2017 / Volume 55 / Number 2
ISSN 1641-4640

Folia NEUROPATHOLOGICA

www.folianeuro.termedia.pl

Official Journal of Mossakowski Medical Research Centre Polish Academy of Sciences
and
Polish Association of Neuropathologists

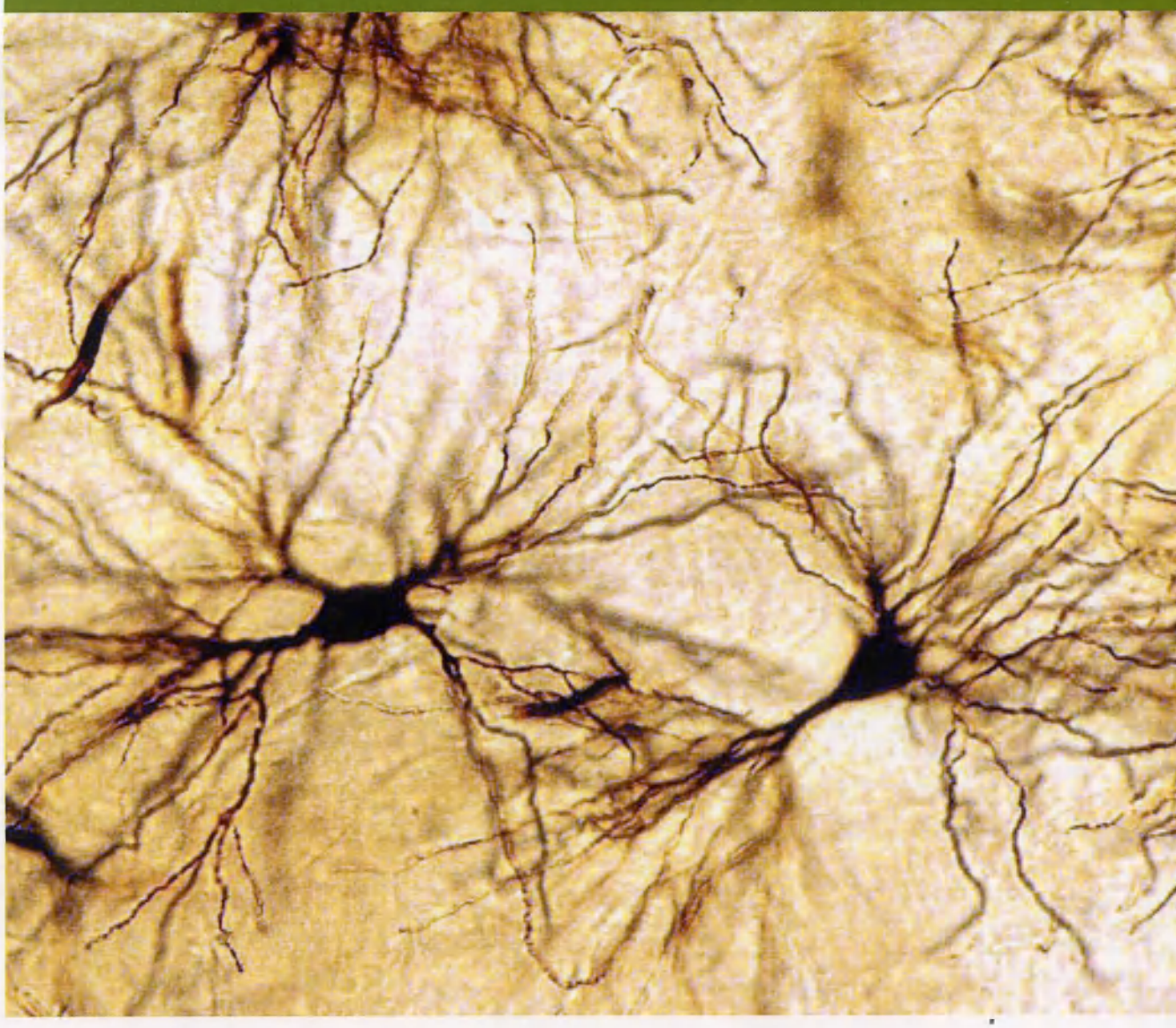

ISSN 1641-4640

Folia Neuropathologica

TERMEDIA Publishing House

Folia
Neuropathologica
former *Neuropatologia Polska*

Official Journal of Mossakowski Medical Research Centre Polish Academy of Sciences
and Polish Association of Neuropathologists

The journal is partly financially supported
by the Ministry of Science and Higher Education

termedia

Termedia Publishing House
Kleeberga 2, 61-615 Poznan, Poland
phone/fax: +48 61 822 77 81
e-mail: termedia@termedia.pl
www.termedia.pl
www.folianeuro.termedia.pl

President of the Management Board
of the Termedia Publishing House
Janusz Michalak

Scientific Director
of the Termedia Publishing House
Maciej Banach

Production Editor
Marzena Demska
e-mail: m.demska@termedia.pl

Marketing and Advertising Department
Renata Dolata
phone: +48 61 822 77 81 ext. 508
e-mail: r.dolata@termedia.pl

Distribution Subscription Department
Jolanta Jankowiak
phone: +48 61 656 22 00
e-mail: prenumerata@termedia.pl

Impact Factor for Folia Neuropathologica equals 1.093
MNiSW score for Folia Neuropathologica equals 20
Index Copernicus Value for Folia Neuropathologica equals 155.68
Position in Index Copernicus ranking systems available at http://www.indexcopernicus.pl

Abstracted and indexed in Index Medicus/MEDLINE, Neuroscience Citation Index, SciSearch, Research Alert, Chemical Abstracts, EMBASE/Excerpta Medica, Polish Medical Bibiography, Index Copernicus

Print run: 450 copies

Folia
Neuropathologica
2017; 55/2: 79-182

Contents

Review paper

Folia Neuropathologica

Neuropathological protocol for the study of unexplained stillbirth

Luca Roncati[1], Francesco Piscioli[2], Teresa Pusiol[2], Anna M. Lavezzi[3]

[1]Department of Diagnostic and Clinical Medicine and of Public Health, Section of Pathology, University of Modena and Reggio Emilia, Modena, [2]Provincial Health Care Services, Institute of Pathology, Santa Maria del Carmine Hospital, Rovereto, [3]Department of Biomedical, Surgical and Dental Sciences, Lino Rossi Research Center, University of Milan, Milan, Italy

Folia Neuropathol 2017; 55 (2): 79-85 DOI: https://doi.org/10.5114/fn.2017.68576

Abstract

An updated neuropathological protocol for the examination of the nervous system in case of unexplained stillbirth has been elaborated and presented in this review. It is focused on the examination of the nervous centers located in the brainstem, which are involved in monitoring the vital functions. Only through a deep analysis of the brainstem it is possible to highlight developmental alterations of these essential centers, and then provide a plausible explanation of the pathogenetic mechanism behind the death. The guidelines, drawn up on the basis of numerous researches performed by the authors, include a histopathological protocol, with an indication of standardized samples, and an immunohistochemical protocol for the study of biological markers, frequently involved in these deaths. The main risk factors that can be related to the neuronal alterations are also reported, together with the indications for the toxicological examination, which should be possibly applied. The authors hope that this protocol will be soon adopted in all the institutions where a fetal death, after a routine autopsy procedure, is diagnosed as "unexplained", in order to make standardized investigations on stillbirth. Nowadays, preventive strategies to decrease the incidence of these very distressing events for both parents and clinicians are necessary.

Key words: *neuropathology, unexplained stillbirth, fetal autopsy, histology, immunohistochemistry, endocrine disrupting compounds.*

Introduction

Inequality in use of fetal autopsy is poorly understood, despite the importance of autopsy in establishing the cause of stillbirth for future prevention [1]. Fetal deaths are in fact the most common adverse pregnancy outcomes in developed countries [4]. Despite a 35% decline in neonatal mortality over the last decades, thanks to public health campaigns promoting back sleep position, the stillbirth rate has not equally decreased [4]. Recently, the World Health Organization (WHO) has communicated that in 2015, 2.6 million stillbirths globally occurred, with more than 7178 deaths a day [4]. Obviously, parents want to know why their baby died in the womb and the chance of recurrence in future pregnancies. Therefore, the detection of the pathogenetic mechanism leading to stillbirth is very important, and not just to give an answer to parents, but above all to introduce preventive measures in order to lower prenatal mortality [1]. The value of a post-mortem examination, as the gold standard investigation following stillbirth, is well documented [18,19,23-26,29]. In particular, the impor-

Communicating author

Luca Roncati, MD, PhD, University of Modena and Reggio Emilia, Policlinico Hospital, 41124 Modena, Italy, phone: +390594224812, fax: +390494224998, e-mail: emailmedical@gmail.com

tance of an adequate fetal examination has been emphasized in a recent policy on the subject by the American Board of Pathology [3]. Nevertheless, the number of fetal autopsies performed worldwide not only has not increased, but it has even declined in the past years, when efforts to decrease stillbirth would just require policies to increase autopsy rates [1]. By contrast, in our unit, the "Lino Rossi" Research Center of Milan University, thanks to Italian law no. 31 "Regulations for diagnostic post mortem investigation in victims of sudden infant death syndrome (SIDS) and unexpected fetal death", there has been a trend for increasing the number of stillbirth autopsy examinations since 2006 [2]. Precisely, this law states that all fetuses, which suddenly died without any apparent cause after 25 weeks of gestation, must be submitted to a diagnostic post-mortem investigation, and that the findings of the in-depth autopsy, the data about pregnancy, fetal development and delivery, and the information related to risk factors, must be collected by the medical personnel (obstetricians, gynecologists, pathologists, etc.) and recorded in the National Data Bank. Researchers can then draw on all the collected results in order to make reliable investigations on the etiology of stillbirth, and improve preventative strategies for these very distressing events for both parents and clinicians. The "Lino Rossi" Research Center has developed an appropriate investigative post-mortem protocol that includes, specifically, the in-depth examination of the autonomic nervous system. The application of this protocol has proved to be greatly useful when a routine fetal autopsy did not show a possible cause of death. It is well known, in fact, that, despite the identification and classification of possible causes of stillborn infants into maternal, fetal, placental and related to external factors, sometimes also combined together, the death remains unexplained in a percentage between 33% and 50% of cases [6]. However, a diagnostic orientation can be obtained from the careful examination, performed by an experienced neuropathologist, of the brain centres checking the vital functions, mostly sited in the brainstem. Detailed examinations of these structures performed in our Institution for several decades, even thanks to Italian law no. 31, in a cohort of over 500 unexplained stillbirths, highlighted, in the great part of cases, their subtle developmental morphological and/or functional alterations, frequently related to environmental risk factors, such maternal smoking. The findings provide insight into the specific pathophysiological process leading to prenatal death. Here, we describe the neuropathologic procedure applied in our Center and which should be adopted in all the anatomopathological institutions where a fetal death, after a standard autopsy procedure, is diagnosed as "unexplained stillbirth" or, more appropriately, "sudden intrauterine unexplained death syndrome" (SIUDS) [20].

Preamble

Only the intact fetal brain (i.e. not macerated or liquefied) can be submitted to the protocol presented below. Then, in case of fetal death, the first assessment consists in the exclusion of cases with brain autolysis. Our previous studies have identified, in well-preserved fetal brains, the main brainstem nuclei and structures that should be examined, hitherto highlighted only in experimental animals. Given the impossibility to perform experiments in humans, the homologous human nuclei have been identified on the basis of morphological criteria of similarity with regard to the location, the cytoarchitecture and number of neurons and applying, when possible, immunohistochemical methods able to highlight the same neurotransmitters expressed in specific nervous structures in rats. Through this original methodology, it was possible to recognize, in particular, the Kölliker-Fuse nucleus, the facial/parafacial complex, the pre-Bötzinger nucleus in the pons/medulla oblongata, and the intermediolateral nucleus in the rostral spinal cord, up to now unidentified in humans [10,12,13,16]. These nervous centers, as demonstrated in experimental studies, are linked together via inter-neuronal synapses into the brainstem in a "respiratory network", able to modulate one another to maintain a regular breathing activity. It should be pointed that, while death related to improper breathing control is easily comprehensible as a possible cause of SIDS, it is difficult to understand how ventilatory alterations can lead to death during intrauterine life, when breathing is not yet a vital condition. We propose, as explanation, that in the last weeks of pregnancy, advancing towards the time of birth, a general check of all the neuronal centers essential for extra-uterine life takes place [17]. Sudden unexpected prenatal deaths could therefore be ascribed to a selective process of self-suppression in the presence of developmental alterations particularly of the respiratory centers, preventing an even more serious and stressful event of a neonatal death [11].

Histopathological protocol

Figure 1 shows a simplified methodology for the brainstem's examination, consisting in the sampling of three specimens (Fig. 1). The first specimen, pontomesencephalic, includes the upper third of the pons and the adjacent portion of caudal mesencephalon. The second extends from the upper part of the medulla oblongata to the adjacent caudal portion of the pons. The third specimen encloses the obex. A fourth sample is taken from the rostral tract of the spinal cord (Fig. 1). Transverse serial sections of each sample are made at intervals of 60 µm. For each level, from eight to ten 5-µm-thick sections are obtained, two of which are stained using hematoxylin-eosin and Klüver-Barrera for histological examination, while the remaining sections are treated, according to the needs, with specific immunohistochemical techniques in order to evaluate the expression of functional markers (as reported in the following paragraph). Any remaining sections are saved for further investigations and stained as deemed necessary. In Figure 2, a schematic representation of the typical histological sections obtained from the four specimens is reported, with the indication of the main nuclei and structures that can be examined (Fig. 2). Overall, they are: the hypoglossus, dorsal motor vagal, tractus solitarius, ambiguus, inferior olivary, pre-Bötzinger, arcuate, dorsal and ventral cochlear, medial inferior vestibular, obscurus and pallidus raphé nuclei in the medulla oblongata; the locus coeruleus, facial/parafacial complex, retrotrapezoid, superior olivary complex, superior and lateral vestibular, Kölliker-Fuse, median and magnus raphé nuclei in the pons; the inferior colliculus, substantia nigra, dorsal and caudal linear raphé nuclei in the caudal mesencephalon. In the spinal cord, the intermedio-lateral nucleus is well recognizable. A diagnosis of "hypoplasia" of a given nucleus is formulated when it shows a significantly decreased number of neurons and/or a decreased area in transverse histological sections, compared to the mean values obtained in age-matched controls. Four of the aforementioned structures, the Kölliker-Fuse nucleus, facial/parafacial complex, pre-Bötzinger nucleus and the intermediolateral nucleus, components of the "respiratory network", are in particular of great interest, and must be always examined in SIUDS. They are entirely enclosed in the four samples taken (Fig. 3). These centers, all components of the respiratory network, are able to coordinate each other through excitatory and/or inhibitory connections, in relation to the need, to control the breathing activity before and after birth. Their evaluation can be speeded by examining a few selected

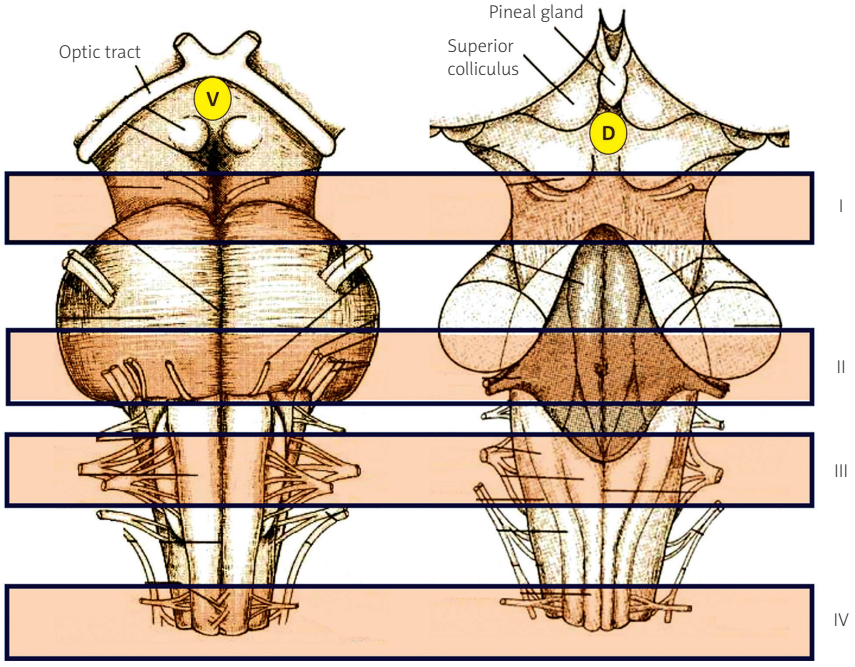

Fig. 1. Schematic representation of the brainstem and spinal cord sampling in four (I, II, III, IV) transversal planes in the ventral (V) and dorsal (D) view.

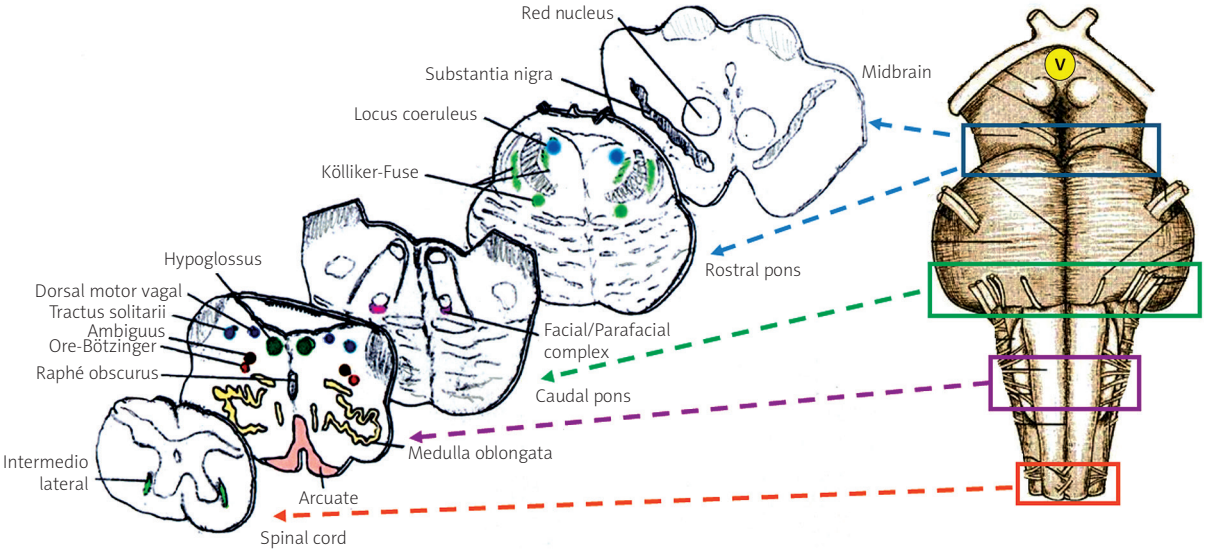

Fig. 2. Schematic representation of the histological sections obtainable from the sampling illustrated in Figure 1, with an indication of the main nuclei and examinable structures.

histological sections. The corresponding specimens are easily recognizable on the basis of precise landmarks that are the presence of the superior cerebellar peduncle decussation in the rostral pons (for the Kölliker-Fuse nucleus analysis), of the medial nucleus of the superior olivary complex in the caudal pons (for the facial/parafacial complex), of the dorsal accessory of the inferior olivary nucleus in the medulla oblongata (for the pre-Bötzinger nucleus) and of dorsal and ventral horns, adjacent to the central canal, in the rostral spinal cord (for the intermediolateral nucleus).

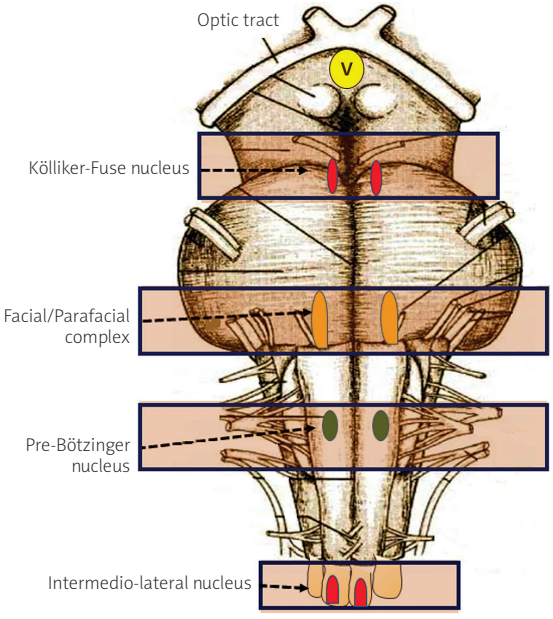

Fig. 3. Schematic representation of the localization of the main respiratory centers (Kölliker-Fuse nucleus, facial/parafacial complex, pre-Bötzinger nucleus and intermedio-lateral nucleus): they are totally included in the four samples obtained.

Immunohistochemical protocol

The reserved sections for the immunohistochemical analyses are treated according to standard procedures in order to evaluate functional parameters, whose altered expression can represent a very significant finding in SIUDS. These biological markers are: neuronal nuclear antigen (NeuN), nicotinic acetylcholine (nACh) receptors (Rs), serotonin (5-HT) Rs, somatostatin (SS) Rs, apoptosis and gliosis.

NeuN

This antigen is strongly expressed in the nucleus of post-mitotic healthy neurons already in fetal life, with the inexplicable exception of several neuronal cell types (precisely, Purkinje cells and dentate nucleus neurons in the cerebellum, neurons of the inferior olivary nucleus in the medulla oblongata, and all the glial cells). By excluding these neurons, a decreased NeuN immunopositivity or absolute negativity can be indicative of neuronal degeneration. In particular, immunoreactivity is significantly weakened after a severe injury, such as

cerebral hypoxia/ischemia [33]. Then, it is very important to apply this technique in all SIUDS to obtain useful information about the physiological general status of neurons. The related detailed immunohistochemical technique is available in our previous article [9].

nACh Rs

The nAChRs regulate critical aspects of brain maturation during the intrauterine life, through neurochemical transmission of acetylcholine among the neurons. These receptors are ion channels in the cytoplasmic membrane, consisting of a different combination of α and β subunits. To date, a total of 10 α and 4 β different subunits have been described [17]. The nAChRs can be opened not only by the neurotransmitter acetylcholine, but also by nicotine (hence the adjective "nicotinic"). Fetal brain damage caused by maternal smoking in pregnancy mainly results from the interaction of nicotine with nAChRs. We specifically suggest addressing the study on the α7-nAChR subtype, given its important involvement in neuronal differentiation, synaptogenesis and formation of brain circuits in fetal life and its demonstrated high vulnerability to toxic effects of nicotine [7].

5-HT Rs

5-HT is a neuromodulator transmitter above all involved in neurotrophic processes during brain development, deputy to the control of neural circuits, including the respiratory network in the ponto-medullary brainstem. It is produced by the serotonergic neurons of the raphé system, a complex of nuclei spread along the midline of the brainstem. In detail, they are the caudal linear raphé nucleus, the dorsal raphé nucleus, the median raphé nucleus, the raphé magnus nucleus, the raphé obscurus nucleus and the raphé pallidus nucleus. A decrease in 5-HT Rs in medullary regions containing raphé neurons has been described by us in SIUDS [8].

SS Rs

SS is a neuropeptide with a wide distribution in the central nervous system. During fetal development, in particular, SS-containing neurons are prevalently concentrated in the brainstem nuclei involved in the ventilatory regulation, as demonstrated by the high immunopositivity of their receptors [5]. This suggests that SS is normally deputy to the inhibition of breathing in utero, while the detection of SS-immunonegativity leads to presume a fatal intrauterine respiratory activity. For this reason, it is definitely recommended to study this transmitter in SIUDS; the related method can be retrieved from our previous works [14,15].

Apoptosis and gliosis

The immunostaining for the detection of apoptosis (TUNEL method) and glial fibrillary acid protein (GFAP) are also recommended to obtain further information about a possible abnormal increase of neuronal death, over the physiological levels, and the presence of reactive gliosis, a well-known marker of neurodegenerative processes [19,21].

Toxicological protocol

It is important, for each case, to collect a complete clinical history, with particular reference to the maternal lifestyle, including information related to the main potential risk factors (such as maternal smoking, alcohol, drug abuse and air pollution).

Nicotine

Among the risk factors, maternal smoking during pregnancy is worldwide recognized as highly associated to fetal death. The mothers must be asked for information about their smoking habit before and during pregnancy. Their reply should be possibly validated through a toxicological research in fetal hair of cotinine, the main metabolite of nicotine, characterized by a long half-life and great stability [32]. The protocol generally includes a qualitative cotinine test to detect the presence or absence of the substance in the hair. A quantitative testing by liquid chromatography-mass spectrometry (LC-MS) system can also be applied to evaluate the cotinine concentration [32].

Pesticides

Recently, our original investigations have demonstrated the adverse effects of persistent pollutants, such as pesticides and household insecticides, on brain development [30,31]. Exactly as nicotine, these harmful chemicals belong to the category of the "endocrine disrupting compounds" (EDCs) [27,28]. Traces of highly toxic substances, as organochlorine and organophosphate pesticides (α and γ-chlordane, chlorfenvinphos, chlorpyrifos, p,p-DDT, p,p-DDE, endrin, α- and β-endosulfans),

have been directly detected in the brain of fetuses, died in agricultural areas where pesticides are used [22].

Conclusions

The post-mortem examination, in case of intrauterine death, is worldwide recognized as important for determining the cause of stillbirth and directing management of subsequent pregnancy [1]. It is necessary, however, to point out that the lack of uniform post-mortem protocols applied in the different centers has hindered significant studies in this field. Furthermore, in the routine fetal autopsy, the examination of the nervous system has received up to now poor attention. Here, we have proposed a neuropathological protocol for a concise and specific examination of the nervous system, and in particular of the brainstem, very useful when the routine autopsy does not reveal a precise cause of fetal death. The application of these guidelines, drawn up after many years of studies in this field, frequently allow to highlight developmental morphological and/or physiological neuronal alterations that could explain the pathogenesis of SIUDS, considering also their correlation with the exposure to environmental risk factors, such as EDCs. The core objective of our work has been to provide, in the simplest way, the steps for the accurate neuropathological examination of the brainstem. The protocol is the culmination of our pluriannual scientific experience in this field. We strongly hope that the examination of the central nervous system, following this protocol, becomes a specialized component of the fetal autopsy, above all when a clear cause of death is not found. The application of this procedure is furthermore the best way to collect a rich body of information about all possible neurological alterations in the fetal brain underlying SIUDS, in order to reduce its incidence and mitigate the surrounding social concern. Pathologists are then invited to adopt this protocol, making it a standardized universal procedure in unexplained stillbirths.

Disclosure

Authors report no conflict of interest.

References

1. Auger N, Tiandrazana RC, Healy-Profitós J, Costopoulos A. Inequality in fetal autopsy in Canada. J Health Care Poor Underserved 2016; 27: 1384-1396.
2. Available at: http://users.unimi.it/centrolinorossi/files/gazz_ufficiale.pdf
3. Available at: http://www.abpath.org/FetalAutopsyPolicy.pdf
4. Available at: http://www.who.int/maternal_child_adolescent/epidemiology/stillbirth/en/
5. Chigr F, Najimi M, Leduque P, Charnay Y, Jordan D, Chayville JA, Tohyama M, Kopp N. Anatomical distribution of somatostatin immunoreactivity in the infant brainstem. Neuroscience 1989; 29: 615-628.
6. Fretts RC. Etiology and prevention of stillbirth. Am J Obstet Gynecol 2005; 193: 1923-1935.
7. Lavezzi AM, Cappiello A, Pusiol T, Corna MF, Termopoli V, Matturri L. Pesticide exposure during pregnancy, like nicotine, affects the brainstem α7 nicotinic acetylcholine receptor expression, increasing the risk of sudden unexplained perinatal death. J Neurol Sci 2015; 348: 94-100.
8. Lavezzi AM, Casale V, Oneda R, Weese-Mayer DE, Matturri L. Sudden infant death syndrome and sudden intrauterine unexplained death: correlation between hypoplasia of raphé nuclei and serotonin transporter gene promoter polymorphism. Pediatr Res 2009; 66: 22-27.
9. Lavezzi AM, Corna MF, Matturri L, Neuronal nuclear antigen (NeuN): a useful marker of neuronal immaturity in sudden unexplained perinatal death. J Neurol Sci 2013; 329: 45-50.
10. Lavezzi AM, Corna MF, Mehboob R, Matturri L. Neuropathology of the intermediolateral nucleus of the spinal cord in sudden unexplained perinatal and infant death. Int J Dev Neurosci 2010; 28: 133-138.
11. Lavezzi AM, Ferrero S, Matturri L, Roncati L, Pusiol T. Developmental neuropathology of brainstem respiratory centers in unexplained stillbirth: What's the meaning? Int J Dev Neurosci 2016; 53: 99-106.
12. Lavezzi AM, Matturri L. Functional neuroanatomy of the human pre-Bötzinger complex with particular reference to sudden unexplained perinatal and infant death. Neuropathology 2008; 28: 10-16.
13. Lavezzi AM, Matturri L. Hypoplasia of the parafacial/facial complex: a very frequent finding in sudden unexplained fetal death. Open Neurosci J 2008; 2: 1-5.
14. Lavezzi AM, Ottaviani G, Matturri L. Involvement of somatostatin in breathing control before and after birth, and in perinatal and infant sudden unexplained death. Folia Neuropathol 2004; 42: 59-65.
15. Lavezzi AM, Ottaviani G, Matturri L. Role of somatostatin and apoptosis in breathing control in sudden perinatal and infant unexplained death. Clin Neuropathol 2004; 23: 304-310.
16. Lavezzi AM, Ottaviani G, Rossi L, Matturri L. Cytoarchitectural organization of the parabrachial/Kölliker-Fuse complex in man. Brain Dev 2004; 26: 316-320.
17. Lindstrom J, Anand R, Gerzanich V, Peng X, Wang F, Wells G. Structure and function of neuronal nicotinic acetylcholine receptors. Prog Brain Res 1996; 109: 125-137.
18. Manganaro L, Scialpi M, Piscioli F, Pusiol T, Roncati L. MRI prenatal diagnosis of genitourinary abnormalities in a case of inconclusive ultrasonography. J Obstet Gynaecol 2016; 36: 762-763.
19. Manganaro L, Vinci V, Giancotti A, Gerli S, Cozzi DA, Pusiol T, Scialpi M, Roncati L. Bi-parametric magnetic resonance imaging applied to obstetrics. J Obstet Gynaecol 2017; 37: 670-672.

20. Martin LJ. Neuronal cell death in nervous system development, disease and injury. Int J Mol Med 2001; 7: 455-478.
21. Matturri L, Pusiol T, Lavezzi AM. Proposal of the acronym "SIUDS" for unexplained stillbirths, like "SIDS". J Neonatal Biol 2014; 3: 5-6.
22. Norenberg MD. Astrocytes responses to CNS injury. J Neuropathol Exp Neurol 1994; 53: 213-220.
23. Pusiol T, Lavezzi A, Matturri L, Termopoli V, Cappiello A, Piscioli F, Roncati L. Impact assessment of endocrine disruptors on sudden intrauterine and infant death syndromes. Eur J Forensic Sci 2016; 3: 8-15.
24. Pusiol T, Lavezzi AM, Piscioli F, Roncati L. Sudden infant death due to imported malignant malaria in Europe. Eur J Forensic Sci 2015; 2: 18-20.
25. Pusiol T. Roncati L, Lavezzi AM, Taddei F, Piscioli F, Ottaviani G. Sudden fetal death due to dualism of the sino-atrial node. Cardiovasc Pathol 2016; 25: 325-328.
26. Roncati L, Barbolini G, Fano RA, Rivasi F. Fatal Aspergillus flavus infection in a neonate. Fetal Pediatr Pathol 2010; 29: 239-244.
27. Roncati L, Barbolini G, Pusiol T, Piscioli F, Maiorana A. New advances on placental hydrops and related villous lymphatics. Lymphology 2015; 48: 28-37.
28. Roncati L, Piscioli F, Pusiol T. The endocrine disrupting chemicals as possible stillbirth contributors. Am J Obstet Gynecol 2016; 215: 532-533.
29. Roncati L, Piscioli F, Pusiol T. The endocrine disruptors among the environmental risk factors for stillbirth. Sci Total Environ 2016; 563-564: 1086-1087.
30. Roncati L, Pusiol T, Piscioli F, Barbolini G, Maiorana A, Lavezzi A. The first 5-year-long survey on intrauterine unexplained sudden deaths from the Northeast Italy. Fetal Pediatr Pathol 2016; 35: 315-326.
31. Roncati L, Pusiol T, Piscioli F, Lavezzi AM. Neurodevelopmental disorders and pesticide exposure: the northeastern Italian experience. Arch Toxicol 2016; 91: 603-604.
32. Roncati L, Termopoli V, Pusiol T. Negative role of the environmental endocrine disruptors in the human neurodevelopment. Front Neurol 2016; 7: 143.
33. Tzatzarakis MN, Vardavas CI, Terzi I, Kavalakis M, Kokkinakis M, Liesivuori J, Tsatsakis AM. Hair nicotine/cotinine concentrations as a method of monitoring exposure to tobacco smoke among infants and adults. Hum Exp Toxicol 2012; 31: 258-265.
34. Unal-Cevik I, Kilinç M, Gürsoy-Ozdemir Y, Gurer G, Dalkara T. Loss of NeuN immunoreactivity after cerebral ischemia does not indicate neuronal cell loss: a cautionary note. Brain Res 2004; 1015: 169-174.

Review paper

Folia Neuropathologica

Neurologic complications in kidney transplant recipients

Piotr C. Piotrowski[1,2], Anna Lutkowska[2], Alexander Tsibulski[2], Marek Karczewski[3], Paweł P. Jagodziński[2]

[1]Department of Experimental and Clinical Neuropathology, Mossakowski Medical Research Centre, Polish Academy of Sciences, Warszawa, [2]Department of Biochemistry and Molecular Biology, Poznań University of Medical Sciences, Poznań, [3]Department of Transplantology, General, Vascular and Plastic Surgery, Clinical Hospital of Poznan University of Medical Sciences, Poznań, Poland

Folia Neuropathol 2017; 55 (2): 86-109 DOI: https://doi.org/10.5114/fn.2017.68577

Abstract

Transplantology experiences continuous growth and kidney transplantation is the most frequently transplanted solid organ. Metabolic, cardiovascular, infectious or kidney function-related aspects are widely recognised and are of key interest for transplant doctors. Neurological complications seen in these patients, although known, are less covered in the literature. According to some reports, neurologic symptoms are experienced by almost 9 per 10 transplant recipients. The intensity, severity and type of abnormalities may vary, and most frequently the complications seem to be associated with a direct or indirect effect of immunosuppressive medications, including their direct effect on cells, on blood vessels, and susceptibility to infections. Increasing age of transplant recipients and relaxation of transplantation eligibility criteria enriches the population with patients already compromised, with a higher present risk of stroke, neuropathy, malignancy etc. Research on and introduction to clinical practice of new agents like belatacept, proteasome inhibitors, or modified release formulations of tacrolimus, changes the picture and type of abnormalities within the nervous or neuromuscular system but does not eliminate them. Thus, it seems justified to remind the society of the whole array of neurologic complications they can see in their practice despite advances in the field.

Key words: *kidney transplantation, immunosuppression, neurotoxicity, PTLD, PRES, opportunistic infections, CNS.*

Introduction

Kidney is the most widely transplanted solid organ associated with high survival rates, which makes renal transplant a growing area of interest in the modern era of nephrology. One of the crucial drawbacks in successful renal transplantation is allograft rejection. Survival rates among transplant recipients have greatly improved due to better understanding of transplant biology and more effective immunosuppressive agents. In the US, less than 30% of the approximately 615,000 patients that were diagnosed with end-stage renal disease (ESRD) have received a kidney transplant and more than 100,000 patients are on the waiting list for a donor kidney [189]. In some other countries, like Spain or the Netherlands, more than 50% of ESRD patients are treated with kidney transplantation [19]. Current immunosuppressive protocols tend to prevent acute rejection of renal allografts better than the old ones despite lower doses of immunosuppressive drugs used nowadays in general. Post-transplant immune monitoring and optimization of the immunosuppressive therapy using non-invasive biomarkers can effectively predict impending graft rejection and may spare the need for renal biopsy. However, drug

Communicating author

Piotr C. Piotrowski, Department of Experimental and Clinical Neuropathology, Mossakowski Medical Research Centre, Polish Academy of Sciences, 5 Pawińskiego St., 02-106 Warsaw, Poland, e-mail: ppiotrow@imdik.pan.pl

toxicity and the unfavourable effects of long-term immunosuppression are associated with significant morbidity and mortality.

The goals of pharmacotherapy in kidney transplantation are to prevent graft rejection, reduce morbidity, and prevent complications. Immunosuppressant drug classes include calcineurin inhibitors (CNIs), corticosteroids, antimetabolites, mammalian target of rapamycin (mTOR) inhibitors, and other immunosuppressants like depleting antibodies (Table I). Transplant recipients are maintained on an immunosuppression regimen based on 1-3 drugs. There is a number of regimens which can be used, including pre-transplantation induction therapy and simple postoperative maintenance therapy; the choice of regimen depends on the patient's profile, training and experience of the transplantation centre, local standards, and reimbursement status of drugs. According to the report of the United States Renal Data System (USRDS) [207], the majority (90% in 2012) of kidney transplant recipients received antibody induction. While the use of anti-IL-2R (interleukin-2 receptor) antagonists has fallen in the US from a peak of 41% in 2002 to 25% in 2012, the use of T-cell depleting agents continues to increase, reaching 65% in 2012 [207] and this trend may continue due to weak data supporting the use of IL-2R antagonists [86,227,228]. However, in Europe, IL2RA induction was more widely used than rabbit antithymocyte globulin (rATG) or other depleting agents [145]. Nearly all transplant recipients in 2012 received a calcineurin inhibitor and an anti-metabolite as components of their initial immunosuppressive regimen. 92% of these patients were prescribed tacrolimus (Tac) as their first-line CNI, and mycophenolate mofetil (MMF) has almost completely replaced azathioprine (Aza) as the anti-metabolite of choice. Use of mTOR inhibitors, both initially and at one year following transplantation, has declined to 2% and 4%,

Table I. Immunosuppressive agents used in organ transplant recipients*

Induction	Maintenance treatment	Treatment of rejections
Polyclonal and monoclonal antibodies	*Corticosteroids*	*Corticosteroids*
Polyclonal (ATG)	Prednisone	Polyclonal and monoclonal antibodies
Monoclonal anti-CD3 (OKT3/Muromonab), withdrawn	*Calcineurin inhibitors*	Reversible 26S proteasome inhibitor (Bortezomib)
Monoclonal anti CD-52 (Alemtuzumab)	Cyclosporine, Tacrolimus	Anti-C5 antibody (Eculizumab)
Monoclonal anti-CD20 (Rituximab)	*Anti-metabolites/Anti-proliferative agents*	
Interleukin-2 receptor antagonists, monoclonal anti-CD25	Azathioprine	
Basiliximab	Mycophenolate mofetil, Mycophenolic acid	
Daclizumab, withdrawn	Mizoribine	
Corticosteroids	Leflunomide	
Methylprednisolone	*m-TOR inhibitors*	
	Sirolimus, Everolimus	
	Co-stimulation blocker	
	Belatacept (fusion protein)	
	Protein kinase C inhibitor	
	Sotrastaurin	
	JAK 3 inhibitors	
	Tofacitinib	
	Alkylating agents	
	Cyclophosphamide	

**Including selected off-label, discontinued and/or currently developed products. Modified classification published by Kumar and Shrestha, 2016 [84,98,106]*

respectively, in 2012, while steroid use seems to be stabilizing at about 67% [207].

Immunosuppressive agents are known to show numerous side effects, including the ones affecting the nervous system directly or indirectly. Majority of solid organ transplant recipients experience neurologic complications after transplantation, and only minority of cases (e.g. femoral neuropathy, stroke) can be attributed to the surgery or the pre-existing comorbidities (e.g. atherosclerosis, hypertension, diabetes) alone [67,160,212]. Immunosuppressive medications, can induce direct or indirect neurotoxicity or increase the risk of central nervous system (CNS) infections and tumours. Neurotoxic effects can manifest either in the central or in the peripheral nervous system (PNS). Immunosuppressive medications used in transplantation that have most frequently been associated with neurologic complications include cyclosporine (CsA), tacrolimus (Tac, FK506), corticosteroids, and muromonab (OKT3) [53,63, 197,220,222,223]. In addition, frequent disturbances of hepatic and kidney metabolism may appreciably prolong the half-life of drugs and increase their plasma levels. The use of various medications interfering with cytochrome CYP3A function may alter the levels of Tac and CsA [130] and affect their safety profile.

Apart from a potentially detrimental effect of immunosuppression, an impaired kidney function itself can be a cause of adverse neurologic outcomes. For example, changes in creatinine, eGFR, serum nitrogen, CRP, 1,25-$(OH)_2D_3$, intact parathyroid hormone (iPTH), phosphorus were found to correlate with psychological and cognitive disorders in patients with treated chronic kidney disease [108].

Neurologic complications following kidney transplantation are more common compared to the general population and the incidence of neurologic alterations is reported in up to 85% of recipients [21,71,177,230]. Somewhat contrary to this prevalent opinion, in a relatively small retrospective analysis of magnetic resonance imaging of transplant recipients in Charleston, SC Medical University, frequency of posterior reversible encephalopathy syndrome, and both acute and chronic lesions/changes in brain did not differ significantly between patients before and after kidney transplantation [26]. They can be classified as several core groups: infection, drug toxicity, structural pathology (stroke, cancer, vasculitis), and metabolic abnormalities including those caused by graft dysfunction [230].

In a retrospective study, it was reported that most frequent neurologic complications following renal transplantation were focal neurologic deficits (20%), acute confusion (16%), seizures (15%) and headache (13%) [21]. An increased frequency of stroke in kidney allograft recipients is attributable to the progression of pre-existing vasculopathy and hypertension [1,173]. Kidney transplantation surgery is also associated with an increased incidence of femoral and lumbosacral plexopathy [56].

This review, although focusing on kidney transplantation is generally applicable to all solid organs as the medications used in e.g. heart or liver transplantology are merely the same although some differences exist when it comes to doses, regimes, and underlying diseases. In the review we analyse firstly the neurotoxicity from selected therapeutic agents perspective, and then we discuss selected most relevant neurotoxicities. Because of volume limitations of the paper we have not been able to cover all relevant topics, including e.g. neurologic complications related directly to an impaired kidney function, linked to use of other medications used in this population of patients, we have barely mentioned importance of genetics/epigenetics behind increased vulnerability to immunosuppression, psychological impact of the transplantation itself, available treatment of the complications etc. We also acknowledge availability of a number of review papers on this subject in contemporary literature. However, we hope that our approach will provide a unique perspective, and by encompassing recent advances in the field, will be a valuable summary for clinicians and scientists interested in this slightly overlooked aspect of transplantology.

Neurotoxicity of immunosuppressive drugs

Calcineurin inhibitors

Cyclosporine is an 11 amino acids polypeptide of fungal origin and a pro-drug, which has been a keystone of immunosuppression in transplantation for four decades. This agent is used for induction and maintenance of immunosuppression. Tacrolimus is a macrolide antibiotic and a calcineurin inhibitor with 2-3 times the potency of cyclosporine. Tac can be used at lower doses than cyclosporine, but its adverse effects include renal dysfunction, neurotoxicity (tremor, insomnia, and paraesthesia of the

extremities), and new-onset diabetes. Tacrolimus has essentially replaced cyclosporine as the CNI of choice, because of a claimed lower rejection rate including decreased steroid-resistant rejection, and according to some studies, superior graft survival [6,135,172]. Some other studies do not support the superiority of Tac vs CsA, though [12,129] and it may partly depend on CYP3A5 (6986 A>G, rs776746) polymorphism [117]. Currently, 80-90% of patients receive Tac after renal transplantation instead of cyclosporine, and this change has persisted for the past 10-15 years.

CsA and Tac induce immunosuppression by inhibiting the first phase of T-cell activation by binding to immunophilins. The immunosuppressive, and possibly neurotoxic, action of both CsA and Tac is exerted through inhibition of the calcium calmodulin-dependent protein phosphatase, calcineurin [82]. Calcineurin is essential for the dephosphorylation of the nuclear factor of activation of T cells (NFAT) which is responsible for activation of T-cells. The first phase of T-cell activation causes transcriptional activation of interleukin (IL)-2, IL-3, IL-4, tumour necrosis factor (TNF) alpha, and interferon gamma that allow T-cells to progress from the G0- to G1-phase [195]. Thus, CsA and Tac both work to inhibit IL-2, which is a critical link in the proliferation of helper T cells. These agents bind to a group of proteins called immunophilins, divided into CsA-binding cyclophilins and FK-binding proteins, to form complexes that then bind to and inhibit the activated calcineurin phosphatase. The tacrolimus: FKBP12 active complex inhibits calcineurin with greater potency than the corresponding cyclosporine complex [83].

Calcineurin and immunophilins have a widespread expression in the central and peripheral nervous systems, but the exact mechanism of CsA- or tacrolimus-induced neurotoxicity is not yet well understood. Protein dephosphorylation by calcineurin may play an important role in neuronal signal transduction due to its ability to regulate the activity of ion channels, glutamate release, and synaptic plasticity [235]. Calcineurin has been shown to regulate the activity of *N*-methyl-*D*-aspartate (NMDA) receptor channels by both altering their ion gating properties and promoting desensitization in cultured hippocampal neurons, which has been ascribed to the enhanced release of glutamate by the presynaptic cells [142,185,213]. Since NMDA receptors are highly permeable to Ca^{2+}, the influx of extracellular Ca^{2+} is considered to be the primary event responsible for glutamate toxicity and neuronal cell death [115].

Mechanisms underlying calcineurin inhibitors neurotoxicity may be related to: (1) upregulation of endothelin receptors A and B and stimulation of endothelin 1 synthesis; (2) damage of the blood–brain barrier (BBB); (3) alterations in the mitochondrial function; (4) interaction with neuromodulatory systems and (5) vascular toxicity. Circulating endothelin, produced in excess in the presence of CNIs can affect the cerebral vascular smooth muscle and could promote systemic hypertension [147,190,203]; the endothelin-mediated effect is also promoted by CsA-dependent upregulation of endothelin receptors A and B [141,238]. On the other hand, if endothelial integrity is disrupted, CsA and Tac could gain access to astrocytes. Under such conditions, local ischemia and consequent white matter oedema could show transient alterations observed in cases of acute hypertensive encephalopathy [143] or in PRES (Posterior Reversible Encephalopathy Syndrome). CsA and Tac are highly lipophilic and are bounded in plasma, especially to low-density lipoprotein (LDL). Since LDL receptors are also expressed on the cell membrane of astrocytes at the blood–brain barrier, increased uptake of these drugs can lead to damage of the BBB as well as the white matter. The vasoconstriction induced by CNI may cause microvascular damage and disrupt the blood-brain barrier [4,177]. In case reports of patients treated with relatively high doses of CsA, published by Shbarou *et al*. [182], lesions in the cerebral white matter associated with abnormally elevated cerebral blood flow velocities on transcranial Doppler ultrasound and abnormal vascular appearance on magnetic resonance angiography were seen. The authors reported the changes as resembling brain lesions seen in pre-eclampsia. CNI can lead to decrease the expression of p-glycoprotein in the brain endothelial cell and cause dysfunction of the blood-brain barrier leading to vasogenic oedema [221]. CsA and Tac increased proinflammatory cytokines and endothelial activation markers in cultured murine endothelial and vascular smooth muscle cells, and in *ex vivo* cultures of murine aortas through TLR4 and with no significant role of calcineurin. In TLR4 knockout mice CNIs were unable to induce inflammation and endothelial activation in aortas. The CNI-induced-TLR4 activity lead to increased $O_2(-)$/ROS production and NF-κB-regulated

synthesis of proinflammatory factors in cultured as well as aortic endothelial and VSMCs [170]. Part of CsA and Tac toxicity may arise from interference with mitochondrial functions [93], such as decrease of mitochondrial energy production and the subsequent activation of anaerobic glycolysis, impaired cellular calcium buffering, activation of proteases and phospholipases, activation of nitric oxide synthase (NOS) and generation of free radicals, leading to either apoptotic or necrotic cell death [180]. CsA and Tac appear to affect neuronal transmission in specific circuits via the following mechanisms: (1) inhibition of the gamma-amino butyric acid (GABA) system that amplifies excitatory response and limits inhibitory response, which may be the mechanism behind the increased seizure activity in transplant recipients; (2) neuronal serotonin depletion, which may explain depression and tremor; (3) glutaminergic NMDA receptor inhibition, suggesting a possible role for psychotic features. In a recent study it was shown in a model of chronic CsA or Tac microinjections into medial prefrontal cortex in rats that calcineurin-inhibition-induced depressive-like behaviour is mediated by blockade of the mTOR signalling pathway and can be reversed by NMDA [237]. Influence on NMDA-dependent signalling through potentiating presynaptic and postsynaptic NMDAR activity in the spinal cord may increase glutamate-mediated nociceptive input and be responsible for calcineurin inhibitor-induced pain syndrome (CIPS) linked to CsA or Tac use [42,45].

Table II. Neurologic side-effects of calcineurin inhibitors

Tremors
Sleep disturbances, insomnia
Paraesthesia, pain syndrome, polyneuropathy
Mood disturbances
Mental status changes: confusion, disorientation, paranoia, hallucinations, lethargy, apathy, depression, irritability, aggression
Leukoencephalopathy, toxic encephalopathy
Seizures
Visual disturbances: hemianopsia, cortical blindness, blurred vision
Motor symptoms: paraplegia, quadriplegia, paresis, dystonia
Speech or language disturbances: akinetic mutism, aphasia, slurred speech
Other movement disorders: asterixis

It was shown that nerve excitability testing demonstrated abnormal nerve function in CNI-treated patients, reflecting nerve membrane depolarization [13]. This can translate into the reduced threshold for action potential generation and easier development of neuropathic symptoms, including paraesthesia and cramps [132]. More severe depolarization may lead to sodium channel inactivation and reduce the size of the action potential, leading to sensory loss and fatigue [105].

Of note, treatment with CsA significantly reduced plasma concentrations of adrenocorticotropic hormone (ACTH), cortisol, and noradrenaline whereas adrenaline levels and state of anxiety remained unaffected [8]. This effect was shown to attenuate stress-responsiveness in animal studies [99].

Neurologic complications have been reported to occur in 10% to 28% of the patients treated with CsA [77,200]. Common complications include tremor, headache, and less frequently, PRES [53,223] (Table II). Mild symptoms in patients treated with CsA are frequent, and encompass tremor, neuralgia, and peripheral neuropathy. Severe symptoms affect up to 5% of transplant recipients such as psychoses, hallucinations, blindness, seizures, cerebellar ataxia and motor weakness [24,40,53,97,111,156,204]. Hypocholesterolemia and hypomagnesemia were suggested as possible precipitating factors for CsA neurotoxicity, however CsA neurotoxicity may be seen in patients with normal cholesterol and magnesium as well [53]. Symptoms typically improve by discontinuation, dosage reduction, or substitution with Tac [223]. Further reports indicate less toxicity associated with the oral route of administration [222]. Epileptiform EEG changes and frank seizures have been described in patients treated with CsA [7,231]. In a small number of patients, myalgia and myopathy have been linked to treatment with CsA. Interference with the mitochondrial function was suggested as the causative mechanism [33]. Use of CNIs in clinical practice in transplantology has significantly changed over the last 20 years. Introduction of microemulsion formulation of cyclosporine, CNI minimization strategies, trough levels monitoring, and introduction of modified release preparations of tacrolimus can be expected to decrease the frequency and severity of neurotoxicity in the longer term [193]. Although in a 12-month large randomized prospective study, no difference in neurotoxicity was seen between standard-dose CsA and low-dose CsA or low-dose Tac groups, it has to be noted that the trough levels of CsA

were not that much different in that study (approx. 150 vs. 100 ng/ml) with levels not exceeding 250 ng/ml for most of the study duration in the standard dosing group [64]. Noteworthy, there was no significant difference in the prevalence of brain abnormalities in early compared with late post-transplant periods when exposure to CI is tapered, and the authors concluded that abnormalities seen in brain MR in kidney transplant recipients are likely not predominantly linked to CNI toxicity [26].

Neurologic complications may be more severe while on Tac than on CsA [120,136], particularly in children [73,126], and it was also reported in liver transplant patients (The US Multicenter FK506 Liver Study Group). Some studies show complications related to Tac are less frequent, 5.4% versus 25% than to CsA [63] while in other publications on solid organ transplantations frequency of neurologic complications is higher in Tac than in CsA-treated groups [126,205]. Complications typically occur in the early post-transplant period, when higher doses and intravenous formulations are used [63]. Common neurologic complications of Tac include tremor, encephalopathy, headache, and seizures [63,220] (Table II). Mild symptoms include tremor, insomnia, nightmares, headache, vertigo, dysesthesia, photophobia and mood disturbances. Severe manifestations include akinetic mutism, seizures, cortical blindness, focal deficits, psychosis and encephalopathy [52]. The most serious complication is PRES, presenting with nausea, hematemesis, headache, loss of vision, seizures and altered consciousness [149], associated with subcortical and deep white matter changes [74,94]. The spontaneous resolution of the syndrome is probably associated with the spontaneous reduction in hemodynamic disorders. A rare but severe side effect of Tac can be peripheral neuropathy. About 0.003% of patients developed severe multifocal demyelinating sensorimotor polyneuropathy 2-10 weeks after the start of treatment with Tac, though similar changes can also be observed with CsA [224]. In another report, a late onset severe chronic inflammatory demyelinating polyradiculoneuropathy was diagnosed 10 years after Tac initiation, and resolved after Tac withdrawal [165].

The treatment of immunosuppressive neurotoxicity consists of correction of electrolyte imbalance and hypertension, immunosuppressant dose reduction and switching from cyclosporine to tacrolimus or vice versa, if necessary [109,196,233]. Use of combinations, such as CNI plus mycophenolate or mTOR inhibitor, enables lower doses of cyclosporine or tacrolimus to be used without weakening the immunosuppressive effect [124]. These approaches lead in most cases to the disappearance of the symptoms and the reversal of neuroimaging anomalies [27].

Corticosteroids

Corticosteroids are used for induction and maintenance immunosuppression, as well as against acute rejection. These agents prevent production of cytokines and vasoactive substances, including IL-1, IL-2, IL-6, tumor necrosis factor-α, chemokines, prostaglandins, major histocompatibility class II and proteases. Corticosteroids act as agonists of glucocorticoid receptors, but at higher doses, have receptor-independent effects. Corticosteroids have three principal mechanisms of action: 1) inhibit the synthesis of inflammatory proteins blocking NF-κB, 2) induce the expression of anti-inflammatory proteins by IkB and MAPK phosphatase I, and 3) inhibit 5-lipoxygenase and cyclooxygenase-2 [44]. Some of the observed effects of corticosteroids depend on the increase in the adrenergic effects of catecholamines and of the synthesis of epinephrine from norepinephrine [65].

Glucocorticoids and, to a lesser extent, mineralocorticoids cross the blood–brain barrier to access corticosteroid receptors within the CNS [206]. There are two major classes of corticosteroid receptors: mineralocorticoid receptors and glucocorticoid receptors [167].

Glucocorticoid receptors in the cytoplasm are in an inactive complex with heat shock proteins. The binding of corticosteroids to the glucocorticoid receptors dissociates heat shock proteins from the glucocorticoid receptors. Active corticosteroid–glucocorticoid receptor complexes migrate to the nucleus and dimerize on palindromic DNA sequences in many genes. The binding of glucocorticoid receptors in the promoter region of the target genes can lead to either induction or suppression of gene transcripts.

The most common corticosteroids used in transplantation are oral prednisolone/prednisone and intravenous methylprednisolone. Their role in maintenance immunosuppression is still under investigation because of severe side effects during long-term use. These agents are metabolized by the liver and excreted by kidneys as inactive metabolites. Drug interactions with P450 inhibitors and inducers are common. The neurologic complications of corticosteroids are reversible with a reduction and/

or withdrawal of their intravenous administration [166]. Common neurological complications linked to steroids are myopathies of skeletal and respiratory muscles and psychiatric disorders [32,55,208]. Psychiatric disorders include confusion, mood disturbances, manic states, psychotic reactions, anxiety, sleeplessness, reduced concentration, cognitive impairment. Steroid-induced psychosis is rare, but complications such as schizophrenic syndromes, affective disorders or delirium can also occur due to steroids use [57,150,214,226]. It was suggested that 50% of patients treated with medium to high doses of steroids for more than 3 weeks develop a proximal myopathy starting in the hip muscles. Steroid myopathy usually resolves slowly and it takes 2 to 8 months following discontinuation [37,47].

High-dosage treatment with corticosteroids and neuromuscular blocking agents may lead to the development of critical illness myopathy [36,107]. Myopathy usually improves gradually with dosage reduction or discontinuation of therapy. Epidural lipomatosis is a rare complication of steroid therapy; spinal compression and radiculopathy have been reported [70].

It has been proposed that cognitive dysfunction caused by corticosteroids may be a result of a combination of impaired hippocampal neurogenesis and subcortical white matter dysfunction [57].

Risk factors predisposing for neuropsychiatric side effects of corticosteroids include a daily dose of prednisone greater than 40 mg, damaged blood-brain barrier, hypoalbuminemia, and prior history of steroid-related psychosis or mania [218].

Prolonged use of steroids may also indirectly lead to numerous non-specific neurologic complications, including those related to opportunistic infections, osteoporosis, diabetes mellitus, obesity, elevated blood pressure etc. [44,60].

Polyclonal and monoclonal antibodies

Biologic agents are polyclonal and monoclonal antibodies that are frequently used in transplantation for induction immunosuppression or treatment of rejection. The three antibodies used for induction therapy are the lymphocyte-depleting agents: (1) antithymocyte globulin (ATG), (2) basiliximab, and (3) alemtuzumab (Table I). However, alemtuzumab has not been granted market approval for use in transplantations and has not been endorsed by recent Cochrane review due to insufficient and inconclusive data [9,87]. Historically, immunosuppressant selection was based solely on efficacy for the prevention of rejection. In the current era of transplantation, it is a common practice in the transplant community to select induction therapy based on risk-benefit considerations for each patient.

Polyclonal antibodies induce lysis of lymphocytes. Antithymocyte globulin rabbit acts against human T-cell surface antigens and depletes CD4 lymphocytes. In addition to T-cell depletion, it induces B-cell apoptosis, interferes with dendritic cell function, modulates adhesion molecules and chemokine receptors and induces regulatory T-cells. Administration of ATG can induce a cytokine-release syndrome, which includes fever, chills and sometimes hypotension and pulmonary oedema, and may mimic neurotoxicity reported after OKT3 use. ATG has many adverse effects (fever, thrombocytopenia, leukopenia, haemolysis, respiratory distress, serum sickness, and anaphylaxis), but some of them may be ameliorated with steroids. It is indicated for prophylaxis and treatment of renal transplant acute rejection in conjunction with concomitant immunosuppression. In comparison with basiliximab it causes a higher rate of infections including opportunistic infections [9,20,87,106,199].

The monoclonal antibodies used (mostly in clinical research except for basiliximab) in transplant patients include anti-CD3 antibody (OKT3, muromonab), anti-CD25 antibody (basiliximab and daclizumab), anti-CD20 antibody (rituximab) and anti-CD52 antibody (alemtuzumab) (Table I). Except for OKT3, their administration to transplant patients is associated with a very low prevalence of neurologic adverse effects.

Basiliximab

Basiliximab is an IL-2R antagonist indicated for prophylaxis of kidney transplant rejection and is used as induction treatment. Its use has not been linked to specific neurotoxicities and has not been shown to increase occurrence of malignancies or opportunistic infections [20,106].

Alemtuzumab

Alemtuzumab is a humanized recombinant monoclonal antibody against CD52 which is present on T-cells, B-cells, NK cells and to a lesser extent on monocytes.

As with ATG, alemtuzumab infusion can be followed by a cytokine-release syndrome [225], however it is much milder than with ATG. It is used off-label as part of various induction regimens in patients undergoing kidney transplantation. The use of alemtuzumab as induction immunosuppression for renal transplantation introduces the possibility of long-term Tac monotherapy, avoiding maintenance with both corticosteroids and MMF. Renal transplantation with alemtuzumab induction followed by Tac monotherapy leads to good graft and patient outcomes, with no major differences detected compared with basiliximab induction and tacrolimus/mycophenolate mofetil maintenance at one year. Higher frequency of opportunistic infections comparing to basiliximab has been suggested [87,106,158], which may translate into the corresponding risk of neurologic complications.

OKT3

OKT3 is a murine monoclonal antibody targeted against the CD3 adhesion molecule on lymphocytes. It was most frequently used in the treatment of rejection, and it was associated with aseptic meningitis, encephalopathy and seizures [197]. OKT3 caused release of systemic proinflammatory cytokines in CSF, which are responsible for the flu-like syndrome and may be involved in the pathogenesis of the cerebral oedema [3]. Approximately 5% to 10% of patients treated with OKT3 developed an acute aseptic meningeal syndrome associated with aseptic meningitis presenting within 72 hours of its administration [90]. Diffuse encephalopathy was rarely seen with coma, seizures, psychosis and brain oedema. The encephalopathy may take up to 2 weeks to resolve. OKT3 is rarely associated with neurologic complications because of its reduced neurotoxicity and its current limited clinical indications. Its use was contraindicated in patients with underlying neurologic problems such as seizures. The product has been withdrawn from the market [22].

Rituximab

Rituximab is a chimeric anti-CD20 monoclonal antibody which acts through depletion of B cells [18]. It has not been approved for use in renal transplantation [169] but its use has been endorsed for specific subpopulations of organ transplant recipients by the international transplantology society expressed in national guidelines [39,159,229] e.g. for ABO blood group incompatible transplantation, for post-transplant lymphoproliferative disorder, HLA antibody incompatible renal transplantation and for treatment of acute rejections. It has been postulated that rituximab may prevent development of chronic antibody mediated rejection [18]. Regarding its toxicity, the drug can cause e.g. cytokine release syndrome, progressive multifocal leukoencephalopathy infusion-associated hypotension, cardiovascular disorders and infections [169]. Cases of PRES linked to rituximab administration were also reported [25].

Belatacept

Belatacept is a selective T-cell costimulation blocker. It comprises of a recombinant extracellular domain of human cytotoxic T lymphocyte antigen-4 (CTLA-4) and a fragment of a modified Fc portion of human IgG1. The drug binds to CD 80/86 ligands of antigen-stimulating cells and thereby inhibits the CD-28-mediated T-cell costimulation. T-cells activation requires two signals of which the first signal is mediated by the interaction of major histocompatibility complex (MHC): T cell receptor (TCR) and the second is mediated by the costimulatory molecules. The costimulatory molecules CD80/86 ligands in the antigen presenting cells bind to CD28 of the T-cells to induce the immunological response. The costimulatory molecules CD28:CD80/86 interaction is also essential for clonal proliferation of cytotoxic T cells which play a main role in the graft rejection [112].

Belatacept has been approved for use in combination therapy to prevent renal graft rejection in patients who are Epstein-Barr virus seropositive. Despite some advantages over calcineurin inhibitor-based regimens it bears a risk of post-transplant lymphoproliferative disorder (PTLD), a rapidly progressing and often lethal malignancy. The occurrence of PTLD, particularly PTLD involving the central nervous system was noted in 0-4% of belatacept-treated patients in clinical trials. Belatacept has also potential to induce progressive multifocal leukoencephalopathy [23,68,106,121].

mTor inhibitors

Mammalian target of rapamycin (mTOR) inhibitors inhibit T-cell activation and proliferation. Unlike calcineurin inhibitors, sirolimus and everolimus inhibit the second phase of T-cell activation [83].

The second phase involves signal transduction and clonal proliferation of T-cells. These agents inhibit interleukin-induced proliferation of T-cells resulting in the cell cycle arrest in the late G1-phase, which prevents progression to the S-phase [80]. Mammalian target of rapamycin (mTOR) is a serine/threonine kinase, integrating multiple signals such as nutrition, oxygen supply, and growth factors [38]. mTOR inhibitors (sirolimus and everolimus) need to bind to the 12-kD immunophilin FK-506-binding protein in order to block the serine/threonine kinase activity of the mTOR/raptor/GbetaL complex [85]. Two TOR proteins have been identified – TOR1 and TOR2 and both everolimus and sirolimus were long thought to act almost only through inhibition of TOR1 complex (TORC1) [239]. However, there has been increasing evidence that the additional hydroxyethyl group at the C(40) of the everolimus is linked to not only different tissue and subcellular distribution, but also to different affinities to active drug transporters and drug-metabolizing enzymes, and interaction with TORC2 than sirolimus [103]. It was suggested that everolimus, but not sirolimus, distributes to brain mitochondria and stimulates mitochondrial oxidation in the brain and contrary to sirolimus, everolimus counteracts CsA-related negative effects in the rat brain energy state [102,178,179]. In contrast to sirolimus, everolimus was shown not to affect cyclosporine concentrations in blood and brain tissue but it reduced cyclosporine concentrations in brain mitochondria by 65% [178].

Sirolimus and everolimus have shown their efficacy in kidney transplantation in a variety of immunosuppression regimes, but their wide use has been limited by relative high discontinuation rates and safety profile. Their most important adverse effects are thrombocytopenia, leukopenia, hypercholesterolemia, stomatitis, diarrhoea, and, interstitial pneumonitis [131]. In a long-term retrospective analysis of 10 prospective randomized trials in kidney transplantation it was shown that the efficacy of *de novo* use of mTOR inhibitor is similar to antimetabolites in kidney transplant recipients receiving calcineurin inhibitor. Patients on mTOR inhibitor benefited from the lower CMV infection rate, but the overall safety profile was unfavourable, showing higher treatment discontinuation rates and higher incidence of proteinuria [54]. In heart transplant recipients patients switched from CNI to mTORi had a higher creatinine clearance but also significantly higher occurrence of adverse effects, which included skin diseases, gastrointestinal side effects, bone marrow suppression, and infections [163]. Also, when compared with mycophenolate as part of the combination with CNI in kidney transplantation, mTOR-I showed no particular superiority to mycophenolate, and instead mTOR-I had an increased risk of graft loss when combined with CNI, even when combined with a reduced dose of CNI. In this retrospective analysis of 4930 patients treated with mTOR-it had a higher risk of new-onset diabetes mellitus, dyslipidemia, proteinuria, peripheral oedema, thrombocytopenia and lymphocele, but a lower risk of CMV infection, malignancy and leukopenia. Neurotoxicity was not reported [234].

Neurotoxicity with mTOR inhibitors is relatively low, however PRES associated with mTOR inhibitors was reported [134,162,202]. Sirolimus rarely causes neurotoxicity since it can alter cell metabolism of astrocytes, thus resulting in similar neurotoxicity as experienced by Tac and CsA (tremor, confusion, agitation and headache) [175]. For everolimus rare adverse effects are dizziness, hypoesthesia, paraesthesia, somnolence, and tremor [11]. Bilateral optic neuropathy was also reported [202]. As mentioned earlier, mTOR intermediates depression-like symptoms which may lead to corresponding psychiatric abnormalities during mTOR inhibitors use [2,237], although scarce evidence exists that mTOR inhibitors may have a more favourable profile than CNIs in this respect [111]. In a small study, no difference between CNIs and everolimus was shown in terms of negative impact on the cognitive function in heart transplant recipients. About 40% of subjects had cognitive impairment, defined as performance at least 1.5 standard deviations below normative mean in one or several cognitive domains in that population [35].

Other immunosuppressants

Apart from a variety of off-label agents used occasionally or in clinical trials in transplantology, there are two other important subgroups of medications which belong to standard of care in solid organ transplantations. The first group comprises agents inhibiting synthesis of nucleotides – purine synthesis inhibitors – mycophenolate and pyrimidine synthesis inhibitors – leflunomide. The second group comprises old drugs – so-called antimetabo-

lites: azathioprine and cyclophosphamide [171]. From this selection, mycophenolate derivatives (mofetil or sodium salt) are most frequently used. Mycophenolate inhibits enzyme – inosine monophosphate dehydrogenase (IMPDH) required for guanosine synthesis and suppresses *de novo* purine synthesis in lymphocytes, thus inhibiting their proliferation [127]. Mycophenolate impairs B and T-cell proliferation, sparing other rapidly dividing cells due to the presence of guanosine salvage pathways in other cells. This agent is frequently used in regimens containing a calcineurin inhibitor and corticosteroids for prevention of renal allograft rejection [171]. Mycophenolate has been shown to decrease prevalence of acute cellular rejection compared with azathioprine and prevalence of chronic rejection [6,154]. The prescribing information for MMF reports psychiatric disorders – common – agitation, confusional state, depression, anxiety, thinking abnormal, insomnia, and nervous system disorders – common – convulsion, hypertonia, tremor, somnolence, myasthenic syndrome, dizziness, headache, paraesthesia, dysgeusia as adverse reactions possible or probable related to MMF. Cases of JC virus related PML have also been reported. It is also possible that the rate of infections is increased in relation to mycophenolate use [137]. A case study reported a 64-year-old woman who developed a severe depressive disorder after the start of therapy [59]. However, it is generally believed that mycophenolate is not causing neurotoxicity [11].

According to Cochrane analysis, mycophenolic acid was superior azathioprine to AZA for improvement of graft survival and prevention of acute rejection after kidney transplantation. However it was noted that these benefits must be weighed against potential harms. The available evidence on safety outcomes is limited and inconsistent [215]. Azathioprine (Aza), a disease-modifying antirheumatic drug (DMARD), was also employed in renal transplantation to prevent graft rejection however due to reported higher efficacy of mycophenolate, its use in organ transplantations has been declining significantly. Its anti-proliferative properties are less selective than those of MMF [66,210]. Azathioprine antagonizes purine metabolism and inhibits synthesis of DNA, RNA, and proteins. It may decrease proliferation of immune cells, which results in lower autoimmune activity [6,156]. Azathioprine has been clearly identified as having potential to increase the neuromuscular blockade produced by depolarising agents such as succinylcholine and can reduce the blockade produced by non-depolarising agents such as tubocurarine [15]. An increased risk of infections and cases of PML were also reported for AZA [15]. Very rare cases of psychiatric complications of AZA were reported [31] and they comprised a complex picture of behavioural changes, forgetfulness, confusion, memory loss and communication difficulty, obsessive-compulsive disorder and panic attacks [31,209].

Neither leflunomide nor cyclophosphamide has been used as part of standard immunosuppression after organ and specifically kidney transplantation [101,159]. However, Johannes *et al*. [216] have published recently a systematic report on cyclophosphamide-based treatment of acute antibody-mediated rejection showing a positive effect of combined regimen (with plasmapheresis and i.v. immunoglobulins) proven with modern diagnostic measures. Cyclophosphamide has been linked with multiple toxicities. According to Summary of Product Characteristics [51], apart from an increased risk of infections, the following side effects are known or suspected to be related to cyclophosphamide a) psychiatric disorders (very rare confusional state), b) nervous system disorders (uncommon – peripheral neuropathy, polyneuropathy, neuralgia, convulsion, dizziness, dysgeusia, hypogeusia, paraesthesia, general neurotoxicity, unknown frequency – PRES, encephalopathy). Also, vision disorders, hearing disorders and muscle symptoms were noted.

Regarding other agents reported in the context of immunosuppression in organ transplantology, it is worth mentioning relatively new agents – bortezomib and eculizumab [106, 159]. Bortezomib (BTZ) is a proteasome inhibitor and an antineoplastic drug that reversibly inhibits mammalian 26S proteasome and interacts with the nuclear factor kappa B (NFκB) system, thus leading to cytoplasmic aggregate accumulation and cell cycle arrest in cancer cells [128]. It is also known to induce neurotoxicity in neuronal cells by several mechanisms that lead to apoptosis [176]. BTZ has been shown to induce peripheral neuropathy characterized by neuropathic pain in a stocking-and-glove distribution and by paraesthesias in distal extremities of limbs, mainly due to unmyelinated and thin myelinated sensory fibers impairment (C and Aδ fibers, respectively) [128]. Eculizumab is a fully humanized monoclonal antibody directed against the C5 component of the complement cas-

cade. There have been inconclusive data on its efficacy in kidney transplantation although some results have been encouraging PTT 2016 [96,114,236]. Eculizumab is known to increase the risk of infections, including increases in the patient's susceptibility to meningococcal infection (*Neisseria meningitidis*) [17]. According to the Summary of Product Characteristics [62], headache has been another typical adverse reaction of eculizumab. Other potential adverse reactions include: psychiatric disorders – insomnia, depression, mood disorder, anxiety, abnormal dreams, sleep disorders; neurologic disorders – dizziness, dysgeusia, tremor, paraesthesia, syncope; other – vision disturbances. tinnitus and vertigo, musculoskeletal symptoms [62].

Neurologic complications of kidney transplantation

Ischemic stroke

Ischemic strokes are relatively common in heart and kidney transplant recipients. Stroke may occur in 8% of renal transplant recipients and may be facilitated by hypertension, diabetes and accelerated atherosclerosis, which may be acquired during dialysis or after transplantation [160]. Apart from immunosuppressive treatment, ischemic strokes may be related to the surgical procedure of transplantation, complications typical for surgery (e.g. bacterial infections, anaesthesia-related negative outcomes, bleeding etc.), presence of bacterial endocarditis and vasoinvasive fungal CNS infections, hypercoagulable states, accelerated atherosclerosis, vasculitis and cardiac arrhythmias after transplantation [160]. While aetiology of strokes in the transplant recipient population is shifted toward perioperative and infectious causes, in medium- and long-term survivors accelerated atherosclerosis after transplantation [48,146] will affect cerebrovascular circulation increasing the risk of stroke [140]. In heart and liver allograft recipients, strokes occur early after transplantation and they tend to occur late after kidney transplantation. In kidney transplant recipients, age over 40 and diabetes were found to be major risk factors for cerebrovascular disease [4].

Ischemic strokes after kidney transplantation are frequently related to atherosclerosis [144]. A significant reduction in stroke incidence has been reported in diabetic patients receiving simultaneous kidney and pancreas transplantation [140]. Concomitant control of the main risk factors (cholesterol, glycaemia and hypertension) is critical as is preventive treatment with antiplatelet agents like aspirin. Cyclosporine, mTOR inhibitors, and to a lesser extent, Tac, may cause hypercholesterolemia, accelerating cerebrovascular disease, especially in patients with prolonged survival [174]. Also, patients who converted from CNI to mTOR inhibitor have a substantially greater risk of e.g. anaemia, hyperlipidaemia and hypercholesterolemia [116]. According to a recent paper published by Simha *et al*. [186], sirolimus is associated with elevation in PCSK9 levels, which is not associated with sirolimus-induced hypercholesterolemia. This suggests an independent pathway for mTOR-inhibitors-induced hypercholesterolemia, as PSCK9 plays a major regulatory role in cholesterol homeostasis, mainly by reducing LDL receptor (LDLR) levels on the plasma membrane. Reduced LDLR levels result in decreased metabolism of LDL-particles, which could lead to hypercholesterolemia [76]. Substituting CsA with Tac may reduce cholesterol levels [198]. On the other hand, it has been postulated that mTOR inhibitors may offer a cardioprotective effect as in experimental settings delayed progression of atherosclerosis is observed consistent with evidence from heart transplant patients where coronary artery intimal thickening and the incidence of cardiac allograft vasculopathy are reduced with everolimus versus cyclosporine therapy. Earlier data exist as well showing that mTOR inhibitors may improve arterial stiffness, which precedes cardiovascular (CV) events, and may reduce ventricular remodelling and decrease left ventricular mass through an anti-fibrotic effect [89]. Thus, cardiovascular /hypercholesterolemia-related effects of mTOR inhibitors may not necessarily contribute to CV-dependent neurologic complications seen during their use. Clinical data support this hypothesis. In a retrospective analysis, patients receiving SRL after liver transplantation had no increased risk of coronary artery disease or cardiovascular accidents (CAD/CVA) as compared with patients maintained on a calcineurin inhibitor [217].

Stroke is more common after kidney transplantation, while encephalopathy, seizures and CPM (central pontine myelinolysis) are characteristic of liver transplantation. In kidney transplant patients, stroke is the most common neurologic complication, whereas cerebral infarction and bleeding are more typical after heart transplantation. Kidney allograft recipients frequently develop post-transplant poly-

cythaemia (17% of patients) and hypercoagulability, which may increase the risk of stroke [5,100]. The risk for aneurismal subarachnoid haemorrhage is increased 10-fold in kidney allograft recipients transplanted for polycystic kidney disease [219]. Diabetic nephropathy as a cause of pre-transplant kidney failure also increases the risk of post-transplant intracranial haemorrhage [219] and it can be anticipated that the same consequence follows from diabetes related to use of immunosuppressants. Calcineurin inhibitors and steroids are best known to induce post-transplant diabetes, with a higher risk of this complication seen with tacrolimus. In a retrospective analysis of kidney transplant recipients, post-transplantation diabetes mellitus occurred more frequently in patients receiving a cadaver organ compared with a living donor organ and in those receiving tacrolimus therapy vs cyclosporine therapy [29,61]. However, also mTOR inhibitors were associated with an increased risk of new-onset diabetes after transplantation (NODAT) [29].

Encephalopathy

Metabolic encephalopathy is common among transplant recipients; the aetiology is as variable as in non-transplant patients, commonly including electrolyte and changes in glucose levels. Patients with pre-existing diabetes are sensitive to treatment with steroids, in addition Tac may precipitate diabetic ketoacidosis. Abrupt, inadvertent steroid discontinuation may also cause a disturbance of consciousness. Patients with a severe systemic infection without CNS involvement typically develop sepsis-related encephalopathy [30,91]. Delayed graft function in orthotopic liver and kidney transplantation is associated with hepatic and uremic encephalopathy, respectively [91].

Common causes of encephalopathy include neurotoxicity from non-immunosuppressive drugs, various metabolic derangements, CNS or systemic infections, and stroke. Immunosuppressant-related encephalopathy has been also described with e.g. CsA, Tac, OKT3 [16,43,88,110,164,194], and as mentioned earlier – rituximab, belatacept and cyclophosphamide. Although neurotoxicity of mTOR inhibitors is relatively low, they can induce PRES in kidney transplantation patients [134,162,202]. Neurotoxicity is usually associated with higher serum concentrations of immunosuppressants, but may also become apparent at serum levels within the therapeutic range. Common adverse signs are tremor, headache and cerebellar or extrapyramidal signs [157].

Neurotoxicity of CNIs is clinically indistinguishable and classical neuroimaging findings are indistinguishable from PRES in eclampsia or hypertensive encephalopathy [88,110,191]. It is not fully understood why posterior circulation is usually more severely affected, but this has been attributed to the less extensive sympathetic vascular innervation posteriorly. Clinically, PRES commonly presents with akinetic mutism, visual symptoms, occipital seizures, and overall impairment of consciousness [16]. Most commonly, Tac or CsA-related PRES presents within the first month after transplantation, but rarely occurs more than a year later [43,164].

Neuromuscular complications

Femoral neuropathy and meralgia paresthetica have been reported in renal and liver transplantation, while phrenic nerve injury is seen in the setting of heart and lung transplantation [14,161,183]. Lumbosacral plexopathy may be associated with retroperitoneal bleeding or iliac artery pseudoaneurysms [119]. Peripheral mononeuritis and polyneuritis may also occur. An acute femoral neuropathy can develop in 2% of the patients as a result of perioperative nerve compression by retractors or nerve ischemia. Patients complain of weakness in the thigh and pain or sensory deficits on the thigh and inner calf. Most patients have an excellent chance of recovery [181,212].

Peripheral toxicity occurs weeks to months after starting immunosuppressive treatment. Both the nerve and the muscle may be involved. Axonal and demyelinating neuropathy have been reported. The more severe forms have been observed during Tac therapy, such as multifocal demyelinating neuropathy resembling chronic inflammatory demyelinating neuropathy (CIDP). Moreover, akinetic mutism and various aphasic and apractic syndromes may be seen in the setting of both Tac and CsA toxicity [28,168]. These usually improve with dosage reduction and careful monitoring of serum drug levels. Paradoxically, Tac showed neuroprotective properties in some experimental models of peripheral nerve injury [113]. The evidence for the existence of Tac-related peripheral neuropathy is still equivocal, and further studies are needed to firmly establish its pathophysiology and relevance.

Muscle-related or neuromuscular adverse reactions have been reported with most of the immunosuppressive medications. As mentioned earlier, those include e.g. steroid-induced myopathy, myalgia and myopathy during CNIs use, myalgia observed in thymoglobulin-treated patients, tremor after mTOR inhibitors use, myasthenic syndrome reported for mycophenolate and neuromuscular block seen with azathioprine, musculoskeletal symptoms described as potentially related to cyclophosphamide and eculizumab.

Behavioural disorders

Corticosteroid therapy is one of cornerstones of immunosuppression protocols, used for maintenance therapy as well as for treatment of acute rejection. Direct neurologic complications include steroid-related psychosis, myopathy, and epidural lipomatosis. The incidence of acute side-effects is 3–4% and the most common neurologic complications are behavioural disorders including confusion, mood disturbances, manic states and psychotic reactions [150]. Behavioural changes associated with steroid use range from minor mood disturbances to florid psychosis. Symptoms usually improve with dosage reduction or discontinuation of therapy, but occasionally, adjunct antidepressant and neuroleptic therapy needs to be considered. Repeated exposure to steroids does not routinely increase the risk of developing psychosis. Behavioural disorders, as already cited, were also linked to CNI, mTOR inhibitors and mycophenolate. Uncommon, rare or very rare cases of psychiatric/behavioural changes were reported with AZA, cyclophosphamide, mycophenolate and eculizumab [9,106].

De novo CNS malignancies

Organ transplant recipients have a three- to fourfold higher incidence of malignant disease compared with the general population [153], due to their reduced immunosurveillance and high incidence of infections involving oncogenic viruses. The incidence of post-transplant lymphoproliferative disorders has been estimated at less than 2% (with higher rates in the paediatric population) and 27% of cases involve the CNS and meninges [46,95,155]. In a recent report from database of 1421 adult patients who underwent renal transplantation from deceased or living donors in the period from 2007 to 2015 in the Slovak transplant centres, frequency of PTLD was found as 2.4% [240]. Patients undergoing heart–lung or liver–bowel transplantation are at the highest risk (5%) for CNS malignancies, while the risk is lower with liver, cardiac and bone marrow allografts (1-2%), and lowest with kidney transplantation (< 1%) [95]. The most frequent malignancies of the brain in renal transplant recipients are lymphomas and metastatic tumours which are, for the most part, *de novo* malignancies from immunosuppression. The most common malignant PTLD subtype is post-transplant diffuse large B-cell lymphoma (PT-DLBCL), followed by Burkitt lymphoma (PT-BL) and plasmablastic lymphoma (PT-PBL). PT-BL and PT-PBL are aggressive, but poorly studied malignant PTLD subtypes [133]. Many of the reported cases of CNS lymphomas are associated with prior EBV infections [151]: this condition is estimated to occur in 3% of liver recipients [194] and in 1-2% of kidney recipients [75]. The clinical manifestations vary and the final diagnosis is often based on cerebral biopsy [152]. Treatment options include reduction of immunosuppression, anti-CD20 monoclonal antibodies, and/or chemotherapy [118]. Localized disease may be successfully treated with radiotherapy or surgery [81].

Immunosuppressed allograft recipients have an increased incidence of cancer. An increased incidence of post-transplant lymphoproliferative disorder (PTLD) was also observed with use of antithymocyte immunoglobulin, OKT3, belatacept, CNIs [9,10,50,106,121,138]. Mycophenolate has not been linked to PTLD while for mTOR inhibitors the data have been inconclusive. As mTOR signalling pathways were shown to be activated in PTLD cases, protective effects were proposed for mTOR-inhibition in PTLD. However, recent studies reported slightly increased PTLD incidences during maintenance therapy with mTOR-I-based immunosuppression [138].

CNS infection

All immunosuppressive medications are associated with an increased rate of opportunistic infections. The presentation of CNS infection in transplant recipients can vary from that seen in normal population, as the anti-inflammatory effects of immunosuppressive therapy may obscure signs of meningeal inflammation associated with meningitis and changes in the level of consciousness may be subtle [72]. CNS infections in renal transplant recipients are associated with significant mortality and morbidity, which makes understanding of the need of special

methods for detection and isolation of pathogens extremely important.

Opportunistic bacterial infections include pathogens such as: *Legionella*, *Nocardia*, *Mycobacterium tuberculosis* and *Listeria monocytogenes*. The involved fungal organisms are often: *Cryptococcus neoformans*, *Aspergillus fumigatus*, *Candida*, *Pneumocystis carinii*. Common viruses include *Cytomegalovirus* (CMV), Varicella-Zoster virus and Epstein-Barr virus (EBV), Herpes viruses 1 and 2 (HSV 1 and 2) and BK/JC polyoma virus are less common. Acute meningitis, usually caused by *L. monocytogenes*, subacute and chronic meningitis caused by *C. neoformans*, focal brain infections caused by *A. fumigatus, Toxoplasma gondii* or *Nocardia asteroids*, and progressive dementia caused by Polyoma J virus were reported to be the most common CNS infections in kidney transplant recipients [160].

Acute and chronic allograft rejections require higher doses of immunosuppressive drugs and thus increase the risk of CNS infection. In reports published before 2000, CNS infections complicated the post-transplant course of 5% to 10% of allograft recipients with a high mortality rate of up to 75% [47] and in autopsy series, the incidence of CNS infections was even higher, reaching 10% to 16% [122,123]. Recent reports indicate a declining incidence of CNS infections, which may be explained by declining immunosuppressive burden especially with polyclonal antibodies, doses of CNIs and steroids, and better diagnostics enabling earlier detection of the infection, and thus preventing its development into CNS infection. According to a review published in 2014, the incidence of the most common CNS infections stands approximately for: 0.1-0.2% for aspergillosis, cryptococci, fungal infection, and less than 0.05% for other infections including nocardiosis, JC virus – PML, and moulds [230]. In a prospective, nation-wide population-based study in the Netherlands [211], carried out between 2006 and 2014, in data from 68,526 patient-years of follow-up of patients after solid organ transplantation, the annual incidence of bacterial meningitis was 7-fold higher (95% confidence interval [CI]: 2.94-17.02, $p < 0.001$) for renal transplant recipients as compared with the general population (9.56 [95% CI: 3.98-22.96] vs. 1.35 [95% CI: 1.28-1.43] per 100,000 patients per year). However, overall, only 6 cases were identified, with one case with the classic presentation of bacterial meningitis (fever, neck stiffness, and change in the mental status). Seizures were more common and were seen in 33% of patients. Pathogens responsible were *Streptococcus pneumoniae* and *Listeria monocytogenes* identified in 2 patients each, and *Escherichia coli* and *Pseudomonas aeruginosa* in the remaining patients [211].

Fungal CNS infections in solid organ transplantation seem more frequent. The overall cumulative incidence during the first year after transplantation is considered to be at the level of 3% depending on the type of the organ transplanted [184]. In the decreasing order, the risk seen in transplantations stands for (incidence rate in brackets) – small bowel (11.6%), lung (8.6%), liver (4.7%), heart (4.0%), pancreas (3.4%) and kidney (1.3%). Candidiasis is the most common invasive fungal infection in SOT recipients and accounts for 50-60% infections, followed by aspergillosis accounting for 20-25% of fungal infections, then *Cryptococcus* species (6-7%), the endemic fungi (5%) and other species [148].

The CNS infection commonly results from dissemination of the systemic infection, where the lungs and gastrointestinal tract constitute common points of entry to the bloodstream. The paranasal sinuses are also critical routes of entry to the CNS, explaining, for instance, how fungal sinusitis may easily become fungal meningitis [139].

There is a correlation between time after transplantation and the organism that is most likely responsible for CNS infection [47]. In the acute perioperative period (first 30 days), the CNS infection is most likely related to nosocomial, pre-existing, or donor-related organisms. The risk of viral and fungal opportunistic infection is greatest one month post-transplantation, as immunosuppression becomes effective. Six months post-transplantation, infections reportedly result from reactivation of infections acquired earlier, opportunistic infections related to chronic immunosuppression, or common organisms found in immunocompetent patients. During the initial month, CNS infection is most often caused by common bacterial pathogens or opportunistic pathogens present in either the transplant environment (e.g. *Aspergillus* species), or host (e.g. *Mycobacterium tuberculosis*). At 1 to 6 months, there is increased susceptibility to CNS infection by the herpesviruses, especially CMV and Epstein-Barr virus (EBV), fungi, and atypical bacteria. Finally, after 6 months, reduction of immunosuppression is accompanied by decreased susceptibility to CNS infection [241].

One of the most frequent opportunistic bacteria infecting immunocompromised patients is *Legionella pneumophila*. It causes serious infection particularly in patients with impaired cellular immunity. However *Legionella* is not known as a frequent cause of CNS infections in solid organ transplant recipients [230].

Acute meningitis is usually caused by *L. monocytogenes*, subacute and chronic meningitis by *C. neoformans*, and focal brain infections by *A. fumigatus*. *L. monocytogenes*, contracted through ingestion of contaminated food, needs to be considered in transplant patients with symptoms and signs of meningoencephalitis. The classic pathogens like *Haemophilus* and *Streptococcus pneumoniae* are infrequently seen in the transplant population. Meningitis, with or without focal neurological signs, is the commonest form of CNS listeriosis; in addition, listeriosis may cause rhombencephalitis, abscesses, and even myelitis [58].

Mycobacterium is rarely implicated as a CNS pathogen in transplant patients [34]. Immunosuppression may facilitate the progression of a latent, quiescent mycobacterial infection. Pulmonary tuberculosis and atypical mycobacterial CNS infections share similar treatment algorithms. CNS infections may be exceedingly difficult to diagnose, requiring multiple lumbar punctures and polymerase chain reaction studies. Three main presentations of *M. tuberculosis* in the CNS have been described: cerebral tuberculoma, meningitis and myelopathy [192].

Nocardia asteroides is another organism that is rarely recognised in immunocompetent persons, but in transplant patients it may cause subacute or chronic meningitis as well as cerebritis. *Nocardia* infections were reported in 1% to 6% of solid organ transplant recipients and in fewer than 5% of renal transplant recipients [41,49]. In nocardiosis, pulmonary infection usually precedes CNS involvement [47]. Guillain-Barré syndrome may also develop, associated in some cases with CMV or *Campylobacter jejuni* infection [79].

Cryptococcal meningitis is the most common subacute meningitis seen in renal transplant recipients, especially in patients who are exposed to birds, and is universally fatal without treatment. Like all other fungi, cryptococci enter the body through the respiratory tract but CNS is the primary target [92,232]. Symptoms may show and disappear over time and include e.g. headaches, fever, lethargy, abnormal mental status, and coma. Elevated CSF pressure without evidence of obstructive hydrocephalus, believed to result from basilar meningitis and impaired reabsorption of CSF across arachnoid villi, was reported as an important complication of cryptococcal meningitis [92]. In a retrospective analysis of solid organ transplant recipients with cryptococcosis, it was found that 30% of them had changes in computed tomography (CT) or MR. Abnormal neuroimaging findings corresponding with the cryptococcal lesions included leptomeningeal lesions in 50% (8/16), parenchymal lesions in 37.5% (6/16), and hydrocephalus in 12.5% (2/16) [188].

It needs to be mentioned that some immunosuppressive agents (cyclosporine, tacrolimus, mTOR inhibitors) have *in vitro* activity against fungi, including *C. neoformans* [92], and its clinical relevance was confirmed by a multivariable analysis of data from a large study showing that the receipt of a CNI was independently associated with a lower mortality (adjusted HR, 0.21; $p = 0.008$) [187].

In invasive aspergillosis, CNS involvement frequently presents with altered mental status, seizures, focal neurologic deficit, with brain abscess most common location being the fronto-parietal region of the cerebral hemispheres, though the cerebellum and brainstem may also be involved. As *Aspergillus* is an angioinvasive pathogen, cerebral infarcts or haemorrhagic lesions can be found [201]. In a recent summary of a series of cases it was reported that mortality among CNS aspergillosis patients remains high, and suggested that the infection may be more common among patients with previous brain pathology [104].

Herpes virus infections are extremely common in renal transplant recipients but meningoencephalitis is a rare and potentially life-threatening complication mostly caused by HSV-1. Varicella-zoster virus, apart from varicella (chickenpox) and herpes zoster (shingles), may lead to CNS complications such as post-varicella cerebellitis, meningoencephalitis (including the Ramsay Hunt syndrome), vasculopathy, and acute aseptic meningitis. Comparing to normal population, post-transplant patients with zoster are more likely to develop post-herpetic neuralgia [241].

Cytomegalovirus (CMV) is an uncommon cause of encephalitis or Guillain-Barré syndrome in solid organ transplant [237]. Reactivated latent JC virus is found in more than 90% of patients with PML [125]. PML symptoms may include mental status changes, visual field deficits, focal neurologic deficit, while in neuroimaging single or multiple non-enhancing

white matter lesions in CT or MRI lesions most often in the parieto-occipital region are seen [241].

In post-transplant patients, EBV infection can be a primary infection or reactivation of latent infection. It can be associated with meningoencephalitis and an abnormal proliferation of lymphoid cells, causing aseptic meningitis, seizures, encephalitis, or PTLD [230,241]. Twenty-eight percent of patients with PTLD have CNS involvement, and EBV-associated PTLD may be characterized by a mental status change, hemiparesis, or other focal neurologic deficit. In neuroimaging, the focal lesion with variable enhancement can be seen and may have associated haemorrhage or leptomeningeal spread [241].

Immunocompromised kidney transplant recipients may also develop other opportunistic infections, like parasite infections, although rarely affecting the nervous system [241]. Toxoplasmosis is an example with CNS involvement occurring very rarely. In a long, multicentre, matched case-control study in Spain, toxoplasmosis developed in 0.14% of solid organ transplant recipients and toxoplasma-related brain abscesses or meningitis developed in approx. 25% of those very few cases [69].

Future considerations

Organ transplantation is one of the most dynamic fields in medicine and continuously improving outcomes have been achieved in the field of renal transplantation. A significant reduction in acute rejection has been attained at many renal transplant centres using contemporary immunosuppressive therapy. Long-term use of these drugs has been associated with the development of chronic allograft nephropathy and other adverse events. The common neurologic complications such as stroke, encephalopathy, behavioural disorders, neuromuscular complications, CNS *de novo* malignancies, and opportunistic infections still persist. Functional data in healthy human subjects are required to clarify the genuine CNS effects of immunosuppressants in order to be able to differentiate between these drug effects and the CNS effects of transplantation. As more patients are experiencing prolonged survival, the number of patients at risk for chronic complications is increasing, therefore personalizing the immunosuppression therapy to the individual needs of the patient may be favourable. The perfect immunosuppressive regimen would limit or eliminate calcineurin inhibitors neurotoxicity while providing enhanced allograft outcomes. Potential improvements to the calcineurin inhibitor class include a prolonged release tacrolimus formulation. On the other hand, PTLD risk has challenged introduction of belatacept, otherwise a promising novel solution. Moreover, new immunosuppressive agents which eliminate these issues are desirable. As the field of organ transplantation continues to evolve, research should be conducted to create suitable drugs that sustain immunotolerance in transplantation medicine, eliminating the previously mentioned adverse effects.

Disclosure

Authors report no conflict of interest.

References

1. Abedini S, Holme I, Fellström B, Jardine A, Cole E, Maes B, Holdaas H; ALERT Study Group. Cerebrovascular events in renal transplant recipients. Transplantation 2009; 87: 112-117.
2. Abelaira HM, Réus GZ, Neotti MV, Quevedo J. The role of mTOR in depression and antidepressant responses. Life Sci 2014; 101: 10-14.
3. Abramowicz D, De Pauw L, Le Moine A, Sermon F, Surquin M, Doutrelepont JM, Ickx B, Depierreux M, Vanherweghem JL, Kinnaert P, Goldman M, Vereerstraeten P. Prevention of OKT3 nephrotoxicity after kidney transplantation. Kidney Int Suppl 1996; 53: S39-43.
4. Adams HP Jr, Dawson G, Coffman TJ, Corry RJ. Stroke in renal transplant recipients. Arch Neurol 1986; 43: 113-115.
5. Ahmed S, Ahmed E, Naqvi R, Qureshi S. Evaluation of contributing factors of post transplant erythrocytosis in renal transplant patients. J Pak Med Assoc 2012; 62: 1326-1329.
6. Ahsan N, Johnson C, Gonwa T, Halloran P, Stegall M, Hardy M, Metzger R, Shield C 3rd, Rocher L, Scandling J, Sorensen J, Mulloy L, Light J, Corwin C, Danovitch G, Wachs M, VanVeldhuisen P, Salm K, Tolzman D, Fitzsimmons WE. Randomized trial of tacrolimus plus mycophenolate mofetil or azathioprine versus cyclosporine oral solution (modified) plus mycophenolate mofetil after cadaveric kidney transplantation: results at 2 years. Transplantation 2001; 72: 245-250.
7. Aksamit AJ, Ellingson RJ, Sharbrough FW, Westmoreland BF, Pfeiffer RF, Steg RE, de Groen PC. Epileptiform electroencephalographic abnormalities in liver transplant recipients. Ann Neurol 1991; 30: 37-41.
8. Albring A, Wendt L, Harz N, Engler H, Wilde B, Witzke O, Schedlowski M. Short-term treatment with the calcineurin inhibitor cyclosporine A decreases HPA axis activity and plasma noradrenaline levels in healthy male volunteers. Pharmacol Biochem Behav 2014; 126: 73-76.
9. Alemtuzumab, Summary of Product Characteristics, 2011, http://www.ema.europa.eu/ docs/en_GB/document_library/ EPAR_-_Product_Information/human/000353/ WC500025270.pdf.

10. Al-Mansour Z, Nelson BP, Evens AM. Post-transplant lymphoproliferative disease (PTLD): risk factors, diagnosis, and current treatment strategies. Curr Hematol Malig Rep 2013; 8: 173-183.
11. Anghel D, Tanasescu R, Campeanu A, Lupescu I, Podda G, Bajenaru O. Neurotoxicity of immunosuppressive therapies in organ transplantation. Maedica (Buchar) 2013; 8: 170-175.
12. Anil Kumar MS, Irfan Saeed M, Ranganna K, Malat G, Sustento-Reodica N, Kumar AM, Meyers WC. Comparison of four different immunosuppression protocols without long-term steroid therapy in kidney recipients monitored by surveillance biopsy: five-year outcomes. Transpl Immunol 2008; 20: 32-42.
13. Arnold R, Pussell BA, Pianta TJ, Lin CS, Kiernan MC, Krishnan AV. Association between calcineurin inhibitor treatment and peripheral nerve dysfunction in renal transplant recipients. Am J Transplant 2013; 13: 2426-2432.
14. Atamaz F, Hepgüler S, Karasu Z, Kilic M. Meralgia paresthetica after liver transplantation: a case report. Transplant Proc 2005; 37: 4424-4425.
15. Azathioprine Summary of Product Characteristics 2016; http://www.medicines.org.uk/emc/medicine/29130/SPC/Azathioprine+50+mg+Tablets.
16. Bakshi R, Bates VE, Mechtler LL, Kinkel PR, Kinkel WR. Occipital lobe seizures as the major clinical manifestation of reversible posterior leukoencephalopathy syndrome: magnetic resonance imaging findings. Epilepsia 1998; 39: 295-299.
17. Barnett AN, Asgari E, Chowdhury P, Sacks SH, Dorling A, Mamode N. The use of eculizumab in renal transplantation. Clin Transplant 2013; 27: E216-29.
18. Barnett AN, Hadjianastassiou VG, Mamode N. Rituximab in renal transplantation. Transpl Int 2013; 26: 563-575.
19. Bart H, Malik SA International Report About Kidney Diseases in 4 European Countries; www.nvn.nl 20153.
20. Basiliximab, Summary of Product Characteristics 2008, http://www.ema.europa.eu/ docs/en_GB/document_library/EPAR_-_Product_Information/human/000207/ WC500053543.pdf.
21. Basso G, Cristelli M, Bichuetti D, Franco M, Baptista A, Sandes-Freitas T, Gusuma L, Gomes P, Tedesco H, Medina-Pestana J. Major Neurological Complications Following Renal Transplantation [abstract]. Am J Transplant 2013; 13 Suppl 5.
22. Becker H, Reichert JM. MuromonabCD3 (Orthoclone OKT®3). In: Handbook of Therapeutic Antibodies. Dübel S, Reichert JM (eds.). WileyVCH Verlag GmbH & Co. KGaA, Weinheim, Germany 2014.
23. Belatacept Summary of Product Characteristics 2014; https://ec.europa.eu/health/documents/community-register/2014/20141216130471/anx_130471_en.pdf.
24. Benchstein WO. Neurotoxicity of calcineurin inhibitors: impact and clinical management. Transplant Int 2000; 13: 313-326.
25. Berger JR, Neltner J, Smith C, Cambi F. Posterior reversible encephalopathy syndrome masquerading as progressive multifocal leukoencephalopathy in rituximab treated neuromyelitis optica. Mult Scler Relat Disord 2014; 3: 728-731.
26. Besenski N, Rumboldt Z, Emovon O, Nicholas J, Kini S, Milutinovic J, Budisavljevic MN. Brain MR imaging abnormalities in kidney transplant recipients. Am J Neuroradiol 2005; 26: 2282-2289.
27. Bianco F, Fattapposta F, Locuratolo N, Pierallini A, Rossi M, Ruberto F, Bozzao L. Reversible diffusion MRI abnormalities and transient mutism after liver transplantation. Neurology 2004; 62: 981-983.
28. Bird GL, Meadows J, Goka J, Polson R, Williams R. Cyclosporin-associated akinetic mutism and extrapyramidal syndrome after liver transplantation. J Neurol Neurosurg Psych 1990; 53: 1068-1071.
29. Bodziak KA, Hricik DE. New-onset diabetes mellitus after solid organ transplantation. Transpl Int 2009; 22: 519-530.
30. Bolton CF, Young GB, Zochodne DW. The neurological complications of sepsis. Ann Neurol 1993; 33: 94-100.
31. Bouguen G, Evans E, Sandborn WJ. Azathioprine-induced neuropsychiatric disorders. J Crohns Colitis 2014; 8: 180.
32. Bowyer SL, LaMothe MP, Hollister JR. Steroid myopathy: incidence and detection in a population with asthma. J Allergy Clin Immunol 1985; 76: 234-242.
33. Breil M, Chariot P. Muscle disorders associated with cyclosporine treatment. Muscle Nerve 1999; 22: 1631-1636.
34. Bronster DJ, Emre S, Boccagni P, Sheiner PA, Schwartz ME, Miller CM. Central nervous system complications in liver transplant recipients – incidence, timing and long-term follow-up. Clin Transplantation 2000; 14: 1-7.
35. Bürker BS, Gullestad L, Gude E, Relbo Authen A, Grov I, Hol PK, Andreassen AK, Arora S, Dew MA, Fiane AE, Haraldsen IR, Malt UF, Andersson S. Cognitive function after heart transplantation: Comparing everolimus-based and calcineurin inhibitor-based regimens. Clin Transplant 2017; 31: e12927.
36. Campellone JV, Lacomis D, Kramer DJ, Van Cott AC, Giuliani MJ. Acute myopathy after liver transplantation. Neurology 1998; 50: 46-53.
37. Campellone JV, Lacomis D. Neuromuscular disorders. In: Wijdicks EFM (Hrsg). Neurologic complications in organ transplant recipients. Butterworth Heinemann, Boston 1999; 169-192.
38. Cejka D, Hayer S, Niederreiter B, Sieghart W, Fuereder T, Zwerina J, Schett G. Mammalian target of rapamycin signaling is crucial for joint destruction in experimental arthritis and is activated in osteoclasts from patients with rheumatoid arthritis. Arthritis Rheum 2010; 62: 2294-2302.
39. Chadban SJ, Barraclough KA, Campbell SB, Clark CJ, Coates PT, Cohney SJ, Cross NB, Eris JM, Goodman D, Henderson L, Howell MR, Isbel NM, Kanellis J, Kotwal SS, Manley P, Masterson R, Mulley W, Murali K, O'Connell P, Pilmore H, Pussell B, Rogers N, Russ GR, Walker RG, Webster AC, Wiggins KJ, Wong G, Wyburn KR. The Kidney Health Australia-Caring for Australasians with Renal Impairment (KHA-CARI) Guidelines: KHA-CARI adaptation of the KDIGO Clinical Practice Guideline for the Care of Kidney Transplant Recipients. Nephrology 2012; 17: 204-214.
40. Chang SH, Lim CS, Low TS, Chon HT, Tan SY. Cyclosporine associated encephalopathy: a case report and literature review. Transplant Proc 2001; 8: 3700-3701.
41. Chapman SW, Wilson JP. Nocardiosis in transplant recipients. Semin Respir Infect 1990; 5: 74.
42. Chen SR, Hu YM, Chen H, Pan HL. Calcineurin inhibitor induces pain hypersensitivity by potentiating pre- and postsynaptic NMDA receptor activity in spinal cords. J Physiol 2014; 592: 215-227.

43. Chtioui H, Zimmermann A, Dufour JF. Unusual evolution of posterior reversible encephalopathy syndrome (PRES) one year after liver transplantation. Liver Transpl 2005; 11: 588-590.
44. Ciriaco M, Ventrice P, Russo G, Scicchitano M, Mazzitello G, Scicchitano F, Russo E. Corticosteroid-related central nervous system side effects. J Pharmacol Pharmacother 2013; 4 Suppl 1: S94-98.
45. Collini A, De Bartolomeis C, Barni R, Ruggieri G, Bernini M, Carmellini M. Calcineurin-inhibitor induced pain syndrome after organ transplantation. Kidney Int 2006; 70: 1367-1370.
46. Collins MH, Montone KT, Leahey AM, Hodinka RL, Salhany KE, Belchis DA, Tomaszewski JE. Autopsy pathology of pediatric posttransplant lymphoproliferative disorder. Pediatrics 2001; 107: E89.
47. Conti DJ, Rubin RH. Infection of the central nervous system in organ transplant recipients. Neurol Clin 1988; 6: 241-260.
48. Coplin WM, Cochran MS, Levine SR, Crawford SW. Stroke after bone marrow transplantation: frequency, aetiology and outcome. Brain 2001; 124: 1043-1051.
49. Coussement J, Lebeaux D, van Delden C, Guillot H, Freund R, Marbus S, Melica G, Van Wijngaerden E, Douvry B, Van Laecke S, Vuotto F, Tricot L, Fernández-Ruiz M, Dantal J, Hirzel C, Jais JP, Rodriguez-Nava V, Lortholary O, Jacobs F; European Study Group for Nocardia in Solid Organ Transplantation. Nocardia Infection in Solid Organ Transplant Recipients: A Multicenter European Case-control Study. Clin Infect Dis 2016; 63: 338-345.
50. Curtis RE, Travis LB, Rowlings PA, Socié G, Kingma DW, Banks PM, Jaffe ES, Sale GE, Horowitz MM, Witherspoon RP, Shriner DA, Weisdorf DJ, Kolb HJ, Sullivan KM, Sobocinski KA, Gale RP, Hoover RN, Fraumeni JF Jr, Deeg HJ. Risk of lymphoproliferative disorders after bone marrow transplantation: a multi-institutional study. Blood 1999; 94: 2208–2216.
51. Cyclophosphamide Summary of Product Characteristics 2014; https://www.medicines.org.uk/emc/medicine/29593 (Acces: 21.05.2017).
52. Dawson FM. Immunosoppressants, immunophilins and the nervous system. Ann Neurol 1996; 40: 559-560.
53. de Groen PC, Aksamit AJ, Rakela J, Forbes GS, Krom RA. Central nervous system toxicity after liver transplantation. Role of cyclosporine and cholesterol. N Engl J Med 1987; 317: 861-866.
54. de Paula MI, Medina Pestana JO, Nicolau Ferreira A, Pontello Cristelli M, Fabiano Franco M, Aguiar WF, Tedesco-Silva H, Rosso Felipe C. Long-Term Follow-Up of De Novo Use of mTOR and Calcineurin Inhibitors After Kidney Transplantation. Ther Drug Monit 2016; 38: 22-31.
55. Decramer M, Stas KJ. Corticosteroid-induced myopathy involving respiratory muscles in patients with chronic obstructive pulmonary disease or asthma. Am Rev Respir Dis 1992; 146: 800-802.
56. Dhillon SS, Sarac E. Lumbosacral plexopathy after dual kidney transplantation. Am J Kidney Dis 2000; 36: 1045-1048.
57. Dietrich J, Rao K, Pastorino S, Kesari S. Corticosteroids in brain cancer patients: benefits and pitfalls. Expert Rev Clin Pharmacol 2011; 4: 233-242.
58. Doganay M. Listeriosis: clinical presentation. FEMS Immunol Med Microbiol 2003; 35: 173-175.
59. Draper HM. Depressive disorder associated with mycophenolate mofetil. Pharmacotherapy 2008; 28: 136-139.
60. Eberlein WR, Bongiovanni AM, Rodriguez CS. Diagnosis and treatment: the complications of steroid treatment. Pediatrics 1967; 40: 279-282.
61. Eckhard M, Schindler RA, Renner FC, Schief W, Padberg W, Weimer R, Bretzel RG, Brendel MD. New-onset diabetes mellitus after renal transplantation. Transplant Proc 2009; 41: 2544-2545.
62. Eculizumab Summary of Product Characteristics 2012ł http://www.ema.europa.eu/docs/en_GB/document_library/EPAR__Product_Information/human/000791/WC500054208.pdf.
63. Eidelman BH, Abu-Elmagd K, Wilson J, Fung JJ, Alessiani M, Jain A, Takaya S, Todo SN, Tzakis A, Van Thiel D, Shannon W, Starzl TE. Neurologic complications of FK 506. Transplant Proc 1991; 23: 3175-3178.
64. Ekberg H, Tedesco-Silva H, Demirbas A, Vítko S, Nashan B, Gürkan A, Margreiter R, Hugo C, Grinyó JM, Frei U, Vanrenterghem Y, Daloze P, Halloran PF, ELITE-Symphony Study. Reduced exposure to calcineurin inhibitors in renal transplantation. N Engl J Med 2007; 357: 2562-2575.
65. Ellul-Micallef R, Fenech FF. Effect of intravenous prednisolone in asthmatics with diminished adrenergic responsiveness. Lancet 1975; 2: 1269-1271.
66. Eugui EM, Almquist SJ, Muller CD, Allison AC. Lymphocyte-selective cytostatic and immunosuppressive effects of mycophenolic acid in vitro: role of deoxyguanosine nucleotide depletion. Scand J Immunol 1991; 33: 161-173.
67. Fallon B, Rayhill S. Ranal Transplantation: Surgical Procedure and Complications. In: Dreger D (ed.). Hospital Physician Urology Board Review Manual. Turner White Communications, Inc., Wayne 2004; 2-12.
68. FDA Department of Health and Human Services Belatacept BLA Approval Letter 2011; https://www.accessdata.fda.gov/drugsatfda_docs/appletter/2011/125288s000ltr.pdf.
69. Fernàndez-Sabé N, Cervera C, Fariñas MC, Bodro M, Muñoz P, Gurguí M, Torre-Cisneros J, Martín-Dávila P, Noblejas A, Len O, García-Reyne A, Del Pozo JL, Carratalà J. Risk factors, clinical features, and outcomes of toxoplasmosis in solid-organ transplant recipients: a matched case-control study. Clin Infect Dis 2012; 54: 355-361.
70. Fessler RG, Johnson DL, Brown FD, Erickson RK, Reid SA, Kranzler L. Epidural lipomatosis in steroid-treated patients. Spine 1992; 17: 183-188.
71. Findlay MD, Thomson PC, MacIsaac R, Jardine AG, Patel RK, Stevens KK, Rutherford E, Clancy M, Geddes CC, Dawson J, Mark PB. Risk factors and outcome of stroke in renal transplant recipients. Clin Transplant 2016; 30: 918-924.
72. Fishman JA, Rubin RH. Infection in organ-transplant recipients. N Engl J Med 1998; 338: 1741-1751.
73. Flynn JT, Bunchman TE, Sherbotie JR. Indications, results, and complications of tacrolimus conversion in pediatric renal transplantation. Pediatr Transplant 2001; 5: 439-446.
74. Furukawa M, Terae S, Chu BC, Kaneko K, Kamada H, Miyasaka K. MRI in seven cases of Tacrolimus FK 506 encephalopathy: utility of flair and diffusion-weighted imaging. Neuroradiology 2001; 43: 615-621.

75. Gill D, Juffs HG, Herzig KA, Brown AM, Hawley CM, Cobcroft RG, Petrie JJ, Marlton P, Kennedy G, Thomson DB, Campbell SB, Nicol DL, Norris D, Johnson DW. Durable and high rates of remission following chemotherapy in posttransplantation lymphoproliferative disorders after renal transplantation. Transpl Proc 2003; 35: 256-257.
76. Giunzioni I, Tavori H. New developments in atherosclerosis: clinical potential of PCSK9 inhibition. Vasc Health Risk Manag 2015; 11: 493-501.
77. Goldstein LS, Haug MT 3rd, Perl J 2nd, Perl MK, Maurer JR, Arroliga AC, Mehta AC, Kirby T, Higgins B, Stillwell PC. Central nervous system complications after lung transplantation. J Heart Lung Transplant 1998; 17: 185-191.
78. Griffiths PD, Clark DA, Emery VC. Betaherpesviruses in transplant recipients. J Antimicrob Chemother 2000; 45 Suppl T3: 29-34.
79. Grygorczuk S, Zajkowska J, Kondrusik M, Pancewicz S, Hermanowska-Szpakowicz T. Guillain-Barré syndrome and its association with infectious factors. Neurol Neurochir Pol 2005; 39: 230-236.
80. Guertin DA, Sabatini DM. The pharmacology of mTOR inhibition. Sci Signal 2009; 2: pe24.
81. Habibeh O, Elsayad K, Kriz J, Haverkamp U, Eich HT. Post-transplant lymphoproliferative disorder in the pelvis successfully treated with consolidative radiotherapy. Strahlenther Onkol 2017; 193: 80-85.
82. Halloran P, Kung L, Noujaim J. Calcineurin and the biological effect of cyclosporine and tacrolimus. Transplant Proc 1998; 30: 2167-2170.
83. Halloran PF. Immunosuppressive drugs for kidney transplantation. N Engl J Med 2004; 351: 2715-2729.
84. Hardinger KL, Brennan DC. Novel immunosuppressive agents in kidney transplantation. World J Transplant 2013; 3: 68-77.
85. Heitman J, Movva NR, Hall MN. Targets for cell cycle arrest by the immunosuppressant rapamycin in yeast. Science 1991; 253: 905-909.
86. Hellemans R, Bosmans JL, Abramowicz D. Induction Therapy for Kidney Transplant Recipients: Do We Still Need Anti-IL2 Receptor Monoclonal Antibodies? Am J Transplant 2017; 17: 22-27.
87. Hill P, Cross NB, Barnett AN, Palmer SC, Webster AC. Polyclonal and monoclonal antibodies for induction therapy in kidney transplant recipients. Cochrane Database Syst Rev 2017; 1: CD004759.
88. Hinchey J, Chaves C, Appignani B, Breen J, Pao L, Wang A, Pessin MS, Lamy C, Mas JL, Caplan LR. A reversible posterior leukoencephalopathy syndrome. N Engl J Med 1996; 334: 494-500.
89. Holdaas H, Potena L, Saliba F. mTOR inhibitors and dyslipidemia in transplant recipients: a cause for concern? Transplant Rev (Orlando) 2015; 29: 93-102.
90. Hopkins S, Jolles S. Drug-induced aseptic meningitis. Expert Opin Drug Saf 2005; 4: 285-297.
91. Huberlant V, Cosnard G, Hantson PE. Brain death in a septic patient: possible relationship with posterior reversible encephalopathy syndrome? Anaesth Intensive Care 2009; 37: 1017-1020.
92. Husain S, Wagener MM, Singh N. Cryptococcus neoformans infection in organ transplant recipients: variables influencing clinical characteristics and outcome. Emerg Infect Dis 2001; 7: 375-381.
93. Illsinger S, Janzen N, Lücke T, Bednarczyk J, Schmidt KH, Hoy L, Sander J, Das AM. Cyclosporine A: impact on mitochondrial function in endothelial cells. Clin Transplant 2011; 25: 584-593.
94. Inoha S, Inamura T, Nakamizon A, Ikezaki K, Amono T, Fukui M. Magnetic resonance imaging in cases with encephalopathy secondary to immunosuppressive agents. J Clin Neurosci 2002; 9: 305-307.
95. Jaffe ES, Harris NL, Stein H. In: Pathology and Genetics of Tumor and Haematopoietic Tissues. Jaffe ES (ed.). World Health Organization Classification of Tumors. IARC Press: Oxford University Press, Lyon 2001; 264-270.
96. Johnson CK, Leca N. Eculizumab use in kidney transplantation. Curr Opin Organ Transplant 2015; 20: 643-651.
97. Kahan BD. Role of cyclosporine: present and future. Transplant Proc 1994; 26: 3082-3087.
98. Kalluri HV, Hardinger KL. Current state of renal transplant immunosuppression: Present and future. World J Transplant 2012; 2: 51-68.
99. Kapur S, Jones WG 2nd, Barber AE, Minei JP, Fahey TJ 3rd, Shires GT 3rd, Shires GT. Effect of cyclosporine on adrenocortical response to injury and infection. J Surg Res 1992; 53: 357-361.
100. Kazory A, Ducloux D. Acquired hypercoagulable state in renal transplant recipients. Thromb Haemost 2004; 91: 646-654.
101. Kidney Disease: Improving Global Outcomes (KDIGO) Transplant Work Group. KDIGO clinical practice guideline for the care of kidney transplant recipients. Am J Transplant 2009; 9 Suppl 3: S1-155.
102. Klawitter J, Gottschalk S, Hainz C, Leibfritz D, Christians U, Serkova NJ. Immunosuppressant neurotoxicity in rat brain models: oxidative stress and cellular metabolism. Chem Res Toxicol 2010; 23: 608-619.
103. Klawitter J, Nashan B, Christians U. Everolimus and sirolimus in transplantation-related but different. Expert Opin Drug Saf 2015; 14: 1055-1070.
104. Kourkoumpetis TK, Desalermos A, Muhammed M, Mylonakis E. Central nervous system aspergillosis: a series of 14 cases from a general hospital and review of 123 cases from the literature. Medicine (Baltimore) 2012; 91: 328-336.
105. Krishnan AV, Lin CS, Kiernan MC. Activity-dependent excitability changes suggest Na+/K+ pump dysfunction in diabetic neuropathy. Brain 2008; 131: 1209-1216.
106. Kumar A, Shrestha BM. Evolution of Immunosuppressive Agents in Renal Transplantation: An Updated Review. Int J Stem Cell Res Transplant 2016; 04(3): 158-172.
107. Lacomis D, Petrella JT, Giuliani MJ. Causes of neuromuscular weakness in the intensive care unit: a study of ninety-two patients. Muscle Nerve 1998; 21: 610-617.
108. Lai S, Mecarelli O, Pulitano P, Romanello R, Davi L, Zarabla A, Mariotti A, Carta M, Tasso G, Poli L, Mitterhofer AP, Testorio M, Frassetti N, Aceto P, Galani A, Lai C. Neurological, psychological, and cognitive disorders in patients with chronic kidney disease on conservative and replacement therapy. Medicine (Baltimore) 2016; 95: e5191.

109. Lake KD, Canafax DM. Important interactions of drugs with immunosuppressive agents used in transplant recipients. J Antimicrob Chemother 1995; 36: 11-22.
110. Lamy C, Oppenheim C, Meder JF, Mas JL. Neuroimaging in posterior reversible encephalopathy syndrome. J Neuroimaging 2004; 14: 89-96.
111. Lang UE, Heger J, Willbring M, Domula M, Matschke K, Tugtekin SM. Immunosuppression using the mammalian target of rapamycin (mTOR) inhibitor everolimus: pilot study shows significant cognitive and affective improvement. Transplant Proc 2009; 41: 4285-4288.
112. Larsen CP, Pearson TC, Adams AB, Tso P, Shirasugi N, Strobert E, Anderson D, Cowan S, Price K, Naemura J, Emswiler J, Greene J, Turk LA, Bajorath J, Townsend R, Hagerty D, Linsley PS, Peach RJ. Rational development of LEA29Y (belatacept), a high-affinity variant of CTLA4-Ig with potent immunosuppressive properties. Am J Transplant 2005; 5: 443-453.
113. Lee M, Doolabh VB, Mackinnon SE, Jost S. FK506 promotes functional recovery in crushed rat sciatic nerve. Muscle Nerve 2000; 23: 633-640.
114. Legendre C, Sberro-Soussan R, Zuber J, Rabant M, Loupy A, Timsit MO, Anglicheau D. Eculizumab in renal transplantation. Transplant Rev (Orlando) 2013; 27: 90-92.
115. Leist M, Nicotera P. Apoptosis, excitotoxicity, and neuropathology. Exp Cell Res 1998; 239: 183-201.
116. Liu J, Liu D, Li J, Zhu L, Zhang C, Lei K, Xu Q, You R. Efficacy and Safety of Everolimus for Maintenance Immunosuppression of Kidney Transplantation: A Meta-Analysis of Randomized Controlled Trials. PLoS One 2017; 12: e0170246.
117. Liu LS, Li J, Chen XT, Zhang HX, Fu Q, Wang HY, Xiong YY, Liu S, Liu XM, Li JL, Huang M, Wang CX. Comparison of tacrolimus and cyclosporin A in CYP3A5 expressing Chinese de novo kidney transplant recipients: a 2-year prospective study. Int J Clin Pract Suppl 2015; 183: 43-52.
118. Llaurador G, McLaughlin L, Wistinghausen B. Management of post-transplant lymphoproliferative disorders. Curr Opin Pediatr 2017; 29: 34-40.
119. Luzzio CC, Waclawik AJ, Gallagher CL, Knechtle SJ. Iliac artery pseudoaneurysm following renal transplantation presenting as lumbosacral plexopathy. Transplantation 1999; 67: 1077-1078.
120. Margreiter R. Efficacy and safety of tacrolimus compared with ciclosporin microemulsion in renal transplantation: a randomised multicentre study. Lancet 2002; 359: 741-766.
121. Martin ST, Powell JT, Patel M, Tsapepas D. Risk of posttransplant lymphoproliferative disorder associated with use of belatacept. Am J Health Syst Pharm 2013; 70: 1977-1983.
122. Martinez AJ. The neurology and neuropathology of hepatobiliary and pancreatic transplantation. In: Handbook of Clinical Neurology. Goetz CG, Aminoff MJ (eds.). Systemic diseases, Part II. Elsevier, Amsterdam 1998; 249-266.
123. Martinez AJ. The neuropathology of organ transplantation: comparison and contrast in 500 patients. Pathol Res Pract 1998; 194: 473-486.
124. McAlister VC, Peltekian KM, Malatjalian DA, Colohan S, MacDonald S, Bitter-Suermann H, MacDonald AS. Orthotopic liver transplantation using low dose tacrolimus and sirolimus. Liver Transpl 2001; 7: 701-708.
125. McGuire D, Barhite S, Hollander H, Miles M. JC virus DNA in cerebrospinal fluid of human immunodeficiency virus-infected patients: Predictive value for progressive multifocal leukoencephalopathy. Ann Neurol 1995; 37: 395-399. Published erratum in Ann Neurol 37: 687, 1995.
126. McTaggart S. The CARI guidelines. Calcineurin inhibitors in paediatric renal transplantation. Nephrology (Carlton) 2007; 12 Suppl 1: S106-110.
127. Mele TS, Halloran PF. The use of mycophenolate mofetil in transplant recipients. Immunopharmacology 2000; 47: 215-245.
128. Meregalli C. An Overview of Bortezomib-Induced Neurotoxicity. Toxics 2015; 3: 294-303.
129. Michael M, Minard CG, Kale AS, Brewer ED. Outcomes of two-drug maintenance immunosuppression for pediatric renal transplantation: 10-yr follow-up in a single center. Pediatr Transplant 2016; 20: 49-58.
130. Mignat C. Clinically significant drug interactions with new immunosuppressive agents. Drug Safety 1997; 16: 267-278.
131. Moes DJ, Guchelaar HJ, de Fijter JW. Sirolimus and everolimus in kidney transplantation. Drug Discov Today 2015; 20: 1243-1249.
132. Mogyoros I, Bostock H, Burke D. Mechanisms of paresthesias arising from healthy axons. Muscle Nerve 2000; 23: 310-320.
133. Morscio J, Tousseyn T. Recent insights in the pathogenesis of post-transplantation lymphoproliferative disorders. World J Transplant 2016; 6: 505-516.
134. Moskowitz A, Nolan C, Lis E, Castro-Malaspina H, Perales MA. Posterior reversible encephalopathy syndrome due to sirolimus. Bone Marrow Transplant 2007; 39: 653-654.
135. Mourad G, Garrigue V, Squifflet JP, Besse T, Berthoux F, Alamartine E, Durand D, Rostaing L, Lang P, Baron C, Glotz D, Antoine C, Vialtel P, Romanet T, Lebranchu Y, Al Najjar A, Hiesse C, Potaux L, Merville P, Touraine JL, Lefrancois N, Kessler M, Renoult E, Pouteil-Noble C, Cahen R, Legendre C, Bedrossian J, Le Pogamp P, Rivalan J, Olmer M, Purgus R, Mignon F, Viron B, Charpentier B. Induction versus noninduction in renal transplant recipients with tacrolimus-based immunosuppression. Transplantation 2001; 72: 1050-1055.
136. Mueller AR, Platz KP, Bechstein WO, Schattenfroh N, Stoltenburg-Didinger G, Blumhardt G, Christe W, Neuhaus P. Neurotoxicity after orthotopic liver transplantation. A comparison between cyclosporine and FK506. Transplantation 1994; 58: 155-170.
137. Mycophenolate mofetil Summary of Product Characteristics 2006; http://www.ema.europa.eu/docs/en_GB/document_library/EPAR_-_Product_Information/human/000082/WC500021864.pdf.
138. Mynarek M, Schober T, Behrends U, Maecker-Kolhoff B. Post-transplant lymphoproliferative disease after pediatric solid organ transplantation. Clin Dev Immunol 2013; 2013: 814973.
139. Nampoory MR, Khan ZU, Johny KV, Constandi JN, Gupta RK, Al-Muzairi I, Samhan M, Mozavi M, Chugh TD. Invasive fungal infections in renal transplant recipients. J Infect 1996; 33: 95-101.
140. Nankivell BJ, Lau SG, Chapman JR, O'Connell PJ, Fletcher JP, Allen RD. Progression of macrovascular disease after transplantation. Transplantation 2000; 69: 574-581.

141. Nasser SA, Elmallah AI, Sabra R, Khedr MM, El-Din MM, El-Mas MM. Blockade of endothelin ET(A), but not thromboxane, receptors offsets the cyclosporine-evoked hypertension and interrelated baroreflex and vascular dysfunctions. Eur J Pharmacol 2014; 727: 52-59.
142. Nichols RA, Suplick GR, Brown JM. Calcineurin-mediated protein dephosphorylation in brain nerve terminals regulates the release of glutamate. J Biol Chem 1994; 269: 23817-23823.
143. Nishiguchi T, Mochizuki K, Shakudo M, Takeshita T, Hino M, Inoue Y. CNS Complications of Hematopoietic Stem Cell Transplantation. AJR 2009; 192: 1003-1011.
144. Oliveras A, Roquer J, Puig JM, Rodríguez A, Mir M, Orfila MA, Masramon J, Lloveras J. Stroke in renal transplant recipients: epidemiology, predictive risk factors and outcome. Clin Transplant 2003; 17: 1-8.
145. Opelz G, Döhler B; Collaborative Transplant Study. Influence of immunosuppressive regimens on graft survival and secondary outcomes after kidney transplantation. Transplantation 2009; 87: 795-802.
146. Ozdemir FN, Akgul A, Altunoglu A, Bilgic A, Arat Z, Haberal M. The association between cytomegalovirus infection and atherosclerotic events in renal transplant recipients. Transplant Proc 2007; 39: 990-992.
147. Papachristou E, Papadimitropoulos A, Kotsantis P, Goumenos DS, Katsoris PG, Vlachojannis JG. Cyclosporine induces endothelin-1 mRNA synthesis and nitric oxide production in human proximal tubular epithelial cell cultures. Ren Fail 2009; 31: 372-376.
148. Pappas PG, Alexander BD, Andes DR, Hadley S, Kauffman CA, Freifeld A, Anaissie EJ, Brumble LM, Herwaldt L, Ito J, Kontoyiannis DP, Lyon GM, Marr KA, Morrison VA, Park BJ, Patterson TF, Perl TM, Oster RA, Schuster MG, Walker R, Walsh TJ, Wannemuehler KA, Chiller TM. Invasive fungal infections among organ transplant recipients: results of the Transplant-Associated Infection Surveillance Network (TRANSNET). Clin Infect Dis 2010; 50: 1101-1111.
149. Parvex P, Pinsk M, Bell LE, O'Gorman AM, Patenoude YG, Gupta IR. Reversible encephalopathy associated with tacrolimus in pediatric renal transplant. Pediatr Nephrol 2001; 16: 537-542.
150. Patchell RA. Neurological complications of organ transplantation. Ann Neurol 1994; 36: 688-703.
151. Paya CV, Fung JJ, Nalesnik MA, Kieff E, Green M, Gores G, Habermann TM, Wiesner PH, Swinnen JL, Woodle ES, Bromberg JS. EBV-induced posttransplant lymphoproliferative disorders. ASTS/ASTP EBV PTLD Task Force and the Mayo Clinic Organized International Consensus Development Meeting. Transplantation 1999; 68: 1517-1525.
152. Penn I. Posttransplant malignancies. Transplant Proc 1999; 31: 1260-1262.
153. Penn I. Some problems with posttransplant lymphoproliferative disease. Transplantation 2000; 79: 705.
154. Pescovitz MD, Govani M. Sirolimus and mycophenolate mofetil for calcineurin-free immunosuppression in renal transplant recipients. Am J Kidney Dis 2001; 38 (4 Suppl 2): S16-21.
155. Pickhardt PJ, Siegel MJ, Hayashi RJ, Kelly M. Posttransplantation lymphoproliferative disorder in children: clinical, histopathologic and imaging features. Radiology 2000; 217: 16-25.
156. Pinho de Oliveira Ribeiro N, Rafael de Mello Schier A, Ornelas AC, Pinho de Oliveira CM, Nardi AE, Silva AC. Anxiety, depression and suicidal ideation in patients with rheumatoid arthritis in use of methotrexate, hydroxychloroquine, leflunomide and biological drugs. Compr Psychiatry 2013; 54: 1185-1189.
157. Pirsch JD, Miller J, Deierhoi MH, Vincenti F, Filo RS. A comparison of tacrolimus and cyclosporine for immunosuppression after cadaveric renal transplantation. Kidney transplant Study Group. Transplantation 1997; 63: 977.
158. Plata-Munoz JJ, Vaidya A, Fuggle SV, Friend PJ. Effect of alemtuzumab or basiliximab induction therapy on graft function and survival of kidneys from donors after cardiac death. Transpl Int 2009; 22: 1024-1027.
159. Polskie Towarzystwo Transplantacyjne, Zalecenia Dotyczące Leczenia Immunosupresyjnego Po Przeszczepieniu Narządów Unaczynionych. In: Durlik M, Zieniewicz K (ed). Fundacja Zjednoczeni dla Transplantacji, Warszawa, 2016. https://p-t-t.org/index.php/content/download/8785/128648/file/Zalecenia_immunopresyjne_2016.pdf.
160. Ponticelli C, Campise MR. Neurological complications in kidney transplant recipients. J Nephrol 2005; 18: 521-528.
161. Pontin AR, Donaldson RA, Jacobson JE. Femoral neuropathy after renal transplantation. S Afr Med J 1978; 53: 376-378.
162. Qin W, Tan CY, Huang X, Huang Z, Tao Y, Fu P. Rapamycin-induced posterior reversible encephalopathy in a kidney transplantation patient. Int Urol Nephrol 2011; 43: 913-916.
163. Qiu Y, Wang X, Fan J, Rao Z, Lu Y, Lin T. Conversion From Calcineurin Inhibitors to Mammalian Target-of-Rapamycin Inhibitors in Heart Transplant Recipients: A Meta-Analysis of Randomized Controlled Trials. Transplant Proc 2015; 47: 2952-2956.
164. Reinohs M, Straube T, Baum P, Berrouschot J, Wagner A. Recurrent reversible cerebral edema after long term immunosuppression with tacrolimus. J Neurol 2002; 249: 780-781.
165. Renard D, Gauthier T, Venetz JP, Buclin T, Kuntzer T. Late onset tacrolimus-induced life-threatening polyneuropathy in a kidney transplant recipient patient. Clin Kidney J 2012; 5: 323-326.
166. Resener M, Martin E, Zipp F, Dichgans J, Martin R. Neurological side-effects of pharmacologic corticoid therapy. Neverarzt 1996; 67: 983.
167. Reul JM, de Kloet ER. Two receptor systems for corticosterone in rat brain: microdistribution and differential occupation. Endocrinology 1985; 117: 2505-2511.
168. Reyes J, Gayowski T, Fung J, Todo S, Alessiani M, Starzl TE. Expressive dysphasia possibly related to FK506 in two liver transplant recipients. Transplantation 1990; 50: 1043-1045.
169. Rituximab, Summary of Product Characteristics 2008, http://www.ema.europa.eu/ docs/en_GB/document_library/EPAR_-_Product_Information/human/000165/ WC500025821.pdf.
170. Rodrigues-Diez R, González-Guerrero C, Ocaña-Salceda C, Rodrigues-Diez RR, Egido J, Ortiz A, Ruiz-Ortega M, Ramos AM. Calcineurin inhibitors cyclosporine A and tacrolimus induce vascular inflammation and endothelial activation through TLR4 signaling. Sci Rep 2016; 6: 27915.
171. Rowe I, Neuberger JM. Pharmacology of transplantation. In: Primer on Transplantation. Hricik D (ed.). 3rd ed. Wiley-Blackwell, American Society of Transplantation 2011.

172. Sahutoglu T, Akgul SU, Caliskan Y, Yazici H, Demir E, Kara E, Temurhan S, Savran FO, Turkmen A. Tac-MMF Versus CsA-MMF/CsA-AZA-Based Regimens in Development of De Novo Complement-Binding Anti-HLA Antibodies After Kidney Transplantation. Transplant Proc 2017; 49: 454-459.
173. Salzberg DJ, Karadsheh FF, Haririan A, Reddivari V, Weir MR. Specific management of anemia and hypertension in renal transplant recipients: influence of renin-angiotensin system blockade. Am J Nephrol 2014; 39: 1-7.
174. Satterthwaite R, Aswad S, Sunga V, Shidban H, Bogaard T, Asai P, Khetan U, Akra I, Mendez RG, Mendez R. Incidence of new-onset hypercholesterolemia in renal transplant patients treated with FK506 or cyclosporine. Transplantation 1998; 65: 446-449.
175. Schacherer D, Zeitoun M, Buttner R, Gelbmann C, Obed A, Schlitt HJ, Scholmerich J, Kirchner GI. Sirolimus-induced drug fever and ciclosporin-induced leukencephalopathia with seizures in one liver transplant recipient. World J Gastroenterol 2007; 13: 6090-6093.
176. Schiff D, Wen PY, van den Bent MJ. Neurological adverse effects caused by cytotoxic and targeted therapies. Nat Rev Clin Oncol 2009; 6: 596-603.
177. Senzolo M, Ferronato C, Burra P. Neurologic complications after solid organ transplantation. Transpl Int 2009; 22: 269-278.
178. Serkova N, Jacobsen W, Niemann CU, Litt L, Benet LZ, Leibfritz D, Christians U. Sirolimus, but not the structurally related RAD (everolimus), enhances the negative effects of cyclosporine on mitochondrial metabolism in the rat brain. Br J Pharmacol 2001; 133: 875-885.
179. Serkova N, Litt L, Leibfritz D, Hausen B, Morris RE, James TL, Benet LZ, Christians U. The novel immunosuppressant SDZ-RAD protects rat brain slices from cyclosporine-induced reduction of high-energy phosphates. Br J Pharmacol 2000; 129: 485-492.
180. Serkova NJ, Christians U, Benet LZ. Biochemical Mechanisms of Cyclosporine Neurotoxicity. Mol Interv 2004; 4: 97-107.
181. Sharma KR, Cross J, Santiago F, Ayyar DR, Burke G. Incidence of acute femoral neuropathy following renal transplant. Arch Neurol 2002; 59: 541-545.
182. Shbarou RM, Chao NJ, Morgenlander JC. Cyclosporin A-related cerebral vasculopathy. Bone Marrow Transplant 2000; 26: 801-804.
183. Sheridan PH Jr, Cheriyan A, Doud J, Dornseif SE, Montoya A, Houck J, Flisak ME, Walsh JM, Garrity ER Jr. Incidence of phrenic neuropathy after isolated lung transplantation. J Heart Lung Transplant 1995; 14: 684-691.
184. Shoham S, Marr KA. Invasive fungal infections in solid organ transplant recipients. Future Microbiol 2012; 7: 639-655.
185. Sihra TS, Nairn AC, Kloppenburg P, Lin Z, Pouzat C. A role for calcineurin (protein phosphatase-2B) in the regulation of glutamate release. Biochem Biophys Res Commun 1995; 212: 609-616.
186. Simha V, Qin S, Shah P, Smith BH, Kremers WK, Kushwaha S, Wang L, Pereira NL. Sirolimus Therapy Is Associated with Elevation in Circulating PCSK9 Levels in Cardiac Transplant Patients. J Cardiovasc Transl Res 2017; 10: 9-15.
187. Singh N, Alexander BD, Lortholary O, Dromer F, Gupta KL, John GT, del Busto R, Klintmalm GB, Somani J, Lyon GM, Pursell K, Stosor V, Munoz P, Limaye AP, Kalil AC, Pruett TL, Garcia-Diaz J, Humar A, Houston S, House AA, Wray D, Orloff S, Dowdy LA, Fisher RA, Heitman J, Wagener MM, Husain S; Cryptococcal Collaborative Transplant Study Group. Cryptococcus neoformans in organ transplant recipients: impact of calcineurin-inhibitor agents on mortality. J Infect Dis 2007; 195: 756-764.
188. Singh N, Lortholary O, Dromer F, Alexander BD, Gupta KL, John GT, del Busto R, Klintmalm GB, Somani J, Lyon GM, Pursell K, Stosor V, Munoz P, Limaye AP, Kalil AC, Pruett TL, Garcia-Diaz J, Humar A, Houston S, House AA, Wray D, Orloff S, Dowdy LA, Fisher RA, Heitman J, Wagener MM, Husain S; Cryptococcal Collaborative Transplant Study Group. Central nervous system cryptococcosis in solid organ transplant recipients: clinical relevance of abnormal neuroimaging findings. Transplantation 2008; 86: 647-651.
189. Skelton SL, Waterman AD, Davis LA, Peipert JD, Fish AF. Applying best practices to designing patient education for patients with end-stage renal disease pursuing kidney transplant. Prog Transplant 2015; 25: 77-84.
190. Sklar EM. Post-transplant neurotoxicity: what role do calcineurin inhibitors actually play? AJNR Am J Neuroradiol 2006; 27: 1602-1603.
191. Small SL, Fukui MB, Bramblett GT, Eidelman BH. Immunosuppression-induced leukoencephalopathy from tacrolimus (FK506). Ann Neurol 1996; 40: 575-580.
192. Smith JA. CNS Infections in Solid Organ Transplant Recipients. In: Hospital Physician Neurology Board Review Manual. Gallagher C (ed.). Turner White Communications, Inc., Wayne 2005; 2-15.
193. Srinivas TR, Meier-Kriesche HU. Minimizing immunosuppression, an alternative approach to reducing side effects: objectives and interim result. Clin J Am Soc Nephrol 2008; 3 Suppl 2: S101-S116.
194. Stracciari A, Guarino M. Neuropsychiatric complications of liver transplantation. Metab Brain Dis 2001; 16: 3.
195. Tedesco D, Haragsim L. Cyclosporine: a review. J Transplant 2012; 2012: 230386.
196. Tezcan H, Zimmer W, Fenstermaker R, Herzig GP, Schriber J. Severe cerebellar swelling and thrombotic thrombocytopenic purpura associated with FK506. Bone Marrow Transplant 1998; 21: 105-109.
197. Thistlethwaite JR Jr, Stuart JK, Mayes JT, Gaber AO, Woodle S, Buckingham MR, Stuart FP. Complications and monitoring of OKT3 therapy. Am J Kid Dis 1988; 11: 112-119.
198. Thorp M, DeMattos A, Bennett W, Barry J, Norman D. The effect of conversion from cyclosporine to tacrolimus on gingival hyperplasia, hirsutism and cholesterol. Transplantation 2000; 69: 1218-1220.
199. Thymoglobuline Summary of Product Characteristics, 2016; http://www.medicines.org.uk/emc/medicine/20799/SPC.
200. Tolou-Ghamari Z, Mortazavi M, Palizban A-A, Najafi M-R. The investigation of correlation between Iminoral concentration and neurotoxic levels after kidney transplantation. Adv Biomed Res 2015; 4: 59.
201. Torre-Cisneros J, Lopez OL, Kusne S, Martinez AJ, Starzl TE, Simmons RL, Martin M. CNS aspergillosis in organ transplanta-

tion: a clinicopathological study. J Neurol Neurosurg Psychiatry 1993; 56: 188-193.
202. Touhami S, Arzouk N, Darugar A, Heron E, Clarençon F, Bodaghi B, LeHoang P, Barrou B, Touitou V. Everolimus-induced posterior reversible encephalopathy syndrome and bilateral optic neuropathy after kidney transplantation. Transplantation 2014; 98: e102-104.
203. Truwit CL, Denaro CP, Lake JR, DeMarco T. MRI imaging of reversible cyclosporine A-induced neurotoxicity. AJNR Am J Neuroradiol 1991; 12: 651-659.
204. Trzepacz PT, Levenson JL, Tringali RA. Psychopharmacology and neuropsychiatric syndromes in organ transplantation. Gen Hosp Psychiatry 1991; 13: 233-245.
205. U.S. Multicenter FK506 Liver Study Group. A comparison of tacrolimus (FK 506) and cyclosporine for immunosuppression in liver transplantation. N Engl J Med 1994; 331: 1110-1115.
206. Uhr M, Holsboer F, Müller MB. Penetration of endogenous steroid hormones corticosterone, cortisol, aldosterone and progesterone into the brain is enhanced in mice deficient for both mdr1a and mdr1b P-glycoproteins. J Neuroendocrinol 2002; 14: 753-759.
207. United States Renal Data System (USRDS), annual data report; www.usrds.org.
208. van Balkom RH, van der Heijden HF, van Herwaarden CL, Dekhuijzen PN. Corticosteroid-induced myopathy of the respiratory muscles. Neth J Med 1994; 45: 114-122.
209. van der Hoeven J, Duyx J, de Langen JJ, van Royen A. Probable psychiatric side effects of azathioprine. Psychosom Med 2005; 67: 508.
210. van Sandwijk MS, Bemelman FJ, Ten Berge IJ. Immunosuppressive drugs after solid organ transplantation. Neth J Med 2013; 71: 281-289.
211. van Veen KE, Brouwer MC, van der Ende A, van de Beek D. Bacterial meningitis in solid organ transplant recipients: a population-based prospective study. Transpl Infect Dis 2016; 18: 674-680.
212. Van Veer H, Coosemans W, Pirenne J, Monbaliu D. Acute femoral neuropathy: a rare complication after renal transplantation. Transplant Proc 2010; 42: 4384-4388.
213. Victor RG, Thomas GD, Marban E, O'Rourke B. Presynaptic modulation of cortical synaptic activity by calcineurin. Proc Natl Acad Sci 1995; 92: 6269-6273.
214. Viswanathan R, Glickman L. Clonazepam in the treatment of steroid-induced mania in a patient after renal transplantation. N Engl J Med 1989; 320: 319-320.
215. Wagner M, Earley AK, Webster AC, Schmid CH, Balk EM, Uhlig K. Mycophenolic acid versus azathioprine as primary immunosuppression for kidney transplant recipients. Cochrane Database Syst Rev 2015; 12: CD007746.
216. Waiser J, Duerr M, Budde K, Rudolph B, Wu K, Bachmann F, Halleck F, Schönemann C, Lachmann N. Treatment of Acute Antibody-Mediated Renal Allograft Rejection with Cyclophosphamide. Transplantation 2016; Dec 22; doi: 10.1097/TP.0000000000001617.
217. Weick A, Chacra W, Kuchipudi A, Elbatta M, Divine G, Burmeister C, Moonka D. Incidence of cardiovascular and cerebrovascular events associated with sirolimus use after liver transplantation. Transplant Proc 2015; 47: 460-464.
218. West S, Kenedi C. Strategies to prevent the neuropsychiatric side effects of corticosteroids: a case report and review of the literature. Curr Opin Organ Transplant 2014; 19: 201-208.
219. Wijdicks EF, Torres VE, Schievink WI, Sterioff S. Cerebral hemorrhage in recipients of renal transplantation. Mayo Clin Proc 1999; 74: 1111-1112.
220. Wijdicks EF, Wiesner RH, Dahlke LJ, Krom RA. FK-506-induced neurotoxicity in liver transplantation. Ann Neurol 1994; 35: 498-501.
221. Wijdicks EF. Neurotoxicity of immunosuppressive drugs. Liver Transpl 2001; 7: 937-942.
222. Wijdicks EFM, Dahlke L, Wiesner RH. Oral cyclosporine decreases severity of neurotoxicity in liver transplant recipients. Neurology 1999; 52: 1708-1710.
223. Wijdicks EFM, Wiesner RH, Krom RAF. Neurotoxicity in liver transplant patients with cyclosporine immunosuppression. Neurology 1995; 45: 1962-1964.
224. Wilson JR, Conwit RA, Eidelman BH, Starzl T, Abu-Elmagd K. Sensorimotor neuropathy resembling CIDP in patients receiving FK506. Muscle Nerve 1994; 17: 528-532.
225. Wing MG, Moreau T, Greenwood J, Smith RM, Hale G, Isaacs J, Waldmann H, Lachmann PJ, Compston A. Mechanism of first-dose cytokine-release syndrome by CAMPATH 1-H: involvement of CD16 (FcgammaRIII) and CD11a/CD18 (LFA-1) on NK cells. J Clin Invest 1996; 98: 2819-2826.
226. Wise MG, Brannan SK, Shanfield SB, Moeller FG. Psychiatric aspects of organ transplantation. JAMA 1988; 260: 3437.
227. Wiseman AC. Immunosuppressive Medications. Clin J Am Soc Nephrol 2016; 11: 332-343.
228. Wiseman AC. Induction Therapy in Renal Transplantation: Why? What Agent? What Dose? We May Never Know. Clin J Am Soc Nephrol 2015; 10: 923-925.
229. Working Party of The British Transplant Society, Guidelines for Antibody Incompatible Transplantation. 3rd Edition, 2015; https://bts.org.uk/wp-content/uploads/2016/09/02_BTS_Antibody_Guidelines-1.pdf (Access 21.05.2017).
230. Wright AJ, Fishman JA. Central nervous system syndromes in solid organ transplant recipients. Clin Infect Dis 2014; 59: 1001-1011.
231. Wszolek ZK, Steg RE. Seizures after liver transplantation. Liver Transplant Surg 1995; 1: 334-339.
232. Wu G, Vilchez RA, Eidelman B, Fung J, Kormos R, Kusne S. Cryptococcal meningitis: an analysis among 5,521 consecutive organ transplant recipients. Transpl Infect Dis 2002; 4: 183-188.
233. Wu G, Weng FL, Balaraman V. Tacrolimus-induced encephalopathy and polyneuropathy in a renal transplant recipient. BMJ Case Rep 2013; pii: bcr2013201099.
234. Xie X, Jiang Y, Lai X, Xiang S, Shou Z, Chen J. mTOR inhibitor versus mycophenolic acid as the primary immunosuppression regime combined with calcineurin inhibitor for kidney transplant recipients: a meta-analysis. BMC Nephrol 2015; 16: 91.
235. Yakel JL. Calcineurin regulation of synaptic function: from ion channels to transmitter release and gene transcription. Trends Pharmacol Sci 1997; 18: 124-134.

236. Yamamoto T, Watarai Y, Futamura K, Okada M, Tsujita M, Hiramitsu T, Goto N, Narumi S, Takeda A, Kobayashi T. Efficacy of Eculizumab Therapy for Atypical Hemolytic Uremic Syndrome Recurrence and Antibody-Mediated Rejection Progress After Renal Transplantation With Preformed Donor-Specific Antibodies: Case Report. Transplant Proc 2017; 49: 159-162.
237. Yu JJ, Zhang Y, Wang Y, Wen ZY, Liu XH, Qin J, Yang JL. Inhibition of calcineurin in the prefrontal cortex induced depressive-like behavior through mTOR signaling pathway. Psychopharmacology (Berl) 2013; 225: 361-72.
238. Zheng JP, Cheng Z, Jiang J, Ke Y, Liu Z. Cyclosporin A upregulates ETB receptor in vascular smooth muscle via activation of mitogen-activating protein kinases and NF-κB pathways. Toxicol Lett 2015; 235: 1-7.
239. Zheng XF, Florentino D, Chen J, Crabtree GR, Schreiber SL. TOR kinase domains are required for two distinct functions, only one of which is inhibited by rapamycin. Cell 1995; 82: 121-130.
240. Zilinska Z, Sersenova M, Chrastina M, Breza J Sr, Bena L, Baltesova T, Jurcina A, Roland R, Lackova E, Cellar M, Laca L, Dedinska I. Occurrence of malignancies after kidney transplantation in adults: Slovak multicenter experience. Neoplasma 2017; 64: 311-317.
241. Zunt JR. Central nervous system infection during immunosuppression. Neurol Clin 2002; 20: 1-22.

Original paper

Folia Neuropathologica

Functional properties of different collagen scaffolds to create a biomimetic niche for neurally committed human induced pluripotent stem cells (iPSC)

Krystyna Pietrucha[1], Marzena Zychowicz[2], Martyna Podobinska[2], Leonora Buzanska[2]

[1]Department of Material and Commodity Sciences and Textile Metrology, Lodz University of Technology, Lodz, [2]Stem Cell Bioengineering Unit, Mossakowski Medical Research Centre, Polish Academy of Sciences, Warsaw, Poland

Folia Neuropathol 2017; 55 (2): 110-123 DOI: https://doi.org/10.5114/fn.2017.68578

Abstract

The biomimetic, standardized conditions for in vitro cultures of human neural progenitors derived from induced pluripotent stem cells (hiPSC-NPs) should meet the requirements to serve as the template and protective environment for therapeutically competent cell population. In this study, two different collagen scaffolds: bi-component consisting of collagen and chondroitin sulphate (Col-CS), and collagen modified by crosslinking agent 2,3-dialdehyde cellulose (Col-DAC) have been used for the first time to encapsulate hiPSC-NPs and compared for the ability to create permissive microenvironment enabling cell survival, growth and differentiation. In our previous report, physicochemical comparison of the scaffolds revealed different elasticity, and diverse size and distribution of the pores within the 3D structure. Binary systems of Col-CS and Col-DAC tested in the current study have the correct balance of properties to serve as a biomimetic niche: they accommodate hiPSC-NPs sustaining their ability to proliferate and differentiate into neural lineages. However, a dense, network structure and rounded in shape pores of the Col-DAC microenvironment resulted in differential cell distributions within the scaffolds, with a tendency for augmented formation of highly proliferating cell aggregates as compared to Col-CS scaffolds. In contrast, Col-CS, which exhibited formation of the network of ellipsoidal and inner interconnected parallel pore channels, promoted enhanced cell viability and neuronal differentiation.

Key words: *collagen scaffolds, chondroitin sulphate, crosslinking by DAC, hiPSC-derived neural progenitors.*

Introduction

Under certain pathological conditions, in which the central nervous system (CNS) microenvironment is altered due to disease-induced stress, infections or trauma, clinically effective therapies are currently lacking [7]. Restoring the function of a damaged brain or spinal cord has always been a challenge due to their limited capacity for regeneration. Stem cell-based therapy opens new opportunities and challenges but is still in its infancy [40], however, when combined with tissue engineering, may result in a spectacular outcome [38]. Numerous tissue engineering strategies have been evaluated for their ability to support reconstruction and regeneration of the nervous system [10,15,21,23,39]. Currently, the important approach towards neural tissue

Communicating author

Professor Leonora Buzanska, Stem Cell Bioengineering Unit, Mossakowski Medical Research Centre, Polish Academy of Sciences, 5 Pawinskiego St., 02-106 Warsaw, Poland, phone: +48 22 60 86 449, fax: +48 22 668 55 32, e-mail: buzanska@imdik.pan.pl

engineering involves the *in vitro* culturing of stem cells on a biodegradable and bioactive scaffold to form hybrid tissue-like structures that are feasible for implantation into the injured site of the brain or spinal cord. Such scaffolds must have a stable micro-architecture and suitable biophysical properties. The design criteria for scaffold biomaterial greatly depend on the tissue engineering applications. In neural tissue engineering, proteins, such as collagen (Col) and Col additions: laminin; fibronectin; peptides (e.g., RGD, IKVAV and YIGSR); and polysaccharides, such as chitosan, alginate and hyaluronan are preferred for preparing these scaffolds [3,33,42]. These natural polymers contain attachment sites for cell membrane integrins and serve as scaffold receptors, thereby constituting a major recognition system for cell adhesion [15]. Comprehensive data on polymer scaffolding in neural tissue engineering have been published in several excellent review articles [1,3,5,14] indicating that the scaffolds used in tissue engineering must be designed to meet a number of properties. They include hydrophilicity, cell-adhesion and growth, biocompatibility, degradability, adapted pore size and structure, specific surface area, mechanical strength and thermo-mechanical stability [1]. Even small changes in the elastic modulus of the scaffold can affect the differentiation of the neuron, astrocyte, and oligodendrocyte populations [17]. It has also been demonstrated that the scaffold mean pore size greatly affects cellular activity and that subtle changes in the pore size and pore distribution can have significant effects on cell adhesion [20]. To date, creating an engineered construct that perfectly mimics all of the functions of the neuronal extracellular matrix (ECM) has not been successful.

Col, mostly type I, comprises a large portion of the ECM for most tissue types and is widely used as a cellular scaffold biomaterial for tissue engineering. It was found that within biocompatible Col scaffolds, embryonic stem cells differentiate into cells of the neural lineage and express neuronal lineage markers, such as NESTIN and β-TUBULIN III [19]. The microstructured collagen scaffold with seeded human neural progenitor cells can promote significant neurite outgrowth from dorsal root glia in both 2D and 3D cultures [8] and seems to be an important factor for future repair strategies for traumatically injured nervous tissues. Proteoglycans, including hyaluronic acid (HA) and chondroitin sulphate (CS), in CNS niches, are mainly responsible for providing structural and functional support to neural stem cells but exert different, sometimes contradictory, influence depending upon the niche's physiological context [4,29]. In the light of this information, we have asked whether the specific 3D template based on Col functionalized with CS can meet *in vitro* requirements to sustain neural developmental capacity within the population of neural progenitors derived from human induced pluripotent stem cells (hiPSC-NPs). The scaffold based on Col modified by crosslinking agent 2,3-dialdehyde cellulose (Col-DAC) was also investigated in this study. DAC was selected as the chemically crosslinking agent because it is biodegradable, biocompatible and toxicologically acceptable [11]. Since the capability of the CNS to regenerate depends on the mutual interaction of cells with the *in vivo* microenvironment, *in vitro* evaluation of such interactions is required in biomimetic conditions (scaffolds), which resemble a natural stem cell niche. The nature of this interaction is determined by the functional properties of the scaffold as well as the source and type of seeded cells. Human induced pluripotent stem cells (hiPSC) hold great promise for the future application in personalized medicine. Although many cell types have been transplanted into the injured spinal cord and brain tissue, including Schwann cells, olfactory ensheathing glia, activated macrophages, adult neural stem/progenitor cells and mesenchymal stem cells [19,22,41], induced pluripotent stem cells remain incompletely understood and should be further explored.

Recently we have prepared a new three-dimensional (3D) structure Col-based scaffolds, including composite system Col with immobilized chondroitin sulphate (Col-CS) crosslinked by carbodiimide [28,30] and Col cross-linked by DAC [24-26], which could serve as carriers for neural cell cultures. The use of such scaffolds for the maintenance of neural stem cells (NSC*) in vitro* and in the regeneration of the nervous system has not yet been well studied. In this *in vitro* study, neurally committed hiPSC seeded within different types of biochemical highly standardized 3D porous Col-CS and Col-DAC scaffolds were examined, evaluated and discussed.

Material and methods

Preparation of collagen-based scaffolds

Col type I was derived from porcine tendon by pepsin digestion and acetic acid dissolution to pre-

pare a 0.5% w/v dispersion [27]. The characteristic parameters of Col dispersion are as follows: pH 3.2, molecular weight 380,000 and denaturation temperature (Td) of 39°C.

Bi-component 3D scaffolds consisting of Col and CS were synthesized using a two-stage process: multiple freeze-drying steps followed by 1-ethyl-3-(3-dimethyl aminopropyl) carbodiimide hydrochloride (EDC) cross-linking according to the methods described by Pietrucha [28]. In brief, sponge-shape matrices were obtained by freezing the dispersion of Col with CS at –40°C. Next, the frozen dispersion was lyophilized at –55°C. The crosslinking reaction was carried out by immersing sponges in an ethanol solution containing a mixture of EDC, (morpholino)ethanesulphonic acid (MES) and N-hydroxysuccinimide (NHS). After crosslinking, the sponges were refrigerated at –40°C and subsequently lyophilized at –55°C. The synthesis of the Col-DAC scaffold was performed in three steps: (i) preparation of 2,3 DAC by a selective oxidation of cellulose, (ii) construction of the 3D Col sponge-shapes and (iii) cross-linking of Col samples using DAC. A detailed description of the method has been provided previously [24]. 3D porous sponges were incubated in a solution of DAC at 25°C for 24 h, at pH 8.0. The cross-linked Col matrices were then thoroughly washed with deionised water. Finally, the sponge was refrigerated at –40°C and subsequently lyophilized at –55°C. Recently, comprehensive biochemical, spectroscopic, morphological and structural properties of those modified Col scaffolds have also been presented [24,26,28].

Cell culture

Induced pluripotent stem cell culture, neural commitment and differentiation

The iPSC line derived by the episomal system from human CD34-positive fractions of cord blood cells was obtained from Life Technologies (Gibco® Human Episomal iPSC, Thermo Fisher Scientific). The cells were cultured on vitronectin (Thermo Fisher Scientific) and maintained in Essential 8 Medium (Thermo Fisher Scientific), according to the manufacturer's protocol. The medium was replaced every day. As cells reached ~80% confluence, they were passaged using DPBS without Ca^{2+} and Mg^{2+} for washing and 0.5 mM EDTA for detaching from culture vessels every 5 days at a ratio of 1 : 6. The neural commitment of induced pluripotent stem cells was performed according to Yan *et al*. [44]. Briefly, the iPS cells were seeded onto vitronectin in Neural Induction Medium (Gibco® PSC Neural Induction Medium, Thermo Fisher Scientific) for 7 days. After reaching confluency, cells were passaged on Matrigel (Corning, BD)-coated dishes and expanded as neural stem cells (NSC) in a neural expansion medium (Neural Induction Supplement 1 : 50, Neurobasal and Advanced D-MEM [1 : 1], Thermo Fisher Scientific). To obtain from hiPS-NSC neural progenitors (hiPSC- NPs) that were more advanced in differentiation, the hiPS-NSCs at passage 6 were used for neuronal and glial differentiation. The cells were seeded at 5 x 10^6 cells/cm^2 on the Matrigel-covered 6-well plates in a differentiating medium containing DMEM/F12/Neurobasal (1 : 1, Thermo Fisher Scientific), 1% FBS, 1% N2 (Thermo Fisher Scientific), 20 ng/ml EGF (Sigma-Aldrich), 10 ng/ml bFGF (Thermo Fisher Scientific). Cells were cultured in these conditions for at least 2 weeks, passaged using Accutase (BD) at a ratio of 1 : 6.

Preparation of scaffolds/hiPSC-NPs hybrids

Sterilization of scaffold samples

All of the constructed sponges' samples were sterilized using an electron beam (accelerator ELU6-Linac) with dose of 18 kGy. Further handling of the scaffolds proceeded under the laminar flow in sterile conditions.

Cell harvesting and seeding on the scaffolds

Following the process of neural commitment and differentiation, hiPSC-NPs were harvested using Accutase (Corning, BD), centrifuged and seeded in the density of 2.5 × 10^6 cells/ml on the scaffolds placed in the Eppendorf tubes. After 24 hours in the incubator, samples were transferred into 24-well culture plates in fresh medium. Samples were fixed for immunocytochemistry after 6 days of culture in standard culture conditions (5% CO_2, 37°C, 90% humidity).

Viability assay

To determine the viability of cell culture on the investigated Col-based scaffolds, after 1, 3 and 6 days of culture Col-CS and Col-DAC scaffolds seeded with hiPSC-NPs were washed with warm PBS and placed in a 96-well plate in the Live/Dead® Viability/Cytotoxicity Kit (Thermo Fisher Scientific), using

2 µM calcein and 4 µM EthD-1 solution, according to the manufacturer's instructions. After 30 minutes of incubation, 6 scaffolds per group were measured using FLUOstar plate reader Omega (BMG, Labtech, Germany) at a wavelength Ex 494/Em517 for calcein and Ex528/Em617 for EthD-1. The units used to estimate intensity for the fluorescence are shown as the Fluorescent intensity units (pixels). The conditions of the experiment for each time-point were optimized with the same number of scaffolds and the same number of seeded cells to be comparable between time-points and different scaffolds.

At day 6, living and dead cell distributions in the scaffolds were visualised using Confocal Laser Microscope LSM 510 (Zeiss).

Immunocytochemistry and image acquisition

Conventional 2D culture and scaffolds with cells were washed with PBS, fixed with 4% of PFA (15 min), permeabilised with 0.1% Triton X-100 and blocked with 10% goat serum. The following primary antibodies were applied overnight: O4 (1 : 100), GalC (mouse IgG3, 1 : 200, Millipore), PDGFRa (1 : 200), NESTIN (1 : 300), NF200 (mouse IgG1, 1 : 400, Sigma Aldrich), GFAP (rabbit polyclonal, 1 : 500, Cappel), β-TUBULIN III (mouse IgG2a, 1 : 1000, Sigma Aldrich), DOUBLECORTIN (DCX 1 : 500), and MAP-2 (mouse IgG1, 1 : 500, Sigma Aldrich), OCT4 (mouse IgG2b, 1 : 200, Santa Cruz), NANOG (rabbit polyclonal, 1 : 200, Abcam), Ki67 (mouse IgG1, 1 : 500, Leica/Novocastra). After washing with PBS, appropriate secondary antibodies (Goat anti-mouse or Goat anti-rabbit AlexaFluor 488 or AlexaFluor 546, 1 : 1000, Thermo Fisher Scientific) were applied for 1 hour, and cell nuclei were contra-stained with Hoechst 33258. Images were prepared in Laboratory of Advanced Microscopy Techniques, Mossakowski Medical Research Centre Polish Academy of Sciences using Confocal Laser Microscope LSM 510 (Zeiss) with objective: Plan_Neofluar 20×/0.5 (in Figs. 5-7 we used additional 1.5× zoom). Scale bars are added as an integral indicator of magnification in Zen Black Edition Software (Zeiss). 3D reconstruction of Z-stack images was performed using the same software.

Statistical analysis

The results are expressed as mean ±SD. Statistical analysis was performed using One Way ANOVA, followed by Bonferroni Multiple Comparison Test. The statistical significance of the results was determined for $p < 0.001$ (**); $p < 0.0001$ (***); $p < 0.00001$ (****).

Results

Characterization of hiPS-NSCs and hiPSC-NPs at 2-dimensional culture

The hiPS cells were used to derive a neurally committed cell population, because of well defined protocol and to avoid ethical concerns: primary human neural stem cell are available only from neurogenic zones of adult brains or from human miscarried embryos. The process of neural stem cell commitment from iPSCs was rapid (7 days of neural induction) and effective (we were able to obtain approximately 20 million of hNSC from one million of hiPSCs). In contrast to hiPSC, the obtained human iPSC-derived neural stem cells (hiPSC-NSC) did not express pluripotency markers OCT4 or NANOG [2], while the multipotent neural differentiation was manifested by expression of markers typical for a neural stem cell population (NESTIN), as well as markers for neuronal (β-TUBULIN III, DOUBLECORTIN, MAP-2) and glial differentiation (GFAP, GalC) (Fig. 1A). After further differentiation applied *in vitro,* neural progenitor population (hiPSC-NPs) was obtained (Fig. 1B). The expression profile of neural markers in hiPSC-NPs was similar to the hiPS-NSC, but the morphology had changed to more typical for neuronal cells, i.e., with long protrusions and small cell body (Fig. 1B). Further, the number of cells expressing MAP-2, β-TUBULIN III and GalC was significantly higher (Fig. 1B). However, some cells expressing NESTIN in the population of hiPSC-NPs could still be detected.

Three dimensional culture of hiPSC-NPs on modified scaffolds

Viability, adhesion and distribution of hiPSC-NPs

In our study, the population of hiPSC-NPs reveals an ability to adhere to and colonize bi-component Col-CS or modified Col-DAC scaffold. Viability of the hiPSC-NPs seeded on Col-CS and Col-DAC scaffolds was evaluated after 1, 3 and 6 days of culture. Living cells were distributed all over both kinds of tested scaffolds (Fig. 2C). The signal coming from living, calcein AM stained hiPSC-NPs was increasing during the culture time in all tested experimental conditions, but a significant rise in viability at 6 DIV (days

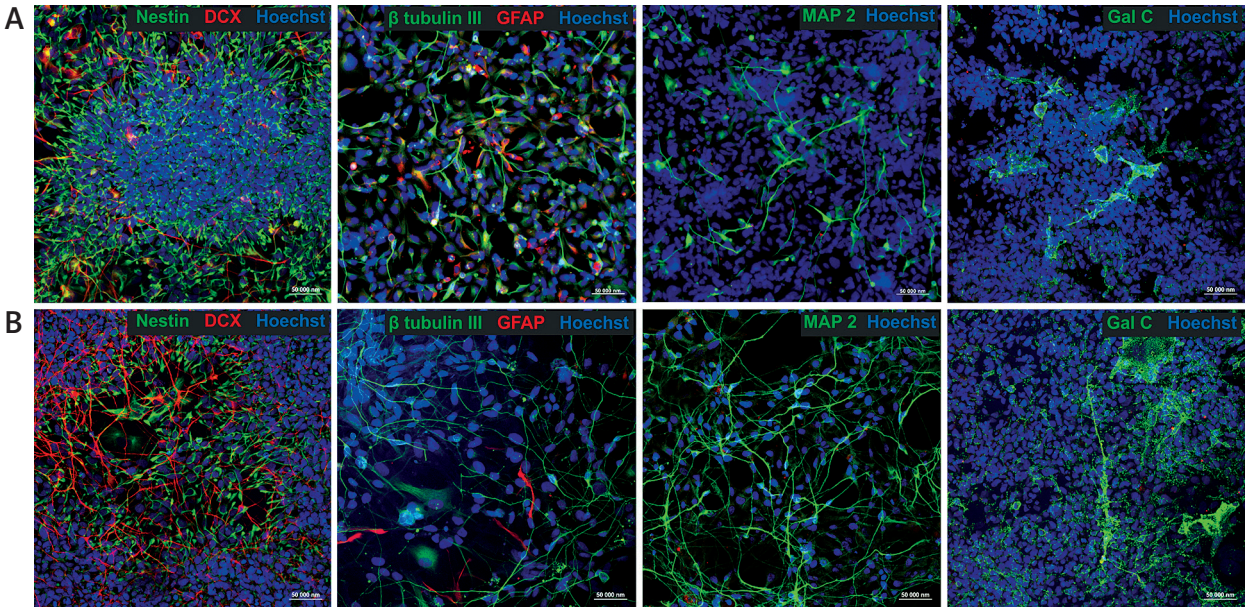

Fig. 1. Human neural stem cell population derived from iPSC (hiPS-NSC) cultured as a monolayer expressed both neuronal and glial markers **(A)**. After prolonged differentiation (2 weeks), the expression of neuronal and glial markers in the population of neural progenitors (hiPSC-NPs) was more abundant, however a number of progenitor cells expressing NESTIN were also detected **(B)**. Scale bar is 50 µm.

in vivo) was revealed only for the cells seeded on Col-CS (Fig. 2A). In contrast, the intensity of fluorescence of ethidium homodimer-1 (EthD-1), which labels cells with damaged membranes, was the same for both types of scaffolds. The highest intensity of fluorescence from dead cells was recorded at the first day of the experiment (DIV1) and significantly dropped after DIV1. From day 3 (DIV3) of the experiment, the constant and stable level of cell viability was observed (Fig. 2B). Moreover, at the 6th day of culture we observed only a few dead cells when Z-stacks were measured and visualised (Fig. 2C).

In both types of investigated scaffolds, the cells have been found across the sample, effectively adhering to the inner and outer surface of the scaffolds (Figs. 3 and 4). Seeded cells, depending upon the surface available, were forming: 1) aggregates within smaller pores with proliferating, Ki67 positive cells and at the edges differentiating β-TUBULIN III positive cells (Figs. 3A and C) or 2) were spreading out to cover the collagen surface of greater pore walls, thus forming a monolayer of cells with flattened and branched morphology (as shown for NESTIN positive cells on Figs. 3B and D). In any case, the population of seeded, hiPSC-NPs was able to penetrate inside the spongy structure of both types of the scaffold (Col-CS or Col-DAC) and populate across the accessible surface. This is illustrated by the confocal Z-stack series of images of Col-DAC (Fig. 4A) and Col-CS (Fig. 4B) samples as well as on their 200 µm depth 3D reconstruction (Fig. 4C), where cells are found at different arrangements (aggregates or spread sheets of differentiated cells). While neuronal marker β-TUBULIN III is widely present throughout the Z-stack in cells populating both types of scaffolds, astrocytic marker GFAP appears sporadically on Col-CS, compared to a more evident expression on Col-DAC scaffold.

Proliferation of hiPSC-NPs cultured on Col scaffolds

To estimate the proliferation rate of hiPSC-NPs, the proliferation marker binding to the nuclear proteins of dividing cells – Ki67 was used. The Ki67-positive cells were found predominantly within the cell aggregates/clumps that were placed inside the pores, while the proliferating cells outside the aggregates were only sporadically observed (Figs. 5A and D). Morphologically mature, β-TUBULIN III positive neuronal cells, with long protrusions aliening longitudinal pockets (pore edges), are in majority post-mitotic (arrows in Figs. 5B, C and F), however few of them were still mitotically active (Ki67 posi-

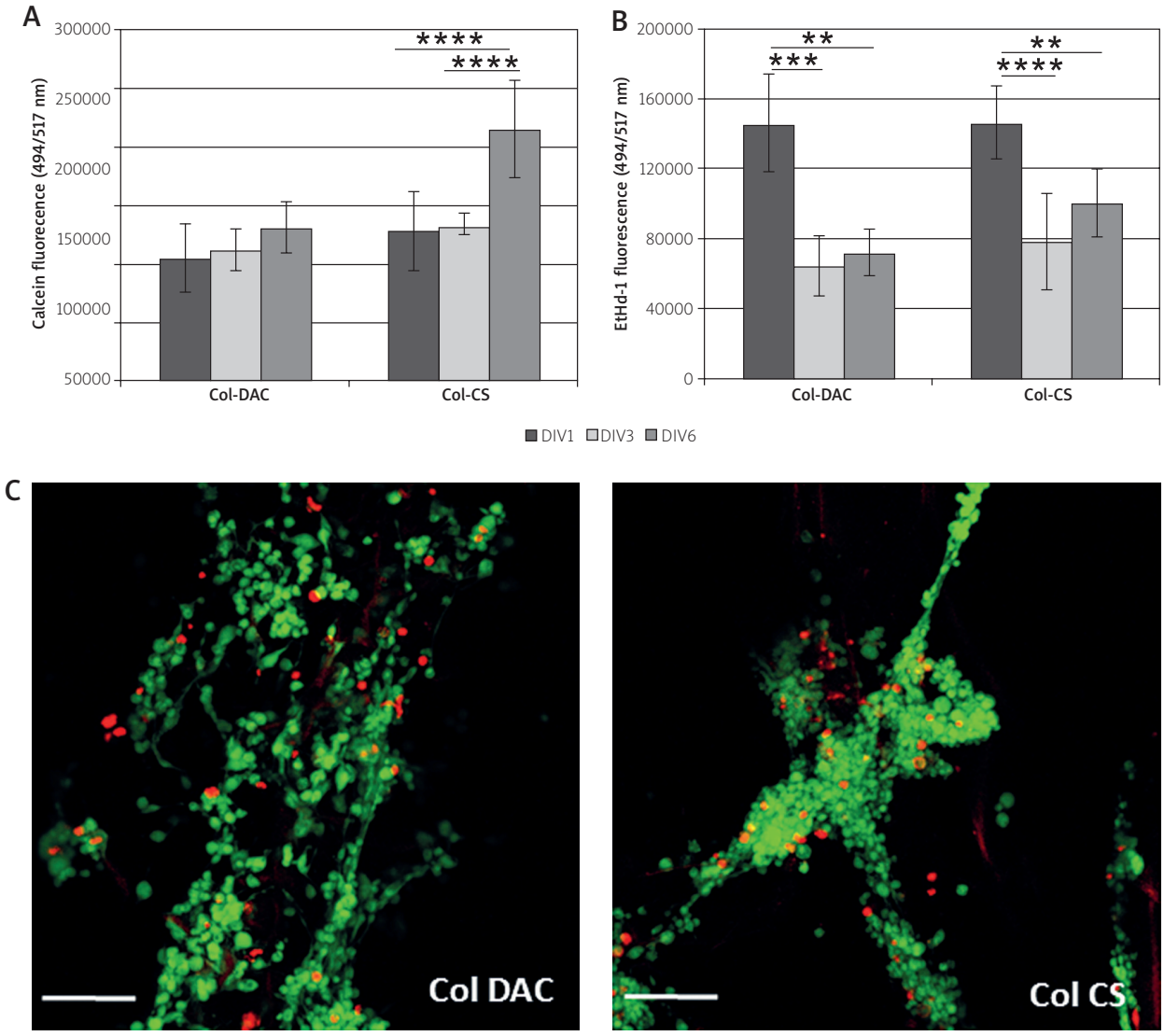

Fig. 2. Viability of hiPSC-NP cells cultured on Col-CS and Col-DAC scaffolds measured at day 1, 3 and 6 of the culture. The calcein-AM staining of living cells (**A, C** – green cells) revealed the increasing cell number during culture time, statistically significant only for Col-CS, while the EthD-1 fluorescence revealed a significant drop of dead cells after DIV1 and was constant further in the experiment (**B, C** – red cells). The units used to estimate intensity for the fluorescence are shown as the fluorescent intensity units (pixels) recorded by the FLUOstar plate reader at given wavelength (Ex 494/Em517 for calcein and Ex528/Em617 for EthD-1). Results represent fluorescence intensity (pixels) at the given wavelength from 12 scaffolds for each time point and are presented as mean ± SD, $p < 0.001$ (**); $p < 0.0001$ (***); $p < 0.00001$ (****). Scale bar is 50 µm.

tive cells, arrowheads on Figs. 5C, E and F). The exact number of proliferating cells was difficult to determine due to the relatively high autofluorescence of Col-DAC samples in the blue channel (total cell number), but our rough estimation of the percentage of Ki67+ cells resulted in about 38% for Col-DAC and 33% for Col-CS, indicating not significant difference between samples.

Differentiation of hiPSC-NPs seeded on the modified Col scaffolds

The input population of cells used for 3D culture was already pre-differentiated, as described above. It is demonstrated that the seeding process and biocompatible properties of both types of investigated Col scaffolds enabled hiPSC-NPs to sustain their

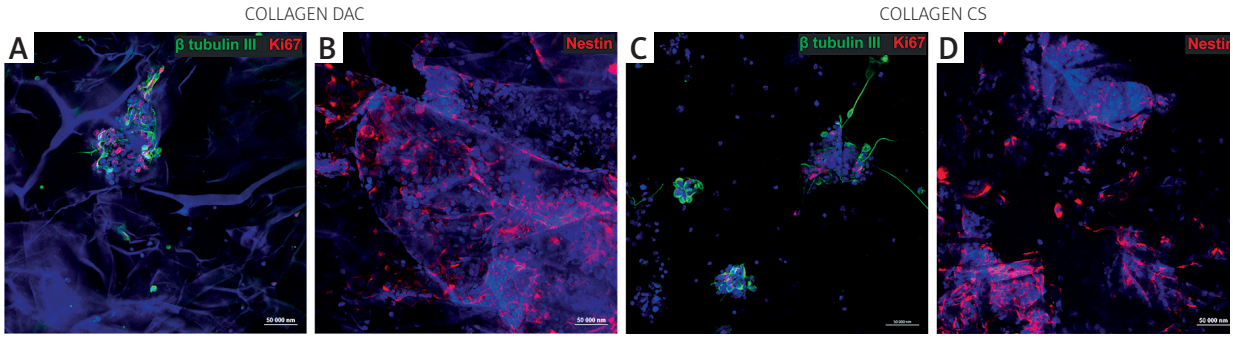

Fig. 3. Cells distribution on the Col scaffolds (DIV6). Cells seeded on Col scaffolds modified by crosslinking with DAC: **(A, B)** and bi-component Col-CS scaffold: **(C, D)** stained for neuronal marker β-TUBULIN III (green), proliferation marker Ki67 **(A, C)** and for NESTIN **(B, D)** (red). Cell nuclei are contra-stained with Hoechst (blue). Scale bar is 50 µm.

morphology and expression of typical markers for neuronal and glial differentiation. The cells within the cell-laden constructs were found mostly as the cell aggregates of different size, as well as monolayers from the cell aggregates, to cover the walls of bigger pores or connecting lamellas (Figs. 4, 5, 6 and 7). Randomly single cells, lacking markers of differentiation were also visible. The porous structure of Col-based scaffolds allows for neurite outgrowth from the cell clumps. We have observed the β-TUBULIN III positive hiPSC-NPs with neurites that aligned edges of the walls in the pore structure (Figs. 5 and 6B). Within the aggregates or clusters, the neuronal cells expressing β-TUBULIN III, MAP-2 and DCX were detected as mostly abundant. Neuronal morphology characterized by protrusions extended from the cell bodies was observed on both Col-CS and Col-DAC scaffolds (Figs. 5 and 7). While the differentiated cells appeared predominantly on the edges of the clusters (DCX presented in Fig. 7 and GalC in Fig. 8), cells found in the core of the aggregates were less differentiated (Figs. 7 and 8). In addition, the astrocytic marker (GFAP) was detected among differentiated cells growing in the clusters on both types of scaffolds (Figs. 4 and 7), however to a lesser extent than the neuronal markers. The early glial markers, such as PDGFRα or oligodendrocyte marker Galactocerebroside (GalC) (Figs. 6A, 7 and 8), have also been observed within the cell clusters in both types of scaffolds. The intense scaffold autofluorescence can be detected (blue tissue-like background in the Hoechst channel) after DAC crosslinking of the collagen (Figs. 4A, 5A and 8), while the functionalization of Col with CS gives almost no visible structure of the scaffolds in the fluorescence channels.

Discussion

In the present study, two types of Col scaffolds have been evaluated: bi-component Col-CS matrices crosslinked by EDC and collagen sponges modified using DAC. DAC was selected as a chemically crosslinking agent because it is biodegradable, biocompatible, and toxicologically acceptable [24]. None of the considered materials, Col, CS or DAC, are ideal for tissue engineering when used alone [18,28]. However, a binary system of Col-CS and Col-DAC may provide the correct balance of properties as a biomimetic niche for neural cell culture. In this study we have shown that both types of scaffold can serve as biomimetic niche to accommodate hiPSC-NPs and sustain their ability to proliferate and differentiate into neuronal, astrocytic and oligodendroglial lineages. Col-CS composite scaffolding has been prepared for regenerating *in vivo* the skin, bone, cartilage and peripheral nerves, yet has rarely been utilized in the restoration of the CNS [19,20]. To our knowledge, Col-DAC matrix has never been used to create a biomimetic environment for human neural cell cultures and Col-CS for neural stem/progenitor cells derived from hiPSC.

The hiPSC were applied in this study due to their exceptional features: they can be derived from the adult tissues of the human body and have the ability to differentiate into almost all types of cells [35]. Since they possess great potential for personalized regenerative medicine, they are investigated as a possible therapeutically competent cell population by our [37] and other groups [reviewed in 43]. Neural progenitors (hiPS-NSC) used in this study were derived from human iPSC and seeded on Col-CS and Col-DAC scaffolds for further investigation. The scaf-

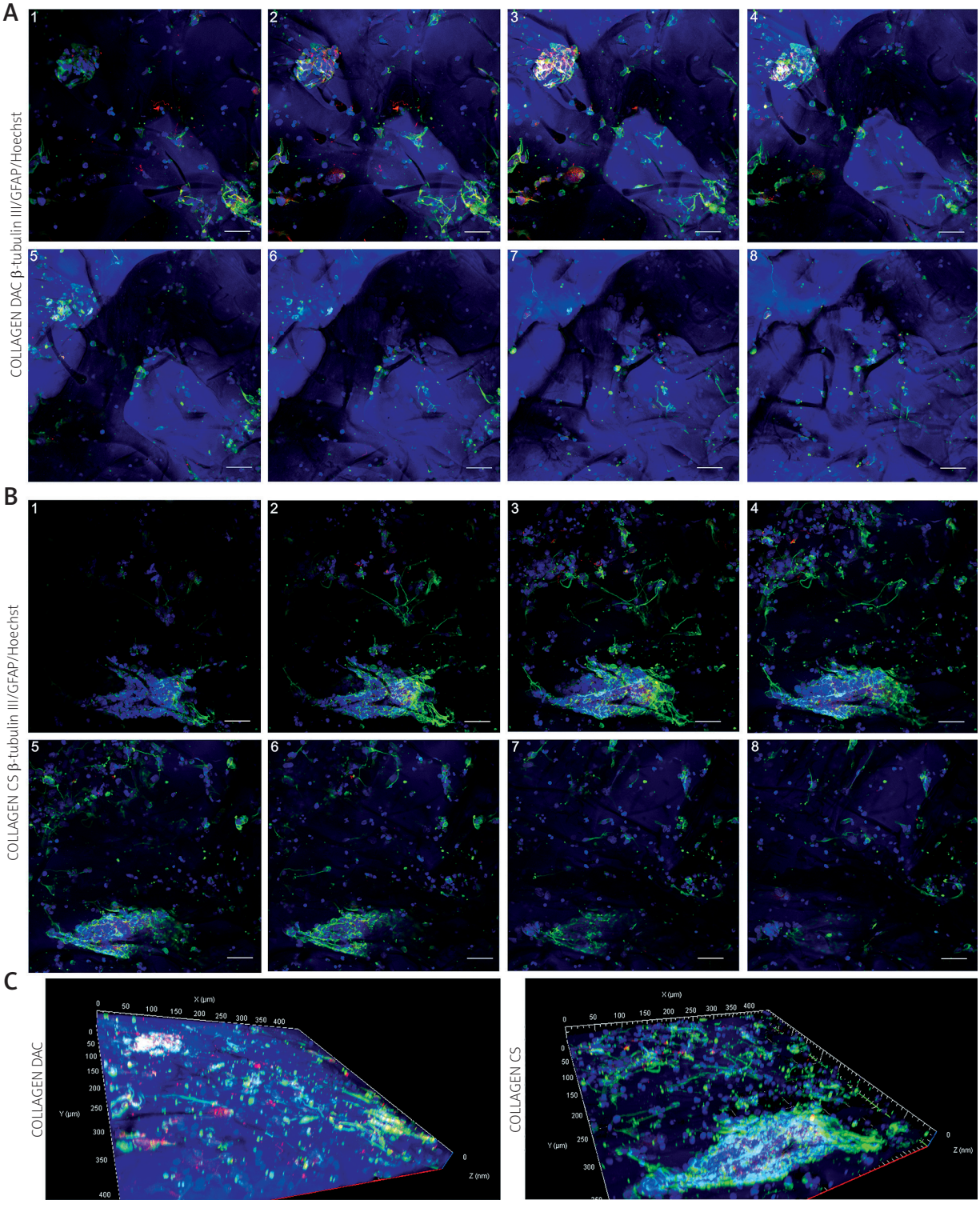

Fig. 4. Cells distribution through the scaffold sample (200 µm Z-stack). Each panel presents 8 subsequent optical sections. Each slice was of about 2.5 µm depth, space between slices 25 µm. Panel **A** shows distribution of cells seeded on Col-DAC scaffold. Intensive autofluorescence of Col-DAC scaffold was observed. Panel **B** shows cells seeded on Col-CS scaffold. Panel **C** shows 3D reconstruction of optical sections presented in **A** and **B**. Cells were stained for neuronal marker β-TUBULIN III (green) and astrocytic marker – GFAP (red). Cell nuclei were contra-stained with Hoechst (blue). Scale bar is 50 µm.

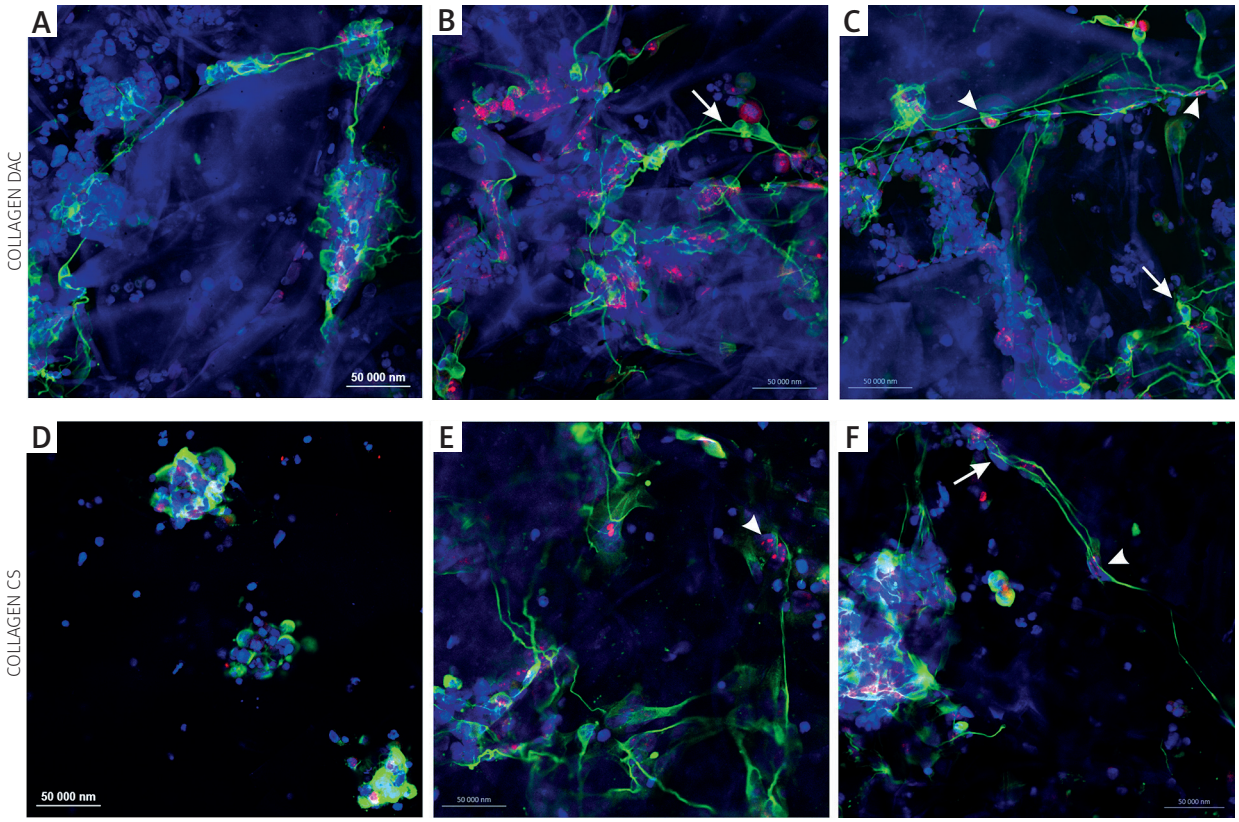

Fig. 5. Proliferation of neural progenitors (hiPSC-NPs) cultured on the Col scaffolds (DIV6): Col-DAC **(A, B, C)**, and Col-CS **(D, E, F)**. The proliferation marker Ki67 (red) is found predominantly within the cell clusters and nearly absent in the cells growing in the monolayer. Morphologically differentiated β-TUBULIN III (green) positive cells were mainly postmitotic (arrows), however some of the neuron-like cells were still dividing (arrowheads). Scale bar is 50 µm.

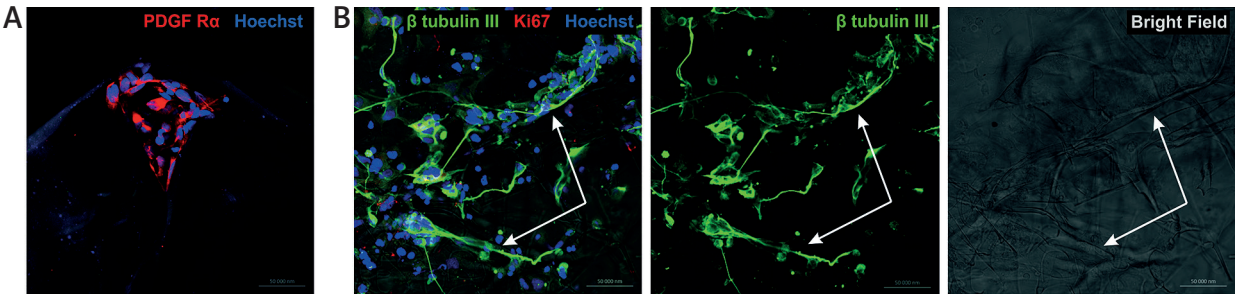

Fig. 6. Alignment of the neural cells protrusions on the porous structure of the Col-DAC scaffold (DIV6). Note the cell clustering in the 'corners' of the scaffold pores (cells stained with PDGFRα) **(A)** as well as long protrusions extended from the cell aggregates **(B)**. Arrows indicate the rows/longitudinal pockets (pores) in the scaffold structure and protrusions of neuron-like cells aligning the edges of these pores. Scale bar is 50 µm.

folds Col-CS and Col-DAC, crosslinked by EDC and DAC, respectively, were shown to immobilize hiPSC-NPs to the active biofunctional surface and allow for their further commitment into three neural lineages: neuronal, astrocytic and oligodendroglial. This is consistent with the study of Drobnik *et al.* [6] that collagen-based scaffolds using different cross-linking methods were shown to be suitable in elaborateing environments for primary nerve cells isolated from murine embryonic brains.

Both EDC and DAC were selected as chemical crosslinking agents due to their unique properties.

When a Col-CS sponge reacts with EDC, two essential processes occur, resulting in the formation of Col-Col cross-link and covalent graft CS to the Col backbone without the addition of any toxic catalysts (zero-length EDC) [28]. Finally, 3D semi- and interpenetrating networks are created. The Col-DAC scaffold is formed by a crosslinking reaction between the aldehyde groups (-CHO) of DAC with the free amine ($–NH_2$) groups of Col, resulting in a product that is biodegradable, biocompatible and toxicologically acceptable [24].

The viability of human neural progenitors seeded on the scaffolds was measured with the life/dead fluorescent assay and quantitatively evaluated. The significantly increased level of fluorescence indicating living cells show that the cells survive and proliferate (Fig. 2). Interestingly, at day 1 we have observed a significantly higher level of the signal from dead cells as compared to day 3 and day 6. However it is likely that this difference is artificially elevated by the presence of the cells dying from the seeding and harvesting procedure, not related to the biocompatibility of the scaffolds.

To trace the cellular processes (attachment, proliferation and differentiation – axonal outgrowth) of the hiPSC derived neural progenitors cultured on the scaffolds, immunocytochemical/immunofluorescent marker proteins identification and confocal microscopy analysis were applied. The proliferation rate of the hiPS-NSC cultured on the scaffolds was investigated by immunostaining with Ki67 antibody (Figs. 3 and 5), which binds to the nuclear protein MKI67, present during all active phases of the cell cycle (G1, S, G2, and mitosis), but is absent in resting cells (G0) [34]. Markers applied to detect neural stem/progenitor cells (NESTIN) and their commitment into neuronal (β-TUBULIN III, NF200, DOUBLECORTIN, MAP-2), astrocytic (GFAP) and oligodendroglial (PDGFRα, GalC) lineages have been used before in the study of our group [2,36,46] and are typical for characterization of neural lineages *in vitro* and *in vivo* [31]. It is important to note that the results of this study based on immunofluorescent images are only qualitative due to the high autofluorescence of the Col-DAC scaffolds (Figs. 3A, B, 4A, 5 and 8), which was not the case of Col-CS matrix (Figs. 3B and 4B). The autofluorescence of Col-DAC samples may be assigned to the formation of stable covalent imine bonding between the amino groups of lysine, hydroxylysine and arginine from Col and aldehyde group of DAC through the Schiff base reaction. As reported in the literature [9], Schiff base compounds containing an imine group (–RC=N–) are usually formed by the condensation of a primary amine with an active carbonyl responsible for the fluorescence.

However, the detailed analysis of the confocal microscope Z-stack panels allowed the qualitative assessment for not only the presence of the cells, but also their stage of differentiation, detailed distribution through the scaffold and alignment within the scaffold architecture (Fig. 4). The alignment of the cells in the scaffolds is in accordance with the pore distribution within biomaterial architecture. Cells cover the walls of bigger pores creating a monolayer (Figs. 4, 5 and 6), allowing space for cell protrusions and promote differentiation of hiPSC-NPs, while in the smaller pores and in the edges of the bigger pores cell aggregates are formed. According to our previous results [24,28], the distribution of the pore sizes depends on the type of components and the method of modifying the scaffold. For Col-CS sponges, the largest fraction, at least 55% of the total pore volume that comprises the sponge is occupied by pores ranging from 20 to 100 µm in size, only 25% of the total pore volume is larger than 100 µm. Whereas, the sponge-like scaffold Col-DAC had 70% pores ranging from 20 to 100 µm. These results agree with those presented by Yannas [45], showing that regenerative scaffolds based on collagen have a narrowly specified pore structure with a pore diameter of 20 to 125 µm. Such pores are ideal for cell aggregates to adhere and develop a micro-niche. The pore size between 80-100 µm of dextran or gelatin cryogels was previously shown to be optimal for stem cells derived from human cord blood adhesion and neural differentiation [12]. Subsequently it was shown that gelatin-based cryogels scaffolds with the pore size ranging from 20 to 120 allow encapsulation of bigger in size mesenchymal stem cells (hUCMSCs) and when supplemented with neuromorphogenes promote their neural differentiation *in vitro* [32].

In our study, pore size-dependent encapsulation and differentiation of stem cells within spongy collagen scaffolds was confirmed. The hiPSC-NSC are smaller than MSC discussed above, thus the pores about 100 µm are suitable for the formation of cell aggregates. The larger amount and specific alignment of pores smaller than 100 µm in Col-DAC as compared to Col-CS might promote formation of cell aggregates with proliferative centres (Fig. 3A).

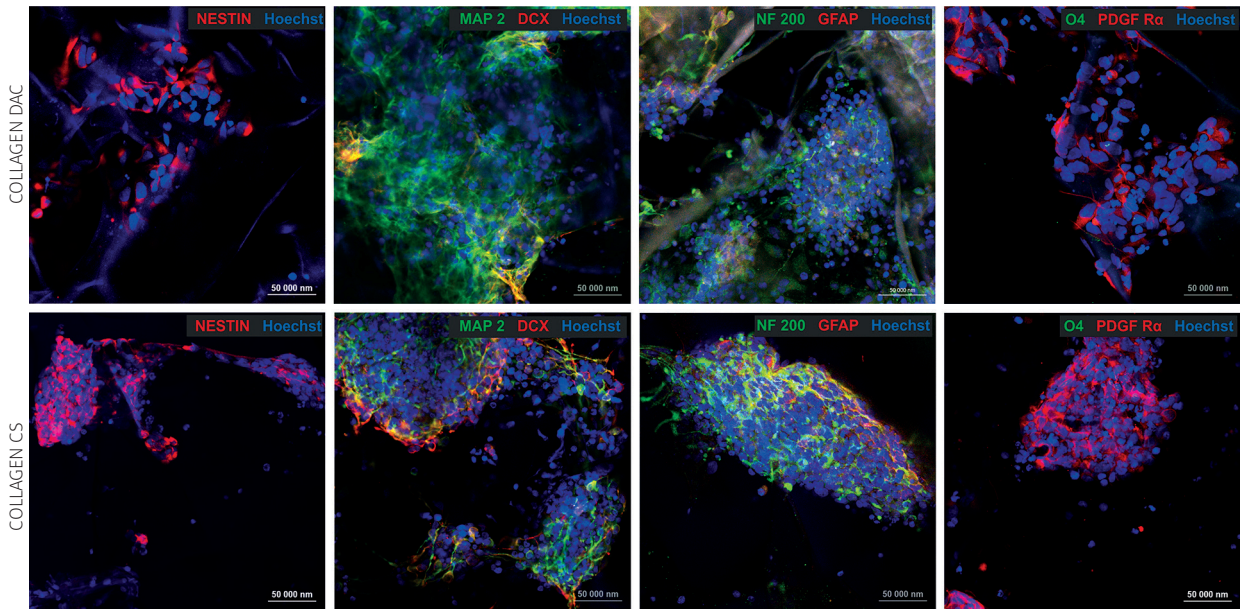

Fig. 7. Neuronal and glial differentiation of hiPSC-NPs cultured on Col-DAC and Col CS scaffolds (DIV6). Some of the cells express markers typical for a neural stem cell population (NESTIN) as well as markers for neuronal (NF200, DOUBLECORTIN, MAP-2) and glial differentiation (GFAP, PDGFRα). Cell nuclei are contra-stained with Hoechst (blue). Scale bar is 50 µm.

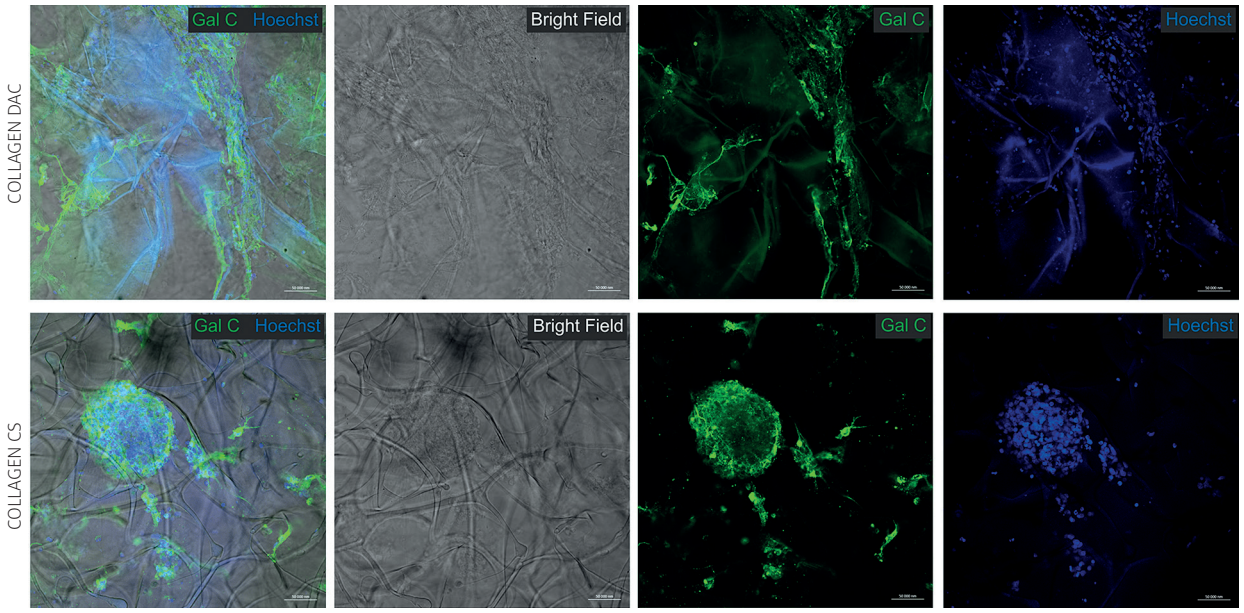

Fig. 8. Oligodendroglial differentiation of hiPSC-NPs cultured on the Col-DAC and Col-CS scaffolds (DIV6). Some of the cells exhibit oligodendroglial marker GalC. Intense scaffold autofluorescence may be observed (blue tissue-like background in the Hoechst channel), after DAC crosslinking of the collagen, while the functionalization of collagen with CS gives almost no visible structure of samples in the fluorescence channels. Scale bar is 50 µm.

The dual composition of both investigated scaffolds, having smaller and bigger pores, provides an ability to preserve both the proliferative, Ki67-positive, NESTIN-positive population of neural progenitors and the cells committed into different neural lineages. The proliferation marker Ki67 is found

predominantly within the cell clusters and nearly absent in the cells growing in the monolayer (Fig. 5). The hiPSC-NPs proliferate in the centre of the aggregates, while at the peripheral part they migrate out of the cluster and differentiate predominantly into neurons. As shown in this study, the cells expressing neuronal markers expand protrusions along the pore edges and their interconnecting lamellas. It was earlier noted [31,32] that the pores in Col-CS sponges are ellipsoidal in shape and are oriented parallel to the surface within the sponge, what may influence cell distribution with a tendency to form cell monolayers as compared to aggregates found on Col-DAC. This may explain the preferential appearance of the differentiated cells forming the monolayers on the Col-CS as compared to cell aggregates with defined centres of proliferation on Col-DAC, as revealed by immunofluorescence in Fig. 4. Both types of tested scaffolds allow for the proliferation and further differentiation of neurally pre-differentiated hiPS-NSCs. The seeding population of hiPSC-NPs in 2D conditions revealed markers typical for all three neural lineages, however the porous structure of collagen scaffolds promote/allow neurite outgrowth from the cell clumps supporting further neuronal differentiation, as shown by the expression of DOUBLECORTIN and MAP-2 markers in Col-DAC and Col-CS scaffolds. The astrocytic marker (GFAP), while to a lesser extent than the neuronal markers, was also detected among differentiated cells growing in clusters on both types of scaffolds. The glial markers such as PDGFRα (typical for early glial differentiation) or oligodendrocyte marker GalC, have also been observed at the edges of the cell clusters in both types of scaffold, confirming multilineage potential of differentiation of the encapsulated hiPSC-NPs.

Recently, binary systems more complicated than used in this study, the hybrid scaffolds comprised of collagen, hyaluronic acid, and alginate and additionally functionalized with GRGDSP and Ln5-P4 were shown to support efficient differentiation of hiPSC into neuronal cells [16]. The Col scaffolds tested in this study were stable during the culture time and did not produce any toxic forms of degradation. The surface of tested biomaterial provided proper adhesion and different pore sizes, which immobilised cells in the smaller or bigger aggregates or allowed for cell spreading on the lamella of the Col structures. The encapsulating of living cells inside the scaffold can help to prevent apoptosis caused by induced active inflammation after transplantation of such hybrids into the host nerve tissue [13]. The sustained proliferation and neuronal differentiation capacity of hiPSC-NPs on these modified biomaterials enables further migration from the scaffold or extending protrusions outside the biomaterial into host tissue. The important difference between tested scaffolds was that Col-CS maintain *in vitro* viable cells significantly longer than Col-DAC. However, we did not observe any significant differences of proliferation and cell differentiation between the two Col scaffolds investigated, therefore this supports the conclusion that using both types of Col-CS and Col-DAC biomaterials in tissue engineering and regenerative medicine is justified, when different physicochemical features are required.

Conclusions

The Col-based (Col-CS, Col-DAC) binary scaffold systems presented in this study possess appropriate physicochemical properties and are biocompatible, easy to handle and non-toxic. They allow for good cell attachment as well as sustain the proliferation and differentiation capacity of seeded human neural progenitors derived from iPSC. The current study demonstrated that the binary system of Col-CS and Col-DAC scaffolds can be considered as the potential tool for delivery of neural progenitor cells to the injured brain or spinal cord.

Acknowledgments

This work is supported by the National Science Centre via Grant No. DEC-2011/03/B/ST8/05867 and statutory funds to MMRC.

Disclosure

Authors report no conflict of interest.

References

1. Ai J, Kiasat-Dolatabadi A, Ebrahimi-Barough S, Ai A, Lotfibakhshaiesh N, Norouzi-Javidan A, Saberi H, Arjmand B, Aghayan HR. Polymeric scaffolds in neural tissue engineering: A review. Arch Neurosci 2013; 1: 15-20.
2. Augustyniak J, Lenart J, Zychowicz M, Lipka G, Gaj P, Kolanowska M, Stepien PP, Buzanska L. Sensitivity of hiPSC-derived neural stemcells (NSC) to Pyrroloquinoline quinone depends on their developmental stage. Toxicol In Vitro 2017; doi:10.1016/j.tiv.2017.05.017

3. Das RK, Zouani OF. A review of the effects of the cell environment physicochemical nano-architecture on stem cell commitment. Biomaterials 2014; 35: 5278-5293.
4. Dityatev A, Seidenbecher CI, Schachner M. Compartmentalization from the outside: the extracellular matrix and functional microdomains in the brain. Trends Neurosci 2010; 33: 503-512.
5. Donaghue IE, Tam R, Sefton MV, Shoichet MS. Review: Cell and biomolecule delivery for tissue repair and regeneration in the central nervous system. J Control Release 2014; 190: 219-227.
6. Drobnik J, Pietrucha K, Kudzin M, Mader K, Szymański J, Szczepanowska A. Comparison of various types of collagenous scaffolds applied for embryonic nerve cell culture. Biologicals 2017; 45: 1-7.
7. Forostyak O, Dayanithi G, Forostyak S. CNS Regenerative Medicine and Stem Cells. OM & P 2016; 69-76.
8. Fuhrmann T, Hillen LM, Montzka K, Wöltje M, Brook GA. Cell-cell interactions of human neural progenitor-derived astrocytes within micro-structured 3D-scaffold. Biomaterials 2010; 31: 7705-7715.
9. Guo B, Wang LJ, Li BG, Cao XZ, Zhang QS, Li PX. Synthesis and characterization of fluorescent wood pulp cellulose derivative based on Schiff base reaction. Cellulose Chem Technol 2016; 50: 57-63.
10. Hoffman-Kim D, Mitchel JA, Bellamkonda RV. Topography, cell response, and nerve regeneration. Annu Rev Biomed Eng 2010; 12: 203-231.
11. Huang K F, Hsu WC, Chiu WT, Wang JY. Functional improvement and neurogenesis after collagen-GAG matrix implantation into surgical brain trauma. Biomaterials 2012; 33: 2067-2075.
12. Jurga M, Dainiak M. B, Sarnowska A, Jablonska A, Tripathi A, Plieva FM, Savina IN, Strojek L, Jungvid H, Kumar A, Lukomska B, Domanska-Janik K, Forraz N, McGuckin CP. The performance of laminin-containing cryogel scaffolds in neural tissue regeneration. Biomaterials 2011; 32: 3423-3434.
13. Karus M, Ulc A, Ehrlich M, Czopka T, Hennen E, Fischer J, Mizhorova M, Qamar N, Brüstle O, Faissner A. Regulation of oligodendrocyte precursor maintenance by chondroitin sulphate glycosaminoglycans. Glia 2016; 64: 270-286.
14. Khaing ZZ, Schmidt CE. Advances in natural biomaterials for nerve tissue repair. Neurosci Lett 2012; 519: 103-114.
15. Kim H, Cooke MJ, Shoichet MS. Creating permissive microenvironments for stem cell transplantation into the central nervous system. Trends in Biotechnol 2012; 30: 55-63.
16. Kuo YC, Hsueh CH. Neuronal production from induced pluripotent stem cells in self-assembled collagen-hyaluronic acid-alginate microgel scaffolds with grafted GRGDSP/Ln5-P4. Mater Sci Eng C Mater Biol Appl 2017; 76: 760-774.
17. Leipzig ND, Shoichet MS. The effect of substrate stiffness on adult neural stem cell behaviour. Biomaterials 2009; 30: 6867-6878.
18. Lu D, Mahmood A, Qu C, Hong X, Kaplan D, Chopp M. Collagen scaffolds populated with human marrow stromal cells reduce lesion volume and improve functional outcome after traumatic brain injury. Neurosurgery 2007; 61: 596-602.
19. Michelini M, Franceschini V, Chen SS, Papini S, Rosellini A, Ciani F, Margolis L, Revoltella RP. Primate embryonic stem cells create their own niche while differentiating in three-dimensional culture systems. Cell Prolif 2006; 39: 217-229.
20. Murphy CM, Haugh MG, O'Brien FJ. The effect of mean pore size on cell attachment, proliferation and migration in collagen-glycosaminoglycan scaffolds for bone tissue engineering. Biomaterials 2010; 31: 461-466.
21. Norman LL, Stroka K, Aranda-Espinoza H. Guiding axons in the central nervous system: a tissue engineering approach. Tissue Eng Part B 2009;15: 291-305.
22. Oudega M, Moon LD, de Almeida Leme RJ. Schwann cells for spinal cord repair. Braz J Med Biol Res 2005; 38: 825-835.
23. Pérez-Garnes M, Barcia JA, Gómez-Pinedo U et al. Materials for Central Nervous System Tissue Engineering: Cells and Biomaterials in Regenerative Medicine. In: Eberli D (ed.). 2014 Chapter 7.
24. Pietrucha K, Marzec E, Kudzin M. Pore structure and dielectric behaviour of the 3D collagen-DAC scaffolds designed for nerve tissue repair. Int J Biol Macromol 2016; 92: 1298-1306.
25. Pietrucha K, Safandowska M. Dialdehyde cellulose-crosslinked collagen and its physicochemical properties. Process Biochem 2015; 50: 2105-2111.
26. Pietrucha K. Development of collagen cross-linked with dialdehyde cellulose as a potential 3D scaffold for neural tissue engineering. Int Fed Med Biol Eng Proc 2015; 45: 349-352.
27. Pietrucha K. Effect of irradiation on collagen solutions in relation to biomedical applications. Polym Med 1989; 19: 3-18.
28. Pietrucha K. Physicochemical properties of 3D collagen-CS scaffolds for potential use in neural tissue engineering. Int J Biol Macromol 2015; 80: 732-739.
29. Riquelme PA, Drapeau E, Doetsch F. Brain micro-ecologies: neural stem cell niches in the adult mammalian brain. Philos Trans R Soc Lond B Biol Sci 2008; 363: 123-137.
30. Safandowska M, Pietrucha K. Effect of fish collagen modification on its thermal and rheological properties. Int J Biol Macromol 2013; 53: 32-37.
31. Sarnat HB. Clinical neuropathology practice guide 5-2013: markers of neuronal maturation. Clin Neuropathol 2013; 32: 340-369.
32. Sarnowska A, Jablonska A, Jurga M, Dainiak M, Strojek L, Drela K, Wright K, Tripathi A, Kumar A, Jungvid H, Lukomska B, Forraz N, McGuckin C, Domanska-Janik K. Encapsulation of mesenchymal stem cells by bioscaffolds protects cell survival and attenuates neuroinflammatory reaction in injured brain tissue after transplantation. Cell Transplant 2013; 22 Suppl 1: S67-82.
33. Sarnowska A, Zychowicz M, Buzanska L. Tissue engineering and Bioengineering. In: Neurorestoratology. Volume 1. Huang H, Raisman G, Sanberg PR, Sharma HS (eds.). Nova Science Publisher, Inc., New York 2015; Chapter 8: 187-212.
34. Scholzen T, Gerdes J. The Ki-67 protein: from the known and the unknown. J Cell Physiol 2000; 182: 311-322.
35. Stadtfeld M, Hochedlinger K. Induced pluripotency: history, mechanisms, and applications. Genes Dev 2010; 24: 2239-2263.
36. Sypecka J, Sarnowska A. Heterogeneity of local tissue microenvironment influences differentiation of oligodendroglial progenitors. Folia Neuropathol 2013; 51: 103-110.
37. Szablowska-Gadomska I, Sypecka J, Zayat V, Podobinska M, Pastwinska A, Pienkowska-Grela B, Buzanska L. Treatment with

small molecules is an important milestone towards the induction of pluripotency in neural stem cells derived from human cord blood. Acta Neurobiol Exp (Wars) 2012; 72: 337-350.
38. Tabakow P, Jarmundowicz W, Czapiga B, Fortuna W, Miedzybrodzki R, Czyz M, Huber J, Szarek D, Okurowski S, Szewczyk P, Gorski A, Raisman G. Transplantation of autologous olfactory ensheathing cells in complete human spinal cord injury. Cell Transplant 2013; 9: 1591-1612.
39. Tam RY, Fuehrmann T, Mitrousis N Shoichet MS. Regenerative therapies for central nervous system diseases: a biomaterials approach. Neuropsychopharmacology 2014; 39: 169-188.
40. Tang YH, Ma YY, Zhang ZJ, Wang YT, Yang GY. Opportunities and challenges: stem cell-based therapy for the treatment of ischemic stroke. CNS Neurosci Ther 2015; 21: 337-347.
41. Tetzlaff W, Okon EB, Karimi-Abdolrezaee S, Hill CE, Sparling JS, Plemel JR, Plunet WT, Tsai EC, Baptiste D, Smithson LJ, Kawaja MD, Fehlings MG, Kwon BK.. A systematic review of cellular transplantation therapies for spinal cord injury. J Neurotrauma 2011; 28: 1611-1682.
42. Wang X, Yan C, Ye K, He Y, Li Z, Ding J. Effect of RGD nanospacing on differentiation of stem cells. Biomaterials 2013; 34: 2813-2874.
43. Xie IN, Tang B. The Application of Human iPSCs in Neurological Diseases: From Bench to Bedside. Stem Cells Int 2016; 2016: 6484713.
44. Yan Y, Shin S, Jha BS, Liu Q, Sheng J, Li F, Zhan M, Davis J, Bharti K, Zeng X, Rao M, Malik N, Vemuri MC. Efficient and rapid derivation of primitive neural stem cells and generation of brain subtype neurons from human pluripotent stem cells. Stem Cells Transl Med 2013; 2: 862-870.
45. Yannas V. Emerging rules for inducing organ regeneration. Biomaterials 2013; 34: 321-330.
46. Zychowicz M., Mehn D, Ruiz A, Frontczak-Baniewicz M, Rossi F, Buzanska L. Patterning of human cord blood-derived stem cells on single cell posts and lines: Implications for neural commitment. Acta Neurobiol Exp (Wars) 2012; 72: 325-336.

Original paper

Folia Neuropathologica

Propofol attenuates intermittent hypoxia induced up-regulation of proinflammatory cytokines in microglia through inhibiting the activation of NF-κB/p38 MAPK signalling

Song Liu[1], Jin-Yuan Sun[1], Lian-Ping Ren[1], Kui Chen[2], Bo Xu[2]

[1]Xinhua Hospital Affiliated to Shanghai Jiao Tong University School of Medicine, Shanghai, [2]Beijing Friendship Hospital, Capital Medical University, Beijing, China

Folia Neuropathol 2017; 55 (2): 124-131 DOI: https://doi.org/10.5114/fn.2017.68579

Abstract

As immune sentinels of the central nervous system (CNS), microglia is pivotal cellular mediator of neuroinflammatory processes. Activation of microglia might elicit the expression of proinflammatory cytokines involved in the progression of neuroinflammatory diseases. Numerous studies have demonstrated that propofol (2,6-diisopropylphenol) has an effective anti-inflammatory property. Intermittent hypoxia (IH), as a result of obstructive sleep apnoea (OSA), could lead to neuron damage and neuroinflammation in the CNS. Here, we determined the effects of propofol on the inflammatory response in microglia during IH. The levels of nuclear factor-κB (NF-κB) inhibitor (IκB) and activated p38 mitogen-activated protein kinase (MAPK) exposed to IH with or without propofol treatment were detected by Western blot. The viability of cells exposed to various concentrations of propofol was monitored with MTT assay. The production and mRNA levels of tumor necrosis factor-α (TNF-α) and interleukin-6 (IL-6) were evaluated by qRT-PCR and ELISA, respectively. As results, IH exposure obviously promoted the activation of NF-κB/p38 MAPK signalling and the secretion of TNF-α and IL-6. Propofol was not toxic to microglia. Compared with the control group, propofol attenuated the IH-induced activation of NF-κB and p38 MAPK, which accompanied with reduction of proinflammatory cytokine secretion. These data suggested that propofol down-regulated the IH-induced secretion of proinflammatory cytokine, and inhibit inflammatory responses in microglia, and might be involved in attenuation of the p38 MAPK and NF-κB signalling pathways. Overall, propofol could contribute to alleviating IH-induced CNS diseases in patients by inhibiting p38 MAPK and NF-κB mediated inflammation in microglia.

Key words: *propofol, intermittent hypoxia, proinflammatory cytokine, microglia.*

Introduction

Neuroinflammation mediated by the activation of glia has been shown to be associated with the progressive neuronal damage in a variety of neurodegenerative diseases, such as Alzheimer's disease (AD), Huntington's disease (HD), and amyotrophic lateral sclerosis (ALS) [1,12]. Microglia are considered to be the resident immune cells in the central nervous system (CNS), which can be activated by various stimuli. Under inflammatory conditions, microglia will be activated and play a vital role in regulating inflammatory reactions by releasing diverse inflammatory

Communicating author

Song Liu, Xinhua Hospital Affiliated to Shanghai Jiao Tong University School of Medicine, 1665 Kongjiang Road, 200092 Shanghai, China, phone: +86-21-25077383, e-mail: liusongyy@hotmail.com

factors including cyclooxygenase-2 (COX-2), nitric oxide (NO) and proinflammatory cytokines such as interleukin-1 beta (IL-1β), necrosis factor-α (TNF-α) and interleukin-6 (IL-6) [5,17,20]. However, overactive microglia lead to excessive secretion of neurotoxic mediators, which can result in severely detrimental neuronal damage and neurodegenerative diseases. Consequently, blockade of the activation of microglia could reduce subsequent neuroinflammation, providing a promising therapy for the treatment of inflammation-mediated neurodegenerative diseases.

Propofol, with potent sedation/hypnotic properties, is a widely used intravenous agent for induction and maintenance of anaesthesia, as well as sedation in the intensive care unit [21]. Accumulated studies suggested that propofol exhibits anti-inflammatory effects. For instance, propofol inhibited inflammatory responses in lipopolysaccharide (LPS)-induced alveolar epithelial type II cells [18]. And it attenuated secretion of proinflammatory cytokines in a hepatocyte nuclear factor-1α-dependent manner [19]. Emerging reports suggested that propofol effectively down-regulated inflammatory responses by inhibiting the phosphorylation of nuclear factor-κB (NF-κB) and p38 mitogen-activated protein kinase (MAPK) [25,26,33]. Propofol blocked astrocyte activation upon stimulation with LPS via presenting the NF-κB, p38 MAPK and extracellular signal-regulated protein kinases (ERK) 1/2 pathways [33]. Moreover, propofol exerted effectively anti-inflammatory properties in human neuroglioma cells treated by sevoflurane through suppressing the NF-κB signalling pathway [26]. An earlier report supported that anti-inflammatory mechanisms of propofol were shown through decreasing the level of phosphorylated p38 MAPK [25]. The anti-inflammatory property of propofol in microglia has become one of the most exciting research topics.

Intermittent hypoxia (IH), one of the pathophysiologic changes resulting from obstructions of the upper airway during sleep, may play a key role in the structural neuron damage in the CNS, especially excitotoxicity in hippocampal neurons [8,9,36]. Moreover, IH would lead to the up-regulation of ROS, NO, and downstream pro-inflammatory responses [2,30]. Thus, we investigated the effects of propofol on the secretion of proinflammatory molecules in IH-exposed microglia, and evaluated the activation of NF-κB and p38 MAPK during these processes.

Material and methods

Cell culture

BV2 microglial cells were provided by the State Key Laboratory of Brain and Cognitive Science, Institute of Biophysics, Chinese Academy of Science. The cells were seeded into six-well plates in Dulbecco's Modified Eagle Medium (DMEM) (Thermo Scientific, Rockford, Illinois, USA) containing 10% foetal bovine serum (Gibco, Grand Island, NY, USA), 1% penicillin, and 1% streptomycin (Invitrogen, Shanghai, China), and incubated in a humidified 5% CO_2 atmosphere at 37°C. After incubation for 24 h, the cells were cultured with fresh medium and used as microglia for later experiments.

Intermittent hypoxia exposure and propofol treatment

Microglia cells in the IH exposure group were maintained at 37°C and 5% CO_2 in the hypoxic chamber with shifted O_2 levels between 1% and 21% for 400 sec/cycle. Cells in the control group were cultured at 5% CO_2 and normoxic conditions (21% O_2). Both groups were treated for 8 h.

Referring to the clinically relevant blood concentration of propofol [10,22], different concentrations of 0, 25, 50 and 100 μM of prepared propofol were used to pre-treat the microglia 0.5 h prior to IH exposure. Cells in the control group were treated with neither propofol nor IH.

Western blot

Cells were homogenized in lysis buffer and then the total proteins were isolated through centrifuging at 12,000 × g for 15 min at 4°C. Proteins were separated by sodium dodecyl sulphate polyacrylamide gel electrophoresis (SDS-PAGE) and transferred to polyvinylidene fluoride (PVDF) membrane (Amersham Life Science, West Chester, PA, USA). The PVDF membrane was blocked in tetrapropyl benzene sulfonate (TPBS) with 5% skimmed milk for 2 h at room temperature. Followed by incubation with primary rabbit Monoclonal Antibodies (Cell Signaling Technology, Beverly, MA, USA): anti-IκB (cat. no. 4812, 1 : 100), anti-p38 MAPK (cat. no. 9212, 1 : 1,000), anti-phosphorylated p38 MAPK (cat. no. 9211, 1 : 500), and mouse anti-β-actin (1 : 200) for 2-4 h at room temperature, respectively. Next, the membranes were incubated with secondary anti-

bodies for 1 h at room temperature. The blotting signals were detected using enhanced chemiluminescence (ECL) reaction reagents.

MTT assay

The effect of propofol on cell viability was determined with 3-(4,5-dimethylthiazol-2-yl)-2,5-diphenyltetrazolium bromide (MTT) kits (Sigma-Aldrich, St. Louis, MO, USA). Cells in various concentrations of the propofol pre-treated group and the control group were plated at a density of 4×10^6 per well, and incubated for 8 h. Then, 10 µl MTT solution was added to each well and continued to incubate for 4 h. The supernatant was removed when the reaction terminated. Finally, the optical density (OD) at 570 nm was measured by a microplate reader (Bio-Rad 550, California, USA).

qRT-PCR

Total RNA was extracted from microglia with Trizol reagent (Invitrogen, Shanghai, China) and reverse transcribed to complementary DNA (cDNA) by using RNA PCR kit (Takara, Shiga, Japan) according to the instructions described by the manufacturer. qRT-PCR was performed in the 7500 Fast Real Time PCR System (Applied Biosystems, Foster City, CA, USA). Relative gene expression was done by the comparative CT method with β-actin gene as the internal control. The primer sequences were as follows: β-actin-F (5' CCGCCACCAGTTCGCCATG 3') and β-actin-R (5' AGGAAGAGGATGCGGCAGTGG 3'); TNF-α-F (5' GCCTCTTCTCATTCCTGCTCGT 3') and TNF-α-R (5' GCTGACGGTGTGGGTGAGGA 3'); IL-6-F (5' AAATGCCAGCCTGCTGACGAAC 3') and IL-6-R (5' AACAACAATCTGAGGTGCCCATGCTAC 3'). The following PCR condition was applied: 95°C for 30 sec, 40 cycles at 95 °C for 5 sec, and 60°C for 30 sec. The relative expression fold change of mRNAs was calculated using the $2^{-\Delta\Delta Ct}$ methods.

ELISA

The levels of proinflammatory cytokines (TNF-α and IL-1β) were detected using TMB enzyme-linked immunosorbent assay (ELISA) kit (Enzyme-linked Biotechnology Co., Ltd, Shanghai, China) according to the manufacturer's protocol. The absorbance was detected at 450 nm in a microplate reader (Bio-Rad 550, California, USA).

Statistical analysis

All experiments were repeated three times, and data were expressed as the means ± standard error of the mean. Significant differences were evaluated by one-way analysis of variance (ANOVA) followed by Tukey's multiple comparison post hoc analysis using GraphPad Prism 5. $P < 0.05$ was considered statistically significant.

Results

Intermittent hypoxia-induced activation of NF-κB/p38 MAPK signalling and expressions of TNF-α and IL-6

Considering that the activity of NF-κB was involved in phosphorylation of p38 MAPK and expression of NF-κB inhibitor, IκB, western blot was conducted to identify the level of phosphorylated p38 MAPK and the expression level of IκB in IH treated microglia. The results showed that the phosphorylation level of p38 MAPK was dramatically increased with IH treatment for 8 h, while the expression level of IκB was significantly decreased with IH treatment for 4 h, especially after treatment with IH for 8 h (Fig. 1A). These results indicated that NF-κB signalling pathway was activated by IH treatment.

Since NF-κB is a potent regulator of the expression of proinflammation cytokines including TNF-α and IL-6, and the expressions of these two proinflammatory cytokines are dramatically induced by IH, we detected the mRNA levels of TNF-α and IL-6 in microglia with IH treatment by qRT-PCR. Compared with normal conditions, IH exposure gave rise to obviously increased TNF-α ($p < 0.05$) and IL-6 mRNA levels ($p < 0.05$) (Fig. 1B). Furthermore, we measured secretion levels of TNF-α and IL-6 in the serum by ELISA. Consistent with the qRT-PCR, IH-induced remarkably secretions of TNF-α ($p < 0.001$) and IL-6 ($p < 0.05$) (Fig. 1C), confirming that IH could induce inflammatory response in microglia.

Non-cytotoxicity of propofol to BV2 microglia

To further investigate the effect of propofol on IH-induced activation of NF-κB signalling and inflammatory response, cytotoxic effects of propofol were monitored by evaluating the alteration in the

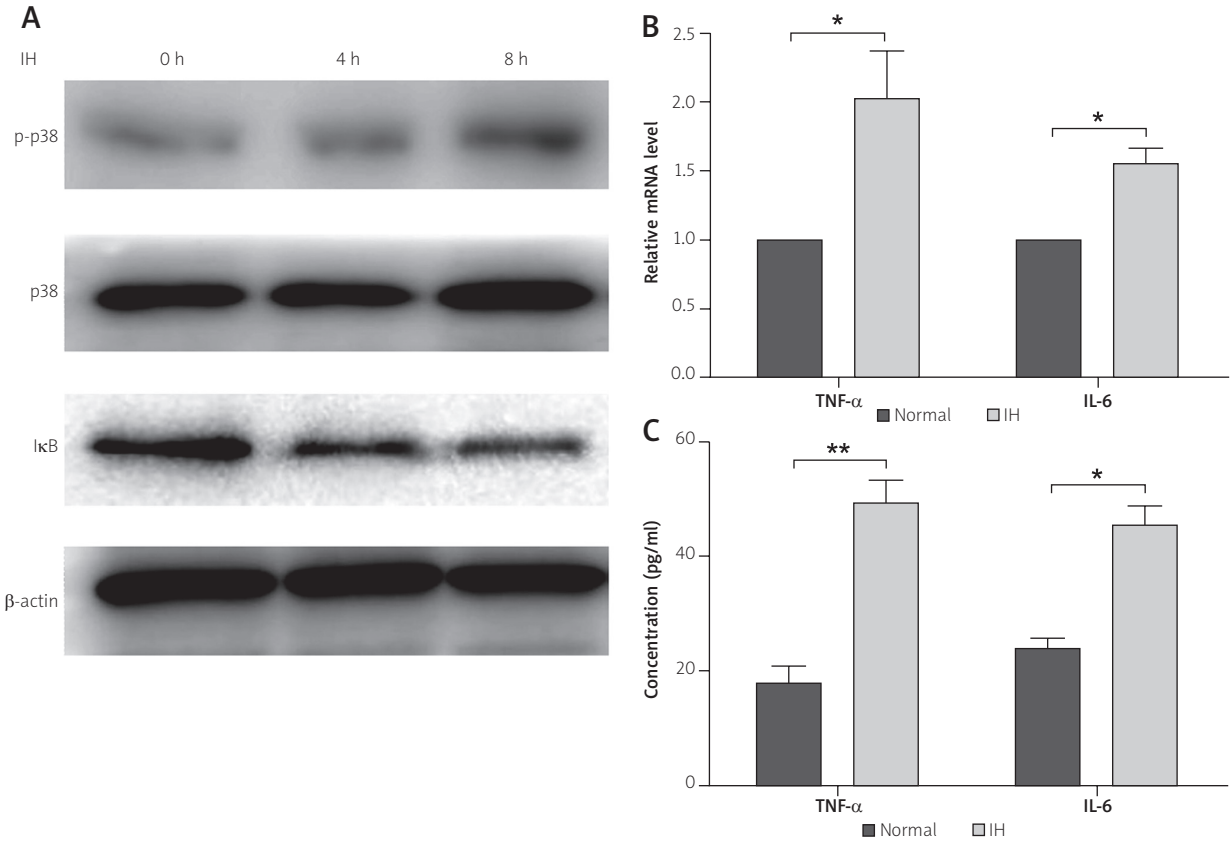

Fig. 1. Effect of intermittent hypoxia (IH) on activation of NF-κB/p38 MAPK signalling and expressions of TNF-α and IL-6. **A)** Effects of IH on p38 MAPK phosphorylation and IκB expression were assayed by western blot. **B)** Effects of IH on TNF-α and IL-6 mRNA levels were demonstrated by qRT-PCR. **C)** Effects of IH on TNF-α and IL-6 protein levels were demonstrated by ELISA analysis. Data are presented as the mean ± standard error of the mean. *$p < 0.05$, **$p < 0.001$. p-38 – p-38 MAPK, p-p38 – phosphorylated p-38 MAPK, IκB – inhibitor of NF-κB, TNF-α – tumor necrosis factor-α, IL-6 – interleukin-6.

viability of microglia via the MTT assay. Compared with controls, there was no significant difference in the viability of BV2 microglia with treatment of diverse concentration (0-250 μM) of propofol (Fig. 2).

Propofol attenuated intermittent hypoxia-induced activation of NF-κB/p38 MAPK signalling in microglia

To examine whether propofol exerts any effects on the phosphorylation level of p38 MAPK and the expression level of IκB in microglia during IH exposure, we investigate the protein levels using western blot. Without IH exposure, the phosphorylation of p38 MAPK remains at a relatively low level, while IH obviously improved the phosphorylation level of p38 MAPK in microglia, and this effect was partially suppressed by pre-treatments with different concentrations of propofol (25 μM, 50 μM, 100 μM) (Fig. 3). Correspondingly, compared with the controls, IH dramatically decreased the level of IκB, this effect was alleviated with propofol pre-treatment in a concentration-dependent manner. With pre-treatment of 50 μM propofol following IH stimulation, the level of IκB increased a little, and the effect was the most notable with pre-treatment of 100 μM propofol (Fig. 3). These observations suggested that propofol could interfere with the IH-induced NF-κB signalling through regulating the phosphorylation level of p38 MAPK and the expression level of IκB.

Propofol suppressed intermittent hypoxia-induced TNF-α and IL-6 production in microglia

To investigate whether pre-treatment with propofol could inhibit IH-induced production of TNF-α and IL-6 in microglia, we measured the mRNA expression

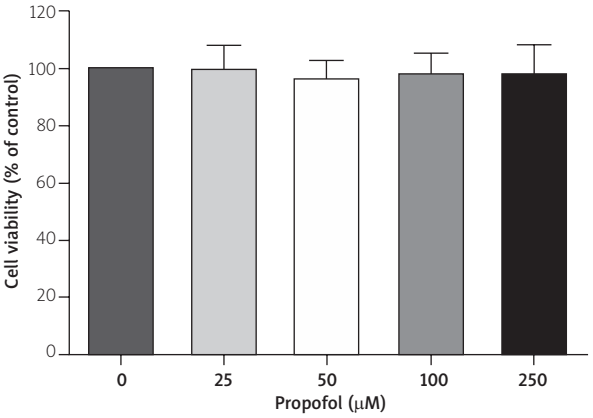

Fig. 2. Effect of propofol on cell viability of microglia was detected by MTT assay. Data are presented as the mean ± standard error of the mean.

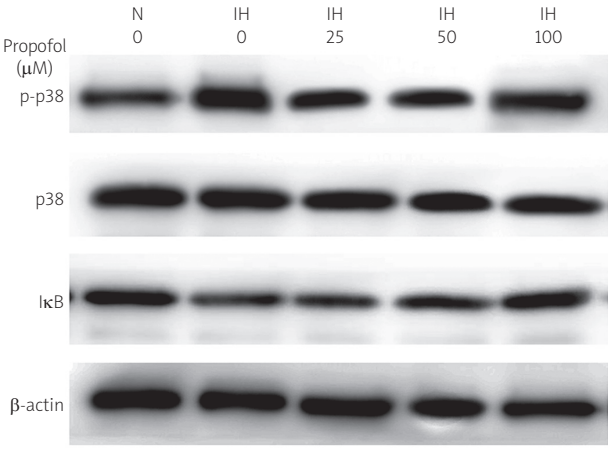

Fig. 3. Effects of propofol on IH-induced alterations of p38 MAPK phosphorylation and IκB expression were analyzed by western blot. p-38 – p-38 MAPK, p-p38 – phosphorylated p-38 MAPK, IκB – inhibitor of NF-κB.

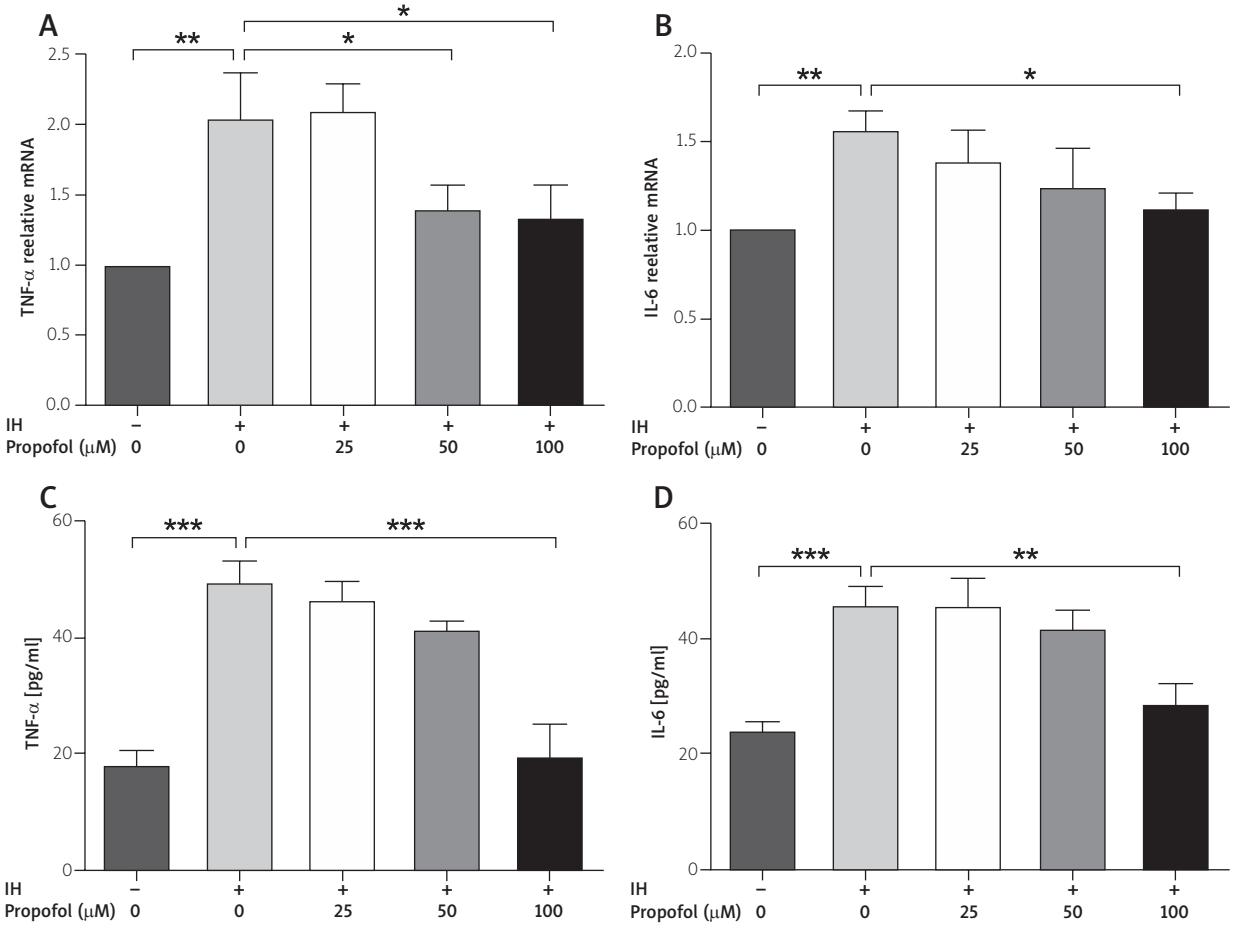

Fig. 4. Effects of propofol on IK-induced TNF-α and IL-6 expression. **A)** TNF-α mRNA level was detected by qRT-PCR. **B)** IL-6 mRNA level was detected by qRT-PCR. **C)** TNF-α protein level was detected by ELISA analysis. **D)** IL-6 protein level was detected by ELISA analysis. Data are presented as the mean ± standard error of the mean. *$p < 0.05$, **$p < 0.001$, ***$p < 0.001$. TNF-α – tumor necrosis factor-α, IL-6 – interleukin-6.

level of TNF-α and IL-6 after microglia treatment with IH in the presence or absence of propofol via qRT-PCR. IH exposure led to a remarkable increase in the TNF-α ($p < 0.001$) and IL-6 ($p < 0.001$) levels (Fig. 4A and B). Propofol at a concentration of 25 μM had no effect on IH-induced mRNA levels of TNF-α and IL-6. However, propofol at a concentration of 50 or 100 μM significantly suppressed the IH-induced TNF-α level ($p < 0.05$) (Fig. 4A), and pre-treatment with 100 μM propofol remarkably reduced IH-induced IL-6 level ($p < 0.05$) (Fig. 4B). Furthermore, the secretion amount of TNF-α and IL-6 into serum under aforementioned conditions were determined by ELISA. We found that IH exposure gave rise to an extremely remarkable rise of TNF-α ($p < 0.0001$) and IL-6 ($p < 0.0001$) in serum, and these effects were obviously attenuated by pre-treatment with 100 μM propofol (Fig. 4C and D).

Discussion

Microglia, as resident immune cells of the CNS, would be activated under inflammatory conditions and followed by inflammatory cascade in the CNS [4,23]. Previous reports confirmed that IH can lead to the activation of microglia and further induce neuron dysfunction and neuroinflammation [32]. Recently, the anti-inflammatory property of propofol has attracted increasing attention. A wealth of information linking that propofol prohibited inflammatory response through preventing the NF-κB and p38 MAPK signalling and then reducing the release of inflammatory mediators is published [25,26]. In addition, emerging evidence showed that propofol selectively attenuated the activation of NF-κB and p38 MAPK in vascular endothelium during IH exposure [16]. The effect of propofol on IH treated microglia was still unclear. Thus, in the current study, we focused on microglia and examined whether propofol exerts an efficient effect on microglia exposed to IH.

Among the inflammatory mediators induced by activated microglia, TNF-α and IL-6 are two of the main proinflammatory cytokines. TNF-α plays a core role in the proinflammatory cytokines and its temporary existence will promote the secretion of IL-1, IL-6, and other secondary inflammatory mediators. IL-6 could serve a dual function by also causing inflammation and resisting inflammation. Considering that its clearance rate is far below than that of other cytokines, the level of IL-6 can reflect the severity of the disease and prognosis. Overproduction of TNF-α and IL-6 can cause various neurodegenerative diseases, including AD and Parkinson's disease (PD) [3,29]. It has been reported that propofol can inhibit the release of inflammatory factors such as TNF-α and IL-6 [11,27]. This study first reported that propofol significantly reduced the IH-induced secretion of proinflammatory cytokines, TNF-α and IL-6, in microglia.

NF-κB, a pleiotropic regulator involved in microglial cell responses, can suppress the production of proinflammatory enzymes and cytokines, including NO, PGE2, TNF-α and IL-6 [13,24,34]. Under normal circumstances, NF-κB binds to IκB to form an inactive heterodimer in the cytoplasm. While suffering from inflammation, IκB is phosphorylated and subjected to degradation by proteasomes. Consequently, NF-κB will be disassociated from IκB and translocate into nucleus, followed by the activation of NF-κB-dependent proinflammatory molecules [6,7]. It has been demonstrated that propofol suppresses the IH-induced NF-κB activity by preventing the phosphorylation of IκB and accompanied by down-regulated secretion of proinflammatory cytokines in the vascular endothelial cells [16].

Additionally, MAPKs, including the extracellular signal-regulated kinase (ERK), the c-jun NH2-terminal kinases (JNK) and the p38 MAPK, can be phosphorylated and then positively regulate the expression of inflammatory genes and cytokines [31,35]. Among these, p38 MAPK acts as a crucial regulator for the production of NF-κB-mediated proinflammatory cytokines and other mediators [15]. Glaucocalyxin A (GLA) can inhibit pro-inflammatory cytokines expression in microglial cells through NF-κB and p38 MAPK signalling pathways [14]. A recent report clarified that triroside attenuated the neuroinflammation in microglia via NF-κB and p38 MAPK signalling pathways [28]. Furthermore, propofol suppressed the NF-κB-mediated inflammation by prohibiting the activation of p38 MAPK in IH-treated vascular endothelium [16]. Consistently with previous reports, IH-induced activation of NF-κB and p38 MAPK both were dramatically reduced by propofol treatment in the present study. Combined with all the results, we showed that propofol alleviates IH-induced secretion of proinflammatory cytokines in microglia probably via inhibiting NF-κB and p38 MAPK signalling.

In conclusion, the present study highlighted the crucial role of propofol in hampering IH-induced

microglia inflammation, which would result in serious neuron damage and dysfunction and further leads to neurodegenerative diseases. Therefore, propofol with the effect of neuroprotection is a novel therapeutic objective for neurodegenerative disorders.

Acknowledgments

The study was supported by the National Natural Science Foundation of China (81670083). We are grateful to Professor Qingyun Li, the Ruijin hospital affiliated to the Shanghai Jiao Tong University School of Medicine, for providing the intermittent hypoxia cell culture chamber and intermittent hypoxia control system.

Disclosure

Authors report no conflict of interest.

References

1. Amor S, Puentes F, Baker D, van der Valk P. Inflammation in neurodegenerative diseases. Immunology 2010; 129: 154-169.
2. Boutahar N, Reynaud E, Lassabliere F, Borg J. Brain-derived neurotrophic factor inhibits cell cycle reentry but not endoplasmic reticulum stress in cultured neurons following oxidative or excitotoxic stress. J Neurosci Res 2010; 88: 2263-2271.
3. Cameron B, Landreth GE. Inflammation, microglia, and Alzheimer's disease. Neurobiol Dis 2010; 37: 503-509.
4. Chen C, Qian Y. Protective role of dexmedetomidine in unmethylated CpG-induced inflammation responses in BV2 microglia cells. Folia Neuropathol 2016; 54: 382-391.
5. Choi Y, Lee MK, Lim SY, Sung SH, Kim YC. Inhibition of inducible NO synthase, cyclooxygenase-2 and interleukin-1beta by torilin is mediated by mitogen-activated protein kinases in microglial BV2 cells. Br J Pharmacol 2009; 156: 933-940.
6. Dai JN, Zong Y, Zhong LM, Li YM, Zhang W, Bian LG, Ai QL, Liu YD, Sun J, Lu D. Gastrodin inhibits expression of inducible NO synthase, cyclooxygenase-2 and proinflammatory cytokines in cultured LPS-stimulated microglia via MAPK pathways. PLoS One 2011; 6: e21891.
7. Fang IM, Yang CH, Yang CM, Chen MS. Linoleic acid-induced expression of inducible nitric oxide synthase and cyclooxygenase II via p42/44 mitogen-activated protein kinase and nuclear factor-kappaB pathway in retinal pigment epithelial cells. Exp Eye Res 2007; 85: 667-677.
8. Feng J, Wu Q, Zhang D, Chen BY. Hippocampal impairments are associated with intermittent hypoxia of obstructive sleep apnea. Chin Med J (Engl) 2012; 125: 696-701.
9. Fung SJ, Xi MC, Zhang JH, Sampogna S, Yamuy J, Morales FR, Chase MH. Apnea promotes glutamate-induced excitotoxicity in hippocampal neurons. Brain Res 2007; 1179: 42-50.
10. Gepts E, Camu F, Cockshott ID, Douglas EJ. Disposition of propofol administered as constant rate intravenous infusions in humans. Anesth Analg 1987; 66: 1256-1263.
11. Hsing CH, Lin MC, Choi PC, Huang WC, Kai JI, Tsai CC, Cheng YL, Hsieh CY, Wang CY, Chang YP, Chen YH, Chen CL, Lin CF. Anesthetic propofol reduces endotoxic inflammation by inhibiting reactive oxygen species-regulated Akt/IKKbeta/NF-kappaB signaling. PLoS One 2011; 6: e17598.
12. Jha MK, Jeon S, Suk K. Glia as a Link between Neuroinflammation and Neuropathic Pain. Immune Netw 2012; 12: 41-47.
13. Jung HW, Yoon CH, Park KM, Han HS, Park YK. Hexane fraction of Zingiberis Rhizoma Crudus extract inhibits the production of nitric oxide and proinflammatory cytokines in LPS-stimulated BV2 microglial cells via the NF-kappaB pathway. Food Chem Toxicol 2009; 47: 1190-1197.
14. Kim BW, Koppula S, Hong SS, Jeon SB, Kwon JH, Hwang BY, Park EJ, Choi DK. Regulation of microglia activity by glaucocalyxin-A: attenuation of lipopolysaccharide-stimulated neuroinflammation through NF-kappaB and p38 MAPK signaling pathways. PLoS One 2013; 8: e55792.
15. Kumar S, Boehm J, Lee JC. p38 MAP kinases: key signalling molecules as therapeutic targets for inflammatory diseases. Nat Rev Drug Discov 2003; 2: 717-726.
16. Li D, Wang C, Li N, Zhang L. Propofol selectively inhibits nuclear factor-kappaB activity by suppressing p38 mitogen-activated protein kinase signaling in human EA.hy926 endothelial cells during intermittent hypoxia/reoxygenation. Mol Med Rep 2014; 9: 1460-1466.
17. Lima IV, Bastos LF, Limborco-Filho M, Fiebich BL, de Oliveira AC. Role of prostaglandins in neuroinflammatory and neurodegenerative diseases. Mediators Inflamm 2012; 2012: 946813.
18. Ma L, Wu X, Chen W, Fujino Y. Propofol has anti-inflammatory effects on alveolar type II epithelial cells. Acta Anaesthesiol Scand 2010; 54: 362-369.
19. Ma X, Hu YW, Zhao ZL, Zheng L, Qiu YR, Huang JL, Wu XJ, Mao XR, Yang J, Zhao JY, Li SF, Gu MN, Wang Q. Anti-inflammatory effects of propofol are mediated by apolipoprotein M in a hepatocyte nuclear factor-1alpha-dependent manner. Arch Biochem Biophys 2013; 533: 1-10.
20. Magni P, Ruscica M, Dozio E, Rizzi E, Beretta G, Maffei Facino R. Parthenolide inhibits the LPS-induced secretion of IL-6 and TNF-alpha and NF-kappaB nuclear translocation in BV-2 microglia. Phytother Res 2012; 26: 1405-1409.
21. Marik PE. Propofol: an immunomodulating agent. Pharmacotherapy 2005; 25: 28S-33S.
22. Short TG, Aun CS, Tan P, Wong J, Tam YH, Oh TE. A prospective evaluation of pharmacokinetic model controlled infusion of propofol in paediatric patients. Br J Anaesth 1994; 72: 302-306.
23. Streit WJ, Mrak RE, Griffin WS. Microglia and neuroinflammation: a pathological perspective. J Neuroinflammation 2004; 1: 14.
24. Tak PP, Firestein GS. NF-kappaB: a key role in inflammatory diseases. J Clin Invest 2001; 107: 7-11.
25. Tang J, Chen X, Tu W, Guo Y, Zhao Z, Xue Q, Lin C, Xiao J, Sun X, Tao T, Gu M, Liu Y. Propofol inhibits the activation of p38 through up-regulating the expression of annexin A1 to exert its anti-inflammation effect. PLoS One 2011; 6: e27890.
26. Tian Y, Guo S, Guo Y, Jian L. Anesthetic Propofol Attenuates Apoptosis, Abeta Accumulation, and Inflammation Induced by Sevo-

flurane Through NF-kappaB Pathway in Human Neuroglioma Cells. Cell Mol Neurobiol 2015; 35: 891-898.
27. Tsao CM, Ho ST, Chen A, Wang JJ, Tsai SK, Wu CC. Propofol ameliorates liver dysfunction and inhibits aortic superoxide level in conscious rats with endotoxic shock. Eur J Pharmacol 2003; 477: 183-193.
28. Velagapudi R, Aderogba M, Olajide OA. Tiliroside, a dietary glycosidic flavonoid, inhibits TRAF-6/NF-kappaB/p38-mediated neuroinflammation in activated BV2 microglia. Biochim Biophys Acta 2014; 1840: 3311-3319.
29. Wang XJ, Yan ZQ, Lu GQ, Stuart S, Chen SD. Parkinson disease IgG and C5a-induced synergistic dopaminergic neurotoxicity: role of microglia. Neurochem Int 2007; 50: 39-50.
30. Wang Y, Zhang SX, Gozal D. Reactive oxygen species and the brain in sleep apnea. Respir Physiol Neurobiol 2010; 174: 307-316.
31. Yang H, Wang S, Yu L, Zhu X, Xu Y. Esculentoside A suppresses Abeta-induced neuroinflammation by down-regulating MAPKs pathways in vivo. Neurol Res 2015; 37: 859-866.
32. Zhang SX, Wang Y, Gozal D. Pathological consequences of intermittent hypoxia in the central nervous system. Compr Physiol 2012; 2: 1767-1777.
33. Zhou CH, Zhu YZ, Zhao PP, Xu CM, Zhang MX, Huang H, Li J, Liu L, Wu YQ. Propofol Inhibits Lipopolysaccharide-Induced Inflammatory Responses in Spinal Astrocytes via the Toll-Like Receptor 4/MyD88-Dependent Nuclear Factor-kappaB, Extracellular Signal-Regulated Protein Kinases1/2, and p38 Mitogen-Activated Protein Kinase Pathways. Anesth Analg 2015; 120: 1361-1368.
34. Zhu C, Xiong Z, Chen X, Peng F, Hu X, Chen Y, Wang Q. Artemisinin attenuates lipopolysaccharide-stimulated proinflammatory responses by inhibiting NF-kappaB pathway in microglia cells. PLoS One 2012; 7: e35125.
35. Zhu Y, Li H, Long C, Hu L, Xu H, Liu L, Chen S, Wang DC, Shao F. Structural insights into the enzymatic mechanism of the pathogenic MAPK phosphothreonine lyase. Mol Cell 2007; 28: 899-913.
36. Zielinski J. Effects of intermittent hypoxia on pulmonary haemodynamics: animal models versus studies in humans. Eur Respir J 2005; 25: 173-180.

Original paper

Folia Neuropathologica

Neuronal vacuolation and spinocerebellar degeneration associated with altered neurotransmission

Aggeliki Giannakopoulou

Laboratory of Anatomy, Histology and Embryology, School of Veterinary Medicine, Faculty of Health Sciences, Aristotle University of Thessaloniki, Thessaloniki, Greece and Department of Hematology, G. Papanikolaou General Hospital, Thessaloniki, Greece

Folia Neuropathol 2017; 55 (2): 132-145 DOI: https://doi.org/10.5114/fn.2017.68580

Abstract

Inherited neurodegenerative disorders are debilitating diseases that occur across different species, such as the domestic dog (Canis lupus familiaris), and many are caused by mutations in the same genes as corresponding human conditions. In the present study, we report an inherited neurodegenerative condition, termed 'neuronal vacuolation and spinocerebellar degeneration' (NVSD) which affects neonatal or young dogs, mainly Rottweilers, which recently has been linked with the homozygosity for the RAB3GAP1:c.743delC allele. Mutations in human RAB3GAP1 cause Warburg micro syndrome (WARBM), a severe developmental disorder characterized predominantly by abnormalities of the nervous system including axonal peripheral neuropathy. RAB3GAP1 encodes the catalytic subunit of a GTPase activator protein and guanine exchange factor for Rab3 and Rab18 proteins, respectively. Rab proteins are involved in membrane trafficking in the endoplasmic reticulum, autophagy, axonal transport and synaptic transmission.

The present study attempts to carry out a detailed histopathological examination of NVSD disease, extending from peripheral nerves to lower brain structures focusing on the neurotransmitter alterations noted in the cerebellum, the major structure affected. NVSD dogs presented with progressive cerebellar ataxia and some clinical manifestations that recapitulate the WARBM phenotype. Neuropathological examination revealed dystrophic axons, neurodegeneration and intracellular vacuolization in specific nuclei. In the cerebellum, severe vacuolation of cerebellar nuclei neurons, atrophy of Purkinje cells, and diminishing of GABAergic and glutamatergic fibres constitute the most striking lesions. The balance of evidence suggests that the neuropathological lesions are a reaction to the altered neurotransmission. The canine phenotype could serve as a model to delineate the disease-causing pathological mechanisms in RAB3GAP1 mutation.

Key words: *spinocerebellar ataxia, Purkinje cells atrophy, neurotransmitters, neurodegeneration.*

Introduction

Several inherited disorders of men are characterized by progressive cerebellar degeneration, but attempts to correlate the observed clinical signs with the neuropathological lesions are complicated by problems associated with the analysis of human post-mortem material [49]. Moreover, in most disorders, the relationship between the appearance of a lesion and the underlying disease process is unclear [5]. Recently, a well-documented inherited disease of Rottweiler dogs named neuronal vacuolation spi-

Communicating author

Aggeliki Giannakopoulou, MD, DVM, PhD, Department of Hematology, G. Papanikolaou General Hospital, Thessaloniki, Greece, e-mail: agiann@auth.gr

nocerebellar degeneration (NVSD) has been linked with the homozygosity for the RAB3GAP1:c.743delC allele [32]. Mutations in human RAB3GAP1 cause Warburg micro syndrome (WARBM), a severe developmental disorder characterized predominantly by abnormalities of the nervous system including axonal peripheral neuropathy. In WARBM and NVSD, the effect of gene mutation encoding RAB3GAP1 on the degeneration of specific anatomical pathways, has not yet been clarified.

WARBM is a rare autosomal recessive genetic disorder, caused by changes in one of at least four different genes, *RAB3GAP1*, *RAB3GAP2*, *RAB18* and *TBC1D20*. In relation to *RAB3GAP1*, which is also mutated in NVSD, is a 130-kDa protein that forms, together with the 150 kDa *RAB3GAP2*, the heterodimeric RAB3GAP complex. This complex regulates the activity of members of the RAB3 family that are master regulators of vesicle trafficking and exocytosis of hormones and neurotransmitters [20,39]. RAB family members cycle between a GDP-bound inactive and a GTP-bound active form. The GTP-bound active form of RAB3 family members is inactivated by GTP hydrolysis before, during, and after the fusion of the vesicle by the stimulation of RAB3GAP [14]. Rab3GAP not only functions as a GAP for the Rab3s but also functions as a guanine exchange factor (GEF) for Rab18. Specifically, Rab3GAP localizes to the endoplasmatic reticulum (ER) and some point mutations in RAB3GAP1 that cause WARBM in humans affect Rab18 GEF activity [16]. Supporting the view that Rab18 activity is important for the ER structure, direct loss of Rab18 function or loss of Rab18 activation at the ER by the absence of Rab3GAP activity can cause WARBM [19].

WARBM and NVSD share considerable clinical similarities, although some differences do exist. NVSD affects puppies younger than 6 months, often as young as 6 to 8 weeks and sometimes littermates. It has been recognised mainly in Rottweiler dogs [13,27,41,43,52] and their cross [12]. Typical signs of the disease include progressive cerebellar ataxia, spastic tetraparesis, dysmetria, ocular motor disorders such as episodic nystagmus, microphthalmia and congenital cataracts, axonal peripheral neuropathy with laryngeal paralysis and rarely behavioural changes [27,30]. Children with WARBM have severe developmental delays, ocular abnormalities including congenital cataracts and microphthalmia, and a predominantly axonal peripheral neuropathy and never develop the ability to walk [18,20,38]. Histopathological hallmarks in NVSD, which have been described so far, are the bilateral and symmetrical neuronal vacuolation involving brainstem and deep cerebellar nuclei (DCN), the Purkinje cell (PC) atrophy, the degeneration of the dorsolateral fasciculi in the spinal cord (SC) and the axonal neuropathy in peripheral nerves with spheroid formation and loss of thick myelinated fibres. There are no reports describing histopathology in WARBM, but MRIs of affected children have shown predominantly cerebellar atrophy [20,33].

The present study investigates the four key features mentioned below, proposed by Armstrong [4] as the 'primary determinants' of a neurodegenerative disease, to provide a descriptive framework of NVSD. These features are the anatomical pathways affected by the disease, the target cell populations, the molecular pathology and the morphological degeneration, which are used to reveal the similarities and differences between NVSD and WARBM. The main focus of this study was the identification of neurotransmitter disturbances noted in the cerebellum of NVSD-affected animals, to clarify the underlying mechanisms involved. Herein we provide a comprehensive histological picture of NVSD and we suggest that the specific neuropathology is a reaction to degenerative processes due to altered neurotransmission caused by the RAB3GAP1 mutation.

Material and methods

Phenotypes

Animal experimentation received the approval of the Veterinary Directorate of Thessaloniki and was conducted under compliance with the National Institutes of Health guidelines, Greek Government guidelines and the local ethics committee. The first dog was a 3-month-old female Rottweiler, which was initially admitted with acute inspiratory dyspnoea and stridor, both of which resolved after treating the animal in the intensive care unit. Neurological examination revealed ataxia, spastic tetraparesis, hypermetria and proprioceptive deficits, hyperreflexia and hypertonicity that were more pronounced in the hind limbs.

One month later, its littermate (second dog), a four-month-old male was also admitted with ataxia and weakness as the main complaints, as well as abnormal swallowing and failure to bark. Mild inspiratory stridor, ataxia, spastic tetraparesis, hypermetria, positional strabismus and nystagmus were detected in neuro-

logical examination. A unilateral laryngeal paresis was diagnosed with laryngoscopy. Motor signs worsened progressively over the next two months in both puppies, finally leading to severe tetraparesis. Due to the severely incapacitating signs and poor prognosis, the puppies were eventually euthanized.

The third dog was a 6-month-old male from the same progenitors, which was presented with the wide base posture, hind limb weakness progressing to paraparesis and difficulty in swallowing and breathing associated to megaesophagus. This led to the compression of the trachea and difficulty in breathing. Motor signs worsened progressively over the next month leading to ataxia, spastic tetraparesis (more severe in hind limbs) with slowed proprioceptive placing reactions in all neurologically examined limbs. The breeder declined further examinations and requested euthanasia because of poor prognosis.

Animal handling, tissue processing, and histopathology techniques

All dogs were euthanized under pentothal deep anaesthesia, following xylazine sedation, and were transcardially perfused with normal saline followed by 4% paraformaldehyde in 0.1 M phosphate buffer. Two age-matched dogs sacrificed during unrelated non-neurological diseases, were processed in parallel. Tissue samples were taken from the brain (brain stem and cerebellum), spinal cord (cervical, thoracic and lumbar segments), nerve dorsal roots (DR), dorsal root ganglia (DRG), and peripheral nerves both from fore- and hindlimbs. Median, ulnar and radial, sciatic, common peroneal, tibial, sural and musculocutaneous nerves were collected. Also, the vagus nerve, external and internal branches of the superior laryngeal nerve (SLN) and the recurrent laryngeal nerve (RLN) were taken and embedded in paraffin and routinely processed for 6 µm-thick sections. Dewaxed sections were stained with the following histological techniques: hematoxylin and eosin (H&E), Luxol-fast blue-Klüver Barrera and Bielschowsky (BLS) or processed for immunohistochemistry (IHC) with appropriate primary antibodies. Masson's trichrome stain was performed in DRG and peripheral nerves to reveal possible fibrosis. In addition, small blocks of sciatic, sural, median, superior laryngeal nerve and RLN nerves were fixed in 2.5% glutaraldehyde, dehydrated through alcohol solutions, stained with 4% osmium tetroxide and embedded in Araldite. Semithin sections obtained were stained with toluidine blue and observed under the light microscope.

Histologically stained sections were examined by two independent researchers and evaluated for neuronal and axonal degeneration and loss, as revealed by BLS. Demyelination and other myelin abnormalities were evaluated in Luxol fast blue-Klüver Barrera paraffin sections or toluidine blue stained semithin sections. The spatial distribution of neuronal vacuolation was also investigated.

Immunohistochemistry

A set of IHC and immunofluorescence (IF) techniques were performed on paraffin sections to reveal astrocytic/microglia activation and neurotransmitter alterations in the cerebellum. Glutamate is the prevalent excitatory neurotransmitter for both the mossy fibre and climbing fibre system. Mossy fibres form synapses on granule cells in the GCL of the cortex and on neurons in the DCN. Climbing fibres coming from inferior olive nuclei form excitatory synapses directly on PCs and are strongly enriched in glutamate. In DCN, there are large glutamatergic neurons that project to premotor areas and directly regulate the motor control. On the other hand, GABA is the primary inhibitory neurotransmitter known to counterbalance the action of glutamate. PCs, the sole output neurons of the cerebellar cortex are GABAergic and project to the DCN and vestibular nuclei neurons. The DCN and vestibular nuclei are involved in motor control in animals through their communication with the nuclei of the thalamus and brainstem. GABA is also the predominant transmitter of cerebellar interneurons (basket cells, stellate cells, Golgi cells, Lugaro cells), except for unipolar brush cells, which are glutamatergic interneurons. In DCN, apart from the large glutamatergic neurons, there are small GABAergic projection neurons that send outputs to inferior olive nuclei and GABAergic local interneurons. The activities of GABA are mediated by vesicular or non-vesicular release after GABA is synthesized by glutamate decarboxylase (GAD), an enzyme that catalyses the decarboxylation of glutamate to GABA. The availability of antibodies against the neurotransmitters glutamate and GABA, and their receptors, such the *N*-methyl-*D*-aspartate receptor1 (NMDAR1), which mediates neuronal functions in glutamate neurotransmission,

Table I. Primary antibodies used

Antibody		Supplier	Dilution	*Ad hoc* References
Anti-GFAP	Rabbit polyclonal	Dako Corporation, Carpinteria, CA	1 : 1000	De Nevi *et al*. Eur J Histochem 2013; 57: e9
Anti-Iba1	Rabbit polyclonal	Wako, Osaka, Japan	1 : 1000	Lab Anim Res 2012; 28: 165-170 Ahmed *et al*. J Histochem Cytochem 2007; 55: 687-700
Anti-GABA	Rabbit polyclonal	Sigma, St. Louis, USA	1 : 500	Am J Med Genet 1995; 57: 204-212
Anti-GAD67	Mouse monoclonal	Millipore, Temecula, CA	1 : 1000	Neurosci Lett 2008; 431: 251-255
Anti-glutamate	Rabbit polyclonal	Millipore, Temecula, CA	1 : 500	Am J Vet Res 2005; 66: 791-799 J Vet Med Sci 2005; 67: 1119-1126
Anti-NMDAR1	Mouse monoclonal	BD Pharmingen	1 : 250	Brain Res 1996; 723: 77-89
Anti-calbindin	Rabbit polyclonal	Millipore, Temecula, CA	1 : 800	Res Vet Sci 2010; 88: 122-126

has made it possible to examine the neurohumoral synaptic transmission in the cerebellum and brain stem that are of interest in NVSD. Details of the antibodies used and their dilutions are given in Table I.

IHC was carried out using the avidin-biotin-peroxidase complex (ABC) method. In brief, antigen retrieval was performed by incubating deparaffinized – rehydrated sections in citrate buffer 0.01 M (pH 6) under microwave treatment at 750 Watt for 3 minutes and thereafter at 350 Watt for 7 minutes. These sections were cooled down at RT for 20 minutes and thereafter were treated with 2% hydrogen peroxide in 5% methanol for 20 minutes followed by 5% normal goat serum for 2 h, and subsequently one of the primary antibodies were applied overnight at 4°C. Labelling was visualized with DAB (Vector) after pre-treatment with the ABC kit (Vector, Vectastain) and sections were counterstained with haematoxylin. For IF the following secondary antibody: anti-mouse Alexa Fluor 488 and anti-rabbit Alexa fluor 488 (all in dilution 1 : 400, Molecular Probes) were used. Two observers, blinded to the identity of tissue sections, reviewed the IHC and IF preparations independently.

Quantitative analysis of neurotransmitter alterations and their receptors

Seven to ten representative sections IHC stained for each antigenic marker were used for quantifications and photomicrographs were captured using a Nikon upright fluorescence microscope D-Eclipse 80i C1. Photomicrographs were subjected to digital optical densitometry with ImageJ, version 1.51f (National Institutes of Health, Bethesda, Maryland, USA), and were analysed by the following methods. One method, which was used to quantify the intracellular GABA, NMDAR1 and calbindin integrated optical density (IOD) in neurons, integrates the grey value of the inverted image. For GAD, IF labelling was used and for the measurement of IOD there was no need to invert the images. The second method, which measures the area over which the immunoreactivity exceeds a given threshold, was applied to the glutamate and GABA staining for the quantification of glutamatergic and GABAergic fibres, respectively.

Statistical analyses

Statistical analyses were performed with non-parametric tests. Differences between two groups (NVSD vs. controls) per anatomical area were assessed with Wilcoxon Mann-Whitney *U* tests. SPSS v20.0 statistical software system (IBM Corporation, Armonk, New York, USA) was used for calculations. The reported *p* values were the result of two-tailed tests; *p* values smaller or equal to 0.05 were considered statistically significant.

Results

Lesions in peripheral nerves and the spinal cord

Major histopathological lesions observed are summarized in Table II and have already been described by others. In relation to peripheral nerves, there was axonopathy with dystrophic axons, which was more severe in sensory nerves. In semithin sections, there was lack of large myelin sheaths and endoneurial fibrosis. RLN and SLN showed a prevalence of small-diameter fibres with axonal degeneration. Shrinkage of DRs with lack of large axons and mild fibrosis constitute the major abnormality of the DRG on NVSD. Vacuolation of

Table II. Histopathological findings in NVSD-affected dogs

Peripheral nerves	1. Loss of large-diameter myelinated fibres and prevalence of small-diameter fibres. 2. Lack of large myelin sheaths. 3. Thinning of axons and their myelin sheaths. 4. Axonopathy with dystrophic axons. 5. Endoneurial fibrosis.	
Dorsal spinal roots	1. Shrinkage. 2. Lack of large axons. 3. Predominance of small myelinated fibres. 4. Mild fibrosis.	
Ventral spinal roots	Well preserved.	
Dorsal root ganglia	1. Increase of satellite cells (S-100+ and GFAP+ cells) 2. Presence of residual nodes. 3. Reactive fibrosis (proliferation of small spindle-shaped cells). 4. Reduction of large pseudounipolar neurons. 5. Presence of dystrophic axons.	
Spinal cord		
White matter	1. Fasciculi mainly affected: gracile and cuneate fascicles, dorsal and lateral spinocerebellar, lateral corticospinal fasciculi. 2. Loss of large myelinated fibres. 3. Axonal degeneration, with axons forming spheroids or ovoids. 4. Myelin pallor.	
Grey matter	1. Shrinkage of dorsal horns. 2. Neuronal loss in Clarke's column. 3. Vacuolated interneurons in laminae VI and VII.	
Brain stem		
Vestibular nuclei	1. Neuronal vacuolation in the following nuclei: 1) dorsal column nuclei (gracilis and cuneatus), 2) spinal trigeminal nucleus, 3) Deiter's nucleus (nD) or nucleus vestibularis inferior, 4) triangular nucleus or nucleus vestibularis medialis, 5) nucleus of Roller (nR) or sublingual nucleus and 6) nucleus of the solitary tract. 2. Microglia activation and mild astrocytosis.	
White matter	Axonal degeneration and myelin pallor.	
Olivary nuclei	1. Vacuolated neurons. 2. Partially spongiform appearance of the structure. 3. Atrophy of large neurons and diffuse axonal loss.	
Cerebellum		
Cerebellar nuclei	1. Profound neuronal vacuolation. 2. Loss of large neurons. 3. Atrophy of cerebellar nuclei and their efferent myelinated fibres. 4. Astrocytosis and focal microgliosis. 5. Spongiform appearance. 6. Myelin pallor and axonal loss in neuropils.	
Cerebellar cortex	Molecular layer	Altered fragmented dendritic trees of Purkinje cells.
	Purkinje cell layer	Atrophy and loss in most cerebellar lobules. Mild Bergmann gliosis.
	Granular layer	Axonal torpedoes belonging to the axons of Purkinje cells.

pseudounipolar neurons of DRG was not observed, but moderate neuronal loss of large neurons was evident. Dystrophic axons characterized by focal dilations and bulb like structures were also noted.

In the white matter of SC, lesions were mainly located in gracile and cuneate fascicles, in dorsal spinocerebellar and lateral corticospinal fasciculi. In these areas, myelin sheaths were found either empty or occasionally containing swollen axons forming spheroids or ovoids. In cervical SC, the axonal degeneration and myelin loss were most prominent in the lateral spinocerebellar tract. In spinal grey matter,

the most profound finding was the shrinkage of the dorsal horn and its neuronal loss, most evident in Clarke's column. Vacuolated neurons were found mainly in the medial part of laminae VI and VII presumably representing interneurons and observed sparsely only in the ventral horn of SC.

Neuropathology of the brain stem

In the brain stem, there was a moderate vacuolation of neurons bilaterally in many nuclei of the dorsal medulla oblongata (Table II and Fig. 1). Neuronal vacuolation was characterized by intracytoplasmic single or multiple vacuoles of variable size, ranging from 3 to 40 µm, arranged either individually or in clusters. Vacuoles were round and empty and in paraffin-embedded sections, were not stained with histochemical methods (Figs. 2A and B). Neuronal vacuolation was accompanied by microglia activation and mild astrocytosis. In the inferior olivary nucleus, the presence of vacuolated neurons resulted in the spongiform appearance of the structure. Atrophy of large neurons in the olivary nucleus and diffuse axonal loss were also evident. IHC showed that the median IOD of GAD in the remaining neurons of the olivary nucleus of NVSD animals was elevated approximately twofold compared with controls and this difference was statistically significant. Medians of GAD IODs in NVSD and controls were 52,023 and 18,556, respectively; the distributions in the two groups differed significantly (Mann-Whitney $U = 11.5$, $z = -5.307$, $p < 0.001$ two-tailed, Fig. 4C).

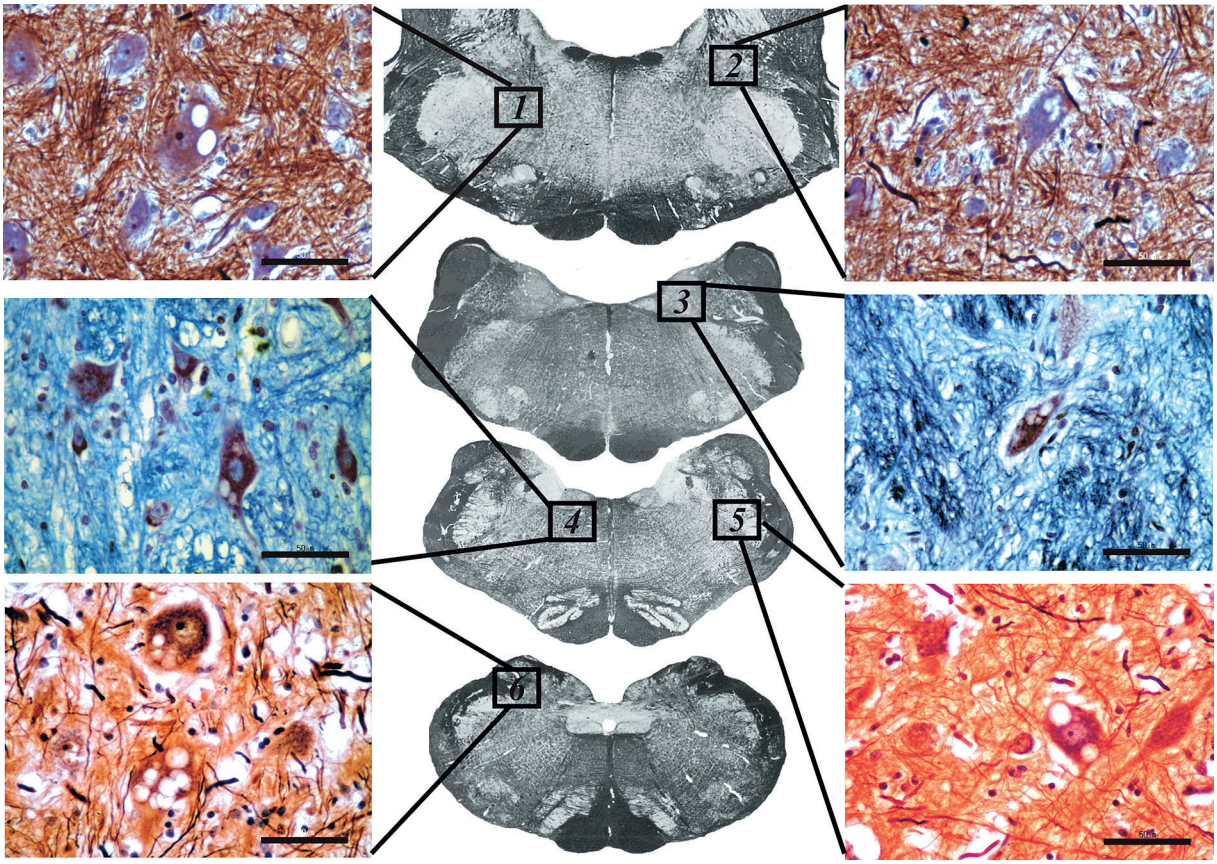

Fig. 1. Photomicrographs of transverse sections through different segments of the brain stem in NVSD animals stained with either BLS or Luxol Fast blue-Klüver Barrera. Vacuolated neurons were detected mainly at: 1 – the reticular formation, 2 – the descent vestibular nucleus, 3 – the medial vestibular nucleus, 4 – the nucleus of Roller, 5 – the nucleus of the trigeminal nerve, 6 – the external nucleus of fasciculus cuneatus. Scale bars are 50 µm.

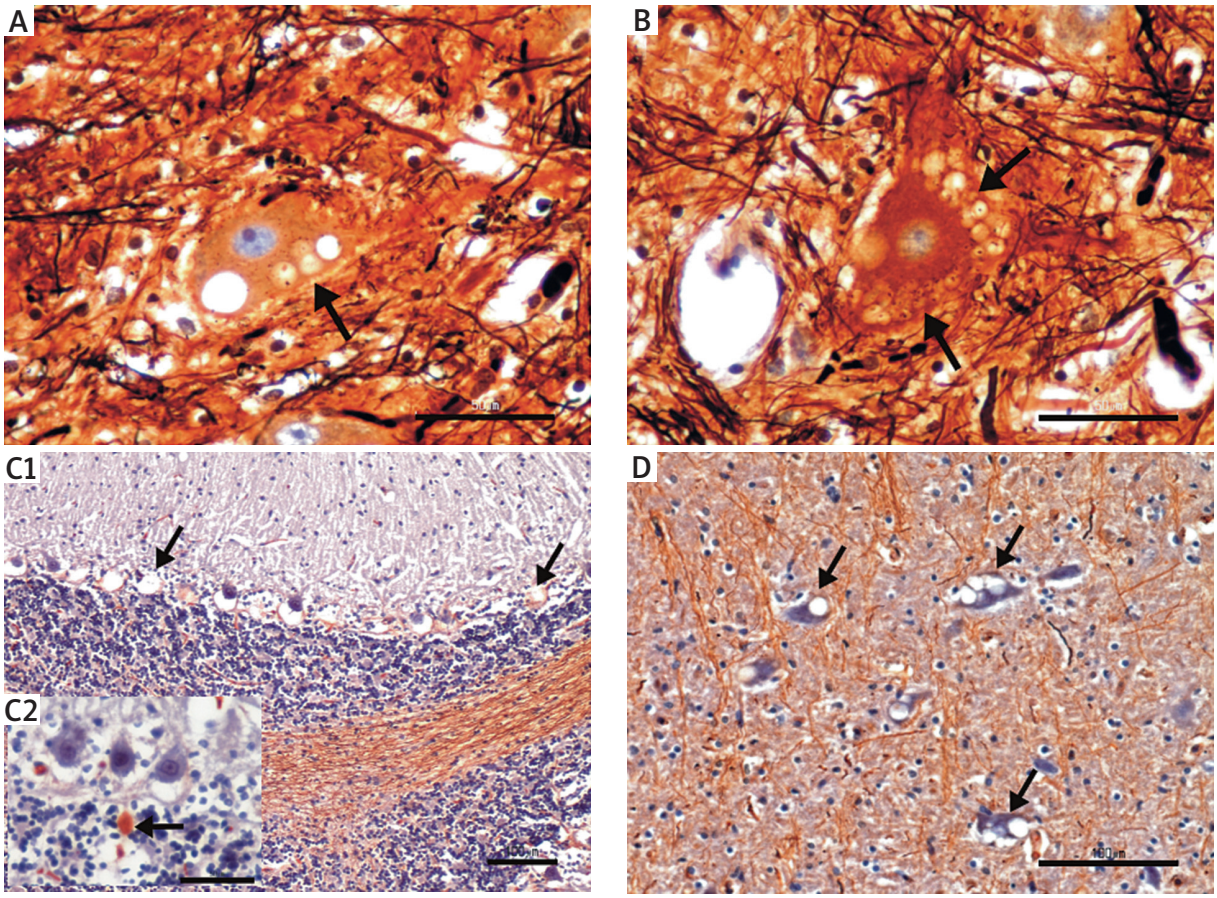

Fig. 2. Representative photomicrographs of cerebellum paraffin sections stained with BLS summarizing the neuropathology in NVSD animals. **A, B**) Neuronal vacuolation was characterized by single or multiple vacuoles (of variable size) and was more profound in cerebellar nuclei. Scale bars in **A, B** are 50 µm. **C1-2,D**) In the cerebellar cortex (**C1**), the atrophy and loss of Purkinje cells were evident leaving empty baskets (arrows). Axonal torpedoes in the granular cell layer belonging to degenerative Purkinje cells were also detected (arrow in **C2**). In cerebellar nuclei (**D**), the neuronal vacuolation (arrows) and axonal loss were profound, resulting in spongiform appearance of the parenchyma. Scale bars in **C, D** are 50 µm.

Neuropathology of the cerebellum

Loss of the large (glutamatergic) neurons and neuronal vacuolation of the remaining cells constitute the most striking histopathological lesions seen in the DCN of NVSD animals. DCN neurons showed single or multiple sharply demarcated cytoplasmic vacuoles which sometimes resulted in peripheral margination of the nucleus (Fig. 2D). In NVSD animals, IOD of GAD in the remaining neurons either vacuolated or not, significantly declined (medians of GAD IOD in NVSD and controls were 16,189 and 128,583; the distributions in the two groups differed significantly (Mann-Whitney U = 0.00, z = –5.477, p < 0.001, two-tailed, Figs. 3A, B and 4C). Similarly, the median IOD of GABA in NVSD animals was reduced by 45% compared to controls. Medians of GABA IOD in NVSD and controls were 19.17 x 10^6 and 34.75 x 10^6, respectively; the distributions in the two groups differed significantly (Mann-Whitney U = 24.00, z = –2.225, p = 0.024, two-tailed, Figs. 3C, D and 4F). In contrast, the median IOD of NMDAR1 in DCN neurons of NVSD animals was elevated by 47% compared with control animals and this difference reached statistical significance (medians were 49.08 x 10^6 and 33.41 x 10^6, respectively; Mann-Whitney U = 27.00, z = –2.2, p = 0.028, two-tailed, Figs. 3F, G and H). DCN neurons were positive for calbindin, although variations on staining inten-

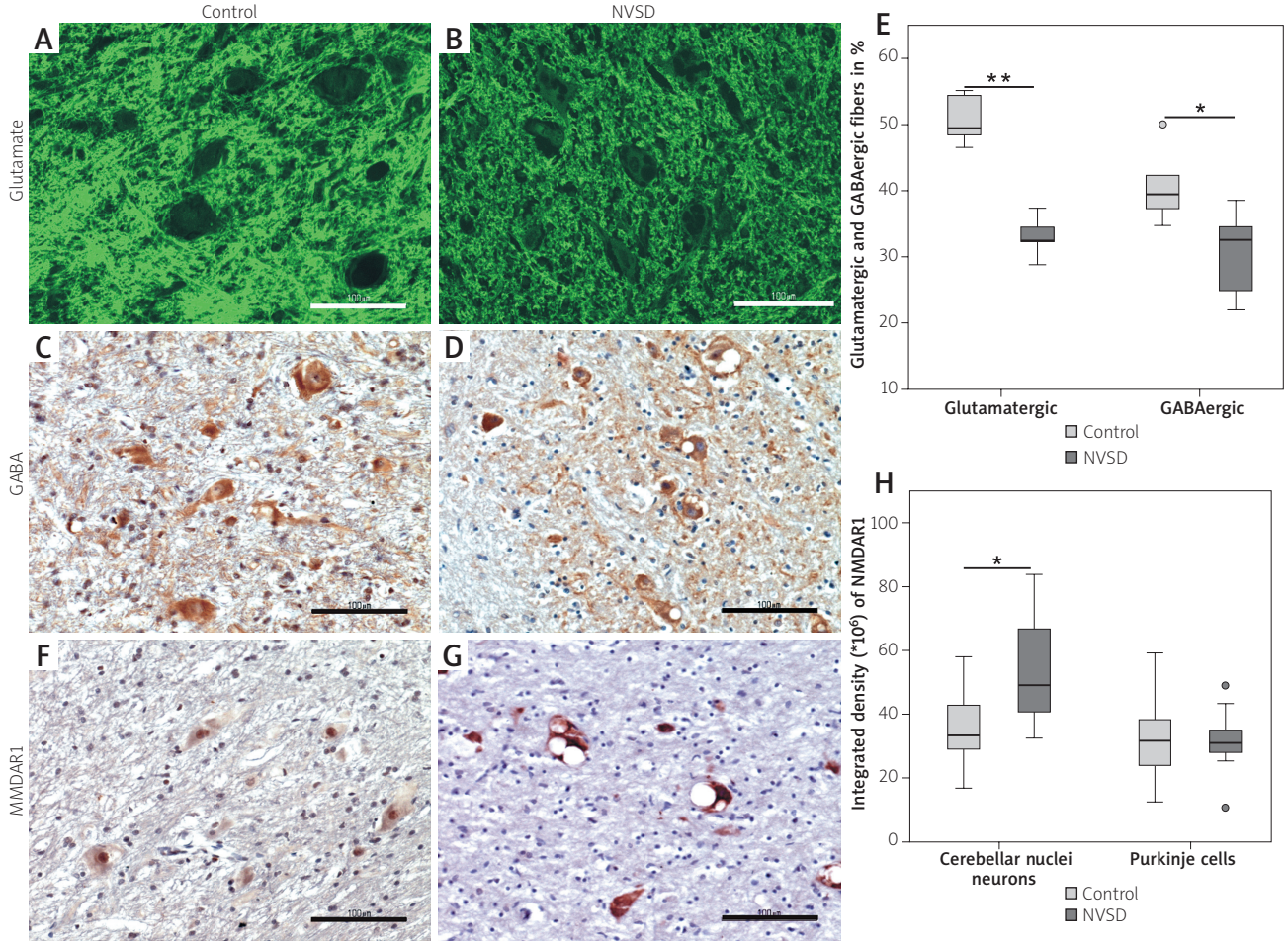

Fig. 3. A-D, F, G) Photomicrographs of paraffin sections of the cerebellum depicting various areas of cerebellar nuclei in control and NVSD animals immunohistochemically stained for glutamate **(A, B)**, GABA **(C, D)** and NMDAR1 **(F, G)**. **A, B)** IHC for glutamate revealed a reduction in glutamatergic fibres, which is expressed as a reduction in the pixel area % per optical field in graph E. **C, D)** Apart from the reduction in IOD of GABA in neuronal somata, there was also a significant reduction in the GABAergic fibres in cerebellar nuclei of NVSD animals. **F, G)** Cerebellar nuclei neurons exhibited a strong immunoreactivity for NMDAR1 in NVSD animals (*$p < 0.05$). Scale bars are 100 µm. **E)** Graph illustrating the percentage of the pixel area of glutamatergic and GABAergic fibres per optical field in cerebellar nuclei in control and NVSD animals. The boxplots represent the median value (50th percentile) and the range of % area of immunoreactive fibres. The outliers (values that are > 1.5 the interquartile range [IQRs]) are marked with a circle. There was a significant reduction in glutamatergic and GABAergic fibres in NVSD animals (**$p < 0.01$, *$p < 0.05$). **H)** Graph illustrating the integrated optical density (IOD) of NMDAR1 in cerebellar nuclei neurons and Purkinje cells in control and NVSD animals. The boxplots represent the median value (50th percentile) and the range of IOD. The IOD of NMDAR1 was significantly higher in cerebellar nuclei neurons of NVSD animals compared to controls (*$p < 0.05$).

sity were noted. The cytoplasm of DCN neurons showed a severe decrease in IOD of calbindin compared to controls (medians were 8.74 × 10^6 and 45.65 × 10^6, respectively; Mann-Whitney U = 0.00, z = –3.182, p = 0.001, two-tailed, Fig. 4I), suggesting an altered Ca^+ dependent metabolism.

In parallel with the vacuolation, the applied histological techniques revealed a spongiform change, myelin pallor and axonal loss within the neuropil. Astrocytosis and focal microgliosis were confirmed by GFAP and Iba1 IHC, respectively. In DCN there was a 24.4% loss of GABAergic fibres in NVSD compared

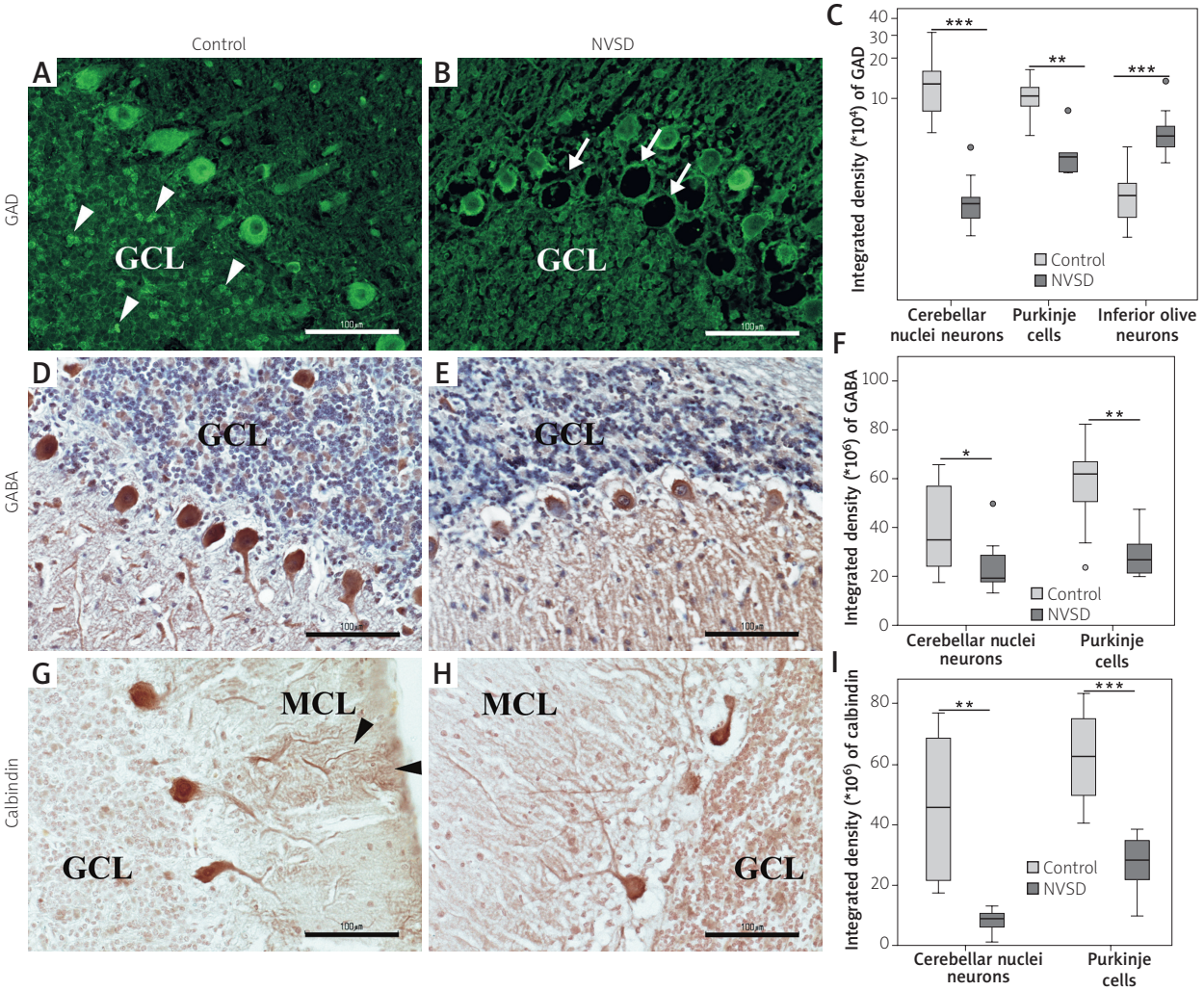

Fig. 4. A, B, D, E, G, H) Photomicrographs of paraffin sections of the cerebellum depicting the cerebellar cortex in control and NVSD animals immunohistochemically stained for GAD **(A, B)**, GABA **(D, E)** and calbindin **(G, H)**. **A, B)** IHC for GAD revealed a reduction in immunoreactivity of GAD in Purkinje cells and elimination of GAD positive terminals in the granular cell layer (GCL) of NVSD animals (arrowheads in **A** indicate the GAD positive terminals in GCL). "Empty baskets" (arrows) in **B** indicate the sites of atrophic Purkinje cells. Atrophy of Purkinje cells was accompanied by a decrease in immunoreactivity of GABA **(E)** and calbindin **(H)** in NVSD animals. Calbindin IHC revealed the characteristic dendritic trees of Purkinje cells (arrowheads in **G**) in the molecular cell layer (MCL) of control animals. Scale bars are 100 µm. **C, F, I)** Graphs illustrating the integrated optical density (IOD) of GAD, GABA and calbindin respectively, in cerebellar nuclei neurons and Purkinje cells (and in olive neurons for GAD) in control and NVSD animals. The boxplots represent the median value (50th percentile) and the range of IOD. The outliers (values that are > 1.5 the interquartile range [IQRs]) are marked with a circle. The IODs of GAD, GABA and calbindin were significantly lower (*$p < 0.05$, **$p < 0.01$, ***$p < 0.001$) in cerebellar nuclei neurons and in Purkinje cells of NVSD animals compared to controls.

with control animals and this difference reached statistical significance (medians were 32.563% and 39.446%, respectively; Mann-Whitney $U = 2.00$, $z = -2.373$, $p = 0.018$, two-tailed, Figs. 3C-E) indicative of the impaired cerebellar corticonuclear connections. In parallel, there was a severe reduction (32%) in glutamatergic fibres in NVSD animals (32.361% vs. 49.431%; Mann-Whitney $U = 0.00$, $z = -2.611$, $p = 0.009$, two-tailed, Figs. 3A, B and E), suggesting the decline of glutamatergic inputs in DCN.

In the cerebellar cortex, atrophy and irregular loss of PCs were prominent in all dogs, accompa-

nied by mild Bergmann gliosis and "empty baskets" in the cerebellar cortex (Fig. 2 C1). The GCL exhibited shrinkage and BLS staining revealed occasional axonal torpedoes in this layer belonging to the axons of the PCs (Fig. 2 C2). The median IOD of GAD in PCs of NVSD animals significantly declined compared to controls. Medians of GAD IODs were 36,324 and 104,648 respectively; the distributions in the two groups differed significantly (Mann-Whitney U = 2.00, z = –2.817, p = 0.005, two-tailed, Figs. 4A-C). In PCs IOD of GABA severely reduced in NVSD compared to control animals. Medians of GABA IODs were 26.70 × 10^6, and 61.64 × 10^6, respectively; the distributions in the two groups differed significantly (Mann-Whitney U = 7.00, z = –3.207, p = 0.001, two-tailed, Figs. 4D-F). Similarly, IHC for calbindin, revealed a significant reduction in IOD of PCs in NVSD compared to controls (medians were 28.23 × 10^6 and 62.60 × 10^6, respectively; Mann-Whitney U = 0.00, z = –3.919, p < 0.001, two-tailed) and altered fragmented dendritic trees in the molecular cell layer (Figs. 4G-I). IOD of NMDAR1 by PCs did not differ significantly between NVSD and control animals (medians were 30.97 × 10^6 and 31.49 × 10^6, respectively; Mann-Whitney U = 73.20, z = –0.189, p = 0.85, two-tailed, Fig. 3H).

Discussion

Recently the RAB3GAP1:c.743delC variant has been identified in the homozygous state in all NVSD-affected Rottweilers. None of the normal Rottweilers or the Rottweilers with signs beginning at > 1 year of age were homozygous for the variant. The RAB3GAP1:c.743delC produces a frame shift that predicts a premature stop codon and a truncated gene product RAB3GAP1:p.P248Lfs4, missing 730 *C*-terminal amino acids, including the catalytic domain, therefore it is doubtful that the truncated gene product retains biological activity [32].

RAB3GAP1 codes for the catalytic subunit that combines with a non-catalytic subunit encoded by RAB3GAP2 to form Rab3GAP. Rab3GAP was first recognized as a GTPase activator protein (GAP) that greatly enhances the inherent GTPase activity of Rab3 [14,23,37]. Rab proteins function as molecular switches that regulate the formation, transport, tethering and fusion of a variety of membrane structures by cycling between inactive GDP-bound and active GTP-bound states [8,23]. These proteins play a vital role in membranous transport within the cell, allowing movement of cell organelles, and endocytosis and exocytosis [11,17,46] reviewed in [40,53]. The mechanism by which they achieve this has been well characterized for certain members of the family, and depends on their GTP state, and their ability to prenylate and thus cycle on and off membranes [1]. However, the precise point of action of Rab3 GAP in synaptic vesicle transport has not been clear so far.

It has been found that in Rab3 GAP p130-deficient mice, the GTP-bound form of Rab3A accumulates in the brain and the Ca^{2+}-dependent glutamate release from cerebrocortical synaptosomes is inhibited [42]. This observation suggests that Rab3 GAP inactivates Rab3A in nerve terminals and thereby regulates neurotransmitter release and synaptic plasticity [23,34,47]. Consistent with this prediction, mutations in p130 have recently been reported to cause WARBM and the altered neurotransmission could be involved in the pathogenesis of this syndrome [2,3]. Gerondopoulos *et al*. [16] reported that Rab3GAP not only functions as a GAP for the Rab3s but also functions as a guanine exchange factor (GEF) for Rab18. Supporting the view that Rab18 activity is important for ER structure, in the absence of either Rab3GAP subunit or Rab18 function, ER tubular networks were disrupted, and ER sheets spread out into the cell periphery [16]. It has been suggested that the intra-neuronal vacuoles may be microscopic and ultrastructural manifestations of a malfunctioned ER that has been aberrantly distributed due to the absence of Rab3GAP activity [32].

A predominant clinical feature of the NVSD phenotype is the juvenile onset laryngeal paralysis and polyneuropathy due to axonopathy. Dystrophic changes in nerves of NVSD-affected dogs have been extensively studied and confirmed by others [7,9] and are characterized by accumulations of normal or abnormal appearing organelles and clusters of vesicular structures resembling proliferating ER, arising from an altered axoplasmic flow [29]. Dystrophic changes were reported in axons of the sciatic nerve in Rab18 knockout mice with disorganization of neurofilaments and collections of microtubules predominantly at the neuromuscular junctions [10]. WARBM can be caused directly by loss of RAB18, or indirectly through loss of RAB18 regulators, RAB3GAP or TBC1D20 [6,19]. In Rab18 knockout mice, neurons with longer axons are more severely affected than those with shorter axons. Interestingly, also in NVSD

the thick myelinated axons are more severely affected. Finding such changes remote from the cell body suggests that axonal transport of membranes and/or vesicles is disrupted by the RAB3GAP1 mutation. Moreover, it is tempting to speculate that an anterograde trans-synaptic degeneration is involved in the pathogenesis of neuronal vacuolation.

The link between axonopathy and neuronal vacuolar degeneration at distinctive anatomical pathways has been reported in several animal models at both spontaneous and experimental lesions [21,36,50]. Neurons within some nuclei in the CNS can atrophy and degenerate via vacuolation in response to deafferentation. Examples are neurons in the inferior and accessory olivary nuclei, which undergo an unusual form of trans-synaptic degeneration after a destructive lesion of the ipsilateral central tegmental tract. The olivary ribbon becomes thickened and neurons show marked enlargement, cytoplasmic vacuolation, and some dispersion of Nissl bodies [48]. In NVSD, large vacuoles were visible mainly within neurons of the DCN, vestibular nuclei and inferior olive. In other areas in the CNS, neuronal vacuolation was either absent or limited, indicating a selective susceptibility of specific neuronal types to vacuolation. Overall, vacuolation occurred in interconnected extrapyramidal and oculomotor structures and this spatial pattern of distribution suggests the spread of this disorder across synaptic connections [44]. However, we cannot exclude the possibility that any abnormalities in other neurons are not gross, but might be subtler at the subcellular level.

Many studies have addressed the selective vulnerability of DCN neurons to NVSD [13,15,27,41,43], however none of them examined either the subtypes of neurons mainly affected or the relative importance of neurohumoral synaptic dysfunction in this structure. The normal DCN contains mainly three populations of neurons: small GABAergic neurons, which send projections to the inferior olive, small GABAergic local interneurons and larger glutamatergic neurons, which project to premotor areas and regulate the motor control [22]. These cells are GAD positive with a mild expression of GABA and NMDAR1. In NVSD cerebellar nuclei, large neurons are severely in decline in parallel with a reduction in GABA and GAD immunoreactivity of the remaining cells.

Moreover, in normal DCN, nuclear neurons receive mostly inhibitory GABAergic inputs from PCs and excitatory glutamatergic inputs from mossy fibres. The latter originate from the second order neuron of Clarke's nuclei and from axon collaterals of inferior olive neurons. In NVSD animals, the glutamatergic inputs in DCN severely declined in parallel with the overexpression of NMDAR1 by the neuronal somata. This upregulation probably serves as a compensatory mechanism in the reduction of excitatory glutamatergic inputs from mossy fibres. However, GABAergic synapses formed by the axons of PCs outnumber the glutamatergic and GABAergic synapses formed by local interneurons [51]. The reduction of GABAergic fibres in DCN in NVSD animals is substantial suggesting that GABAergic inhibition from PCs is heavily missing.

Intraneuronal vacuoles with a similar distribution pattern as in NVSD have been recently reported in a spontaneous neurodegenerative disease in Lagotto Romagnolo dogs associated with abnormal autophagosome maturation and a mutation in the autophagy-related gene *ATG4D* [28]. There are a variety of studies, either in transgenic mice or canine hereditary ataxias providing compelling evidence that a primary defect in autophagy can induce neurodegenerative disease. Autophagy is the process by which more long-lived proteins and organelles are incorporated into autophagosomes for delivery to vacuoles or lysosomes for degradation. Constitutive autophagy plays an important role as a basal source of energy in cells with high metabolic needs, such as the PCs, in the global turnover of cellular organelles and in the clearance of potentially toxic protein aggregates [24-26]. Is it well acknowledged that the heterodimeric RAB3GAP complex regulates the RAB GTPase RAB3 and the release of neurotransmitters at the neuronal synapse; however, recently it has been found that RAB3GAP1/2 also affects intracellular protein aggregation and modulate autophagosomal maturation in basal and rapamycin-induced conditions [45]. Deficiencies of glutamatergic and GABAergic terminals in the DCN of NVSD animals may induce a compromised function of proteins involved in the organelles' integrity. Moreover, vacuolation in DCN neurons may provide evidence for an altered autophagy as a stress response to anterograde transneuronal deafferentation and neurotransmitters deprivation [35].

Atrophy and loss of PCs constitute a major histopathological hallmark in the cerebellum of NVSD animals. The remaining PCs showed reduced IOD for GAD, GABA and calbindin. In addition, histopathology revealed axonal torpedoes, which are

ellipsoid swellings of PC axons in the GCL and are considered to be non-specific changes in various disorders, such as spinocerebellar degeneration [31]. Torpedo formation has been linked to the loss of DCN neurons as a consequence of a retrograde change based on the synaptic detachment of PC axon terminals. It is unlikely that primary changes in PC bodies are involved in the torpedo formation seen in these conditions. On the contrary, the fact that there is a severe damage of DCN but a number of PCs is preserved raises the possibility that the neuronal loss leads secondarily to torpedo formation. Moreover, it has been shown that torpedoes do not develop until the density of neurons in DCN is reduced to about half of that in controls, because the terminal arborisation of the axon of each PC occurs in the DCN to make synaptic contact with multiple neurons [31].

In conclusion, vacuolation in diseases such as NVSD could be a histopathological manifestation of intense intracellular degradation of specific neuronal types, due to neurotransmitters deprivation in the terminals of afferent fibres. The RAB3GAP1:c.743delC dogs could serve as a model for investigating the role of Rab3GAP in membrane trafficking and the pathogenesis of diseases such as WARBM.

Acknowledgements

Dr Polyzopoulou Zoi is thanked for the generous donation of affected dogs, Dr Tsingotjidou Anastasia and Dr Bekiari Chryssa for their valuable contribution, Chiotelli Maria for her excellent technical assistance, and Dr Papadopoulos GC for his constructive criticism on the original manuscript. The study was supported by National Funds.

Disclosure

The author reports no conflict of interest.

References

1. Agler C, Nielsen DM, Urkasemsin G, Singleton A, Tonomura N, Sigurdsson S, Tang R, Linder K, Arepalli S, Hernandez D, Lindblad-Toh K, van de Leemput J, Motsinger-Reif A, O'Brien DP, Bell J, Harris T, Steinberg S, Olby NJ. Canine hereditary ataxia in old english sheepdogs and gordon setters is associated with a defect in the autophagy gene encoding RAB24. PLoS Genet 2014; 10: e1003991.
2. Aligianis IA, Johnson CA, Gissen P, Chen D, Hampshire D, Hoffmann K, Maina EN, Morgan NV, Tee L, Morton J, Ainsworth JR, Horn D, Rosser E, Cole TR, Stolte-Dijkstra I, Fieggen K, Clayton-Smith J, Megarbane A, Shield JP, Newbury-Ecob R, Dobyns WB, Graham JM, Jr., Kjaer KW, Warburg M, Bond J, Trembath RC, Harris LW, Takai Y, Mundlos S, Tannahill D, Woods CG, Maher ER. Mutations of the catalytic subunit of RAB3GAP cause Warburg Micro syndrome. Nat Genet 2005; 37: 221-223.
3. Aligianis IA, Morgan NV, Mione M, Johnson CA, Rosser E, Hennekam RC, Adams G, Trembath RC, Pilz DT, Stoodley N, Moore AT, Wilson S, Maher ER. Mutation in Rab3 GTPase-activating protein (RAB3GAP) noncatalytic subunit in a kindred with Martsolf syndrome. Am J Hum Genet 2006; 78: 702-707.
4. Armstrong RA. Can neurodegenerative disease be defined by four 'primary determinants': anatomy, cells, molecules, and morphology? Folia Neuropathol 2016; 54: 89-104.
5. Armstrong RA, Cairns NJ, Lantos PL. Are pathological lesions in neurodegenerative disorders the cause or the effect of the degeneration? Neuropathology 2002; 22: 133-146.
6. Bem D, Yoshimura S, Nunes-Bastos R, Bond FC, Kurian MA, Rahman F, Handley MT, Hadzhiev Y, Masood I, Straatman-Iwanowska AA, Cullinane AR, McNeill A, Pasha SS, Kirby GA, Foster K, Ahmed Z, Morton JE, Williams D, Graham JM, Dobyns WB, Burglen L, Ainsworth JR, Gissen P, Muller F, Maher ER, Barr FA, Aligianis IA. Loss-of-function mutations in RAB18 cause Warburg micro syndrome. Am J Hum Genet 2011; 88: 499-507.
7. Bennett PF, Clarke RE. Laryngeal paralysis in a rottweiler with neuroaxonal dystrophy. Aust Vet J 1997; 75: 784-786.
8. Bhuin T, Roy JK. Rab proteins: the key regulators of intracellular vesicle transport. Exp Cell Res 2012; 328: 1-19.
9. Braund KG, Steinberg HS, Shores A, Steiss JE, Mehta JR, Toivio-Kinnucan M, Amling KA. Laryngeal paralysis in immature and mature dogs as one sign of a more diffuse polyneuropathy. J Am Vet Med Assoc 1989; 194: 1735-1740.
10. Carpanini SM, McKie L, Thomson D, Wright AK, Gordon SL, Roche SL, Handley MT, Morrison H, Brownstein D, Wishart TM, Cousin MA, Gillingwater TH, Aligianis IA, Jackson IJ. A novel mouse model of Warburg Micro syndrome reveals roles for RAB18 in eye development and organisation of the neuronal cytoskeleton. Dis Model Mech 2014; 7: 711-722.
11. Corbeel L, Freson K. Rab proteins and Rab-associated proteins: major actors in the mechanism of protein-trafficking disorders. Eur J Pediatr 2008; 167: 723-729.
12. de Lahunta A, Summers BA. The laryngeal lesion in young dogs with neuronal vacuolation and spinocerebellar degeneration. Vet Pathol 1998; 35: 316-317.
13. Eger CE, Huxtable CR, Chester ZC, Summers BA. Progressive tetraparesis and laryngeal paralysis in a young rottweiler with neuronal vacuolation and axonal degeneration: an Australian case. Australian Veterinary Journal 1998; 76: 733-737.
14. Fukui K, Sasaki T, Imazumi K, Matsuura Y, Nakanishi H, Takai Y. Isolation and characterization of a GTPase activating protein specific for the Rab3 subfamily of small G proteins. J Biol Chem 1997; 272: 4655-4658.
15. Geiger DA, Miller AD, Cutter-Schatzberg K, Shelton GD, de Lahunta A, Schatzberg SJ. Encephalomyelopathy and polyneuropathy associated with neuronal vacuolation in two Boxer littermates. Veterinary Pathology 2009; 46: 1160-1165.

16. Gerondopoulos A, Bastos RN, Yoshimura S, Anderson R, Carpanini S, Aligianis I, Handley MT, Barr FA. Rab18 and a Rab18 GEF complex are required for normal ER structure. J Cell Biol 2014; 205: 707-720.
17. Goody RS, Rak A, Alexandrov K. The structural and mechanistic basis for recycling of Rab proteins between membrane compartments. Cell Mol Life Sci 2005; 62: 1657-1670.
18. Graham JM Jr., Hennekam R, Dobyns WB, Roeder E, Busch D. MICRO syndrome: an entity distinct from COFS syndrome. Am J Med Genet A 2004; 128A: 235-245.
19. Handley MT, Carpanini SM, Mali GR, Sidjanin DJ, Aligianis IA, Jackson IJ, FitzPatrick DR. Warburg Micro syndrome is caused by RAB18 deficiency or dysregulation. Open Biol 2015; 5: 150047.
20. Handley MT, Morris-Rosendahl DJ, Brown S, Macdonald F, Hardy C, Bem D, Carpanini SM, Borck G, Martorell L, Izzi C, Faravelli F, Accorsi P, Pinelli L, Basel-Vanagaite L, Peretz G, Abdel-Salam GM, Zaki MS, Jansen A, Mowat D, Glass I, Stewart H, Mancini G, Lederer D, Roscioli T, Giuliano F, Plomp AS, Rolfs A, Graham JM, Seemanova E, Poo P, Garcia-Cazorla A, Edery P, Jackson IJ, Maher ER, Aligianis IA. Mutation spectrum in RAB3GAP1, RAB3GAP2, and RAB18 and genotype-phenotype correlations in warburg micro syndrome and Martsolf syndrome. Hum Mutat 2013; 34: 686-696.
21. He L, Lu XY, Jolly AF, Eldridge AG, Watson SJ, Jackson PK, Barsh GS, Gunn TM. Spongiform degeneration in mahoganoid mutant mice. Science 2003; 299: 710-712.
22. Hirano T, Kawaguchi SY. Regulation of inhibitory synaptic plasticity in a Purkinje neuron. Cerebellum 2012; 11: 453-454.
23. Hutagalung AH, Novick PJ. Role of Rab GTPases in membrane traffic and cell physiology. Physiol Rev 2011; 91: 119-149.
24. Komatsu M, Kominami E, Tanaka K. Autophagy and neurodegeneration. Autophagy 2006; 2: 315-317.
25. Komatsu M, Ueno T, Waguri S, Uchiyama Y, Kominami E, Tanaka K. Constitutive autophagy: vital role in clearance of unfavorable proteins in neurons. Cell Death Differ 2007; 14: 887-894.
26. Komatsu M, Waguri S, Chiba T, Murata S, Iwata J, Tanida I, Ueno T, Koike M, Uchiyama Y, Kominami E, Tanaka K. Loss of autophagy in the central nervous system causes neurodegeneration in mice. Nature 2006; 441: 880-884.
27. Kortz GD, Meier WA, Higgins RJ, French RA, McKiernan BC, Fatzer R, Zachary JF. Neuronal vacuolation and spinocerebellar degeneration in young Rottweiler dogs. Veterinary Pathology 1997; 34: 296-302.
28. Kyostila K, Syrja P, Jagannathan V, Chandrasekar G, Jokinen TS, Seppala EH, Becker D, Drogemuller M, Dietschi E, Drogemuller C, Lang J, Steffen F, Rohdin C, Jaderlund KH, Lappalainen AK, Hahn K, Wohlsein P, Baumgartner W, Henke D, Oevermann A, Kere J, Lohi H, Leeb T. A missense change in the ATG4D gene links aberrant autophagy to a neurodegenerative vacuolar storage disease. PLoS Genet 2015; 11: e1005169.
29. Lampert PW. A comparative electron microscopic study of reactive, degenerating, regenerating, and dystrophic axons. J Neuropathol Exp Neurol 1967; 26: 345-368.
30. Mahony OM, Knowles KE, Braund KG, Averill DR Jr., Frimberger AE. Laryngeal paralysis-polyneuropathy complex in young Rottweilers. J Vet Intern Med 1998; 12: 330-337.
31. Matsumoto R, Nakano I, Arai N, Oda M, Yagishita S, Hashizume Y. Loss of the dentate nucleus neurons is associated with torpedo formation: a morphometric study in progressive supranuclear palsy and dentatorubro-pallidoluysian atrophy. Acta Neuropathol 1998; 95: 149-153.
32. Mhlanga-Mutangadura T, Johnson GS, Ashwini A, Shelton GD, Wennogle SA, Johnson GC, Kuroki K, O'Brien DP. A Homozygous RAB3GAP1:c.743delC Mutation in Rottweilers with Neuronal Vacuolation and Spinocerebellar Degeneration. J Vet Intern Med 2016; 30: 813-818.
33. Morris-Rosendahl DJ, Segel R, Born AP, Conrad C, Loeys B, Brooks SS, Muller L, Zeschnigk C, Botti C, Rabinowitz R, Uyanik G, Crocq MA, Kraus U, Degen I, Faes F. New RAB3GAP1 mutations in patients with Warburg Micro Syndrome from different ethnic backgrounds and a possible founder effect in the Danish. Eur J Hum Genet 2010; 18: 1100-1106.
34. Muller M, Pym EC, Tong A, Davis GW. Rab3-GAP controls the progression of synaptic homeostasis at a late stage of vesicle release. Neuron 2011; 69: 749-762.
35. Murrow L, Debnath J. Autophagy as a stress-response and quality-control mechanism: implications for cell injury and human disease. Annu Rev Pathol 2013; 8: 105-137.
36. Nagahama M, Suzuki M, Hamada Y, Hatsuzawa K, Tani K, Yamamoto A, Tagaya M. SVIP is a novel VCP/p97-interacting protein whose expression causes cell vacuolation. Mol Biol Cell 2003; 14: 262-273.
37. Nagano F, Sasaki T, Fukui K, Asakura T, Imazumi K, Takai Y. Molecular cloning and characterization of the noncatalytic subunit of the Rab3 subfamily-specific GTPase-activating protein. J Biol Chem 1998; 273: 24781-24785.
38. Nassogne MC, Henrot B, Saint-Martin C, Kadhim H, Dobyns WB, Sebire G. Polymicrogyria and motor neuropathy in Micro syndrome. Neuropediatrics 2000; 31: 218-221.
39. Oishi H, Sasaki T, Nagano F, Ikeda W, Ohya T, Wada M, Ide N, Nakanishi H, Takai Y. Localization of the Rab3 small G protein regulators in nerve terminals and their involvement in Ca2+-dependent exocytosis. J Biol Chem 1998; 273: 34580-14585.
40. Pereira-Leal JB, Seabra MC. The mammalian Rab family of small GTPases: definition of family and subfamily sequence motifs suggests a mechanism for functional specificity in the Ras superfamily. J Mol Biol 2000; 301: 1077-1087.
41. Pumarola M, Fondevila D, Borras D, Majo N, Ferrer I. Neuronal vacuolation in young Rottweiler dogs. Acta Neuropathologica 1999; 97: 192-195.
42. Sakane A, Manabe S, Ishizaki H, Tanaka-Okamoto M, Kiyokage E, Toida K, Yoshida T, Miyoshi J, Kamiya H, Takai Y, Sasaki T. Rab3 GTPase-activating protein regulates synaptic transmission and plasticity through the inactivation of Rab3. Proc Natl Acad Sci U S A 2006; 103: 10029-10034.
43. Salvadori C, Tartarelli CL, Baroni M, Mizisin A, Cantile C. Peripheral nerve pathology in two rottweilers with neuronal vacuolation and spinocerebellar degeneration. Veterinary Pathology 2005; 42: 852-855.
44. Saper CB, Wainer BH, German DC. Axonal and transneuronal transport in the transmission of neurological disease: potential role in system degenerations, including Alzheimer's disease. Neuroscience 1987; 23: 389-398.

45. Spang N, Feldmann A, Huesmann H, Bekbulat F, Schmitt V, Hiebel C, Koziollek-Drechsler I, Clement AM, Moosmann B, Jung J, Behrends C, Dikic I, Kern A, Behl C. RAB3GAP1 and RAB3GAP2 modulate basal and rapamycin-induced autophagy. Autophagy 2014; 10: 2297-2309.
46. Stenmark H. Rab GTPases as coordinators of vesicle traffic. Nat Rev Mol Cell Biol 2009; 10: 513-525.
47. Sudhof TC. The synaptic vesicle cycle. Annu Rev Neurosci 2004; 27: 509-547.
48. Takamine K, Okamoto K, Fujita Y, Sakurai A, Takatama M, Gonatas NK. The involvement of the neuronal Golgi apparatus and trans-Golgi network in the human olivary hypertrophy. J Neurol Sci 2000; 182: 45-50.
49. Tiemeyer MJ, Singer HS, Troncoso JC, Cork LC, Coyle JT, Price DL. Synaptic neurochemical alterations associated with neuronal degeneration in an inherited cerebellar ataxia of Gordon Setters. J Neuropathol Exp Neurol 1984; 43: 580-591.
50. Twiss JL, Baisch M, Horoupian DS. Neonatal encephalopathy with neuronal vacuolar degeneration. Acta Neuropathol 1993; 86: 536-541.
51. Uusisaari MY, Knopfel T. Diversity of neuronal elements and circuitry in the cerebellar nuclei. Cerebellum 2012; 11: 420-421.
52. van den Ingh TS, Mandigers PJ, van Nes JJ. A neuronal vacuolar disorder in young rottweiler dogs. Veterinary Record 1998; 142: 245-247.
53. Zerial M, McBride H. Rab proteins as membrane organizers. Nat Rev Mol Cell Biol 2001; 2: 107-117.

Original paper

Folia Neuropathologica

Neuropathological characteristics of the brain in two patients with SLC19A3 mutations related to the biotin-thiamine-responsive basal ganglia disease

Maciej Pronicki[1], Dorota Piekutowska-Abramczuk[2], Elżbieta Jurkiewicz[3], Dariusz Rokicki[4], Elżbieta Ciara[2], Joanna Trubicka[1], Katarzyna Iwanicka-Pronicka[5], Magdalena Pajdowska[6], Marek Migdał[7], Wieslawa A. Grajkowska[1,8]

[1]Department of Pathology, The Children's Memorial Health Institute, Warsaw, [2]Department of Medical Genetics, The Children's Memorial Health Institute, Warsaw, [3]Department of Diagnostic Imaging, The Children's Memorial Health Institute, Warsaw, [4]Department of Paediatrics, Nutrition and Metabolic Diseases, The Children's Memorial Health Institute, Warsaw, [5]Department of Audiology and Phoniatrics, The Children's Memorial Health Institute, Warsaw, [6]Department of Biochemistry, Radioimmunology and Experimental Medicine, The Children's Memorial Health Institute, Warsaw, [7]Department of Anaesthesiology and Intensive Care, The Children's Memorial Health Institute, Warsaw, [8]Department of Clinical and Experimental Neuropathology, The Mossakowski Medical Research Centre Polish Academy of Sciences, Warsaw, Poland

Folia Neuropathol 2017; 55 (2): 146-153 DOI: https://doi.org/10.5114/fn.2017.68581

Abstract

Biotin-thiamine-responsive basal ganglia disease is a severe form of a rare neurogenetic disorder caused by pathogenic molecular variants in the thiamine transporter gene. Nowadays, a potentially effective treatment is known, therefore the early diagnosis is mandatory. The aim of the paper was to assess the contribution of neuropathological and magnetic resonance imaging (MRI) studies to a proper diagnosis. We present the brain study of two Polish patients with SLC19A3 mutations, including (1) an infant with an intriguing "walnut" appearance of the brain autopsied many years before the discovery of the SLC19A3 defect, and (2) a one-year-old patient with clinical features of Leigh syndrome. In patient 2, biotin/thiamine responsiveness was not tested at the time of diagnosis and causal treatment started with one-year delay.

The central nervous system lesions found in the patients displayed almost clearly a specific pattern for SLC19A3 defect, as previously proposed in diagnostic criteria. Our study presents a detailed description of neuropathological and MRI findings of both patients.

We confirm that the autopsy and/or MRI of the brain is sufficient to qualify a patient with an unknown neuropathological disorder directly for SLC19A3 mutations testing and a prompt trial of specific treatment.

Key words: *basal ganglia disease, SLC19A3 mutations, MRI, autopsy, neuropathology, thiamine transporter.*

Introduction

A neurogenetic disorder related to homozygous or compound heterozygous mutations in the *SLC19A3* gene was firstly described in 2005 [7] and is known by two acronyms: BBGD (biotin-responsive basal ganglia disease) and BTRBGD (biotin-thiamine-respon-

Communicating author

Prof. Wieslawa A. Grajkowska, Department of Pathology, The Children's Memorial Health Institute, Aleja Dzieci Polskich 20, 04-730 Warsaw, Poland, phone: +48 22 815 19 60, e-mail: w.grajkowska@ipczd.pl

sive basal ganglia disease). Since its discovery, almost a hundred patients have been reported, mainly from Saudi Arabia [2], but also from Japan, Lebanon, Mexico, Sweden and other countries. The natural history of the condition is quite well recognized, pointing to a remarkable clinical heterogeneity, even inside the same family and the wide range of severity and prognoses [6]. Recently this has been comprehensively reviewed [1,2].

The distinctive feature of this rare disease is a potential effectiveness of the treatment with biotin and thiamine in high doses [3,5,18]. Pathogenic variants in the *SLC19A3* [NM_025243.3] coding for thiamine transporter 2 lead to a decrease in the free-thiamine concentration in cells [10]. Brain imaging most commonly shows a basal ganglia involvement of Leigh-like syndrome type [4,5,15] and/or Wernicke encephalopathy features resembling acquired vitamin B_1 deficiency [7]. Progressive brain atrophy is a relatively common finding [15].

Although in the literature there are numerous magnetic resonance imagining (MRI) series of *SLC19A3* defect illustrating both specific changes in detail [6,17] and the response to specific treatment [1,2], only few reports focus on brain pathology in affected patients [15]. Herein, we present our unique autopsy findings ("walnut" appearance of the brain) in a Polish child who died many years ago, and in whom the underlying *SLC19A3* homozygous mutation has been recently established by WES (whole-exome sequencing). In the second Polish patient bearing other homozygous *SLC19A3* variant we show brain MRI evolution before and after vitamin B_1/biotin administration. The treatment which started one year after the disease onset was not sufficiently effective in this child. The aim of the paper was to focus on brain neuropathological findings.

Material and methods

Neuropathological characteristics of the brain of patients with *SLC19A3* defect were analysed in detail to establish usefulness of diagnostic criteria proposed by van den Knaap *et al*. [6]. Two Polish patients with the *SLC19A3* mutations identified out of 113 mitochondrial patients studied in The Children's Memorial Health Institute (CMHI) in the period of 1995-2016 [13] were included.

Routine methods were applied for autopsy study and MRI.

The study was conducted according to the principles of the Helsinki Declaration. The study protocol was approved by the CMHI Bioethics Commission. Informed parental consent was given for the study.

Case reports

Patient 1 was born spontaneously, from the 3rd uncomplicated pregnancy, with the birth weight of 4050 g; he obtained 8 points in Apgar score. His older sister was healthy, while his brother died at the age of six months due to an acute neurological deterioration. Autopsy was performed but it did not confirm clinically suspected meningitis, however focal cortical dysplasia was described in microscopic evaluation of post-mortem material (specimens not available for verification). The patient displayed global developmental delay, spastic tetraparesis, progressive microcephaly up to much below the 3rd centile (weight 25 c; height 97 c) and seizures since the 3rd month of life.

At the age of 8 months, critical deterioration of the general health condition occurred. General brain atrophy was described in MRI (imaging documentation not available). Blood tests showed metabolic acidosis (pH 7.328) accompanied by normal concentrations of lactate (1.8 mmol/l) and alanine (242 µmol/l). Cerebrospinal aminoacidogram revealed increased threonine, decreased serine and normal alanine levels. Classic organic acidurias, biotinidase deficiency, aminoacidopathies and lysosomal storage diseases were excluded. The boy died with hypertension, hypothermia, prolonged coma, respiratory and cardiac insufficiency at the age of 8 months, before the *SLC19A3* gene discovery. Recently, whole exome sequencing has revealed homozygous *SLC19A3* c.74dupT (p.Ser26Leufs*19) mutation. Molecular analysis performed in his family confirmed parental inheritance of the identified variant [13].

Patient 2, a boy was born from the 3rd pregnancy, in term (40 weeks of gestation), with a good clinical status (4350 g; 10 Apgar score). The delivery was complicated by the collarbone fracture and transient hypoxia. The first pregnancy of the mother terminated with intrauterine foetal death. The healthy brother came from the second pregnancy. The patient was under neurological care in infancy due to inappropriate muscle tension, however his motor development was normal. He sat alone between the 7th-8th month of age, stood and walked with support in the

10th month. He started saying his first words on time. At the 12th month of age he stumbled and fell when teething and stopped walking due to hypotonia. The brain MRI revealed basal ganglia changes and diagnosis of Leigh syndrome (LS) was established. Blood and CSF concentrations of lactate were at the upper control range (2.3 and 1.7 mmol/l, respectively), biotinidase deficiency was excluded. In the following year, regression in the boy's development was observed, his emotional contact with parents decreased, he stopped standing up and crawled on all fours. Muscle biopsy revealed mitochondrial complex I deficiency (2.8% of normal value). Further deterioration was observed. This included a complete loss of contact, choking, axial hypotonia with limb hypertonia, strong reflexes, feeding problems requiring a gastric tube and then percutaneous endoscopic gastrostomy (PEG) implantation. Molecular search for the most common LS causative mutations in the *SURF1, MTATP6, MTTL1, POLG, SCO2* and *MTFMT* was negative. At the age of 22 months, a proper diagnosis of BTRBGD associated with *SLC19A3* homozygous c.68G>T (p.Gly23Val) mutation was established by WES [13]. A heterozygous pattern was found in his parents. Vitamin B_1 and biotin were administered one year after the onset of the disease, in high doses of 200 mg and 5 mg daily (and 300 mg and 10 mg since the age of 4). At the start of treatment the boy demonstrated tetraparesis and severe extrapyramidal syndrome with dystonia and sleep-wake phase reversal. Development of brain atrophy was found on second MRI performed two months later. No clear clinical improvement was observed during the vitamin supplementation, but the disease course was without further regression and without exacerbation episodes. Now, at the age of 4, his clinical status is stable, dependent on the type of anticonvulsant treatment with the best response to valproic acid administration (and its good tolerance). Recently, on ketogenic diet, the boy is quieter, has less tensions (spasms) and longer sleep.

Results

The neuropathological abnormalities found in the patients related to the diagnostic criteria proposed in the literature are shown in Table I. Repeatability of all assessed parameters indicates that the brain neuropathology may present a reliable basis to identify patients with *SLC19A3* defect. The detailed findings of autopsy and MRI are described below.

Neuropathological findings on autopsy of patient 1

Gross examination of formalin fixed brain revealed gyral atrophy of frontal, parietal and occipital lobes, as well as cerebellar hemispheres and vermis (Fig. 1). The degree of gyral atrophy appeared less pronounced in temporal lobes. External examination of the brain

Table I. Topography of neuropathological changes in two patients with SLC19A3 mutations

Topography of changes (according to [3])	Patient 1	Patient 2
Method of assessment	Autopsy	MRI
Age of assessment	10 months	12 months/3 years
Stage of the disease at assessment	End stage	Acute/intermediate
Symmetric basal ganglia changes	+	+/+
Nucleus caudatus	+	++/+
Putamen	+	++/+
Globus pallidus	+	++/+
Thalamus	+	++/–
Cerebral white matter changes	+	++/–
Subcortical	+	+/–
Central	+	–/–
With cortex involvement	+	+/–
Cerebellar white matter changes	+	–/–
With cortex involvement	+	–/–
Abnormalities in the pons	+	–/–
In midbrain	+	+/–
Atrophy of affected structures on follow-up	Severe	–/Severe

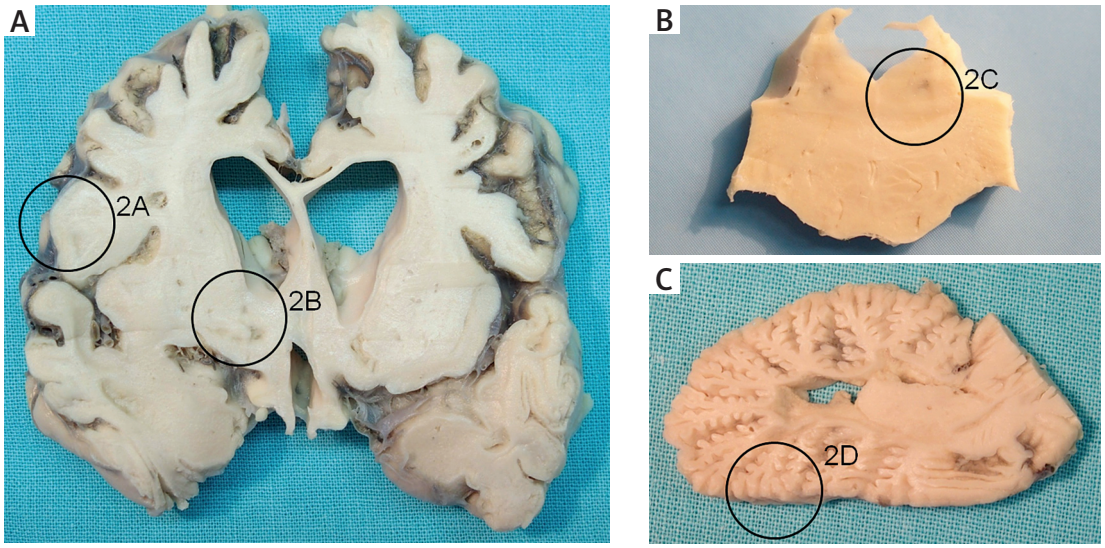

Fig. 1. A) Brain, coronal section showing cortical atrophy, subcortical white matter shrinkage and cavitation, as well as bilateral basal ganglia discoloration and pseudocystic transformation. **B)** Brain stem, pons. Symmetrical discoloration of subventricular areas. **C)** Cerebellum with cortical atrophy and subcortical tissue damage. See corresponding histological findings in Figure 2 (areas indicated by circles).

stem structures, including pituitary gland and vasculature, showed no virtual abnormalities. On coronal sections, cerebral and cerebellar cortex appeared to be atrophic in a diffuse manner. Subcortical white matter showed multiple areas of destruction and cavitation. The ventricular system was symmetrically widened. Basal ganglia showed multiple roughly symmetrical areas of pseudocystic destruction. Symmetrical foci of discoloration were found in mesencephalon in the vicinity of cerebral aqueduct, in the floor of the fourth ventricle and dorsal upper medullary region. Discoloration and tissue rarefaction and cavitation encompassed also cerebellar white matter, with accompanying complete blurring of the dentate nuclei.

Microscopic neuropathological examination revealed diffuse bilateral effacement of hemispheric cortical architecture (Fig. 2). Cortex damage included diffuse neuronal loss, pronounced astroglial gemistocytic reaction and focal massive spongiosis with nervous tissue destruction.

Basal ganglia showed necrosis and calcification of multiple neurons with tissue destruction, as well as formation of cavities. Bilateral "Leigh-like" foci of capillary proliferation accompanied by gliosis, spongiosis, oedema and pseudocystic tissue destruction encompassed basal ganglia, periaqueductal mesencephalon, subependymal pontine and medullary areas, as well as cerebellar white matter.

A striking pattern of damage was found in the cerebellar cortex. The most of gyral cerebellar cortical areas showed almost a total loss of neuronal elements. Both external and internal granular layers and Purkinje cells presented multiple areas of whole-cell calcifications or complete cell body disappearance. Diffuse areas of replacement glial proliferation occupied most of collapsed, atrophic gyral structures. Only some peripheral "apical" regions of gyri retained some preserved neuronal cortical elements, although also with signs of damage.

Olivary nuclei and spinal cord appeared to be relatively well preserved.

Patient 2 – brain magnetic resonance examination

Brain MR examination performed at the age of 12 months, during the acute phase, demonstrated swelling of the basal ganglia with cystic degeneration in both lenticular nuclei on T2-weighted images. Bilateral lesions in the crus cerebri, cortex and grey-white matter junction were seen in both cerebral hemispheres. The areas of the cytotoxic oedema were recognized in the cortex and the parts of putamina (Figs. 3A-C). FLAIR image clearly demonstrates cystic degeneration in both lenticular nuclei (Fig. 3D). Diffusion weighted image (Fig. 3E) and ADC

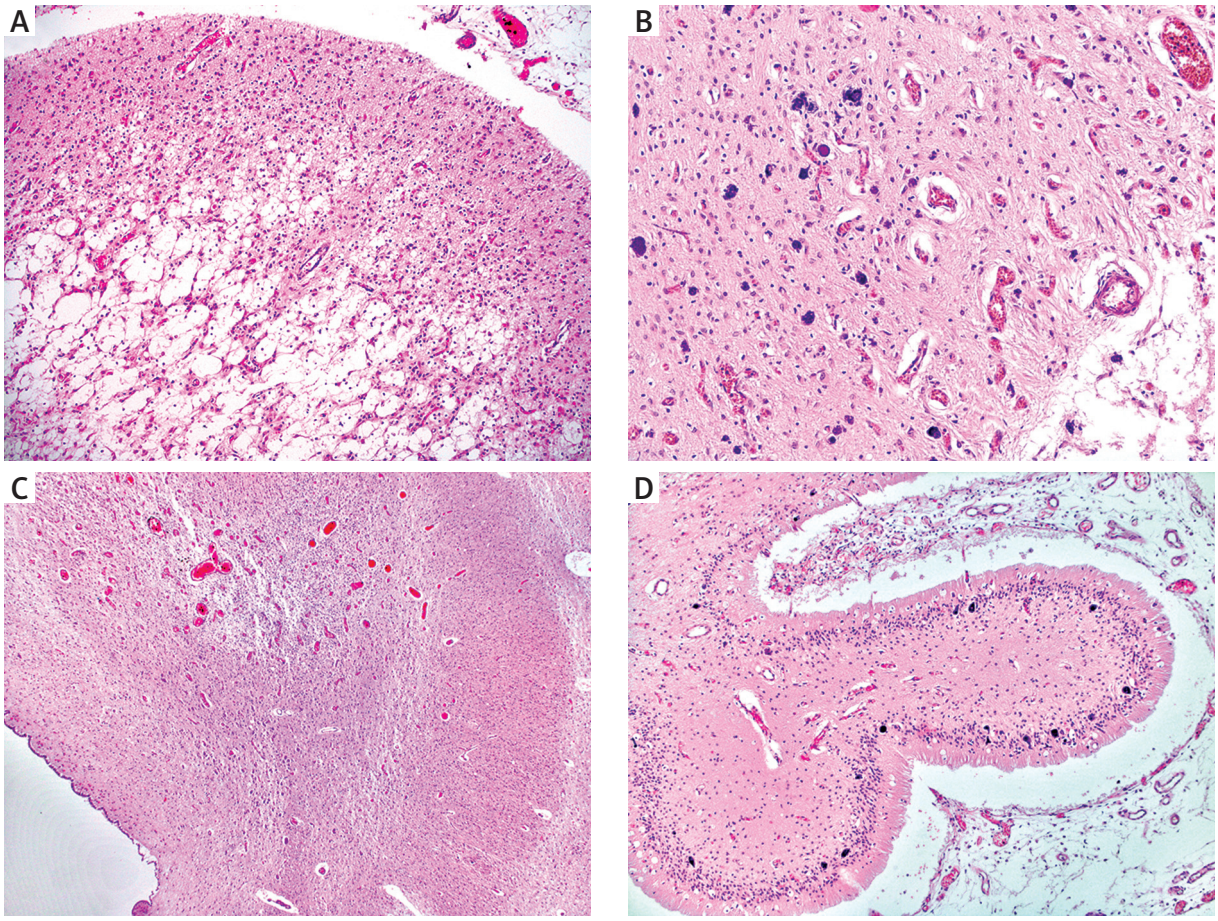

Fig. 2. Central nervous system autopsy material, paraffin sections stained with hematoxylin and eosin. **A)** Cerebral cortical and subcortical damage. Original magnification 100×. **B)** Basal ganglia lesions. Original magnification 200×. **C)** Brain stem (pons). Leigh-like subependymal focus. Original magnification 40×. **D)** Cerebellar cortex atrophy. Original magnification 100×. Detailed description in the text.

map (Fig. 3F) show an increased signal representing vasogenic oedema with multiple areas of restriction diffusion suggesting cytotoxic oedema (Fig. 3F) at both putamen.

Follow-up MR examination at the age of 3 (Fig. 4) revealed generalized infra- and supratentorial cortical and subcortical atrophy (Figs. 4A-D). The signal of both thalami and cerebral cortex normalized. An abnormal signal of the atrophic basal ganglia is decreased and the size of cystic lesions are diminished (Figs. 4A-C). Interestingly, in contrast to patient 1, the cerebellar cortex showed no detectable atrophic changes.

Discussion

In both studied cases, the diagnosis of *SLC19A3* defect was established too late to reliably check the effectiveness of biotin/thiamine administration. Intriguing specificity of brain morphology of "walnut pattern" [8] found at autopsy in patient 1 was the cause of the return to investigation after years, with the advent of the whole exome sequencing, which finally unravelled the disease cause. In patient 2, Leigh syndrome was diagnosed by MRI at onset (in 2013) but *SLC19A3* defect was not considered and therefore biotin/thiamine administration was not tested then. After establishing molecular diagnosis of *SLC19A3* defect, the first MRI was re-assessed and found typical of BTRBGD.

In 2013, the research team of van den Knaap identified a distinct MRI pattern [6] in seven patients with lethal leukoencephalopathy (out of more than 3000 MRIs). Using WES technology they linked this condition to *SLC19A3* mutations. The pattern includ-

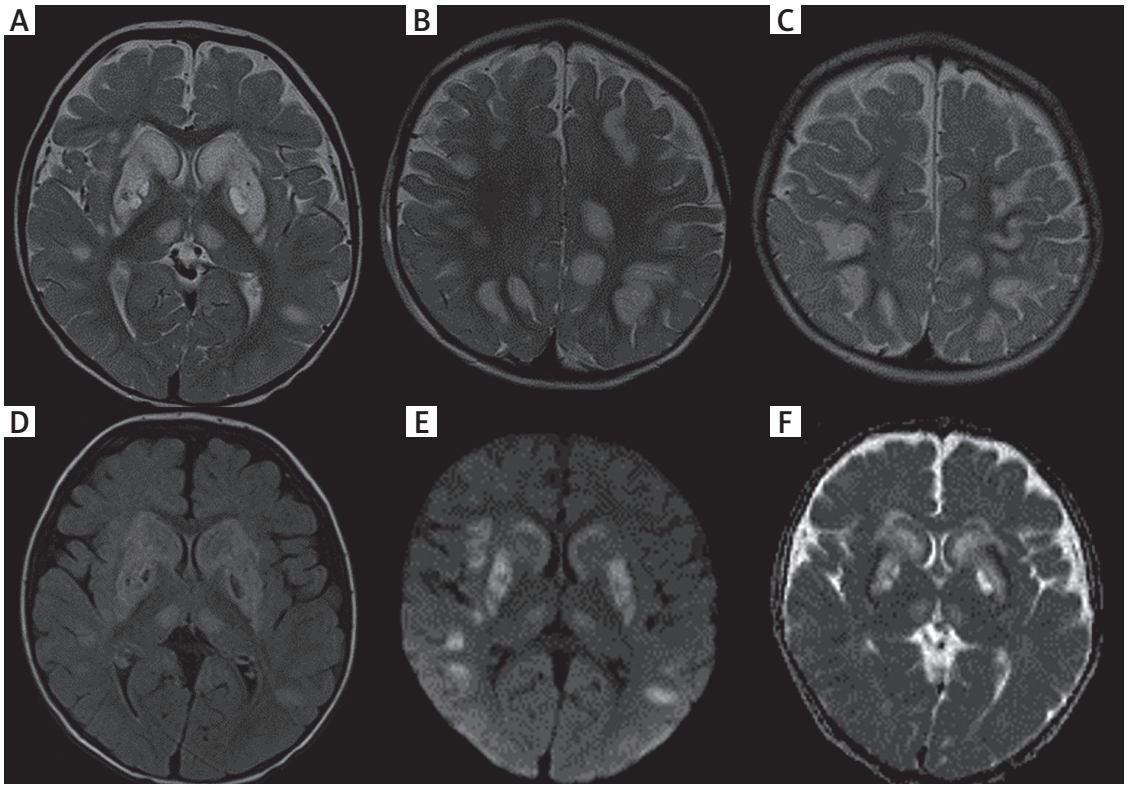

Fig. 3. Brain magnetic resonance imaging at the age of 12 months, the acute phase. Axial T2-weighted images demonstrate a bilateral and symmetric increased signal of the head of the caudate nuclei, putamina, globus pallidi and medial parts of both thalami (**A** and **D**). Abnormal T2-hyperintensities of the cerebral cortex and grey-white matter junction in both cerebral hemispheres (**B** and **C**). Axial FLAIR image **(D)** clearly demonstrates cystic degeneration of both lenticular nuclei. Diffusion weighted image **(E)** and ADC map **(F)** show an increased signal and represents vasogenic oedema with areas of restriction diffusion **(F)** suggesting cytotoxic oedema in parts of both putamina.

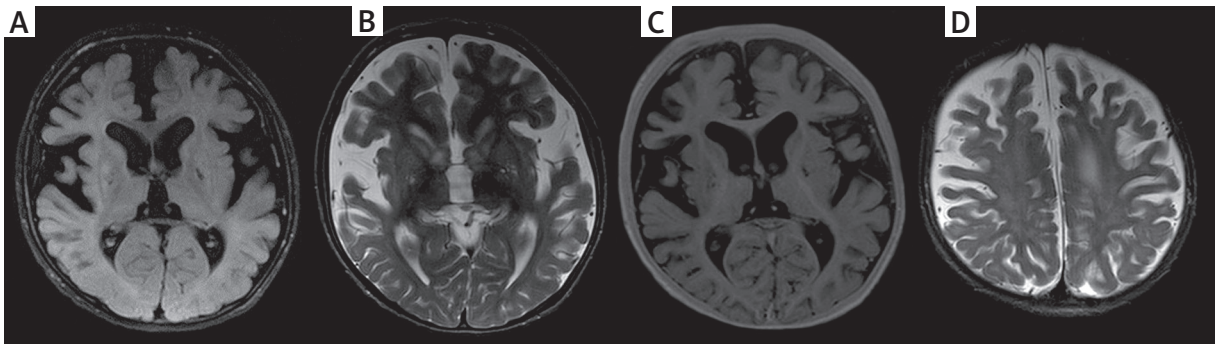

Fig. 4. Follow-up brain magnetic resonance at the age of 3 years. Generalized cortical and subcortical brain atrophy is seen **(A-D)**. The signal of both thalami and cerebral cortex is normalized. Abnormal signal of the atrophic basal ganglia is decreased and the size of cystic lesions is diminished **(A-C)**.

ed: "(i) bilateral signal abnormalities of the nucleus caudatus, putamen, globus pallidus and thalamus; (ii) extensive signal abnormalities of the subcortical and central cerebral white matter and the cerebral cortex; (iii) diffuse signal abnormalities of the cerebellar white matter with or without involvement of the cortex; (iv) extensive signal abnormalities in the pons and midbrain; and (v) in the case of follow-up

MRIs, atrophy of affected structures" [6]. Acute, post-acute, intermediate and end stage of the disease were specified in that study [6]. Up to now more than 75 patients were reported and natural history of the disease was presented in detail [10].

The clinical course of both presented patients demonstrated the most severe type of the *SLC19A3* defect. Neuropathological findings were in full accordance with the diagnostic criteria (Table I) for the disease [6]. We have to emphasize that in both patients a mitochondrial disease in the form of Leigh disease was also expressed, with typical topography and typical histopathological features of capillary proliferation, gliosis, spongiosis, oedema and pseudocystic formation in the affected brain regions, as described first by David Leigh in 1954 [9].

Our detailed description of human brain histology of *SLC19A3* defect is the second report, after the first one [6], which showed almost the same neuropathological damage pattern. Interestingly, there is also an animal model of the disease, studied in detail [16]. The dogs, Alaskan Huskies, demonstrated similar histological features to the affected humans. It included bilateral symmetrical, cavitary, malacic lesions in the thalamus, putamen, claustrum, junctional grey and white matter in the cerebral cortex, brainstem and midline cerebellar vermis [9]. Importantly, an occurrence of some interspecies differences was noticed by the authors [16].

About twenty five mutations including these identified in our study have been reported until today in the *SLC19A3* gene encoding a ubiquitously expressed human thiamine transporter 2 (hTHTR2). Most of them are missense/nonsense changes [HGMD Professional 2016.4].

The c.74dupT variant found in patient 1 is predicted to result in a frameshift starting at codon Ser26 and premature termination of protein translation (Ser26Leufs*19). This mutation was reported twice [3,14] in the compound heterozygous state.

The c.68G>T variant identified in patient 2 in the homozygous state resulted in substitution of highly evolutionary conserved Gly23 into Val. It is a very rare variant as its minor allele frequency (MAF) reported in the Exome Aggregation Consortium (ExAC) database is 0.000008. It was found up to now in three other families [6,10,12,19] including two with the same c.68G>T/c.68G>T genotype [19] as patient 2. One of them, Yemeni originated, presented first symptoms at the age of 12 months, just like our patient 2. The biotin supplementation was started immediately (in 4 days) and its effectiveness was very good [11,19]. The second reported patient with a homozygous c.68G>T variant, of Spanish origin, presented with acute encephalopathy and lactic acidosis during early infancy and also responded quickly to the biotin/thiamine treatment [12], however, on the follow-up observation, brain necrotic changes and cerebral atrophy developed in this patient.

In summary, our observation confirmed that morphological characteristics of the brain (autopsy or MRI) are quite specific to suspect BTRBGD and to start a cascade family study and/or test of biotin/thiamine administration immediately, before the final molecular identification of *SLC19A3* defect.

Acknowledgements

Funding: S136/13, S238/16, 2012/05/B/NZ2/ 01627, N407 075137.

Disclosure

Authors report no conflict of interest.

References

1. Alfadhel M, Almuntashri M, Jadah RH, Bashiri FA, Al Rifai MT, Al Shalaan H, Al Balwi M, Al Rumayan A, Eyaid W, Al-Twaijri W. Biotin-responsive basal ganglia disease should be renamed biotin-thiamine-responsive basal ganglia disease: a retrospective review of the clinical, radiological and molecular findings of 18 new cases. Orphanet J Rare Dis 2013; 8: 83.
2. Algahtani H, Ghamdi S, Shirah B, Alharbi B, Algahtani R, Bazaid A. Biotin-thiamine-responsive basal ganglia disease: catastrophic consequences of delay in diagnosis and treatment. Neurol Res 2017; 39: 117-125.
3. Debs R, Depienne C, Rastetter A, Bellanger A, Degos B, Galanaud D, Keren B, Lyon-Caen O, Brice A, Sedel F. Biotin-responsive basal ganglia disease in ethnic Europeans with novel SLC19A3 mutations. Arch Neurol 2010; 67: 126-130.
4. Fassone E, Wedatilake Y, DeVile CJ, Chong WK, Carr LJ, Rahman S. Treatable Leigh-like encephalopathy presenting in adolescence. BMJ Case Rep 2013; 2013: 200838.
5. Haack TB, Klee D, Strom TM, Mayatepek E, Meitinger T, Prokisch H, Distelmaier F. Infantile Leigh-like syndrome caused by SLC19A3 mutations is a treatable disease. Brain 2014; 137: e295.
6. Kevelam SH, Bugiani M, Salomons GS, Feigenbaum A, Blaser S, Prasad C, Häberle J, Baric I, Bakker IM, Postma NL, Kanhai WA, Wolf NI, Abbink TE, Waisfisz Q, Heutink P, van der Knaap MS. Exome sequencing reveals mutated SLC19A3 in patients with an early-infantile, lethal encephalopathy. Brain 2013; 136: 1534-1543.

7. Kono S, Miyajima H, Yoshida K, Togawa A, Shirakawa K, Suzuki H. Mutations in a thiamine-transporter gene and Wernicke's-like encephalopathy. N Engl J Med 2009; 360: 1792-1794.
8. Laurence KM, Cavanagh JB. Progressive degeneration of the cerebral cortex in infancy. Brain 1968; 91: 261-280.
9. Leigh D. Subacute necrotizing encephalomyelopathy in an infant. J Neurol Neurosurg Psychiatry 1951; 14: 216-221.
10. Ortigoza-Escobar JD, Molero-Luis M, Arias A, Oyarzabal A, Darín N, Serrano M, Garcia-Cazorla A, Tondo M, Hernández M, Garcia-Villoria J, Casado M, Gort L, Mayr JA, Rodríguez-Pombo P, Ribes A, Artuch R, Pérez-Dueñas B. Free-thiamine is a potential biomarker of thiamine transporter-2 deficiency: a treatable cause of Leigh syndrome. Brain 2016; 139: 31-38.
11. Ozand PT, Gascon GG, Al Essa M, Joshi S, Al Jishi E, Bakheet S, Al Watban J, Al-Kawi MZ, Dabbagh O. Biotin responsive basal ganglia disease: a novel entity. Brain 1998; 121: 1267-1279.
12. Pérez-Dueñas B, Serrano M, Rebollo M, Muchart J, Gargallo E, Dupuits C, Artuch R. Reversible lactic acidosis in a newborn with thiamine transporter-2 deficiency. Pediatrics 2013; 131: e1670-5.
13. Pronicka E, Piekutowska-Abramczuk D, Ciara E, Trubicka J, Rokicki D, Karkucińska-Więckowska A, Pajdowska M, Jurkiewicz E, Halat P, Kosińska J, Pollak A, Rydzanicz M, Stawinski P, Pronicki M, Krajewska-Walasek M, Płoski R. New perspective in diagnostics of mitochondrial disorders: two years' experience with whole-exome sequencing at a national paediatric centre. J Transl Med 2016; 14: 174.
14. Sremba LJ, Chang RC, Elbalalesy NM, Cambray-Forker EJ, Abdenur JE. Whole exome sequencing reveals compound heterozygous mutations in SLC19A3 causing biotin-thiamine responsive basal ganglia disease. Mol Genet Metab Rep 2014; 1: 368-372.
15. van der Knaap MS, Kevelam SH. Reply: Infantile Leigh-like syndrome caused by SLC19A3 mutations is a treatable disease. Brain 2014; 137: e297.
16. Vernau KM, Runstadler JA, Brown EA, Cameron JM, Huson HJ, Higgins RJ, Ackerley C, Sturges BK, Dickinson PJ, Puschner B, Giulivi C, Shelton GD, Robinson BH, DiMauro S, Bollen AW, Bannasch DL. Genome-wide association analysis identifies a mutation in the thiamine transporter 2 (SLC19A3) gene associated with Alaskan Husky encephalopathy. PLoS One 2013; 8: e57195.
17. Yamada K, Miura K, Hara K, Suzuki M, Nakanishi K, Kumagai T, Ishihara N, Yamada Y, Kuwano R, Tsuji S, Wakamatsu N. A wide spectrum of clinical and brain MRI findings in patients with SLC19A3 mutations. BMC Med Genet 2010; 11: 171.
18. Ygberg S, Naess K, Eriksson M, Stranneheim H, Lesko N, Barbaro M, Wibom R, Wang C, Wedell A, Wickström R. Biotin and thiamine responsive basal ganglia disease – a vital differential diagnosis in infants with severe encephalopathy. Eur J Paediatr Neurol 2016; 20: 457-461.
19. Zeng WQ, Al-Yamani E, Acierno JS Jr, Slaugenhaupt S, Gillis T, MacDonald ME, Ozand PT, Gusella JF. Biotin-responsive basal ganglia disease maps to 2q36.3 and is due to mutations in SLC19A3. Am J Hum Genet 2005; 77: 16-26.

Original paper

Folia Neuropathologica

Early increased density of cyclooxygenase-2 (COX-2) immunoreactive neurons in Down syndrome

Maria Mulet, José Miguel Blasco-Ibáñez, Carlos Crespo, Juan Nácher, Emilio Varea

Department of Cell Biology, University of Valencia, Burjassot, Spain

Folia Neuropathol 2017; 55 (2): 154-160 DOI: https://doi.org/10.5114/fn.2017.68582

Abstract

Neuroinflammation is one of the hallmarks of Alzheimer's disease. One of the enzymes involved in neuroinflammation, even in early stages of the disease, is COX-2, an inducible cyclooxygenase responsible for the generation of eicosanoids and for the generation of free radicals. Individuals with Down syndrome develop Alzheimer's disease early in life. Previous studies pointed to the possible overexpression of COX-2 and correlated it to brain regions affected by the disease. We analysed the COX-2 expression levels in individuals with Down syndrome and in young, adult and old mice of the Ts65Dn mouse model for Down syndrome. We have observed an overexpression of COX-2 in both, Down syndrome individuals and mice. Importantly, mice already presented an overexpression of COX-2 at postnatal day 30, before neurodegeneration begins; which suggests that neuroinflammation may underlie the posterior neurodegeneration observed in individuals with Down syndrome and in Ts65Dn mice and could be a factor for the premature appearance of Alzheimer's disease.

Key words: *Ts65Dn, Alzheimer's disease, neuroinflammation, microglia.*

Introduction

Down syndrome (DS) is the most common chromosomal aneuploidy [26]. Trisomy of chromosome 21 induces a phenotype with two hallmarks: intellectual disability and early development of Alzheimer's disease (AD) [20].

Alzheimer's disease development may be related to the presence of the amyloid precursor protein (APP) and the S100 genes on chromosome 21 [1,11]. Alzheimer's disease has been widely associated with neuroinflammation, a process that may be responsible for neuronal death observed in patients. One of the key enzymes at the top of the neuroinflammatory cascade is the COX family (cyclooxygenases) which comprises two members: COX-1 that is expressed under basal conditions and COX-2, an inducible isoform, although expressed weakly under basal conditions. Several studies have analysed the expression of COX-2 in AD brains showing contradictory effects, probably due to the different disease stages in which the studies were performed [5,35].

The Ts65Dn mouse is a DS model which is segmentally trisomic for a portion of mouse chromosome 16 and orthologous to the long arm of the human chromosome 21. This segment contains approximately 140 genes, many of which are highly conserved between mice and humans [32]. Ts65Dn mice repro-

Communicating author

Emilio Varea, PhD, Department of Cell Biology, University of Valencia, 50 Dr Moliner St., 46100 Burjassot, Spain, phone: +34963543783, e-mail: emilio.varea@uv.es

duce many of the alterations observed in DS, including the cholinergic degeneration present in AD.

In this study, we aim to characterize COX-2 expression in the human temporal cortex in DS and in the Ts65Dn mouse model with age.

Material and methods

Experimental mice were generated by repeated backcrossing of Ts65Dn females to C57/6Ei 9 C3H/HeSnJ (B6EiC3) F1 hybrid males. The parental generation was obtained from the research colony of Jackson Laboratory. Euploid littermates of Ts65Dn mice served as controls. We used a total of 18 trisomic and 18 euploid mice in three groups: young (1 month), adult (3-4 months) and old (12-14 months). The genotypic characterization was established by qRT-PCR using SYBR Green PCR master mix (Applied Biosystems). The amount of each gene was quantified by the ABI PRISM 7700 (Applied Biosystems). The genes analysed were APP (3 copies) and Apo-B (2 copies) [13,18]. Animal experimentation was conducted in accordance with Directive 2010/63/EU of the European Parliament and Council of 22 September 2010 on the protection of animals used for scientific purposes and was approved by the Committee of Bioethics of the University of Valencia. Every effort was made to minimize the number of animals used and their suffering.

Animals were transcardially perfused under deep anaesthesia (choral hydrate 4%, 1 ml/100 gr bw) using 4% paraformaldehyde in phosphate buffer. Brains were cryoprotected using 30% sucrose. Fifty microns thick sections (6 subseries) were collected from each brain using a sliding freezing microtome.

Human samples were obtained from the BiOBANC HCB – IDIBAPS (Barcelona, Spain). Temporal cortex human brain tissue had been fixed (24 h, paraformaldehyde 4% in buffered solution), cryoprotected (sucrose 30%), stored at –80°C and cut (8-10 µm) with a cryostat. We tested 5 controls (average age 55 years old, 31-78, PMI 11 h, 7-17 h) and 5 individuals with DS (average age 53.6 years old, 36-67, PMI 11.5, 6-18 h).

Single and double immunofluorescence

Tissue was processed "free-floating" (mouse brain sections) or on slides (human sections) for immunofluorescence as follows. Sections were incubated with citrate buffer (0.01 M, pH 6.0) for 1 minute at 100°C. After this, sections were treated for 1 h with 5% normal donkey serum (NDS) (Jackson ImmunoResearch Laboratories, West Grove, PA, USA) in PBS with 0.2% Triton-X100 (Sigma-Aldrich, St. Louis, MO, USA) and incubated overnight at room temperature either with only polyclonal goat IgG anti-COX2 (1 : 500, Santa Cruz) antibody or with a mix of COX-2 antibody and one of the following antibodies: monoclonal mouse IgG anti-NeuN (1 : 100, Chemicon), monoclonal mouse IgG anti-Iba1 (1 : 1000, Chemicon), polyclonal rabbit IgG anti-GFAP (1 : 1000, Sigma-Aldrich) or monoclonal mouse IgG anti-RIP (1 : 500, DSHB). Secondary antibodies were Alexa 488 donkey anti-goat IgG (1 : 200 Molecular Probes) and one of the following: Alexa 555 donkey anti-mouse IgG (1 : 200 Molecular Probes) or Alexa 555 donkey anti-rabbit IgG (1 : 200 Molecular Probes). Sections were mounted using Dako fluorescent medium (Dako North America, California). The sections were analysed using a confocal microscope (Leica TSC-SPE). Stacks (z-step 1.15 µm) were analysed using ImageJ software. All studied sections passed through all procedures simultaneously. All slides were coded prior to analysis until the experiment was completed.

Quantification of COX-2 expression

We analysed (1) the number of cells expressing COX-2 (high expression and low expression cells) and (2) the intensity of expression per cell in the temporal cortex of humans and mice (euploid and trisomic) of different ages. (1) For the number of cells, we counted the immunoreactive cells in 500-µm-wide strips (20 strips per group) running perpendicular to the pial surface including all layers of the temporal cortex. After measuring the area, we calculated cellular density. (2) For the intensity of expression per cell, we measured the intensity of fluorescence emission in 50 cells per individual using ImageJ software. Means were determined for each experimental group and data were statistically analysed using SPSS (version 15). The difference between groups was analysed in humans with one way ANOVA (phenotype) and in mice with two way ANOVA (age and phenotype). Parallel Nissl-stained sections were used to locate the analysed region.

Results

COX-2-positive cells could be found in all layers of the temporal cortex, as well as in other cortical regions of the adult mouse. We observed COX-2

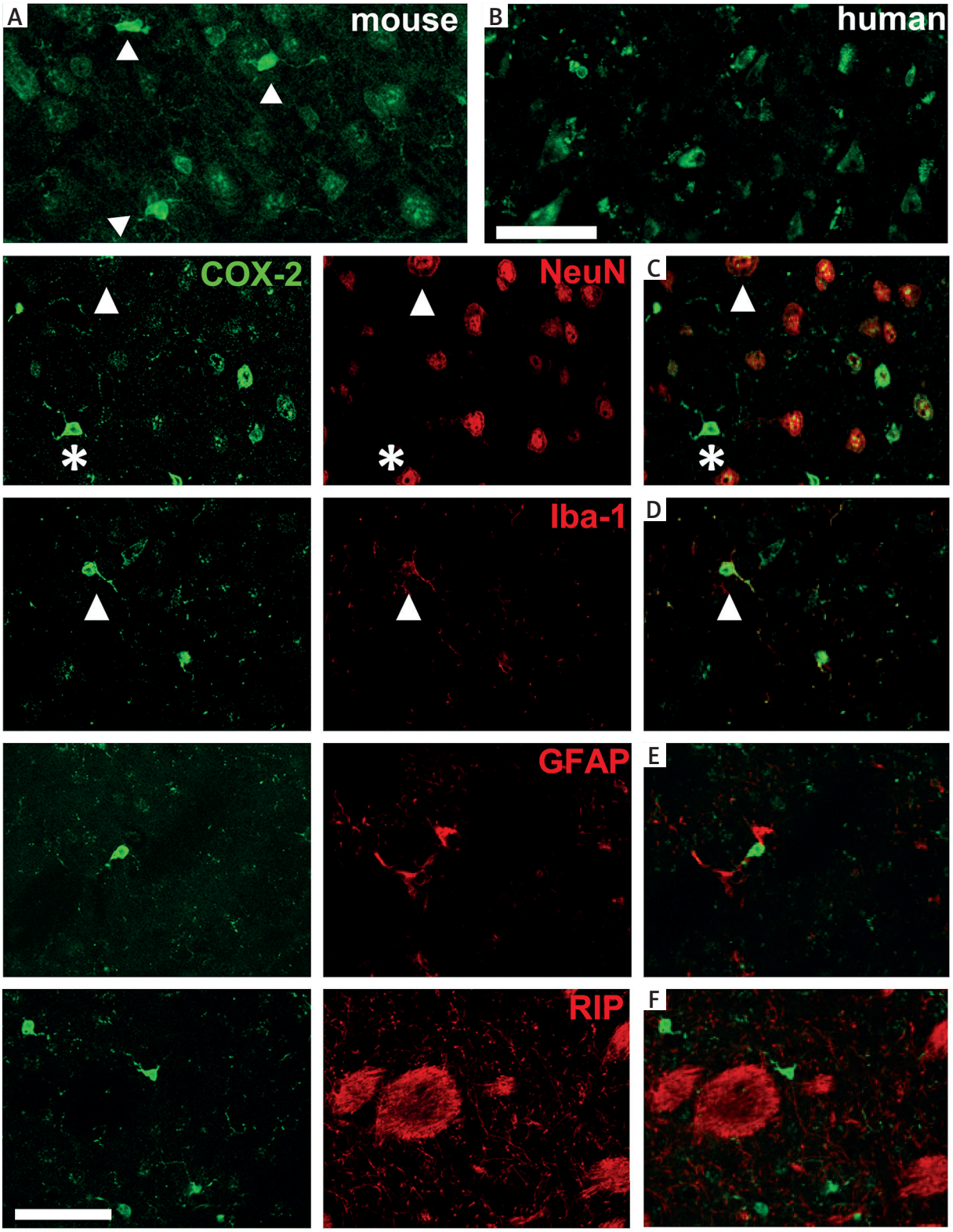

Fig. 1. COX-2 expression in mice and humans. **A)** Adult mouse cortex. High expression of COX-2 in small cells (arrowheads) and low expression in large cells. **B)** COX-2 in the human temporal cortex. **C)** In mice, large COX-2 expressing cells are NeuN positive (neurons, arrowheads) but small cells are not. **D)** COX-2 small cells are Iba-1 (microglia, arrowhead). GFAP-positive astrocytes **(E)** and RIP-positive oligodendrocytes **(F)** lack COX-2. Scale bar 50 µm.

expression in two types of cells: small cells with high expression (arrowheads, Fig. 1A) and large cells with low expression (Fig. 1A). Expression of COX-2 in the temporal cortex of humans presented a similar pattern to that of mouse; however the population of small intensely stained cells was absent (Fig. 1B).

Phenotypic characterization of COX-2-expressing cells in the mouse temporal cortex reflected that the large COX-2-positive cells corresponded to neurons (NeuN positive, Fig. 1C) while the small COX-2 positive cells corresponded to microglia (Iba-1 positive, Fig. 1D). COX-2 was absent in astrocytes (GFAP, Fig. 1E) and oligodendrocytes (RIP, Fig. 1F).

Next, we studied COX-2 expression in DS individuals (5 controls and 5 individuals with DS) and found more COX-2-positive cells in individuals with DS (428.0 ± 29.4 cells/mm^2) than in controls (331.0 ± 25.4 cells/mm^2, $p < 0.05$) (Fig. 2A). Analysis of the intensity of COX-2 expression in both, control and DS individuals, showed that it was similar in the positive cells in the two groups (Fig. 2B).

In the second part of the study we set out to study whether the increase in COX-2-positive cell number observed in humans was present in the temporal cortex of the mouse model for DS Ts65Dn and if so, to determine the time point of onset of the overexpression of this molecule. As shown above, there are two populations of cells in mice (Fig. 1B): small, high COX-2-expressing cells (microglia) and large, low COX-2-expressing cells (neurons) in young (1 month), adult (4 months) and old (12-14 months) mice. Analysis of the microglial cells expressing COX-2 (Fig. 3A) revealed a phenotype-dependent decrease ($p < 0.05$). Moreover, the number of microglial cells expressing COX-2 was reduced with age (young-adult $p < 0.001$, and adult-old $p < 0.05$). Young: control 122.0 ± 11.2 vs. trisomic 94.4 ± 4.1 cells/mm^2; adults: control 70.3 ± 3.0 vs. trisomic 62.5 ± 7.9 cells/mm^2; old: control 48.9 ± 10.6 vs. trisomic 38.4 ± 10.8 cells/mm^2. Analysis of the number of neurons expressing COX-2 in mice (Fig. 3B) (similar population as observed in humans) showed that the COX-2 neuronal density was not altered between age groups, but similar to humans, we found more COX-2-expressing neurons in trisomic mice ($p < 0.001$; Fig. 3B). Control: young 696.9 ± 20.1; adult 680.3 ± 25.2; old 669.7 ± 22.4 cells/mm^2; trisomic: young 843.9 ± 25.7; adult 836.4 ± 30.5; old 824.2 ± 58.2 cells/mm^2. Finally we analysed the intensity of COX-2 expression in the cytoplasm of neurons (Fig. 3C) in the different groups of mice. We observed a decrease in the intensity related to age, however, similar to our findings in humans, there was no difference in the intensity of expression of COX-2 between control and trisomic mice at any age studied.

Discussion

In conclusion, we have found an increased number of COX-2 immunoreactive cells in the human DS temporal cortex as well as in the brain of the mouse model for DS (Ts65Dn) at any age examined. Our findings in humans confirm previous studies where an increased expression of COX-2 has been observed in other brain regions [24].

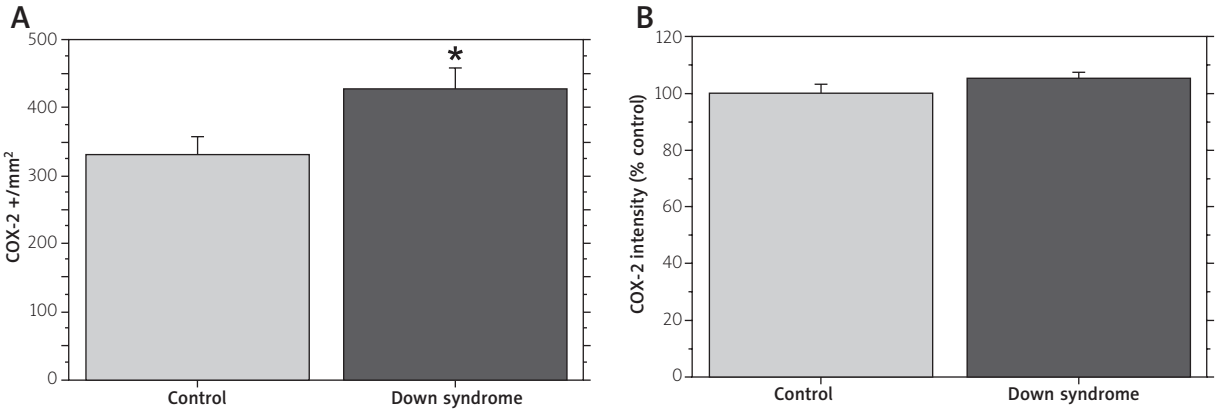

Fig. 2. Alterations in COX-2 expression in the human temporal cortex in DS. **A)** COX-2 cell density in the human temporal cortex (control vs. DS). **B)** Intensity of expression of COX-2 in the cytoplasm of neurons in the human temporal cortex (control vs. DS), values are represented in %, being 100 in control conditions (*$p < 0.05$).

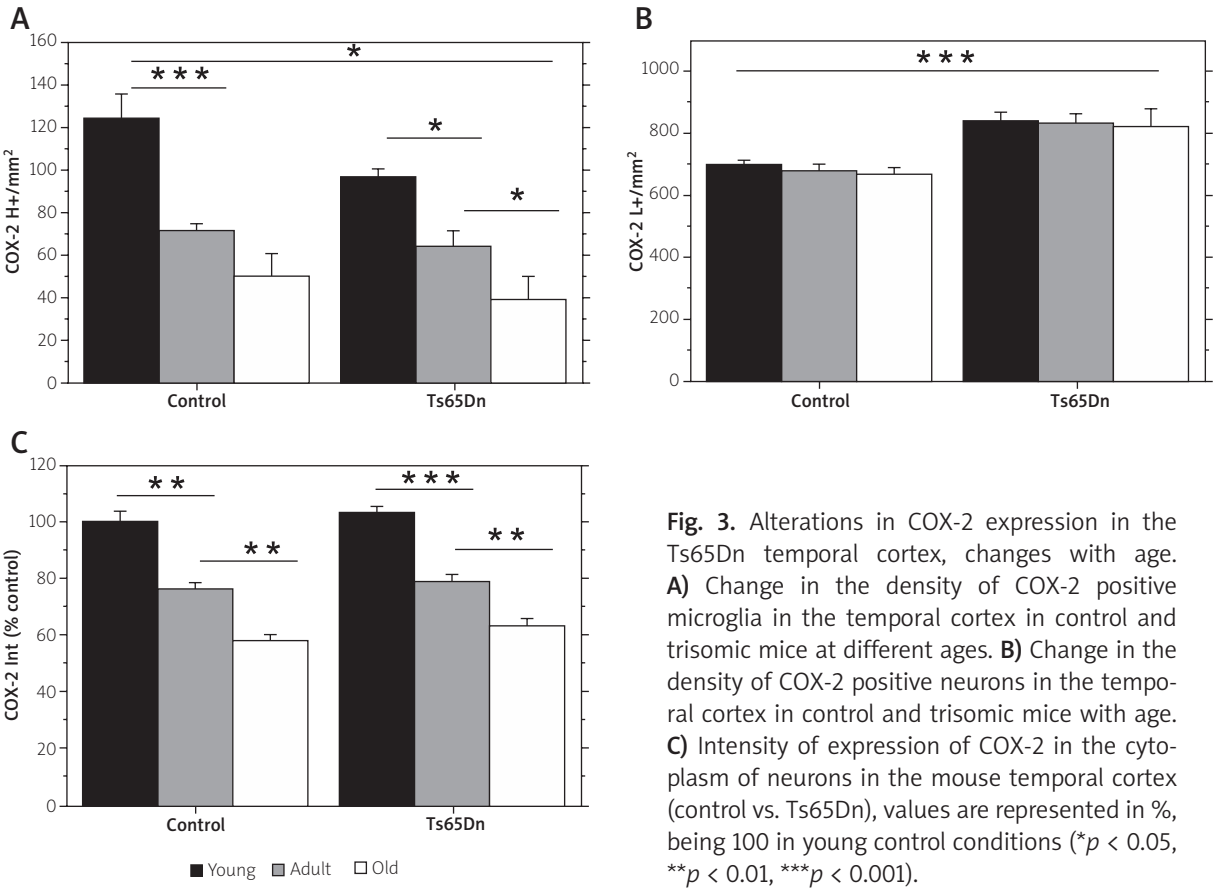

Fig. 3. Alterations in COX-2 expression in the Ts65Dn temporal cortex, changes with age. **A)** Change in the density of COX-2 positive microglia in the temporal cortex in control and trisomic mice at different ages. **B)** Change in the density of COX-2 positive neurons in the temporal cortex in control and trisomic mice with age. **C)** Intensity of expression of COX-2 in the cytoplasm of neurons in the mouse temporal cortex (control vs. Ts65Dn), values are represented in %, being 100 in young control conditions (*$p < 0.05$, **$p < 0.01$, ***$p < 0.001$).

In mice it has been shown previously that COX-2 is present in neurons [16,35], although some studies found it in microglia [4,34], and even astrocytes [14]. Using an antibody previously tested in humans, we and others have shown that in humans COX-2-positive cells are always neurons [22]. However, in the mouse temporal cortex we found, in addition to large COX-2-expressing NeuN-positive cells (neurons, Fig. 1C), small COX-2-expressing cells which were Iba-1-positive and therefore microglia (Fig. 1D). COX-2 was absent in astrocytes (GFAP, Fig. 1E) and oligodendrocytes (RIP, Fig. 1F). Here we show that in the Ts65Dn mouse model, the increased number of COX-2-expressing neurons in DS is independent of age. The principal observation of our study is that this alteration starts early in DS, even in young animals (1 month old). This fact opens the possibility that, given that the alteration in COX-2 is previous to any deleterious observation, perhaps the degeneration observed in DS could be related to the alterations observed in markers such as COX-2.

The mechanism underlying the overexpression of COX-2 in DS has not been elucidated. One possibility is that the higher expression of COX-2 may be related to an extra copy of S100B present in individuals with DS [4]. S100B induces the expression of NF-κB, which is responsible, in turn, for COX-2 transcription.

Overexpression of COX-2 seems to be beneficial in the short run [9]. However, a chronic expression may be deleterious for the brain. In our animals, the density of COX-2 neurons remains unaltered with age, although some studies in old animals reported an increase with age [17]. Perhaps the reduced expression observed in the cytoplasm of old neurons in control and Ts65Dn mice, could lead to an underestimation of the number of positive cells in old animals.

Control of COX-2 expression is fundamental because of the reaction products of COX-2, pro-inflammatory prostanoids and reactive oxygen species, may be cytotoxic and cause CNS injury [29]. However the clear role of COX-2 in the neuroinflammatory process is still a matter of controversy (for a review, see [31]). COX-2 shows a low expression under basal conditions, but is increased during inflammatory responses and can be induced by cytokines and tumour necrosis factor [33]. Pathol-

ogies are AD [23] or epilepsy [27] course with an increment in COX-2. Both pathologies present a high prevalence in DS individuals [20,30]. Moreover, DS is a syndrome that induces a premature ageing process. Human fibroblasts of individuals with DS show an excess of COX-2, and, when submitted to pro-inflammatory treatment, respond strongly by increasing COX-2 expression [24]. The elevated expression of COX-2 in DS could underlie, at least in part, the observed neurodegeneration in this syndrome and could explain the early onset of AD.

COX-2 has been related to adult neurogenesis and neuronal function. The KO mice for COX-2 display a reduction in hippocampal neurogenesis [21], moreover the treatment with COX-2 blockers reduces neurogenesis [8] and impairs the formation of LTP [6]. Even animal models for diabetes display parallel alterations in COX-2 expression and neurogenesis [15]. However, other studies have observed that the increased expression of COX-2 reduced the survival of the newborn cells. [2]. However, the model for DS Ts65Dn, showing an increased expression of COX-2 display a reduction in neurogenesis in the hippocampus [7,19].

This apparent discrepancy could be explained attending to three main facts: (a) the analysis of the increased expression of COX-2 observed in the hippocampus of some animal models of insult, such ischemia, which induces an increase in the expression of COX-2 and neurogenesis reflects that the phenotype of the newly generated cells are mainly glia cells [28]; (b) the second possibility is related to the excess of cellular activity observed in DS [10] as well in the Ts65Dn model (Carbonell in preparation), this overactivation could be the basis of the increased expression of COX-2 and (c) the dysregulation observed in the balance between excitation and inhibition observed in DS [3,12,25]. This dysregulation leads to an increase in some inhibitory neurons, including the so-called IS cells [12,13], which inhibits other inhibitory neurons generating an over-activation that is related with the high prevalence of epilepsy in individuals with DS [30] and could be related to the increased expression of COX-2 observed in neurons in the Ts65Dn model.

Acknowledgments

This study was supported by the Jerome Lejeune Foundation.

Disclosure

Authors report no conflict of interest.

References

1. Antonarakis SE, Lyle R, Dermitzakis ET, Reymond A, Deutsch S. Chromosome 21 and down syndrome: from genomics to pathophysiology. Nat Rev Genet 2004; 5: 725-738.
2. Bastos GN, Moriya T, Inui F, Katura T, Nakahata N. Involvement of cyclooxygenase-2 in lipopolysaccharide-induced impairment of the newborn cell survival in the adult mouse dentate gyrus. Neuroscience 2008; 155: 454-462.
3. Belichenko PV, Kleschevnikov AM, Masliah E, Wu C, Takimoto-Kimura R, Salehi A, Mobley WC. Excitatory-inhibitory relationship in the fascia dentata in the Ts65Dn mouse model of down syndrome. J Comp Neurol 2009; 512: 453-466.
4. Bianchi R, Adami C, Giambanco I, Donato R. S100B binding to RAGE in microglia stimulates COX-2 expression. J Leukoc Biol 2007; 81: 108-118.
5. Chang JW, Coleman PD, O'Banion MK. Prostaglandin G/H synthase-2 (cyclooxygenase-2) mRNA expression is decreased in Alzheimer's disease. Neurobiol Aging 1996; 17: 801-808.
6. Chen C, Magee JC, Bazan NG. Cyclooxygenase-2 regulates prostaglandin E2 signaling in hippocampal long-term synaptic plasticity. J Neurophysiol 2002; 87: 2851-2857.
7. Clark S, Schwalbe J, Stasko MR, Yarowsky PJ, Costa ACS. Fluoxetine rescues deficient neurogenesis in hippocampus of the Ts65Dn mouse model for Down syndrome. Exp Neurol 2006; 200: 256-261.
8. Goncalves MB, Williams E-J, Yip P, Yáñez-Muñoz RJ, Williams G, Doherty P. The COX-2 inhibitors, meloxicam and nimesulide, suppress neurogenesis in the adult mouse brain. Br J Pharmacol 2010; 159: 1118-1125.
9. Gopez JJ, Yue H, Vasudevan R, Malik AS, Fogelsanger LN, Lewis S, Panikashvili D, Shohami E, Jansen SA, Narayan RK, Strauss KI. Cyclooxygenase-2-specific inhibitor improves functional outcomes, provides neuroprotection, and reduces inflammation in a rat model of traumatic brain injury. Neurosurgery 2005; 56: 590-604.
10. Greber-Platzer S, Balcz B, Cairns N, Lubec G. c-fos expression in brains of patients with Down syndrome. J Neural Transm Suppl 1999; 57: 75-85.
11. Helguera P, Pelsman A, Pigino G, Wolvetang E, Head E, Busciglio J. ets-2 promotes the activation of a mitochondrial death pathway in Down's syndrome neurons. J Neurosci 2005; 25: 2295-2303.
12. Hernández-González S, Ballestín R, López-Hidalgo R, Gilabert-Juan J, Blasco-Ibáñez JM, Crespo C, Nácher J, Varea E. Altered distribution of hippocampal interneurons in the murine Down Syndrome model Ts65Dn. Neurochem Res 2015; 40: 151-164.
13. Hernández S, Gilabert-Juan J, Blasco-Ibáñez JM, Crespo C, Nácher J, Varea E. Altered expression of neuropeptides in the primary somatosensory cortex of the Down syndrome model Ts65Dn. Neuropeptides 2012; 46: 29-37.
14. Hirst WD, Young KA, Newton R, Allport VC, Marriott DR, Wilkin GP. Expression of COX-2 by normal and reactive astrocytes in the adult rat central nervous system. Mol Cell Neurosci 1999; 13: 57-68.

15. Hwang IK, Yi SS, Yoo K-Y, Park OK, Yan B, Kim IY, Kim YN, Song W, Moon SM, Won M-H, Seong JK, Yoon YS. Effects of treadmill exercise on cyclooxygenase-2 in the hippocampus in type 2 diabetic rats: Correlation with the neuroblasts. Brain Res 2010; 1341: 84-92.
16. Kaufmann WE, Worley PF, Pegg J, Bremer M, Isakson P. COX-2, a synaptically induced enzyme, is expressed by excitatory neurons at postsynaptic sites in rat cerebral cortex. Proc Natl Acad Sci U S A 1996; 93: 2317-2321.
17. Lee CH, Yoo K-Y, Choi JH, Park OK, Hwang IK, Kang I-J, Won M-H. Cyclooxygenase-2 immunoreactivity and protein level in the gerbil hippocampus during normal aging. Neurochem Res 2010; 35: 99-106.
18. Liu DP, Schmidt C, Billings T, Davisson MT. Quantitative PCR genotyping assay for the Ts65Dn mouse model of Down syndrome. Biotechniques 2003; 35: 1170-1174, 1176, 1178 passim.
19. López-Hidalgo R, Ballestín R, Vega J, Blasco-Ibáñez JM, Crespo C, Gilabert-Juan J, Nácher J, Varea E. Hypocellularity in the Murine Model for Down Syndrome Ts65Dn Is Not Affected by Adult Neurogenesis. Front Neurosci 2016; 10: 75.
20. Lott IT, Head E. Alzheimer disease and Down syndrome: factors in pathogenesis. Neurobiol Aging 2005; 26: 383-389.
21. Nam SM, Kim JW, Yoo DY, Choi JH, Kim W, Jung HY, Won M-H, Hwang IK, Seong JK, Yoon YS. Effects of Treadmill Exercise on Neural Stem Cells, Cell Proliferation, and Neuroblast Differentiation in the Subgranular Zone of the Dentate Gyrus in Cyclooxygenase-2 Knockout Mice. Neurochem Res 2013; 38: 2559-2569.
22. Neri M, Cantatore S, Pomara C, Riezzo I, Bello S, Turillazzi E, Fineschi V. Immunohistochemical expression of proinflammatory cytokines IL-1β, IL-6, TNF-α and involvement of COX-2, quantitatively confirmed by Western blot analysis, in Wernicke's encephalopathy. Pathol Res Pract 2011; 207: 652-658.
23. Oka A, Takashima S. Induction of cyclo-oxygenase 2 in brains of patients with Down's syndrome and dementia of Alzheimer type: specific localization in affected neurones and axons. Neuroreport 1997; 8: 1161-1164.
24. Otsuka Y, Ito M, Yamaguchi M, Saito S, Uesu K, Kasai K, Abiko Y, Mega J. Enhancement of lipopolysaccharide-stimulated cyclooxygenase-2 mRNA expression and prostaglandin E2 production in gingival fibroblasts from individuals with Down syndrome. Mech Ageing Dev 2002; 123: 663-674.
25. Pérez-Cremades D, Hernández S, Blasco-Ibáñez JM, Crespo C, Nacher J, Varea E. Alteration of inhibitory circuits in the somatosensory cortex of Ts65Dn mice, a model for Down's syndrome. J Neural Transm 2010; 117: 445-455.
26. Roizen NJ, Patterson D. Down's syndrome. Lancet 2003; 361: 1281-1289.
27. Rojas A, Jiang J, Ganesh T, Yang M-S, Lelutiu N, Gueorguieva P, Dingledine R. Cyclooxygenase-2 in epilepsy. Epilepsia 2014; 55: 17-25.
28. Sasaki T, Kitagawa K, Sugiura S, Omura-Matsuoka E, Tanaka S, Yagita Y, Okano H, Matsumoto M, Hori M. Implication of cyclooxygenase-2 on enhanced proliferation of neural progenitor cells in the adult mouse hippocampus after ischemia. J Neurosci Res 2003; 72: 461-471.
29. Seibert K, Masferrer J, Zhang Y, Gregory S, Olson G, Hauser S, Leahy K, Perkins W, Isakson P. Mediation of inflammation by cyclooxygenase-2. Agents Actions Suppl 1995; 46: 41-50.
30. Stafstrom CE. Epilepsy in Down syndrome: clinical aspects and possible mechanisms. Am J Ment Retard 1993; 98 Suppl: 12-26.
31. Strauss KI. Antiinflammatory and neuroprotective actions of COX2 inhibitors in the injured brain. Brain Behav Immun 2008; 22: 285-298.
32. Sturgeon X, Gardiner KJ. Transcript catalogs of human chromosome 21 and orthologous chimpanzee and mouse regions. Mamm Genome 2011; 22: 261-271.
33. Vane JR, Bakhle YS, Botting RM. Cyclooxygenases 1 and 2. Annu Rev Pharmacol Toxicol 1998; 38: 97-120.
34. Villa V, Thellung S, Corsaro A, Novelli F, Tasso B, Colucci-D'Amato L, Gatta E, Tonelli M, Florio T. Celecoxib Inhibits Prion Protein 90-231-Mediated Pro-inflammatory Responses in Microglial Cells. Mol Neurobiol 2016; 53: 57-72.
35. Yasojima K, Schwab C, McGeer EG, McGeer PL. Distribution of cyclooxygenase-1 and cyclooxygenase-2 mRNAs and proteins in human brain and peripheral organs. Brain Res 1999; 830: 226-236.

Original paper

Folia Neuropathologica

Commitment of protein p53 and amyloid-beta peptide (Aβ) in aging of human cerebellum

Danuta Maślińska[1,2], Milena Laure-Kamionowska[2], Dariusz Szukiewicz[1], Sławomir Maśliński[1], Krystyna Księżopolska-Orłowska[3]

[1]Department of General and Experimental Pathology, Warsaw Medical University, Warsaw, [2]Department of Experimental and Clinical Neuropathology, Mossakowski Medical Research Centre, Polish Academy of Sciences, Warsaw, [3]Department of Rehabilitation, National Institute of Geriatrics, Rheumatology and Rehabilitation, Warsaw, Poland

Folia Neuropathol 2017; 55 (2): 161-167 DOI: https://doi.org/10.5114/fn.2017.68583

Abstract

Protein p53 is known to induce the cell cycle arrest and apoptosis in response to a variety of cellular distress signals and DNA damage. A recent study has demonstrated that in blood cells of aging subjects, p53 may induce early pathological changes that precede the amyloidogenic cascade. However, it is not clear whether p53 participates in the local deposition of amyloid-beta peptide (Aβ) in the nerve tissue of normal aging subjects. Therefore, in the present study, we analyse the distribution of both (Aβ and p53) proteins in the cerebellum of individuals without any history of dementia or other neurological illness who died suddenly in traffic accidents.

We found that in the subjects at the beginning of their aging process (60-65 years of age) Aβ deposits were localized in subependymal areas of the cerebellar cortex and such deposits were not linked to the presence of p53 in the nerve tissue. In groups of subjects over 65 years of age, numerous Aβ diffuse plaques were scattered throughout the cerebellar cortex. In these subjects, p53 protein was detected in the cytoplasm or in the nucleus of the cerebellar nerve cells.

All the results lead to the conclusion that in nerve tissue p53 participates in the process of neurodegeneration and then it is involved in the deposition of Aβ in the nerve tissue.

Key words: *amyloid-beta (Aβ) deposits, aging, cerebellum, p53, neurodegeneration.*

Introduction

The brain as any other organ shows morphological changes with the increasing age. In humans, most prominent morphological features of the brain aging include extracellular deposits of amyloid and intracellular neurofibrillary tangles. Amyloid deposits may take a form of diffuse, neuritic or senile plaques and angiopathy in small blood vessels. The main component of such deposits is beta-amyloid (Aβ) which is a fragment of the amyloid precursor protein (APP) snipped from APP during its metabolism.

Clinical symptoms at the beginning of human aging are characterized by a decrease in muscle strength, impairment of vision, and diminution of hearing but progress of aging leads to the further symptoms such as loss of memory for recent events, decreased abstract thinking, disorientation and dementia including Alzheimer's disease (AD).

Communicating author

Milena Laure-Kamionowska, PhD, Department of Experimental and Clinical Neuropathology, Mossakowski Medical Research Centre, Polish Academy of Sciences, 5 Pawińskiego St., 02-106 Warsaw, Poland, phone: +48 22 608 65 03, e-mail: mkamionowska@imdik.pan.pl

Currently, with the increasing life expectancy across the world, problems inherent in aging are the focus of the intensive study. A substantial body of evidence suggests that the lifespan is under genetic control but decades of quest for human longevity genes were not successful. Results of the studies suggest that the epigenetic mechanisms probably play a role in modulating the lifespan [13,23,34]. Moreover, these studies document that the heritability of epigenetic age acceleration in various brain regions is different and that the heritability of age acceleration of the cerebellum appears to be higher than that of the frontal cortex, pons or temporal cortex.

The role of the cerebellum in motor coordination of the body movement is well known [8,11,35] but increasing evidence shows that the cerebellum plays also a significant role in cognitive functions such as attention, language, emotional behaviour, sleep, and even non-somatic visceral responses [21,29].

A distinct functional topography for the cerebellum has been shown, reflecting connections to distributed circuits within the central nervous system (CNS) [31,32]. These include loops associated with cognitive processing where the cerebellum exerts a modulating effect that may be impaired in neuropsychiatric diseases [20,24-27].

Coupling within various neural networks and brain systems is known to be affected by amyloid pathology in AD [4,6,18,28], but also in elderly subjects with normal cognitive performance effects of brain amyloidosis on functional integrity of the cerebro-cerebellar system has been documented [2]. Moreover, brain amyloidosis-related changes in cerebro-cerebellar coupling indicate brain regions with particular vulnerability to amyloid-associated pathology [29,30].

For the last few decades, the prevention and treatment of the cognitive disorders including AD has remained a major challenge for clinicians and scientists. In view of existing and emerging therapeutic compounds, the focus has increasingly shifted to accurate detection of the earliest phase of the illness. Results of performed studies with a wide variety of different proteins such as inflammatory markers, markers of oxidative stress, apolipoproteins, and markers of neuronal degeneration suggest [3,36] that the measurement of conformational altered p53 in blood cells has a high ability to early discriminate AD cases from normal aging [14]. It was also observed that such defective p53 when influenced by very low concentrations of soluble Aβ, may induce at a cellular level, early pathological changes that precede the amyloidogenic cascade.

A recent study has demonstrated that Aβ is linked to functional reorganization within the cerebro-cerebellar system, taking place in elderly individuals with normal cognitive performance. However, it is not clear whether p53 protein participates in local deposition of Aβ in cerebellar of normal aging subjects as it was observed in the cells of peripheral tissues. Therefore, in the present study, we analyse the distribution of both proteins in the cerebellum of individuals without any history of dementia or other neurological illness and who died suddenly in traffic accidents.

Material and methods

The study was performed performed on archival material of brain sections collected routinely at autopsies. All subjects were victims of traffic accidents in which they participated as drivers or as pedestrians. Paraffin blocks were drawn from the files of the Mossakowski Medical Research Centre, Polish Academy of Sciences, Warsaw, Poland. Serial sections 5 µm thick were stained with H&E for routine histological examination or used for immuno-histochemical study.

Immunohistochemistry was performed using specific primary antibodies:

- monoclonal mouse anti-human p53 protein Clone DO-7 Code No. M 7001 Lot 075 was purchased from DAKO and supplied in liquid form as tissue culture supernatant (RPMI 1640 medium containing foetal calf serum) dialysed against 0.05 M Tris/HCl, pH 7.2 containing 15 mM NaN_3. The DAKO antibody recognizes an epitope in the *N*-terminus of the human p53 protein. The epitope for the antibody is known to be residing between amino acids 19 to 26;
- monoclonal mouse anti-β-amyloid 4G8 which recognizes an epitope residing between amino acids 17-24 of Aβ protein was purchased from BioLegend;
- polyclonal rabbit anti-β-amyloid which recognizes an epitope residing between amino acids 1-42 protein of Aβ was purchased from Bio-Rad;
- alkaline phosphatase-avidin-biotin conjugate purchased from Santa Cruz Biotechnology, Inc. (USA);
- avidin-biotin-peroxidase complex system purchased from Vector Laboratories (USA);
- and all of them were used according to the manufacturer's recommendations.

Briefly, sections were dewaxed and hydrated through descending alcohols to water. For non-enzymatic antigen retrieval, tissue sections were heated in 0.01 M sodium citrate buffer (pH 6.0) to 95°C and allowed to cool for 20 min at room temperature and washed with PBS. Then, they were incubated in a solution of methanol containing 3% H_2O_2 for 20 min to quench endogenous peroxidase. Washed again in PBS and blocked with a solution of PBS containing 5% appropriate normal serum (rabbit or mouse) for 2 h at room temperature, sections were incubated overnight at 4°C in solutions of the primary antibody. Immunoreactions were visualized using biotinylated secondary antibodies and ABComplex/HRP or an alkaline phosphatase-avidin-biotin conjugate. Then, sections were lightly counterstained with Mayer's haematoxylin.

For negative controls, primary antibodies were replaced with an appropriate isotypic normal mouse or rabbit immunoglobulin fraction at matched protein concentration. These were included for the examination of each specimen and consistently produced negative results.

Results

Data pertaining to the groups of drivers and pedestrians who were victims of traffic accidents are shown in Tables I and II. Amyloid β peptide and p53 protein were found in approximately 50% of subjects. The immunoexpression and distribution of both proteins in cerebella of drivers were similar as in age-matched groups of pedestrians. In the group of subjects of 55-65 years of age, deposits of Aβ in form of diffuse plaques were detected only at the most peripheral areas of the cerebellar cortex (Table I). In groups of the older subjects, such plaques were scattered throughout the molecular and Purkinje cell layers (Fig. 1). Plaques were of different size and peculiar shape (Fig. 2).

Distribution of p53 protein in the cerebellum was clearly linked with the layer of the Purkinje cells (Fig. 3).

In the youngest groups of subjects (55-65 years of age), p53 was not detected in groups of the older individuals, p53 immuno-positive grains were found only in cytoplasm of some Purkinje cells (Table II). These grains were cumulated in the cytoplasm around the nucleus of the cells (Fig. 4).

In numerous Purkinje cells and other nerve cells, p53 was detected also within the cell nucleus (Table II and Fig. 5) but never simultaneously in the nucleus and in cytoplasm of the same cell. Accumulation of p53 protein in the cell nucleus precedes the cell degeneration and death. In the double immunostained tissue

Table I. Distribution of amyloid β deposits in the cerebellum of subjects participating in traffic accidents

Groups	Number	Age	Areas of cerebellar cortex				White matter
Drivers			SM	ML	PC	GL	
	7	55-65	4/7	0/7	0/7	0/7	0/7
	9	66-75	5/9	5/9	3/9	0/9	0/9
	5	76-85	4/5	4/5	4/5	0/5	0/5
Pedestrians	8	55-65	5/8	0/8	0/8	0/8	0/8
	7	66-75	5/7	5/7	5/7	0/7	0/7
	6	76-85	4/6	4/6	4/6	0/6	0/6

SM – submeningeal area of the cerebellar cortex, PC – Purkinje cell layer, ML – molecular layer of the cerebellar cortex (whole), GL – granular layer

Table II. Distribution of p53 protein in the cerebellum of subjects participating in traffic accidents

Groups	Number	Age	Distribution of p53 within the cell					
Drivers			Cytoplasm			Nucleus		
			ML	PC	GL	ML	PC	GL
	7	55-65	0/7	0/7	0/7	0/7	0/7	0/7
	9	66-75	0/9	5/9	0/9	0/9	4/9	0/9
	5	76-85	0/5	3/5	0/5	0/5	4/5	0/5
Pedestrians	8	55-65	0/8	0/8	0/8	0/8	0/8	0/8
	7	66-75	0/7	4/7	0/7	0/7	4/7	0/7
	6	76-85	0/6	3/6	0/6	0/6	4/6	0/6

ML – molecular layer, PC – Purkinje cells, GL – granular layer

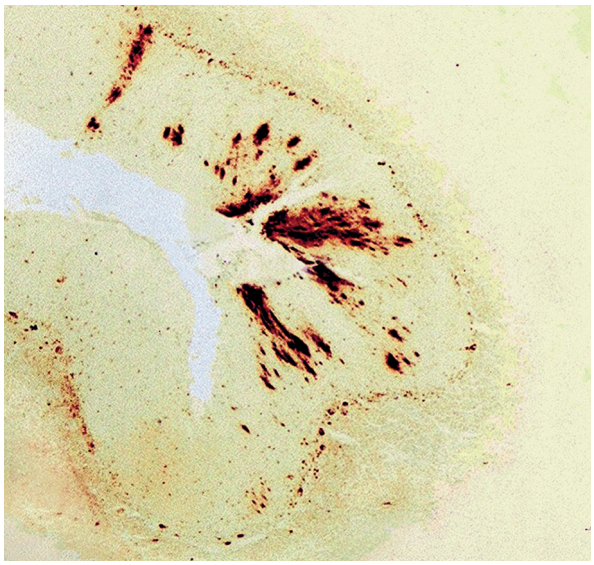

Fig. 1. Diffuse deposits of amyloid β protein in molecular and Purkinje cell layers of the cerebellum. Pedestrian, 68 years of age. Immunoreaction visualized with avidin-biotin-peroxidase system/DAB. Magnification ×200.

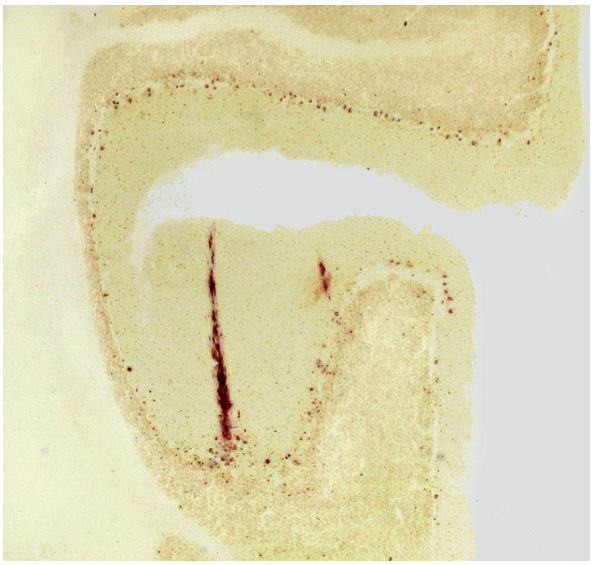

Fig. 2. Peculiar "stick-like" shape of the amyloid β deposit in the cerebellum of the subject (driver), 72 years of age. Immunoreaction visualized with avidin-biotin-peroxidase complex/DAB. Magnification ×200.

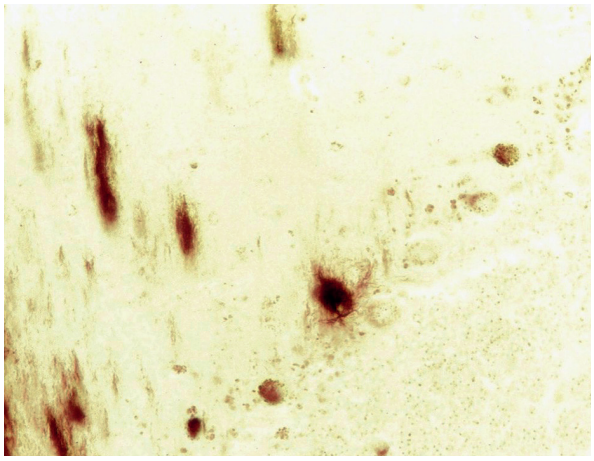

Fig. 3. Amyloid β immunopositive fibrous material coming from degenerating nerve cells of the Purkinje cell layer of the cerebellum. Subject 72 years of age. Immunoreaction visualized with avidin-biotin-peroxidase complex system/DAB. Magnification ×200.

sections, co-localization of Aβ and p53 in the same cells was not found.

Discussion

Cerebro-cerebellar couplings modulate the motor and cognitive functions of the human brain. In aging, these systems may be disordered by Aβ deposits. The source of Aβ is the amyloid precursor protein (APP) which is a normal structural protein of the cell membrane widely distributed throughout the body. Numerous environmental factors including the aging process, increase catabolism of APP and deliver different fragments of Aβ that are quickly removed from the peripheral tissues but some of them may cumulate in cerebro-spinal fluid (CSF). Although, the brain barrier mechanisms control arrival to the CNS of different products and support the clearance of harmful metabolites, the subependymoma regions of the CNS are less controlled by such mechanisms, therefore, they may be affected by some systemic diseases including amyloidogenic processes. In the present study, amyloid deposits of such localization were found in cerebella of our individuals that were at the beginning of their aging process. Moreover, lack of such deposits in any other areas of the cerebellum document that in this period of aging, metabolism of APP and the increased concentration of Aβ in the peripheral tissues preceded the same process in the cerebellum. Protein p53 was not detected in cerebella of those individuals suggesting that p53 did not participate in the formation of Aβ plaques of such subependymoma localization. In addition, results obtained in the present study confirm the previous

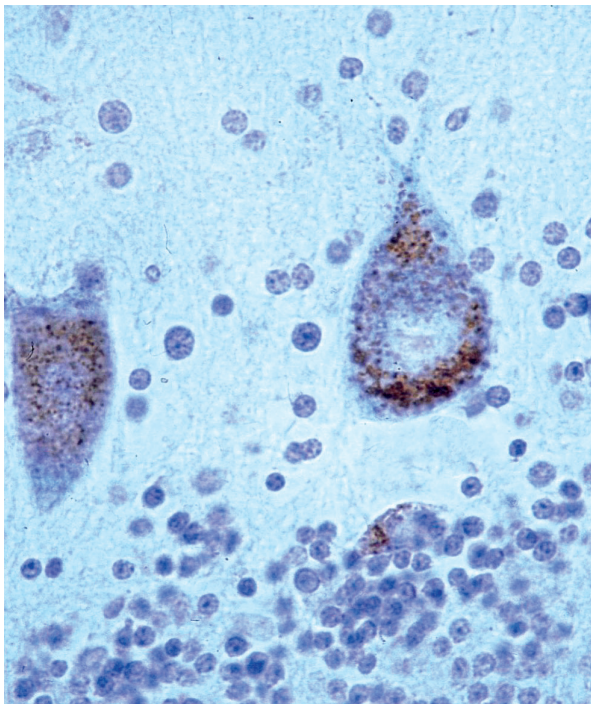

Fig. 4. p53 immuno-positive grains cumulated in the cytoplasm around the nucleus of Purkinje cells. Immunoreaction visualized with avidin-biotin-peroxidase system/DAB, counterstain with haematoxylin. Magnification ×400.

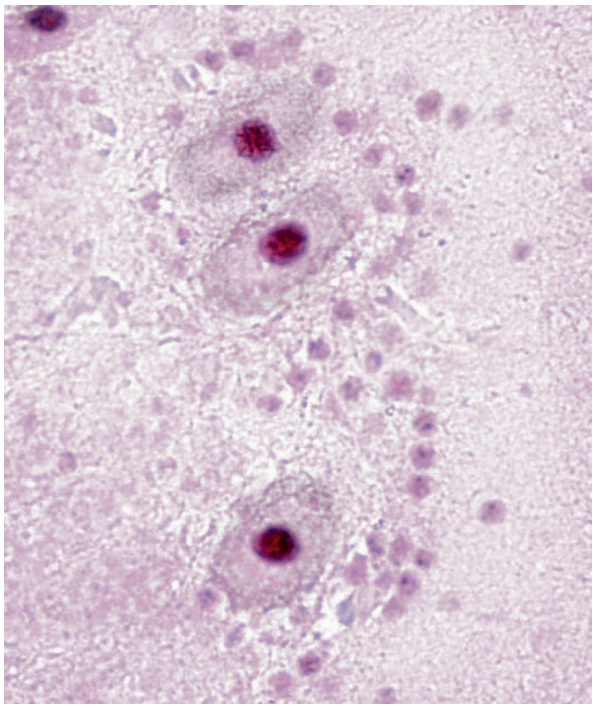

Fig. 5. p53 detected in the nucleus of Purkinje cells of the cerebellum. Pedestrian 75 years of age. Immunoreaction visualized with avidin-biotin/alkaline phosphatase conjugate/AS/TR. Magnification ×400.

observations that in other areas of the CNS, the efficiency of the blood-brain barrier may play an important role in the formation of AB deposits, and suggest also that creation of such deposits is independent of the p53 local activity.

However, in the groups of older subjects (over 65 years of age), p53 was detected in numerous nerve cells of the cerebellar cortex. In some Purkinje cells we found this protein in cytoplasm but in others in the cell nucleus.

In the normal post mitotic cell as nerve cells are, the concentration of p53 protein is generally below the detection level of immunohistochemical methods.

Nevertheless, in all such cells endoplasmic reticulum (ER) is responsible for the synthesis and folding of different proteins including p53 which are entering the secretory/tertiary pathway. Many post-translational modifications that ensure protein function occur in this organelle [9,17].

A variety of physiological perturbations can interfere with processes of protein folding in the ER lumen, leading to the unfolded or misfolded protein accumulation, which is called "ER stress". This stress triggers and activates an adaptive reaction, termed unfolded protein response (UPR) [22].

The protein p53 is known to respond to a variety of cellular distress signals. In response to DNA damage the increased concentration of p53 may induce cell cycle arrest and apoptosis [10,12,15]. The "ER stress" was observed as the first step of p53 reaction in the cytoplasm of cerebellar neurons of our aging subjects.

The next step of p53 reaction in cerebella neurons was the accumulation of p53 in the nucleus of the nerve cells that undergo degeneration. The involvement of p53 in neurodegenerative processes has been previously demonstrated following ischemia and different excitotoxic insults [5,19,37]. Post-transcriptional modification can alter p53 tertiary structure and prevent it from binding to specific DNA structures [38].

It is known that p53 can induce either cell-cycle arrest or apoptosis through transcriptional regulation of several genes. However, p53 can induce apoptosis through multiple mechanisms. Nuclear p53 can bind

to DNA and activate proapoptotic gene expression; alternatively, cytoplasmic p53 can trigger transcription-independent apoptosis by directly interacting with Bcl-2 family members [7]. It has been proposed that after specific death stimuli, posttranslational modification of p53 may regulate its subcellular localization. Phosphorylation and acetylation of p53 sequester p53 in the nucleus [1] whereas monoubiquitination of p53 leads to its nuclear export [16] or mitochondrial translocation. Movement of proteins between the nucleus and the cytoplasm may require interaction with the nuclear pore complex component [33].

Some proteins that shuttle between the nucleus and the cytosol independent of the nuclear pore complex may be controlled purely by their molecular size. Other nuclear proteins, especially those with larger molecular mass, require interaction with nuclear pore components and/or intermediate carriers to escape from the nucleus. The nuclear export receptor regulates nuclear export of specific proteins and p53 is one of them. However, in our study, accumulation of p53 in the cytoplasm precede the immuno-detection of this protein in the cell nucleus suggesting that p53 accumulated in the cytoplasmic compartments has some handicap to enter the cell nucleus.

The results of our present study show that p53 immunopositive degenerating neurons were the source of Aβ fibrillar material, which in the molecular layer of the cerebellum created diffuse Aβ plaques of extraordinary shapes. However, neither Aβ nor p53 appear universal markers for aging of the nerve tissue because in approximately 50% of our aging individuals both proteins were not found in studied cerebellar sections.

In conclusion, all results document that p53 protein is involved in degeneration of cerebellar neurons thus participating also in the amyloidogenic process of the aging cerebellum.

Disclosure

Authors report no conflict of interest.

References

1. Appella E, Anderson CW. Posttranslational modifications and activation of p53 by genotoxic stressors. Eur J Biochem 2001; 268: 2764-2772.
2. Armstrong RA. Laminar distribution of β-amyloid (Aβ) peptide deposits in the frontal lobe in familial and sporadic Alzheimer's disease. Folia Neuropathol 2015; 53: 15-23.
3. Blennow K, Hampel H. CSF markers for incipient Alzheimer's disease. Lancet Neurol 2003; 2: 605-613.
4. Buckner RL, Andrews-Hanna JR, Schacter DL. The brain's default network: anatomy, function, and relevance to disease. Ann NY Acad Sci 2008; 1124: 1-38.
5. Cenini G, Sultana R, Memo M, Butterfield DA. Elevated levels of pro-apoptotic p53 and its oxidative modification by the lipid peroxidation product, HNE, in brain from subjects with amnestic mild cognitive impairment and Alzheimer's disease. J Cell Mol Med 2008; 12: 987-994.
6. Chhatwal JP, Sperling RA. Functional MRI of mnemonic networks across the spectrum of normal aging, mild cognitive impairment, and Alzheimer's disease. J Alzheimers Dis 2012; 31 (Suppl 3): S155-S167.
7. Chipuk JE, Bouchier-Hayes L, Kuwana T, Newmeyer DD, Green DR. PUMA couples the nuclear and cytoplasmic proapoptopic function of p53. Science 2005; 309: 1732-1735.
8. Chol SM. Movement disorders following cerebrovascular lesions in cerebellar circuits. J Mov Disord 2016; 9: 80-88.
9. Denzel A, Molinari M, Trigueros C, Martin JE, Velmurgan S, Brown S, Stamp G, Owen MJ. Early postnatal death and motor disorders in mice congenitally deficient in calnexin expression. Mol Cell Biol 2002; 22: 7398-7404.
10. Glaccia AJ, Kastan MB. The complexity of p53 modulation: emerging patterns from divergent signals. Genes Dev 1998; 12: 2973-2983.
11. Grimaldi G, Manto M. Topography of cerebellar deficits in humans. Cerebellum 2012; 11: 336-351.
12. Ko LJ, Prives C. p53: puzzle and paradigm. Gene Dev 1996; 10: 1054-1072.
13. Kramer A, Challen GA. The epigenetic basis of hemetopoietic stem cell aging. Semin Hematol 2017; 54: 19-24.
14. Lanni C, Racchi M, Mazzini G, Ranzenigo A, Polotti R, Sinforiani E, Olivari L, Barcikowska M, Styczynska M, Kuznicki J, Szybinska A Govoni S, Memo M, Uberti D. Conformationally altered p53: a novel Alzheimer's disease marker? Mol Psychiatry 2008; 13: 641-647.
15. Levine AJ. p53, the cellular gatekeeper for growth and division. Cell 1997; 88: 323-331.
16. Li M, Brooks CL, Wu-Baer F, Chen D, Baer R, Gu W. Monoversus polyubiquitination : differential control of p53 fate by Mdm2. Science 2003; 302: 1972-1975.
17. Luo S, Mao C, Lee B, Lee AS. GRP78/BiP is required for cell proliferation and protecting the inner cell mass from apoptosis during early mouse embryonic development. Mol Cell Biol 2006; 26: 5688-5697.
18. Matthews PM, Filippini N, Douaud G. Brain structural and functional connectivity and the progression of neuropathology in Alzheimer's disease. J Alzheimers Dis 2013; 33 (Suppl 1): S163-S172.
19. McGahan L, Hakim AM, Robertson GS. Hippocampal Myc and p53 expression following transient global ischemia. Brain Res Mol Brain Res 1998; 56: 133-145.

20. Middleton FA, Strick PL. Anatomical evidence for cerebellar and basal ganglia involvement in higher cognitive function. Science 1994; 266: 458-461.
21. Mori F, Okada KI, Nomura T, Kobayashi Y. The pedunculopontine tegmental nucleus as a motor and cognitive interface between the cerebellum and basal ganglia. Front Neuroanat 2016; 10: 109.
22. Ni M, Lee AS. ER chaperones in mammalian development and human diseases. FEBS Lett 2007; 581: 3641-3651.
23. Rea IM, Dellet M, Mills KI. Living long and aging well is epigenetics the missing link between nature and nurture? Biogerontology 2016; 17: 33-54.
24. Schmahmann JD, Caplan D. Cognition, emotion and the cerebellum. Brain 2006; 129: 290-292.
25. Schmahmann JD, Weilburg JB, Sherman JC. The neuropsychiatry of the cerebellum – insights from the clinic. Cerebellum 2007; 6: 254-267.
26. Schmahmann JD. Dysmetria of thought: clinical consequences of cerebellar dysfunction on cognition and affect. Trends Cogn Sci 1998; 2: 362-371.
27. Schmahmann JD. From movement to thought: anatomic substrates of the cerebellar contribution to cognitive processing. Hum Brain Mapp 1996; 4: 174-198.
28. Sheline YI, Raichle ME, Snyder AZ, Morris JC, Head D, Wang S, Mintun MA. Amyloid plaques disrupt resting state default mode network connectivity in cognitively normal elderly. Biol Psychiatry 2010; 67: 584-587.
29. Sokolov AA, Miall RC, Ivry RB. The cerebellum adaptive prediction for movement and cognition. Trends Cogn Sci 2017; 21: 313-332.
30. Steininger SC, Liu X, Gietl A, Wyss M, Schreiner S, Gruber E, Treyer V, Kälin A, Leh S, Buck A, Nitsch RM, Prüssmann KP, Hock C, Unschuld PG. Cortical amyloid beta in cognitively normal elderly adults is associated with decreased network efficiency within the cerebro-cerebellar system. Front Aging Neurosci 2014; 6: 52.
31. Stoodley CJ, Schmahmann JD. Evidence for topographic organization in the cerebellum of motor control versus cognitive and affective processing. Cortex 2010; 46: 831-844.
32. Stoodley CJ, Valera EM, Schmahmann JD. Functional topography of the cerebellum for motor and cognitive tasks: an fMRI study. Neuroimage 2012; 59: 1560-1570.
33. Talcott B, Moore MS. Getting across the nuclear pore complex. Trends Cell Biol 1999; 9: 312-318.
34. Taormina G, Mirisola MG. Longevity epigenetic and biomolecular aspects. Biomol Concepts 2015; 6: 105-117.
35. Thach WT, Goodkin HP, Keating JG. The cerebellum and the adaptive coordination of movement. Annu Rev Neurosci 1992; 15: 403-442.
36. Thal LJ, Kantarci K, Reiman EM, Klunk WE, Weiner MW, Zetterberg H, Galasko D, Pratico D, Griffin S, Schenk D, Siemers E. The role of biomarkers in clinical trials for Alzheimer's disease. Alzheimer Dis Assoc Disord 2006; 20: 6-15.
37. Uberti D, Belloni M, Grilli M, Spano P, Memo M. Induction of tumour-suppressor phosphoprotein p53 in the apoptosis of cultured rat cerebellar neurons triggered by excitatory amino acids. Eur J Neurosci 1998; 10: 246-254.
38. Uberti D, Lanni C, Carsana T, Francisconi S, Missale C, Racchi M, Govoni S, Memo M. Identification of a mutant-like conformation of p53 in fibroblasts from sporadic Alzheimer's disease patients. Neurobiol Aging 2006; 27: 1193-1201.

Original paper

Folia Neuropathologica

Retinal ganglion cell/inner plexiform layer thickness in patients with Parkinson's disease

Maja Živković[1,2], Volkan Dayanir[3], Jelena Stamenović[4], Srdjan Ljubisavljević[1,4], Ana Pražić[4], Marko Zlatanović[2], Gordana Zlatanović[1,2], Vesna Jakšić[5], Marija Radenković[2], Svetlana Jovanović[6]

[1]Faculty of Medicine, University of Nis, Niš, Serbia, [2]Ophthalmology Clinic, Clinical Center Niš, Niš, Serbia, [3]BATIGOZ Health Group Eye Clinic, Cankaya, Izmir, Turkey, [4]Neurology Clinic, Clinical Center Niš, Niš, Serbia, [5]Clinic for Eye Diseases "Prof. Dr Ivan Stanković", Clinical-Hospital Center Zvezdara, Belgrade, Serbia, [6]Faculty of Medical Sciences, University of Kragujevac, Department of Ophthalmology, Kragujevac, Serbia

Folia Neuropathol 2017; 55 (2): 168-173 DOI: https://doi.org/10.5114/fn.2017.68584

Abstract

Introduction: *The aim of the paper was to analyze the changes in the macular ganglion cell layer and inner plexiform layer (GCL-IPL) thickness in patients with Parkinson's disease.*

Material and methods: *The study enrolled 46 patients with established diagnosis of Parkinson's disease and 46 healthy subjects. Both groups were age- and gender-matched. An OCT protocol, namely standardized Ganglion Cell Analysis algorithm was used to measure the thickness of the macular GCL-IPL layer. The average, minimum, and six sectoral (superotemporal, superior, superonasal, inferonasal, inferior, inferotemporal) GCL-IPL thicknesses were measured from the elliptical annulus centered on the fovea.*

Results: *The mean value of the clinical severity of Parkinson's disease was between 2 and 3, according to the Hoehn and Yahr scale. Statistically significant thinning of the GCL-IPL layer was registered in average and minimum GCL-IPL thickness, as well as in the sectoral layer thicknesses in patients with Parkinson's disease in comparison to the controls. There was no correlation between structural changes in the retina and disease duration or severity. A statistically significant difference in thickness between the different stages of the disease was registered only in the inferior sector.*

Conclusions: *Parkinson's disease is accompanied by thinning of the GCL-IPL complex of macula even in the earliest stages. This may indicate a possible retinal dopaminergic neurodegeneration. There is no correlation between duration or severity of Parkinson's disease with thinning of the GCL-IPL complex.*

Key words: *Parkinson's disease, ganglion cell complex, inner plexiform layer, retina.*

Introduction

Parkinson's disease (PD) is a chronic, progressive neurodegenerative disorder mostly affecting the aging population. The most common type of presentation of the disease is idiopathic, although it may occur secondary to the tumor, injury or infection [14,17]. Basically, the disease is a movement disorder caused

Communicating author

Srdjan Ljubisavljević, Neurology Clinic, Clinical Center Niš, Faculty of Medicine, University of Nis, Bul. Dr Zorana Djindjica 81, 18 000 Nis, Serbia, phone: +381 64 67 27 222, e-mail: srljub@gmail.com

by a decrease in a chemical substance, dopamine, in the part of the brain responsible for voluntary motor control (the basal ganglia) [11,24].

Dopaminergic neurons play key roles in the central nervous system (CNS), mediating basic mechanisms of vision, movement, motivation and mood. Dopamine as a neurotransmitter presents in retinal amacrine cells. Dopamine is released by a unique set of amacrine cells and activates D1 and D2 dopamine receptors distributed throughout the retina [2,5,6]. Today's research on the retina focuses a great deal of attention on neurotransmission between the neurons of the retina. Dopaminergic amacrine cells are one of the most sparsely distributed retinal nerve cell types found within the mammalian retina [30]. Amacrine cells are inhibitory neurons, and project their dendritic arbors to the inner plexiform layer (IPL), there interacting with retinal ganglion cells and/or bipolar cells [9].

Amacrine cells operate at the IPL, the second synaptic retinal layer where bipolar cells and retinal ganglion cells form synapses. There are at least 33 different subtypes of amacrine cells based just on their dendrite morphology and stratification. Each type of the amacrine cell releases one or several neurotransmitters where it connects with other cells. They are often classified by the width of their field of connection, the layer(s) of the stratum in the IPL they are in, and by the neurotransmitter type [9,20]. There is still much to be discovered about all of the different functions of all of the different amacrine cells.

Amacrine retinal cells located in IPL can be measured with the segmentation of the ganglion cell layer and inner plexiform layer (GCL-IPL) by the latest version of Cirrus OCT [11]. Measurement of the GCL-IPL layer may prove to be of value in providing an objective criterion in diagnosis and/or monitoring progression of PD. There are previous works demonstrating decreased visual acuity, contrast sensitivity and color vision defects among patients with PD [1], early-onset thinning of the inner retinal layers on OCT [3,31] and functional alterations observed in retinal ganglion cells [29] may strengthen authors' rationale in conducting this study and can make the readers comprehend the aims of the study better.

The aim of the paper was to analyze the changes in macular GCL-IPL layer thickness in patients with early stages of PD in order to assess whether loss of dopaminergic neurons, i.e. amacrine cells, in the retina of patients with PD could be demonstrated as thinning of the respective retinal layers on OCT scans, and whether this thinning is correlated with disease severity and/or duration.

Material and methods

This was a prospective, nonrandomized, observational study conducted between July 2014 and July 2016 at the Neurology Clinic and Eye Clinic, Clinical Center Niš, University of Niš, Serbia. The study followed the tenets of the Declaration of Helsinki. Informed consent was obtained from each patient after explanation of the nature of the study.

Patients with PD were consecutively enrolled as they presented at the Neurology Clinic. The diagnosis of PD was made according to the UK PD Brain Bank criteria [15]. All patients were evaluated by a neurologist who had no access to ophthalmologic findings. All enrolled patients were in a clinically stable phase using substitution therapies at doses of levodopa of 750 mg to 1000 mg per day, in divided doses. Patients who were under treatment for less than one year (6 months to a year) were included. Disease severity was evaluated according to the Hoehn and Yahr (HY) scale [14] which is widely used to categorize the progression of PD symptoms and quantify the patients according to 5 stages.

Exclusion criteria comprised any ocular disease that may confound the assessment of the retina: AMD, diabetic retinopathy, glaucoma, retinal vessel occlusion, retinal dystrophies, uveitis. Patients with myopia and hypermetropia > 2.0 Dsph were excluded. Also patients with previous intraocular surgery were excluded from the study.

All patients underwent a complete ophthalmic examination as follows: best corrected visual acuity (BCVA), intraocular pressure measurement by applanation tonometry, gonioscopy, slit lamp examination of the anterior segment and fundus examination with a plus 90-diopter lens. The OCT protocol was performed according to the standardized operating procedures included in Cirrus SD-OCT device (model 4000, software version 6.0, Carl Zeiss Meditec, Inc.). The Ganglion Cell Analysis algorithm of the aforementioned device was used to process and measure the thickness of the macular GCL-IPL layer. The average (GCavg), minimum (GCmin), and six sectoral (superotemporal, superior, superonasal, inferonasal, inferior, inferotemporal) GCL-IPL thicknesses were measured from the elliptical annulus centered on the fovea. Demarcation of superior sectors was performed from nasal to temporal, thus the superior

nasal sector of GCL+IPL was marked as GC1, superior as GC2, superior-temporal as GC3, while demarcation of inferior sectors was performed from temporal to nasal, marking inferior-temporal as GC4, inferior GC5 and inferior-nasal as GC6. Images with a signal power more than seven were used for analysis.

A sex- and age-matched normal control group was recruited from normal healthy population. Both eyes of healthy participants had to meet the following criteria: (1) no history or evidence of retinal and eye pathology, (2) no history of ocular surgery, (3) IOP < 21 mm Hg, and (4) had to be free of optic nerve damage and without any systemic and neurological disease.

Statistical analysis

Statistical analysis was done using the statistical package SPSS 22 for Windows (SPSS Inc., USA). Primary data obtained were analyzed by descriptive statistical methods and methods for testing hypotheses. The following descriptive statistical methods were used: measures of central tendency (mean, median), rate variability (standard deviation and variation interval) and indicators of structure expressed in percentages. Kolmogorov-Smirnov and Shapiro-Wilk tests, skewness value ("skewing") and kurtosis ("taper/flatness") were used to determine the normality of distribution. The *t* test was used to test the difference of arithmetic mean between the groups. Analysis of variance (ANOVA) was used to test the difference between the stages of the disease. The conclusion was done at the level of a statistical significance of 0.05. Correlation analysis was performed by measuring the correlation of two variables. Spearman correlation coefficient of ranks was used to determine the direction and strength of the connection stages of PD with thickness of GC1-GC6 as well as GCLavg and GCLmin.

Results

The study included 46 eyes of 46 patients suffering from PD. Out of the 46 patients, 20 were males and 26 were females. The mean age was 66.00 ± 9.67 years. Average value of PD stage was 2.49. The control group was composed of 46 eyes of 46 patients, of which 21 were males and 25 were females with a mean age of 64.47 ± 11.33 years.

We analyzed GCL-IPL average thickness (GCavg), minimum thickness (GCmin) and thickness of all six sectors. There was a statistically significant difference between the mean values in the observed and the control groups with respect to all 6 sectors, GCavg and GCmin (Table I).

There was no statistically significant difference in mean values of GC1, GC2, GC3, GC4, GC6, GCavg and GCmin between the stages of the disease. Only the mean GC5 value was statistically different (ANOVA, $p = 0.041$) between different PD stages (stages I and II, $p = 0.046$; stages II and III, $p = 0.012$) (Table II).

Correlation analysis between the stages of disease and the value of GC1, GC2, GC3, GC4, GC5, GC6, GCLavg, GCLmin has shown that there was no sta-

Table I. Clinical characteristics and ganglion cell-inner plexiform layer measurements of Parkinson's disease patients and healthy subjects

	Patients with Parkinson's disease (n = 46)	Control group (n = 46)	p
Age (mean ± SD)	66.00 ± 9.67	64.47 ± 11.33	0.081[a]
Gender (male/female)	20/26	21/25	
GC1	72.45 ± 14.36	86.34 ± 2.52	< 0.001[a]
GC2	69.77 ± 15.64	86.55 ± 2.60	< 0.001[a]
GC3	71.28 ± 14.10	86.45 ± 2.58	< 0.001[a]
GC4	72.05 ± 14.23	86.12 ± 3.45	< 0.001[a]
GC5	70.97 ± 15.38	86.62 ± 2.60	< 0.001[a]
GC6	72.95 ± 14.23	86.31 ± 2.73	< 0.001[a]
GCavg	72.44 ± 13.18	86.01 ± 3.68	< 0.001[a]
GCmin	65.33 ± 19.01	82.49 ± 1.78	< 0.001[a]

[a] *t-test*

GC1 – superonasal sector of the ganglion cell-inner plexiform layer, GC2 – superior sector of the ganglion cell-inner plexiform layer, GC3 – superotemporal sector of the ganglion cell-inner plexiform layer, GC4 – inferotemporal sector of the ganglion cell-inner plexiform layer, GC5 – inferior sector of the ganglion cell-inner plexiform layer, GC6 – inferonasal sector of the ganglion cell-inner plexiform layer, GCavg – ganglion cell-inner plexiform layer average thickness, GCmin – ganglion cell-inner plexiform layer minimum thickness

Table II. Thickness of the ganglion cell-inner plexiform layer in different stages of Parkinson's disease

	Stage I, *n* = 14	Stage II, *n* = 17	Stage III, *n* = 15	*p*
GC1	71.57 ± 15.45	71.42 ± 16.11	77.71 ± 6.02	0.358[a]
GC2	69.43 ± 14.96	68.13 ± 18.52	74.00 ± 7.50	0.503[a]
GC3	70.30 ± 14.04	70.95 ± 15.71	75.00 ± 8.51	0.585[a]
GC4	70.78 ± 15.34	70.29 ± 15.98	69.67 ± 8.74	0.621[a]
GC5	66.65 ± 17.51	69.42 ± 16.62	78.07 ± 5.73	0.041[a]
GC6	68.70 ± 16.74	71.71 ± 14.76	77.64 ± 4.25	0.183[a]
GCavg	69.48 ± 16.41	72.16 ± 13.94	76.07 ± 5.30	0.369[a]
GCmin	64.48 ± 20.91	65.89 ± 20.82	69.64 ± 8.86	0.727[a]

[a]*ANOVA*

GC1 – superonasal sector of the ganglion cell-inner plexiform layer, GC2 – superior sector of the ganglion cell-inner plexiform layer, GC3 – superotemporal sector of the ganglion cell-inner plexiform layer, GC4 – inferotemporal sector of the ganglion cell-inner plexiform layer, GC5 – inferior sector of the ganglion cell-inner plexiform layer, GC6 – inferonasal sector of the ganglion cell-inner plexiform layer, GCavg – ganglion cell-inner plexiform layer average thickness, GCmin – ganglion cell-inner plexiform layer minimum thickness

Table III. Correlation with the stage of the disease (*N* = 46)

	Correlation coefficient*	*p*
GC1	0.152	0.192
GC2	0.098	0.403
GC3	0.129	0.269
GC4	0.098	0.401
GC5	0.203	0.081
GC6	0.209	0.071
GCavg	0.112	0.340
GCmin	0.058	0.619

**Spearman's coefficient*

N – number of patients with Parkinson's disease, GC1 – superonasal sector of the ganglion cell-inner plexiform layer, GC2 – superior sector of the ganglion cell-inner plexiform layer, GC3 – superotemporal sector of the ganglion cell-inner plexiform layer, GC4 – inferotemporal sector of the ganglion cell-inner plexiform layer, GC5 – inferior sector of the ganglion cell-inner plexiform layer, GC6 – inferonasal sector of the ganglion cell-inner plexiform layer, GCavg – ganglion cell-inner plexiform layer average thickness, GCmin – ganglion cell-inner plexiform layer minimum thickness

Table IV. Correlation with duration of the disease (*N* = 46)

	Correlation coefficient*	*p*
GC1	0.228	0.252
GC2	0.042	0.834
GC3	0.341	0.082
GC4	0.436	0.023
GC5	0.338	0.084
GC6	0.338	0.084
GCavg	0.275	0.165
GCmin	0.037	0.854

**Spearman's coefficient*

N – number of patients with Parkinson's disease, GC1 – superonasal sector of the ganglion cell-inner plexiform layer, GC2 – superior sector of the ganglion cell-inner plexiform layer, GC3 – superotemporal sector of the ganglion cell-inner plexiform layer, GC4 – inferotemporal sector of the ganglion cell-inner plexiform layer, GC5 – inferior sector of the ganglion cell-inner plexiform layer, GC6 – inferonasal sector of the ganglion cell-inner plexiform layer, GCavg – ganglion cell-inner plexiform layer average thickness, GCmin – ganglion cell-inner plexiform layer minimum thickness

tistically significant correlation between the stages of the disease and the thickness of GCL-IPL, as presented in Table III.

Correlation analysis between disease duration and the value of GC1, GC2, GC3, GC5, GC6, GCLavg, GCLmin was not statistically significant. However, there was a significant positive correlation between the duration of the PD and the thickness of the inferior (GC4) sector, as shown in Table IV.

Discussion

The most accessible dopaminergic neurons of the vertebrate CNS are the dopaminergic amacrine cells (DA cells) of the retina. Retinal dopamine has multiple roles in vision [4,22,27]. Dopaminergic amacrine cells exhibit two classes of intrinsic bursting in the dark, shaped by inhibitory synaptic inputs, and two classes of light responses, ON-transient and ON-sustained, as well as light-independent activity, tuned to mediate specific dopaminergic functions in vision. The functional heterogeneity revealed in dopaminergic amacrine cells provides a cellular basis for the multiple roles of dopaminergic amacrine neurons in vision and is likely a general property of dopaminergic neurons throughout the CNS [2,5,12,23].

Localization of amacrine cells is very important. Specifically, placed in the inner plexiform layer, the layer which, with the advent of the latest version of

the OCT and segmentation of retinal layers, can be measured together with the ganglion cell layer [8,19]. This made amacrine cells even more accessible. OCT technology might prove useful in the diagnosis and monitoring changes in patients with PD by monitoring changes in the GCL-IPL layer.

Inzelberg *et al*. showed a reduction in the inferotemporal peripapillary retinal nerve fiber layer (RNFL) thickness and pointed out that changes in the level of internal layers of the retina can be of importance for the monitoring PD progression for the first time [17]. Some subsequent studies reported also evidence of peripapillary RNFL thinning in patients with PD [5,21]. RNFL thickness in patients with PD was also monitored by Lee *et al*. who proved the presence of statistically significant thinning of the RNFL and its association with duration and severity of disease. Lee was among the first ones who questioned whether retina could be a biomarker for disease progression [21]. Kaur *et al*. were among the first ones who in addition to RNFL also monitored the changes in the level of GCL-IPL concluding that GCL-IPL complex may be a more reliable parameter than RNFL thickness for structural alterations at the retina of patients with PD [18].

Currently there are not much data in the literature on the thickness of the GCL-IPL layer in PD. The loss of dopaminergic amacrine cells, i.e. failure of stimulation of metabotropic receptors with dopamine and subsequent failure in transition from scotopic to photopic vision by setting the gain of the retina in PD has been demonstrated [13]. The retinal thickness as a biomarker for PD has been investigated in some previous studies [26] and is currently under investigation in a clinical trial (https://clinicaltrials.gov/ct2/show/NCT02443779).

Our results indicate a statistically significant thinning of not only average and minimum GCL-IPL in PD, but also in all 6 sectors. Our results are similar to the results of Bayhan *et al*. who also pointed out thinning but unlike us they monitored ganglion cell complex on SD-OCT (RTVue-100), which includes the RNFL [7]. Cirrus SD-OCT device (model 4000 software version 6.0, Carl Zeiss Meditec, Inc.) used in our study can perform segmentation by subtracting RNFL from the complex, making the sole monitoring of GCL-IPL layer possible. We used ganglion cell analysis algorithm, which can automatically segment macular GCL-IPL thickness with excellent intervisit reproducibility [7,19,25]. Previous studies have evaluated GCL or IPL using different segmentation algorithms with similar results [10]. Sari *et al*. also indicated that the retinal dopaminergic neurodegeneration in patients with PD can be detected with GCL-IPL macular thickness measurements [28]. Our results are however not fully consistent with the results of Sari, who got a statistically significant correlation between the duration and severity of PD and the GCL-IPL thinning. Their conclusion was that GCL-IPL may be used to follow disease progression and the efficacy of neuroprotective treatment in patients with PD. Unlike their results, our study did not confirm the correlation between thickness of GCL-IPL, PD severity and duration. We found only a focal positive correlation between disease duration and the thinning of the GC4 sector.

There was no statistically significant difference in values for GC1, GC2, GC3, GC4, GC6, GCavg and GCmin between the stages of the disease. The only statistically significant differences registered were between stages I and II (p = 0.046), and stages II and III (p = 0.012) at sector GC5. These results lead to the thinking whether lower sectors were more sensitive to dopaminergic neurodegeneration, i.e. whether amacrine cells located at lower sectors are more prone to the progression of the disease. Additional studies are necessary to follow progression of PD using thickness of GCL-IPL complex.

Even in the earliest stages, PD is accompanied by changes in the internal layers of the macula in the form of decreased GCL-IPL layer thickness. This may indicate a possible retinal dopaminergic neurodegeneration. There is no correlation between duration or severity of PD with thinning of the GCL-IPL complex. The inferior sector is the only sector where a statistically significant difference was registered in thickness values between the different stages of the disease. To assess the significance of the findings in the context of their role as a surrogate biomarker for disease progression, further studies are required, which would include a larger number of patients in all stages of the disease.

Disclosure

Authors report no conflicts of interest.

References

1. Armstrong RA. Visual symptoms in Parkinson's disease. Parkinsons Dis 2011; 2011: 908306.

2. Aaker GD, Myung JS, Ehrlich JR, Mohammed M, Henchcliffe C, Kiss S. Detection of retinal changes in Parkinson's disease with spectral-domain optical coherence tomography. Clin Ophthalmol 2010; 4: 1427-1432.
3. Adam CR, Shrier E, Ding Y, Glazman S, Bodis-Wollner I. Correlation of inner retinal thickness evaluated by spectral-domain optical coherence tomography and contrast sensitivity in Parkinson disease. J Neuroophthalmol 2013; 33: 137-142.
4. Almer Z, Klein KS, Marsh LGerstenhaber M, Repka MX. Ocular motor and sensory function in Parkinson's disease. Ophthalmology 2012; 119: 178-182.
5. Altintas O, Işeri P, Ozkan B, Caglar Y. Correlation between retinal morphological and functional findings and clinical severity in Parkinson's disease. Doc Ophthalmol 2008; 116: 137-146.
6. Archibald NK, Clarke MP, Mosimann UP, Burn DJ. The retina in Parkinson's disease. Brain 2009; 132 (Pt 5): 1128-1145.
7. Bayhan HA, Bayhan AS, Tanık N, Gürdal C. The association of spectral-domain optical coherence tomography determined ganglion cell complex parameters and disease severity in Parkinson's disease. Curr Eye Res 2014; 39: 1117-1122.
8. Francoz M, Fenolland JR, Giraud JM, El Chehab H, Sendon D, May F, Renard JP. Reproducibility of macular ganglion cell-inner plexiform layer thickness measurement with cirrus HD-OCT in normal, hypertensive and glaucomatous eyes. Br J Ophthalmol 2014; 98: 322-328.
9. Frederick JM, Rayborn ME, Laties AM, Lam DM, Hollyfield JG. Dopaminergic neurons in the human retina. J Comp Neurol 1982; 210: 65-79.
10. Garcia-Martin E, Larrosa JM, Polo V, Satue M, Marques ML, Alarcia R, Seral M, Fuertes I, Otin S, Pablo LE. Distribution of retinal layer atrophy in patients with parkinson disease and association with disease severity and duration. Am J Ophthalmol 2014; 157: 470-478.
11. Goetz CG, Poewe W, Rascol O, Sampaio C, Stebbins GT, Counsell C, Giladi N, Holloway RG, Moore CG, Wenning GK, Yahr MD, Seidl L. Movement disorder society task force report on the Hoehn and Yahr staging scale: status and recommendations. The movement disorder society task force on rating scales for Parkinson's disease. Mov Disord 2004; 19: 1020-1028.
12. Hajee ME, March WF, Lazzaro DR, Wolintz AH, Shrier EM, Glazman S, Bodis-Wollner IG. Inner retinal layer thinning in Parkinson disease. Arch Ophthalmol 2009; 127: 737-741.
13. Hirasawa H, Betensky RA, Raviola E. Corelease of dopamine and GABA by a retinal dopaminergic neuron. J Neurosci 2012; 32: 13281-13291.
14. Hoehn M, Yahr M. Parkinsonism: onset, progression and mortality. Neurology 1967; 17: 427-442.
15. Hughes AJ, Daniel SE, Kilford L, Lees AJ. Accuracy of clinical diagnosis of idiopathic Parkinson's disease: a clinico-pathological study of 100 cases. J Neurol Neurosurg Psychiatry 1992; 55: 181-184.
16. Inzelberg R, Ramirez JA, Nisipeanu P, Ophir A. Retinal nerve fiber layer thinning in Parkinson disease. Vis Res 2004; 44: 2793-2797.
17. Jankovic J. Parkinson's disease: clinical features and diagnosis. J Neurol Neurosurg Psychiatry 2008; 79: 368-376.
18. Kaur M, Saxena R, Singh D, Behari M, Sharma P, Menon V. Correlation Between Structural and Functional Retinal Changes in Parkinson Disease. J Neuroophthalmol 2015; 35: 254-258.
19. Koh VT, Tham YC, Cheung CY, Whang WL, Baskaran M, Saw S, Wong T, Aung M. Determinants of Ganglion Cell–Inner Plexiform Layer Thickness Measured by High-Definition Optical Coherence Tomography. Invest Ophthalmol Vis Sci 2012; 53: 5853-5859.
20. Langheinrich T, Tebartz van Elst L, Lagreze WA, Bach M, Lücking CH, Greenlee MW. Visual contrast response functions in Parkinson's disease: evidence from electroretinograms, visually evoked potentials and psychophysics. Clin Neurophysiol 2000; 111: 66-74.
21. Lee JY, Ahn J, Kim TW, Jeon BS. Optical coherence tomography in Parkinson's disease: is the retina a biomarker? J Parkinsons Dis 2014; 4: 197-204.
22. Matsui H, Udaka F, Tamura A, Oda M, Kubori T, Nishinaka K, Kameyama M. Impaired visual acuity as a risk factor for visual hallucinations in Parkinson's disease. J Geriatr Psychiatry Neurol 2006; 19: 36-40.
23. Moschos MM, Tagaris G, Markopoulos I, Margetis I, Tsapakis S, Kanakis M, Koutsandrea C. Morphologic changes and functional retinal impairment in patients with Parkinson disease without visual loss. Eur J Ophthalmol 2011; 21: 24-29.
24. Movement disorder society task force on rating scales for Parkinson's disease. The Unified Parkinson's Disease Rating Scale (UPDRS): status and recommendations. Mov Disord 2003; 18: 738-750.
25. Mwanza J-C, Oakley JD, Budenz DL, Chang RT, Knight OJ, Feuer WJ. Macular ganglion cell-inner plexiform layer: automated detection and thickness reproducibility with spectral domain-optical coherence tomography in glaucoma. Invest Ophthalmol Vis Sci 2011; 52: 8323-8329.
26. Normando EM, Davis BM, De Groef L, Nizari S, Turner LA, Ravindran N, Pahlitzsch M, Brenton J, Malaguarnera G, Guo L, Somavarapu S, Cordeiro MF. The retina as an early biomarker of neurodegeneration in a rotenone-induced model of Parkinson's disease: evidence for a neuroprotective effect of rosiglitazone in the eye and brain. Acta Neuropathol Commun 2016; 4: 86.
27. Onofrj M, Bonanni L, Albani G, Mauro A, Bulla D, Thomas A. Visual hallucinations in Parkinson's disease: clues to separate origins. J Neurol Sci 2006; 248: 143-150.
28. Sari ES, Koc R, Yazici A, Sahin G, Ermis SS. Ganglion Cell-Inner Plexiform Layer Thickness in patients with Parkinson Disease and association with disease severity and duration. J Neuroophthalmol 2015; 35: 117-121.
29. Sartucci F, Orlandi G, Lucetti C, Bonuccelli U, Murri L, Orsini C, Porciatti V. Changes in pattern electroretinograms to equiluminant red-green and blue-yellow gratings in patients with early Parkinson's disease. J Clin Neurophysiol 2003; 20: 375-381.
30. Schraermeyer U, Kopitz J, Peters S, Henke-Fahle S, Blitgen-Heinecke P, Kokkinou D, Schwarz T, Bartz-Schmidt KU. Tyrosinase biosynthesis in adult mammalian retinal pigment epithelial cells. Exp Eye Res 2006; 83: 315-321.
31. Yu JG, Feng YF, Xiang Y, Huang JH, Savini G, Parisi V, Yang WJ, Fu XA. Retinal nerve fiber layer thickness changes in Parkinson disease: a meta-analysis. PLoS One 2014; 9: e85718.

Original paper

Folia Neuropathologica

High expression of CX3C chemokine receptor 1 (CX3CR1) in human carotid plaques is associated with vulnerability of the lesions

Marta Masztalewicz[1], Przemysław Nowacki[1], Łukasz Szydłowski[2], Maciej Żukowski[2], Piotr Gutowski[3]

[1]Department of Neurology, Pomeranian Medical University in Szczecin, [2]Department of Anaesthesiology, Intensive Care and Acute Poisoning, Pomeranian Medical University in Szczecin, [3]Department of Vascular Surgery and Angiology, Pomeranian Medical University in Szczecin, Poland

Folia Neuropathol 2017; 55 (2): 174-181 DOI: https://doi.org/10.5114/fn.2017.68585

Abstract

Introduction: *In data based on ex vivo studies and animal models, fractalkine is considered an important mediator in the development and destabilization of atherosclerotic plaques. We do not know how it is associated with human carotid plaques morphology.*

Material and methods: *The study included 126 carotid plaques taken from 126 patients who underwent endarterectomy of internal carotid arteries. We assessed the following characteristics: inflammatory infiltration, connective tissue elements, foam cells, lipid core, plaque vascularisation, calcifications, intraplaque haemorrhage, thrombi built into the plaque structure, and mural thrombi. CX3CR1 expression in plaques as a response to fractalkine was assessed.*

Results: *Compared to those with a low fractalkine receptor expression, plaques with its high expression exhibited more intensive inflammatory infiltrations. They were more likely to contain inflammatory than fibrous components. They were characterized by a large foam cell component and were less calcified. Intraplaque haemorrhages, the large lipid core and mural as well as intraplaque thrombi were more frequent within them.*

Conclusions: *High expression of the fractalkine receptor within human carotid plaques is associated with morphological parameters of plaque instability. Thus we conclude that fractalkine may be involved in vulnerability of human carotid plaque.*

Key words: *fractalkine receptor, carotid plaques, plaques morphology.*

Introduction

In data based on ex vivo studies and animal models, fractalkine (CX3CL1) is considered an important mediator in the development and destabilization of atherosclerotic plaques. These roles are attributable to its proinflammatory and prothrombotic features [13,23-26].

The biological activities of CX3CL1 are mediated by CX3C chemokine receptor 1 (CX3CR1) which is expressed on monocytes, natural killer cells, T cells, platelets, and vascular smooth muscle cells (VSMCs). The protein facilitates the migration, adhesion, and proliferation of these cell types via CX3CR1. All of these processes are involved in atherogenesis [2,4,6,11,13,15,23,25].

Communicating author

Marta Masztalewicz, Department of Neurology, Pomeranian Medical University, Szczecin, Poland, 1 Unii Lubelskiej St., 71-252 Szczecin, Poland, phone: +48 91 425 32 51, faks: +48 91 425 32 60, e-mail: marta.masztalewicz@pum.edu.pl

To date, case studies of patients with carotid atherosclerosis have confirmed an association between fractalkine expression and the development and severity of atherosclerotic changes in carotid arteries. Yadaw *et al*. observed a significant correlation between common carotid artery intima-media thickness and the CX3CL1 serum level [27]. Stolla *et al*. found that fractalkine is expressed in early and advanced carotid lesions, and they observed a relationship between elevated soluble CX3CL1 levels and a high degree of carotid stenosis [26]. However, we do not know how fractalkine is associated with human carotid plaques stability from a morphological point of view. It is unclear whether it is involved in the vulnerability of human carotid plaques. By definition, vulnerable plaques are unstable lesions, prone to rupture, and susceptible to thrombosis [18,20,22].

As mentioned above, fractalkine interacts with a single receptor (CX3CR1) [9,11], and their expressions are positively correlated with each other [26]. Considering that fact, we used CX3CR1 expression in carotid plaques as a marker of response to fractalkine. We aimed to answer the question whether it is associated with plaques morphological instability.

Material and methods

The study included 126 carotid plaques taken from 126 patients (38 females and 88 males, aged between 40 and 92 years) who underwent endarterectomy of internal carotid arteries. Patients after the ischemic stroke or transient ischemic attack (TIA) or with no history of cerebrovascular events were analysed. They suffered from arterial hypertension, type 2 diabetes, dyslipidemia, lower limb obliterative atherosclerosis, and coronary arterial disease. Some patients had multiple conditions.

We excluded individuals after a possible or probable hemodynamic or cardioembolic stroke (coexistence of hemodynamically significant heart failure, atrial fibrillation, sick-sinus syndrome). We also excluded patients with chronic diseases characterized by inflammation and immunological factors (systemic connective tissue diseases, viral hepatitis, cirrhosis, ulcerative colitis, Crohn's disease, multiple sclerosis, Hashimoto's thyroiditis, Graves' disease, proliferative diseases of the hematopoietic system, other cancers). Another exclusion criterion was immunosuppressant drug use (steroids and cytostatics) within 5 years before study enrolment.

The research was approved by the local Bioethical Commission. The study subjects gave informed consent for their participation.

Microscopic carotid plaque evaluation

Intraoperatively harvested atherosclerotic plaques were fixed in 10% formalin solution before they were divided into five parts, including the area most affected by the disease. The material was then submerged in paraffin, sliced into 3-μm-thick fragments, and stained with haematoxylin and eosin (H&E).

We assessed the following characteristics: inflammatory infiltration, connective tissue elements, foam cells, lipid core, plaque vascularisation, calcifications, intraplaque haemorrhage, thrombi built into the plaque structure, and mural thrombi. We differentiated plaque shoulders, fibrous cap, and central part including the lipid core (Figs. 1A and B, magnification 100×).

Several features considered important for plaque stability were taken into consideration. Parameters of instability were: massive inflammatory infiltrations, dominance of inflammation in relation to the plaque connective tissue component, large foam cells component, large lipid core, increased vascularity, intraplaque haemorrhages, intraplaque thrombus, mural thrombus and plaque rupture. Enlarged plaque calcification, chondro-osseus metaplasia as a dominant calcification type were considered as markers of plaque stability [1,16,21].

1. Inflammatory infiltration:

   a) the intensity of inflammation in the plaque shoulder and fibrous cap: inflammatory cells were counted in four visual fields at magnification 400x; infiltration was considered massive if we counted more than 100 cells,

   b) the relationship of inflammatory cells with connective tissue elements: the visual fields infiltrated by inflammatory cells to the fields with connective tissue dominance (without or with single inflammatory cells) at magnification 200x; A – inflammation dominance, B – connective tissue dominance.
2. Foam cells component, separately in plaque shoulders and plaque fibrous cap: the component was considered significant if foam cells occupied more than one-third of the shoulder/fibrous cap thickness.

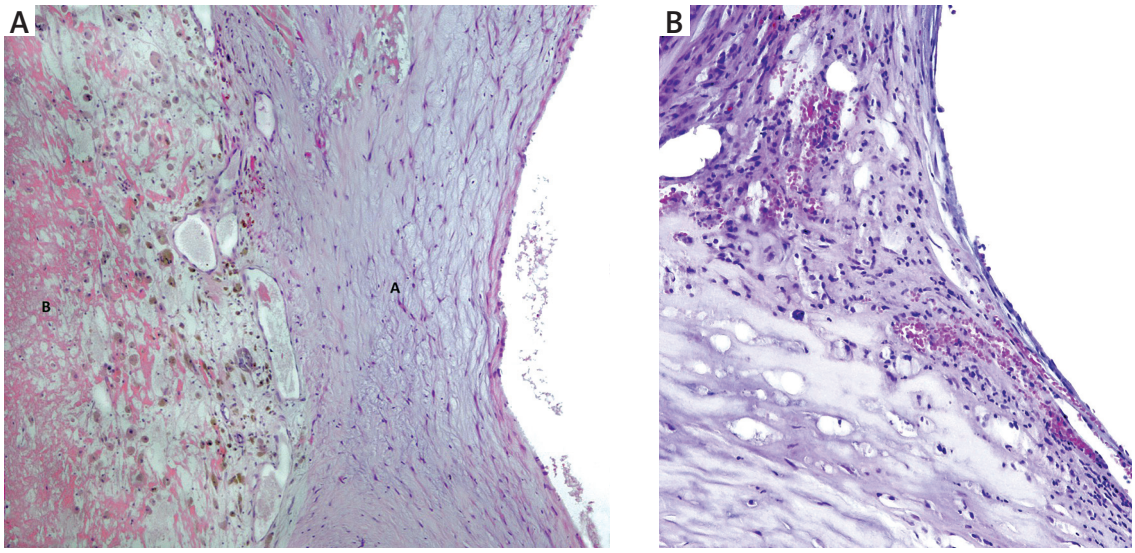

Fig. 1. A) Carotid plaque with visible: A – fibrous cap, B – central part of the lesion; **B)** carotid plaque – visible shoulder of the lesion.

3. Lipid core (amorphous material containing cholesterol crystals): large if occupied more than half of the plaque thickness.
4. Plaque vascularity: vessel sections counted in four visual fields at magnification 400×: 0, none; I, 1 to 9 sections; II, > 9.
5. Plaque calcification:

a) enlargement of plaque calcification: considered large if calcifications occupied more than half of the plaque surface at magnification 400×,

b) calcifications in shoulders, fibrous cap, and core: considered large if they occupied more than half of shoulder/fibrous cap/core thickness at magnification 200×,

c) dominant calcification type: A – small single or dispersed calcifications, B – nodules, C – chondro-osseus metaplasia (separately in the fibrous cap, shoulder, and core).

6. Intraplaque haemorrhage (separately in the fibrous cap, shoulder, and core): area of erythrocytes within the plaque causing disorganization of plaque architecture or evident organized haemorrhage with accumulation of hemosiderin-laden macrophages or iron deposition within plaque connective tissue.
7. Intraplaque thrombus: organized collection of fibrin and red blood cells within the plaque.
8. Mural thrombus: organized collection of fibrin and red blood cells in the vessel lumen.
9. Plaque rupture: clear communication between the lipid core and vessel lumen that was not due to surgery.

CX3CR1 expression in human carotid plaques

Among 5 fragments of each carotid plaque, one fragment – the most affected by the disease was taken for analysis of CX3CR1 expression. There were 126 specimens examined altogether. We analysed 3-µm-thick fragments from plaque hot spots labelled with human anti-CX3CR1 antibodies (Novus Biologicals, 1 : 200). The plaques were divided into two groups based on the CX3CR1 expression level. Group I included 54 lesions with single or dispersed CX3CR1-positive cells (plaques with a low CX3CR1 expression and less fractalkine influence), while group II consisted of 72 plaques with clusters of CX3CR1-positive cells (lesions with a high CX3CR1 expression and stronger fractalkine influence) (Fig. 2A and B, magnification 400×). The two groups were compared with reference to the microscopic features mentioned above.

Evaluations of plaque morphology and fractalkine receptor expression were performed at baseline and 3 months later. Both evaluations were performed by one researcher. The second analysis was blinded to the first one. Both were performed without knowledge about clinical data. An intraobserver agreement for plaques morphology parameters ranged between 85 and 98 percent. It was 96.825 percent for assessment of the CX3CR1 expression.

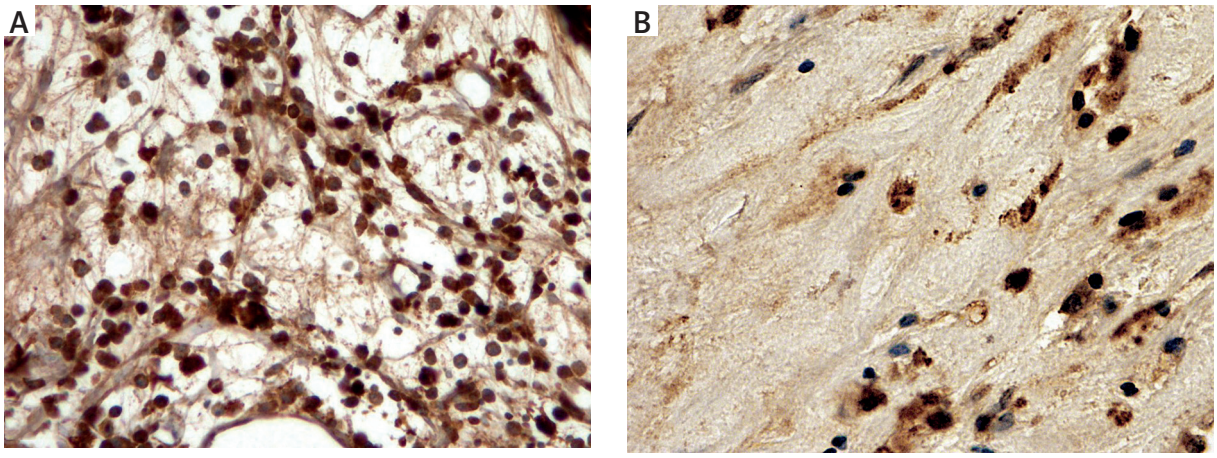

Fig. 2. A) Carotid plaque – high CX3CR1 expression. **B)** Carotid plaque – low CX3CR1 expression.

Statistical analysis

Since distributions of most variables were significantly different from normal (Shapiro-Wilk test), the results were presented as a number (percentage) for qualitative variables. Data were compared between groups using the χ^2 test for categorical variables. The statistical significance threshold was set at $p < 0.05$. Calculations were performed with the use of STATISTICA 10 software.

Results

CX3CR1 expression and inflammatory infiltrations in carotid plaques

Compared to those with a low CX3CR1 expression, plaques with its high expression exhibited more intensive inflammatory infiltrations that were predominantly localized in the plaque shoulders (Table I, Fig. 3, magnification 200×). Notably, high CX3CR1-expressing plaques were more likely to contain inflammatory than fibrous components (Table I).

CX3CR1 expression and foam cell components in carotid plaques

We found a significant positive association between a carotid plaque CX3CR1 expression and enlargement of foam cells component (Table I, Fig. 4, magnification 200×).

CX3CR1 expression and carotid plaque calcifications

The plaques with a high CX3CR1 expression were less calcified than plaques with a low expression of the receptor. This was especially clear within the shoulders (Table II, Fig. 5, magnification 200×).

CX3CR1 expression and carotid plaque vascularisation

We did not find a significant difference in plaque vascularisation between the two groups. High CX3CR1 expression significantly correlated with intraplaque haemorrhages in the plaque fibrous cap, while the

Table I. CX3CR1 expression and cellular component of carotid plaques

	Low CX3CR1 expression, $n = 54$	High CX3CR1 expression, $n = 72$	p
Massive inflammatory infiltration in the fibrous cap	93.5% (46*)	86.4% (66*)	0.8617
Massive inflammatory infiltration in the shoulder	25% (48*)	47.06% (68*)	0.0591
The dominance of inflammation in the fibrous cap in the shoulder	14.89% (47*)	39.71% (68*)	0.0122
	33.33% (45*)	49.27% (69*)	0.0421
Significant foam cells component in the fibrous cap in the shoulder	8.16% (49*)	22.06% (68*)	0.0129
	24.49% (49*)	47.06% (68*)	0.0373

**Number of cases with available assessment of particular morphological features*

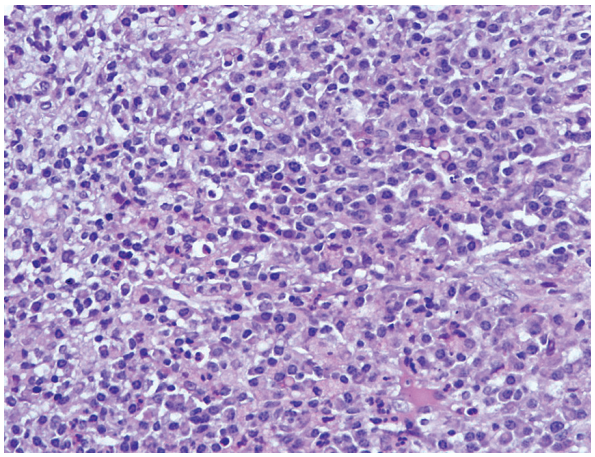

Fig. 3. Visible inflammatory infiltration in the carotid plaque.

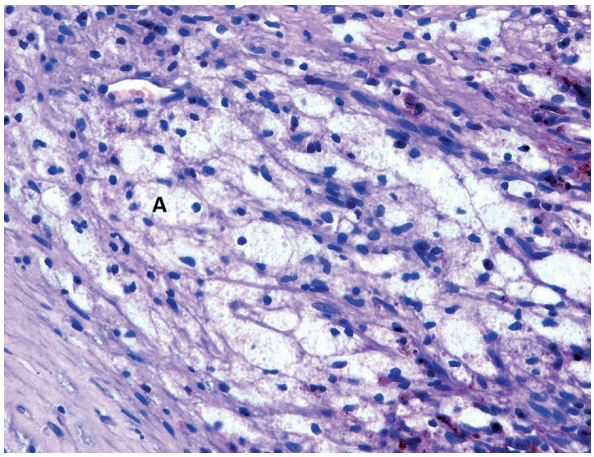

Fig. 4. Visible foam cells component in the carotid plaque. A – foam cell.

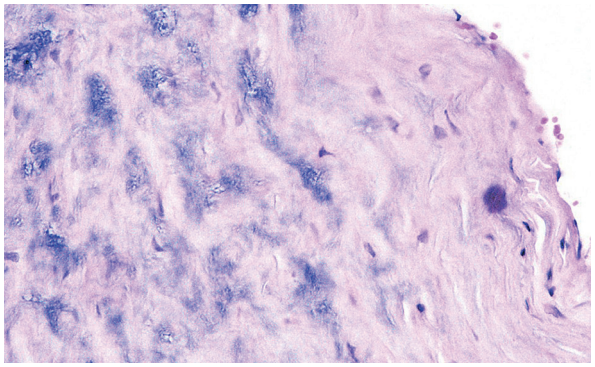

Fig. 5. Visible dispersed calcifications.

trend was toward significance in the shoulder (Table III, Fig. 6 magnification 200×).

CX3CR1 expression and lipid component in carotid plaques

The large lipid core was more frequent within the plaques with a high CX3CR1 expression than those with a low receptor expression. However, the difference was not quite significant (Table IV).

Table II. CX3CR1 expression and carotid plaque calcifications

	Low CX3CR1 expression, *n* = 54	High CX3CR1 expression, *n* = 72	*p*
Large calcifications in the plaque	33.33% (54*)	19.11% (68*)	0.0621
Large calcification in the shoulder	55.55% (54*)	34.72% (72*)	0.0167
Large calcification in the fibrous cap	50% (54*)	38.89% (72*)	0.2133
Dominant calcifications type in the fibrous cap			
A	62.96% (54*)	81.94% (72*)	0.0460
B	5.56% (54*)	1.39% (72*)	
C	31.48% (54*)	16.67% (72*)	
Dominant calcifications type in the plaque shoulder			
A	46.3% (54*)	54.17% (72*)	0.4778
B	7.4% (54*)	5.55% (72*)	
C	46.3% (54*)	40.28% (72*)	
Dominant calcifications type in the central part of the plaque			
A	42% (50*)	60.56% (71*)	0.0587
B	8% (50*)	8.45% (71*)	
C	50% (50*)	30.99% (71*)	

**Number of cases with available assessment of particular morphological features*
A – Small single or dispersed calcifications, B – nodules, C – chondro-osseus metaplasia

Table III. CX3CR1 expression and carotid plaque vascularisation

	Low CX3CR1 expression, *n* = 54	High CX3CR1 expression, *n* = 72	*p*
Vascularity of the fibrous cap			0.5530
0	47.92% (48*)	56.92% (65*)	
I	35.42% (48*)	24.62% (65*)	
II	16.66 (48*)	18.46% (65*)	
Vascularity of the plaque shoulder			0.3363
0	23.4% (47*)	15.15% (66*)	
I	23.4% (47*)	22.73% (66*)	
II	53.2% (47*)	62.12% (66*)	
Vascularity of the plaque central part			0.6729
0	23.91% (46*)	27.9% (61*)	
I	17.39% (46*)	21.3% (61*)	
II	58.7% (46*)	50.8% (61*)	
Intraplaque haemorrhage in the fibrous cap	16.33% (49*)	32.35% (68*)	0.0459
Intraplaque haemorrhage in the plaque shoulder	46.94% (49*)	63.23% (68*)	0.0813
Intraplaque haemorrhage in central part of plaque	50% (48*)	31,14% (61*)	0.1661

**Number of cases with available assessment of particular morphological features*
0 – no vessel sections counted in four visual fields at magnification 400×; I, 1 to 9 vessel sections; II, > 9 vessel sections counted in four visual fields at magnification 400×

Relationships between CX3CR1 expression and plaque rupture and mural and intraplaque thrombi

The percentage of ruptured plaques was significantly lower in group I lesions compared to group II. However, mural thrombi were significantly more frequent in group I plaques (Table IV). Intraplaque thrombi were also more frequent in group I, but this difference was not significant (Table IV).

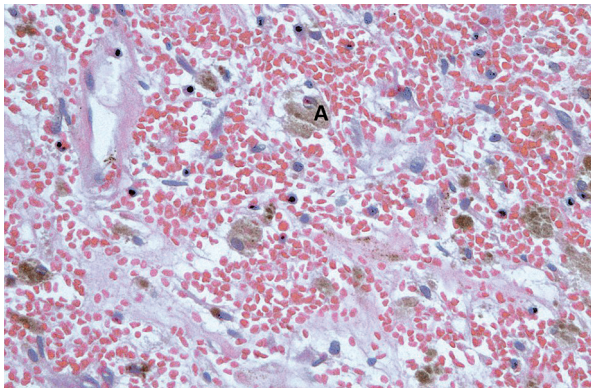

Fig. 6. Visible intraplaque haemorrhage in the carotid plaque. A – hemosiderin-laden macrophage.

Discussion

Our findings demonstrate that fractalkine may influence human carotid plaque morphology. The plaques with a greater CX3CR1 expression (supposed stronger influence of fractalkine) possessed a significantly larger component of inflammatory cells infiltration than lesions with a low CX3CR1 expression. We also observed that plaques in the high CX3CR1 expression group exhibited larger inflammatory components compared to fibrous components. Our results are in agreement with limited data from experimental studies of carotid arteries and fractalkine. Cheng *et al.* assessed apolipoprotein E knockout mice and found that fractalkine stimulated mono-

Table IV. CX3CR1 expression and other features considered important for plaque stability

	Low CX3CR1 expression, *n* = 54	High CX3CR1 expression, *n* = 72	*p*
Large lipid core	54.9% (51*)	56.34% (71*)	0.0656
Plaque rupture	26.53% (49*)	11.76% (68*)	0.0412
Mural thrombi	44.23% (52*)	63.23% (68*)	0.0381
Intraplaque thrombi	4.08% (49*)	15.49% (71*)	0.1611

**Number of cases with available assessment of particular morphological features*

cyte/macrophage accumulation and reduced carotid plaque collagen content [5]. Our results also suggest that fractalkine promotes inflammation in plaques. The imbalance between inflammatory and reparative mechanisms within atherosclerotic plaques is considered to promote plaque destabilization and is a feature of vulnerable plaques [14].

We observed that plaques with a high CX3CR1 expression had significantly more foam cells and were more likely to have a large lipid-necrotic core compared to plaques with a low CX3CR1 expression. Based on this, we hypothesize that fractalkine promotes foam cells accumulation and lipid-necrotic core formation similarly to what has been reported in animal models [5]. A close connection between high CX3CR1 levels and large lipid core, as well as active inflammation and destruction of plaque fibrous elements, are considered major criteria for plaque vulnerability, emphasizing the role of fractalkine in carotid lesion destabilization [1,18].

Calcifications should be also taken into consideration during carotid plaque morphological analysis. Generally, non-calcified/low calcified plaques are treated as high risk lesions because they are associated more with cerebrovascular events than calcified lesions [18-20,22]. We also observed (data not shown) that less calcified plaques were significantly more frequent symptomatic than lesions with enlarged calcification.

The results mentioned above have shown that plaques with a high expression of CX3CR1 (under stronger influence of fractalkine) were significantly less calcified than plaques of the other group. They were more likely to contain small single or dispersed deposits. Conversely, we observed evidence of chondro-osseus metaplasia in group II plaques. These seem to be a further confirmation for association of fractalkine with human carotid plaques vulnerability [7,10].

High CX3CR1 expression was significantly associated with the presence of intraplaque haemorrhages, another feature of plaque instability. Based on the literature, fractalkine is involved in the neovascularisation of atherosclerotic plaques, and these immature vessels may be a source of intraplaque haemorrhage [8,12].

We observed a significant association between a high CX3CR1 expression and mural thrombi; however, these characteristics were not related to plaque rupture frequency (group I) [3]. Our data suggest that fractalkine may promote mural thrombus formation without plaque rupture. Experimental data suggest that fractalkine activates platelets to stimulate their adhesion and aggregation [24]. The interaction between fractalkine receptors (CX3CR1) on platelets with membranous fractalkine on endothelial cells is responsible for platelet adhesion to the endothelium [17,24].

We assessed the fractalkine influence parameter within the plaques and we observed that it is associated with plaques instability. To answer whether fractalkine could be used as a marker of unstable carotid plaques, additional analysis of plaque morphology with a fractalkine blood level should be performed.

Conclusions

High expression of the fractalkine receptor within human carotid plaques is associated with morphological parameters of plaque instability. Thus we conclude that fractalkine may be involved in vulnerability of the human carotid plaque.

Disclosure

Authors report no conflict of interest.

References

1. Alsheikh-Ali AA, Kitsios GD, Balk EM, Lau J, Ip S. The vulnerable atherosclerotic plaque: scope of the literature. Ann Intern Med 2010; 153: 387-395.
2. Apostolakis S, Spandidos D. Chemokines and atherosclerosis: focus on the CX3CL1/CX3CR1 pathway. Acta Pharm Sin 2013; 34: 1251-1256.
3. Badimon L, Vilahur G. Thrombosis formation on atherosclerotic lesions and plaque rupture. J Intern Med 2014; 276: 618-632.
4. Bazan JF, Bacon KB, Hardiman G, Wang W, Soo K, Rossi D, Greaves DR, Zlotnik A, Shall TJ. A new class of membrane-bound chemokine with a CX3C motif. Nature 1997; 385: 640-644.
5. Cheng C, Tempel D, van Haperen R, de Boer HC, Segers D, Huisman M, Zonneveld AJ, Leenen PJM, Steen A, Serruys PW, de Crom R, Krams R. Shear stress-induced changes in atherosclerotic plaque composition are modulated by chemokines. J Clin Invest 2007; 117: 616-626.
6. Cybulsky MI, Hegele RA. The fractalkine receptor CX3CR1 is a key mediator of atherogenesis. J Clin Invest 2003; 111: 1118-1120.
7. Davaine J-M, Quillard T, Brion R, Lapérine O, Guyomarch B, Merlini T, Chatelais M, Guilbaud F, Brennan MA, Charrier C, Heymann D, Gouëffic Y, Heymann MF. Osteoprotegerin, pericytes and bone-like vascular calcification are associated with carotid plaque stability. PLoS One 2014; 9: e107642.
8. Doyle B, Caplice N Plaque neovascularization and antiangiogenic therapy for atherosclerosis. J Am Coll Cardiol 2007; 49: 2073-2080.
9. Haskell CA, Cleary MD, Charo IF. Unique role of the chemokine domain of fractalkine in cell cupture. Kinetics of receptor dis-

sociation correlate with cell adhesion. J Biol Chem 2000; 275: 34183-34189.
10. Hunt J, Fairman R, Mitchell ME, Carpenter JP, Golden M, Khalapyan T, Wolfe M, Neschis D, Milner R, Scoll B, Cusack A, Mohler ER 3rd. Bone formation in carotid plaques. A clinicopathological study. Stroke 2002; 33: 1214-1219.
11. Imai T, Hieshima K, Haskell C, Baba M, Nagira M, Nishimura M, Kakizaki M, Takagi S, Nomiyama H, Shall TJ, Yoshie O. Identification and molecular characterization of fractalkine receptor CX3CR1, which mediates both leukocyte migration and adhesion. Cell 1997; 91: 521-530.
12. Kumar A-S, Martin K, Turner EC, Buneker ChK, Dorgham K, Deterre Ph, Caplice NM. Role of CX3CR1 receptor in monocyte/macrophage driven neovascularization. PLoS One 2013; 8: e57230.
13. Lesnik P, Haskell CA, Charo IF. Decreased atherosclerosis in CX3CR–/–mice reveals a role for fractalkine in atherogenesis. J Clin Invest 2003; 111: 333-340.
14. Libby P, Tabas I, Fredman G, Fisher E. Inflammation and its resolution as determinants of acute coronary syndromes. Circ Res 2014; 114: 1867-1879.
15. Lucas AD, Bursill C, Guzik TJ, Sadowski J, Channon KM, Greaves DR. Smooth muscle cells in human atherosclerotic plaques express the fractalkine receptor CX3CR1 and undergo chemotaxis to the CX3C chemokine fractalkine (CX3CL1). Circulation 2003, 108: 2498-2504.
16. Masztalewicz M, Nowacki P, Bajer-Czajkowska A, Kotfis K, Biernawska J, Safranow K, Żukowski M, Gutowski P. Circulated CD4+CD28– lymphocytes rate and their cytotoxicity and morphological parameters of internal carotid artery atheromatous plaques in patients with atherosclerosis-related ischemic stroke. Folia Neuropathol 2013; 51: 250-260.
17. Meyer dos Santos S, Klinkhardt U, Scholich K, Nelson K, Monsefi N, Deckmyn H, Kuczka K, Zorn A, Harder S. The CX3C chemokine fractalkine mediates platelet adhesion via the von Willebrand receptor glycoprotein Ib. Blood 2011; 117: 4999-5008.
18. Naim C, Douziech M, Therasse E, Robillard P, Giroux MF, Arsenault F, Cloutier G, Soulez G. Vulnerable atherosclerotic carotid plaque evaluation by ultrasound, computed tomography angiography and magnetic resonance imaging: an overview. Can Assoc Radiol J 2014; 65: 275-286.
19. Nandalur KR, Baskurt E, Hagspiel KD, Philips CD, Kramer ChM. Calcified carotid atherosclerotic plaque is associated less with ischemic symptoms than is noncalcified plaque on MDCT. AJR AM J Roentgenol 2005; 184: 295-298.
20. Nighoghossian N, Derex L, Douek P. The vulnerable carotid artery plaque: current imaging methods and new perspectives. Stroke 2005; 36: 2763-2772.
21. Redgrave JN, Lovett JK, Gallagher PJ, Rothwell PM. Histological assessment of 526 symptomatic carotid plaques in relation to the nature and timing of ischemic symptoms. Circulation 2006; 113: 2320-2328.
22. Saba L, Anzidei M, Marincola BC, Piga M, Raz E, Bassareo PP, Napoli A, Manneli L, Catalano C, Wintermark M. Imaging of the carotid artery vulnerable plaque. Cardiovasc Intervent Radiol 2014; 37: 572-585.
23. Saederup N, Chan L, Lira SA, Charo IF. Fractalkine deficiency markedly reduces macrophage accumulation and atherosclerotic lesion formation in CCR2–/– mice: evidence for independent chemokine functions in atherogenesis. Circulation 2008; 117: 1642-1648.
24. Schäfer A, Schultz C, Eigenthaler M, Fraccarollo D, Kobsar A, Gawaz M, Ertl G, Walter U, Bauersachs J. Novel role of the membrane-bound chemokine fractalkine in platelet activation and adhesion. Blood 2004; 103: 407-412.
25. Schultz C, Schäfer A, Stolla M, Kerstan S, Lorenz M, von Brühl ML, Schiemann M, Bauersachs J, Gloe T, Busch DH, Gawaz N, Massberg S. Chemokine fractalkine mediates leukocyte recruitment to inflammatory endothelial cells in flowing whole blood: a critical role for P-selectin expressed on activated platelets. Circulation 2007; 116: 764-773.
26. Stolla M, Pelisek J, von Brühl ML, Schäfer A, Barocke V, Heider P, Schiemann M, Bauersachs J, Gloe T, Busch DH, Gawaz M, Massberg S. Fractalkine is expressed in early and advanced atherosclerotic lesions and supports monocytes recruitment via CX3CR1. PLoS One 2012; 7: e43572.
27. Yadav AK, Lal A, Jha V. Association of circulating fractalkine (CX3CL1) and CX3CR1(+)CD4(+) T cells with common carotid artery intima-media thickness in patients with chronic kidney disease. J Atheroscler Thromb 2011; 18: 958-965.

Instructions to Authors

This instruction is based upon *Uniform Requirements for Manuscripts Submitted to Biomedical Reviews* (the complete document appears in N Engl J Med 1997; 336, 309-315).

Aims and scope

Folia Neuropathologica is an official journal of the Mossakowski Medical Research Centre Polish Academy of Sciences and the Polish Association of Neuropathologists. The journal publishes original articles and reviews that deal with all aspects of clinical and experimental neuropathology and related fields of neuroscience research. The scope of journal includes surgical and experimental pathomorphology, ultrastructure, immunohistochemistry, biochemistry and molecular biology of the nervous tissue. Papers on surgical neuropathology and neuroimaging are also welcome. The reports in other fields relevant to the understanding of human neuropathology might be considered.

Publication charge

Please note that there is an obligatory charge (250 Euro) for the manuscript being accepted for publication in *Folia Neuropathologica*. We send invoice for payment after the article is accepted for publication. There are no additional charges based on color figures or other elements.

Ethical consideration

Papers describing animal experiments can be accepted for publication only if the experiment conforms to the legal requirements in Poland as well as with the European Communities Council Directive of November 24, 1986 or the National Institute of Health Guide (National Institute of Health Publications No. 80-23, Revised 1978) for the care and use of Laboratory Animals for experimental procedure. Authors must provide a full description of their anesthetics and surgical procedures. Papers describing experiments on human subjects must include a statement that experiments were performed with the understanding and consent of each subject, with the approval of the appropriate local ethics committee.

Submission of manuscripts

Articles should be written in English. **All new manuscripts should be submitted through the online submission at http://panel2.termedia.pl/fn**
For authors unable to submit their manuscript online, please contact with Prof. E. Matyja, Editor-in-Chief of *Folia Neuropathologica*, ematyja@imdik.pan.pl
The Editorial Board reserves the right to reject a paper without reviewers' opinion if the content or the form of the paper does not meet minimum acceptance criteria or if the subject of the paper is beyond the aims and scope of the journal.

Legal aspects

In sending the manuscript the author(s) confirm(s) that (s)he has (they have) not previously submitted it to another journal (except for abstracts of no more than 400 words) or published it elsewhere. The author(s) also agree(s), if and when the manuscript is accepted for publication, to automatic and free transfer of copyright to the Publisher allowing for the publication and distribution of the material submitted in all available forms and fields of exploitation. The author(s) accept(s) that the manuscript will not be published elsewhere in any language without the written consent of the copyright holder, i.e. the Publisher.
All manuscripts submitted should be accompanied by an authors' statement including signed confirmation of the above and confirming that this publication has been approved by all co-authors (if any), as well as by the responsible authorities at the institution where the work has been carried out. The authors' statement should be signed by ALL co-authors. Additionally, the author(s) confirm(s) that (s)he is (they are) familiar with and will observe the "Instruction to Authors" included in *Folia Neuropathologica* and also that all sources of financial support have been fully disclosed. Materials previously published should be accompanied by written consent for reprinting from the relevant Publishers. In the case of photographs of identifiable persons, their written consent should also be provided. Any potential conflict of interest will be dealt with by the local court specific to the Publisher. Legal relations between the Publisher and the author(s) are in accordance with Polish law and with international conventions binding on Poland.
Authors agree to waive their royalties.

Anonymous review

All manuscripts will be subject to a process of anonymous editorial review.

Preparation of manuscripts

Articles must be written in English, with British spelling used consistently throughout. Authors not entirely familiar with English are advised to correct the style by professional language editors or native English speakers.
• The length of original article should not exceed 20 printed pages including text, illustrations, tables, and references.

- Manuscripts should be typed using 12pts.font, double-spaced, and fully corrected. Allow a margin at least 2.5 cm at the top, bottom and left side of the page. Text should not be justified.
- The title page should contain: the author's full names, title of the paper, all authors' affiliations, full name and address of the communicating author (including e-mail address and fax number), running title (not exceed 40 characters including spaces).
- The abstract should not exceed 350 words. A list of 3–10 key words is recommended below the abstract.
- The manuscript body should be organized in a standard form with separate sections: Introduction, Material and Methods, Results, Discussion, and References. Review articles should be divided into sections and subsections as appropriate without numbering.
- Do not underline in the text. Avoid footnotes.
- All dimensions and measurements must be specified in the metric system.
- The source of any drug and special reagent should be identified.
- Particular attention needs to be paid to the selection of appropriate analysis of data and the results of statistical test should be incorporated in the results section.
- The nomenclature used should conform to the current edition of the Nomina Anatomica or Nomina Anatomica Veterinaria.
- Acknowledgements should be made in a separate sheet following Discussion and before References. These should contain a list of dedications, acknowledgements, and funding sources.
- Legends of figures and tables should be typed on separate pages.
- The editor reserves the right to make corrections.

Tables

- Tables numbered in Roman numerals require a brief but descriptive heading.
- The major divisions of the table should be indicated by horizontal rules.
- Explanatory matter should be included in footnotes, indicated in the body of the table in order of their appearance.
- Tables must not duplicate material in the text or in illustration.

Illustrations

All figures should be supplied electronically at resolution 300dpi in all standard formats (tiff, jpg, Adobe Photoshop, Corel Draw, and EPS). Name your figure files with "Fig" and the figure number, e.g., Fig1.tif

- The maximum figure size is 84 mm or 174 mm for use in a single or double column width, respectively.
- When possible, group several illustrations on one block for reproduction. Like all other figures, block should be prepared within a rectangular frame to fit within a single or double column width of 84 and 174 mm, respectively, and a maximum page height of 226 mm.
- Each figure should include scale magnification bar; do not use magnification factors in the figure legends.
- All figures, whether photographs, graphs or diagrams, should be numbered using Arabic numerals and cited in the text in consecutive numerical order
- **Immunohistochemical study requires color illustrations of very good quality. The papers with white and black immunohistochemistry will not be accepted.**
- **For the paper accepted before 01.04.2016 the publication charge includes only the expense of color illustrations.** The cost of color print for every successive 8 pages is 200 euro irrespective of the number of color pages, i.e., the price remains the same whether there is one or eight pages.

The Publisher makes out the bill to the communicating Author.

References

The list of references (written on a separate page) should include only those publications that are cited in the text. Avoid citation of academic books, manuals and atlases. References may be arranged alphabetically and numbered consecutively. References should be given in square brackets with no space between the comma and the consecutive number, e.g. [3,4,6-12].

References should be written as follows:

Journal papers: initials and names of all authors, full title of paper, journal abbreviation (according to Index Medicus), year of publication, volume (in Arabic numerals), first and last page (example below):

1. Valverde F. The organization of area 18 in the monkey. Anat Embryol 1978; 154: 305-334.
2. Uray NJ, Gona AG. Calbindin immunoreactivity in the auricular lobe and interauricular granular band of the cerebellum in bullfrogs. Brain Behav Evol 1999; 53: 10-19.

Book and monographs: initials and names of all authors, full title, edition, publisher, place, year (examples below):

1. Pollack RS. Tumor surgery of the head and neck. Karger, Basel 1975.
2. Amaral DG, Price JL, Pitkanen A, Carmichael ST. Anatomical organization of the primate amygdaloid complex. In: Aggleton JP (ed.). The amygdala. Wiley-Liss, New York 1992; pp. 1-66.

Reference to articles that are accepted for publication may be cited as „in press" or Epub.

Proofs

Corrections to the proofs should be restricted to printer's errors only; other alterations will be charged to the authors. In order to maintain rapid publication, proofs should be returned within 48 hours, preferably by e-mail, fax or courier mail. If the Publisher receives no response from the authors after 10 days, it will be assumed that there are no errors to correct and the article will be published.

Subscription information

The journal is published in one volume per year consisting of four numbers. The annual subscription price is 160 PLN for Institutions from Poland and 80 PLN for individual subscribers from Poland and 140 Euro for foreign Institutions and 70 Euro for foreign individual subscribers.
Payment should be made to:
Termedia sp. z o.o., ul. Kleeberga 8, 61-615 Poznań
BZ WBK III O/Poznań PL 61 1090 1359 0000 0000 3505 2645
SWIFT: WBKPPLPP

The publisher must be notified of a cancellation of a subscription not later than two months before the end of the calendar year. After that date the subscription is automatically prolonged for another year.
Publishing, Subscription and Advertising Office:
TERMEDIA Publishing House
ul. Kleeberga 2
61-615 Poznań, Poland
phone/fax +48 61 822 77 81
e-mail: termedia@termedia.pl
http://www.folianeuro.termedia.pl

Folia
Neuropathologica

AUTHOR'S STATEMENT

Title of the article

.....

.....

.....

The author(s) hereby confirm(s) that:

☐ The above-mentioned work has not previously been published and that it has not been submitted to the Publishers of any other journal (with the exception of abstracts not exceeding 400 words).

☐ All co-authors named and the relevant authorities of the scientific institutions at which the work has been carried out are familiar with the contents of this work and have agreed to its publication.

☐ In sending the manuscript together with illustrations and tables agree(s) to automatic and free transfer of copyright to the Publisher allowing for the publication and distribution of the material submitted in all available forms and fields of exploitation, without limits of territory or language, provided that the material is accepted for publication. At the same time the author(s) accept(s) that the submitted work will not be published elsewhere and in whatever language without the earlier written permission of the copyright holder, i.e. the Publisher.

☐ (S)he (they) agree to waive his(her)(their) royalties (fees).

☐ (S)he (they) empower(s) the Publisher to make any necessary editorial changes to the submitted manuscript.

☐ All sources of funding of the work have been fully disclosed.

☐ The manuscript has been prepared in accordance with the Publisher's requirements.

☐ (S)he (they) is (are) familiar with the regulations governing the acceptance of works as published in *Folia Neuropathologica* and agree(s) to follow them.

☐ (S)he (they) agree to accept appropriate invoice from the Publisher in case colour illustrations are implemented.

Date *Signatures of* ***all authors***

The covering letter formula can be found at: www.folianeuro.termedia.pl
-The covering letter should be sent to Associate Editor:

Milena Laure-Kamionowska
-Editorial Office of Folia Neuropathologica
Mossakowski Medical Research Centre, Polish Academy of Sciences
Poland Medical Research Centre
ul. Pawinskiego 5
02-106 Warszawa, Poland

CONTENTS